The preparation of dithiadiazolyl and diselenadiazolyl complexes of platinum and palladium

Iain May

THE PREPARATION OF DITHIADIAZOLYL AND DISELENADIAZOLYL COMPLEXES OF PLATINUM AND PALLADIUM

Iain May BSc (Glasgow)

Graduate Society

A thesis submitted in partial fulfilment for the degree of PhD to the University of Durham

November 1995

to Ann, mum, dad and David
for love and support

Acknowledgements

I would firstly like to thank my supervisor Arthur Banister. He has provided great support both in chemistry and life in general and it is an honour and a privilege to submit the last sulfur-nitrogen thesis from within his research group prior to his retirement.

Thanks to all my research colleagues for putting up with my singing; Stan 'selenium' Hauptman, Jeremy 'what you could do' Rawson, Ian 'golf' Lavender, Simon 'benzene' Lawrence, Christine 'fumehood' Aherne, Tom 'crystal' Hibbert, Colin 'goin tae rixys' Campbell, Owen 'casual but smart' Dawe, Nick 'sulfur' Smith, Penny 'the boss' Herbertson, Pete 'only me' Ivison and the professional Yorkshireman Neil 'me and you will always vote labour' Bricklebank. Owen, Simon and especially Jeremy worked closely with me on my project. The help I recieved from Chris 'tea break' Gregory in physics was also invaluable.

Mention should also be made to various lodgers in lab 100 including Cliff Ludman, Sarah 'filter stick' Lamb, Matt 'Peter Perfect' Davidson, Andrew, Duncan, Jacqui and my two hard working German friends Torsten and Dirk.

My colleagues at the now defunct 24 hour general stores (lab 19) deserve a mention especially the captain of our joint 5-a-side cup team Mike Chan. We would have won the cup if we'd had a decent keeper.

The technical, secretarial and academic staff in the chemistry dept. have provided an invaluable service especially Euan, Jimmy, Joe, George, Tony, Eileen, Jill, Jaraka, Judith, Bob and Keith.

I am also greatly indebted to Johnson Matthey who very generously provided precious metal salts

Thanks to my fellow Scots who I have befriended down here in this foreign land especially Colin Campbell, Douglas Nunn and Graham Robertson. I also must acknowledge my flatmates during my stay in Durham.

Finally thanks to all those who have provided financial support; the E.P.S.R.C., my family, the Bank of Scotland, Dunelm House, the Dept. of Chemistry, the examinations office and Marcos at reflections.

Memorandum

The work described in this thesis was carried out by me in the Department of chemistry at the University of Durham between October 1992 and September 1995. I declare that this work has not been submitted previously for a degree at this or any other University. This thesis is a report of my original work, except where acknowledged by reference. The copyright of this thesis rests with the author. No quotation should be published without his written consent and information derived from it should be acknowledged. Material from this thesis has been included in the following publication:

1. Novel Bonding Modes in Metallo-Dithiadiazolyl Complexes: Preparation and Crystal Structures of [Pt(SNCPhNS-*S,S*)(PPh_3)$_2$].MeCN and [Pt_3(μ_S-$_S$SNCPhNS)$_2$(PPh_3)$_4$].2PhMe, A.J.Banister, I.B.Gorrell, S.E.Lawrence, C.W.Lehmann, I.May, G.Tate, A.J. Blake and J.M. Rawson, J. Chem. Soc., Chem. Commun., 1994, 1779.

2. E.s.r. Spectra of 4-Phenyl-1,2,3,5-Diselenadiazolyl, [PhCNSeSeN]$^{\bullet}$, and the First Diselenadiazolyl Metal Complex, [Pt(SeNCPhNSe-*Se,Se*)(PPh_3)$_2$], J.M.Rawson, A.J.Banister and I.May, *Magn. Reson. Chem.*, 1994, **32**, 487.

3. Metal Insertion into the S-S Bond of Phenyl Dithiadiazolyl, A.J.Banister, I.May, *Phosphorus, Sulfur and Silicon*, 1994, **93-94**, 447.

Abstract

This thesis describes the reaction of phenyl dithiadiazolyl, [PhCNSSN]•, and phenyl diselenadiazolyl, [PhCNSeSeN]•, with zero-valent phosphine complexes of platinum and palladium.

Chapter one outlines the experimental techniques utilised to prepare and characterise the compounds prepared during the course of this research and contains techniques solely employed within the laboratory that this research was undertaken.

The second chapter describes the chemistry of dithiadiazolyls and an improved synthetic route to the ligand [PhCNSSN]•.

The third chapter outlines the chemistry of platinum and palladium and also describes the synthesis of the platinum and palladium complexes used throughout this project.

Chapter four describes the reaction of $[Pt(PPh_3)_4]$, $[Pt(dppe)_2]$ and $[Pd(dppe)_2]$ with [PhCNSSN]• to form the novel monometallic complexes $[Pt(SNC(Ph)NS\text{-}\mathit{S,S})(PPh_3)_2]$, $[Pt(SNC(Ph)NS\text{-}\mathit{S,S})(dppe)]$ and $[Pd(SNC(Ph)NS\text{-}\mathit{S,S})(dppe)]$. These complexes have been extensively studied by x-ray crystallography, magnetic measurements, e.s.r. and u.v./vis spectroscopy. The biological activity of $[Pt(SNC(Ph)NS\text{-}\mathit{S,S})(PPh_3)_2]$ and m.o. calculations on $[Pt(SNC(H)NS\text{-}\mathit{S,S})(PH_3)_2]$ were used as a basis for further study.

In chapter five the formation of trimetallic dithiadiazolyl complexes from the reaction of [PhCNSSN]• with zero-valent phosphine complexes has been described. $[Pt_3(\mu_{S\text{-}S}SNC(Ph)NS)_2(PPh_3)_4]$, $[Pt_3(\mu_{S\text{-}S}SNC(3,4FC_6H_3)NS)_2(PPh_3)_4]$ and $[Pd_3(\mu_{S\text{-}S}SNC(Ph)NS)_2(PPh_3)_4]$ have been structurally characterised. The unique type of bonding in these species has been described with the aid of m.o. calculations undertaken on $[Pt_3(\mu_{S\text{-}S}SNC(H)NS)_2(PH_3)_4]$.

Chapter six describes the decomposition of monometallic to trimetallic dithiadiazolyl complexes with the varying stabilities of different monometallic species rationalised; kinetic measurements made and a mechanism for the decomposition is proposed. N.m.r. and e.s.r. spectroscopy has been used to observe other decomposition products formed.

Chapter seven examines the oxidative decomposition of monometallic dithiadiazolyl complexes electrochemically (by cyclic voltammetry) and chemically (by reaction with $NOBF_4$). The reaction between $[Pd(SNC(Ph)NS\text{-}\mathit{S,S})(dppe)]$, $NOBF_4$ and trace moisture results in the formation of a novel dimetallic species $[Pd_2(\mu_{S\text{-}S}SNC(Ph)N(H)S)(dppe)_2]$ which has been structurally characterised.

Finally, chapter eight outlines an improved synthetic route to $(PhCNSeSeN)_2$ and the frozen glass e.s.r. spectrum of [PhCNSeSeN]•. Reaction between [PhCNSeSeN]• and $[Pt(PPh_3)_4]$ has resulted in the formation of $[Pt(SeNC(Ph)NSe\text{-}\mathit{Se,Se})(PPh_3)_2]$ and reaction between [PhCNSeSeN]• and $[Pd(PPh_3)_4]$ has resulted in the formation of $[Pd_3(\mu_{Se\text{-}Se}SeNC(Ph)NSe)_2(PPh_3)_4]$

Abbreviations

The following abbreviations are used in this thesis:

[RCNSSN]$^{\bullet}$	1,2,3,5 dithiadiazolyl ring system
[RCNSSN]	1,2,3,5 dithiadiazolylium ring system
(SNC(Ph)NS-*S,S*)	chelating 1,2,3,5 dithiadiazolyl ligand
($\mu_{S\text{-}S}$SNC(Ph)NS)	bridging 1,2,3,5 dithiadiazolyl ligand
($\mu_{S\text{-}S}$SN(H)C(Ph)NS)	bridging 1,2,3,5 dithiadiazolyl-imine ligand
[RCNSeSeN]$^{\bullet}$	1,2,3,5 diselenadiazolyl ring system
[RCNSeSeN]	1,2,3,5 diselenadiazolylium ring system
(SeNC(Ph)NSe-*Se,Se*)	chelating 1,2,3,5 diselenadiazolyl ligand
($\mu_{Se\text{-}Se}$SeNC(Ph)NSe)	bridging 1,2,3,5 diselenadiazolyl ligand
cp	cyclopentadienyl
C.V.	cyclic voltammetry
d.s.c.	differential scanning calorimetry
e.s.r.	electron spin resonance
HOMO	highest occupied molecular orbital
IR	infra-red
LUMO	lowest occupied molecular orbital
Me	methyl
MeCN	acetonitrile
n.m.r.	nuclear magnetic resonance
Ph	phenyl
R	substituted phenyl group
SOMO	singly occupied molecular orbital
thf	tetrahydrofuran

CONTENTS

Page No.

CHAPTER ONE
General Experimental

1.1. INTRODUCTION 1
1.2. GENERAL EXPERIMENTAL 1
1.3. THE STORAGE AND HANDLING OF DRY LIQUID SO_2 1
1.4. SPECIALISED GLASSWARE 2
1.4.1. The Closed Soxhlet Extractor. 2
1.4.2. The "Dog". 2
1.5. PHYSICAL METHODS 2
1.5.1. Elemental Analysis. 2
1.5.2. Infrared Spectroscopy. 2
1.5.3. Differential Scanning Calorimetry. 2
1.5.4. Nuclear Magnetic Resonance Spectroscopy. 2
1.5.5. Electron Spin Resonance Spectrometry. 3
1.5.6. Ultra-Violet/Visible Spectroscopy. 3
1.5.7. Mass Spectrometry. 3
1.5.8. Cyclic Voltammetry. 3
1.5.9. Single Crystal X-Ray Diffraction. 3
1.5.10. Magnetic Measurements. 4
1.5.11. Biological Test Measurements. 4
1.6. CHEMICALS AND SOLVENTS 4
1.6.1. Purification of Solvents. 4
1.6.2. Chemicals. 4
1.7. REFERENCES 9

CHAPTER TWO
The Properties of Dithiadiazolyls and the Synthesis of the Ligand 1,2,3,5 Phenyl dithiadiazolyl

2.1. INTRODUCTION 10
2.1.1. General Introduction. 10
2.1.2. 1,3,2,4 Dithiadiazolyls. 10
2.1.3. 1,2,3,5 Dithiadiazolyls. 10
2.1.4. Potential Applications and Synthetic Aims. 11
2.1.5 The Preparation and Properties of [*p*-NCC_6F_4CNSSN]$^{\bullet}$. 13
2.1.6. Formation of Metal Complexes. 15

Page No.

2.1.7. Electron Spin Resonance Spectroscopy. 16
2.1.8. Theoretical Studies. 17
2.1.9. X-Ray Crystallography. 19
2.1.10. Magnetic Measurements. 20
2.1.11. Cyclic Voltammetry. 21
2.1.12. Further Techniques. 21
2.2. RESULTS AND DISCUSSION 22
2.2.1. Synthesis of $(PhCNSSN)_2$. 22
2.2.2. Original Synthetic Routes. 22
2.2.3. Preparation of $(PhCNSSN)_2$ - The Persilylated Amidine Route. 22
2.2.4. Preparation of $[PhCNSSN]_2$ Without Isolation of Amidine . 23
2.2.5. The Preparation of $(PhCNSSN)_2$ Avoiding SO_2 Extraction. 25
2.3. Experimental. 26
2.3.1. The Preparation of [PhCNSSN]Cl. 26
2.3.2. The Reduction of [PhCNSSN]Cl to $(PhCNSSN)_2$. 26
2.3.3. The 'Single Pot' Preparation of $(PhCNSSN)_2$. 27
2.4. CONCLUSION 28
2.5. REFERENCES 29

CHAPTER THREE

The Properties of Platinum and Palladium Co-ordination Compounds and the Synthesis of their Zero-Valent Phosphine Complexes

3.1. INTRODUCTION 32
3.1.1. General Introduction. 32
3.1.2. Complexes of Platinum and Palladium. 32
3.1.3. Zero-valent Chemistry. 33
3.1.4. Chemistry and Applications of Zero-Valent Complexes. 33
3.1.5. Square-planar Chemistry of Platinum and Palladium. 34
3.1.6. Cis-platin and Other Square-Planar Anti-Cancer Drugs. 34
3.1.7. Linear Chain Compounds. 36
3.1.8. Sulphur-Nitrogen Complexes of Platinum and Palladium. 37
3.1.9. ^{31}P n.m.r. Spectroscopy of Phosphine Complexes. 38
3.2. RESULTS AND DISCUSSION 39
3.2.1. Preparation of zero-valent phosphine complexes of Pt and Pd. 39
3.2.2. The preparation of Dppe $(Ph_2PC_2H_4PPh_2)$. 39

		Page No.
3.2.3.	The preparation of $[Pd_2dba_3.CHCl_3]$.	39
3.2.4.	The Preparation of $[Pd(PPh_3)_4]$ and $[Pd(dppe)_2]$ from $[Pd_2dba_3.CHCl_3]$.	40
3.2.5.	The reduction of K_2MCl_4 by $NaBH_4$ in the presence of phosphine.	41
3.2.6.	The Reduction of K_2PtCl_4 by KOH in the presence of Phosphine.	42
3.2.7.	The Preparation of $[Pt(PPh_3)_3]$ from $[Pt(PPh_3)_4]$.	42
3.3.	EXPERIMENTAL	43
3.3.1.	The Preparation of $[Pd_2dba_3.CHCl_3]$.	43
3.3.2.	The Preparation of $[Pd(PPh_3)_4]$ from $[Pd_2dba_3.CHCl_3]$.	43
3.3.3.	The Preparation of $[Pd(PPh_3)_4]$ from $NaBH_4$ reduction of K_2PdCl_4.	44
3.3.4.	The Preparation of dppe.	44
3.3.5.	The Preparation of $[Pd(dppe)_2]$.	45
3.3.6.	The Preparation of $[Pt(PPh_3)_4]$ from K_2PtCl_4 and $NaBH_4$.	45
3.3.7.	The Preparation of $[Pt(PPh_3)_4]$ from K_2PtCl_4/KOH.	46
3.3.8.	The Preparation of $Pt(PPh_3)_3$ from $Pt(PPh_3)_4$.	46
3.3.9.	The Preparation of $[Pt(PMe_2Ph)_4]$.	46
3.3.10.	The Preparation of $[Pt(dppe)_2]$.	47
3.4.	CONCLUSION	48
3.5.	REFERENCES	49

CHAPTER FOUR

The Synthesis and Properties of Monometallic Platinum and Palladium Dithiadiazolyl Complexes

4.1.	INTRODUCTION	52
4.1.1.	The Chelating Bonding Mode of (SNCPhNS).	52
4.1.2.	Requirements for Metal Complex Precursor.	52
4.1.3.	Preliminary Reactions with Zero-Valent Group 10 Complexes.	53
4.2.	RESULTS AND DISCUSSION.	54
4.2.1.	The Synthesis of Monometallic Dithiadiazolyl Complexes.	54
4.2.2.	Crystal Growth of Monometallic Complexes.	55
4.2.3.	X-Ray Structures.	56
4.2.4.	E.s.r. Spectroscopy.	64
4.2.5.	Molecular Orbital Studies on $[Pt(SNCPhNS\text{-}S,S)(PH_3)_2]$.	69
4.2.7.	Magnetic Measurements.	71
4.2.8.	Ultra Violet/Visible Spectroscopy.	80

		Page No.
4.2.9.	Biological Properties.	82
4.2.10.	F.A.B. Spectroscopy of [Pt(SNCPhNS-*S,S*)(PPh_3)$_2$].	84
4.2.11.	Other Techniques.	84
4.3.	EXPERIMENTAL	85
4.3.1.	Preparation of [Pt(SNCPhNS-S,S)(PPh_3)$_2$].MeCN.	85
4.3.2.	Crystal growth of [Pt(SNCPhNS-*S,S*)(PPh_3)$_2$].MeCN.	85
4.3.3.	Preparation of [Pd(SNCPhNS-*S,S*)(dppe)].	85
4.3.4.	Crystal growth of [Pd(SNCPhNS-*S,S*)(dppe)].	86
4.3.5.	Preparation of [Pt(SNCPhNS-*S,S*)(dppe)].	86
4.3.6.	Crystal growth of [Pt(SNCPhNS-*S,S*)(dppe)].	87
4.4.	CONCLUSION	88
4.5.	REFERENCES	89

CHAPTER FIVE

The Synthesis and Properties of Trimetallic Platinum and Palladium Dithiadiazolyl Complexes

5.1.	INTRODUCTION	91
5.1.1.	Decomposition of Monometallic Dithiadiazolyl Complexes.	91
5.1.2.	Reaction Between [$Pd(PPh_3)_4$] and $(PhCNSSN)_2$.	91
5.2.	RESULTS AND DISCUSSION.	92
5.2.1.	Preparation of Trimetallic Complexes.	92
5.2.2.	Crystal Growth of Trimetallic Complexes.	92
5.2.3.	X-Ray Structures of Trimetallic Species.	93
5.2.4.	Rationalisation of Bonding in Trimetallic Complexes.	101
5.2.5.	Molecular Orbital Study of $Pt_3(\mu_{S\text{-}S}SNCHNS)_2(PH_3)_4$.	103
5.2.6.	N.m.r. Studies.	105
5.2.7.	Biological Test Results For $Pt_3(\mu_{S\text{-}S}SNC(Ph)NS)_2(PPh_3)_4$.	108
5.3.	EXPERIMENTAL	109
5.3.1.	Preparation of [$Pt_3(\mu_{S\text{-}S}SNCPhNS)_2(PPh_3)_4$].	109
5.3.2.	Crystal growth of [$Pt_3(\mu_{S\text{-}S}SNCPhNS)_2(PPh_3)_4$].2MePh.	109
5.3.3.	Preparation of [$Pd_3(\mu_{S\text{-}S}SNCPhNS)_2(PPh_3)_4$].$2CH_2Cl_2$.	109
5.3.4.	Crystal growth of [$Pd_3(\mu_{S\text{-}S}SNCPhNS)_2(PPh_3)_4$].$2CH_2Cl_2$.	110
5.3.5.	Preparation of [$Pd_3(\mu_{S\text{-}S}SNCPhNS)_2(dppe)_2$].	110
5.4.	CONCLUSION	111
5.5.	REFERENCES	112

Page No.

CHAPTER SIX

A Study of the Decomposition of Monometallic Platinum and Palladium Dithiadiazolyl Complexes

6.1. INTRODUCTION 113
6.1.1. The Stability of Monometallic Dithiadiazolyl Complexes. 113
6.1.2. Studying the Monometallic To Trimetallic Decomposition. 113
6.2. RESULTS AND DISCUSSION 114
6.2.1. A Rationalisation of the Various Stabilities of [PhCNSSN]•. Monometallic Complexes. 114
6.2.2. The Monometallic to Trimetallic Conversion, a Mechanistic Study by E.s.r. Spectroscopy. 115
6.2.3. The Monmer to Trimer Conversion; a Kinetic Study. 122
6.2.4. Other Decomposition Pathways of Monometallic Complexes. 129
6.2.5. Attempted Rationalisation of the Decomposition Of Monometallic to Trimetallic Species. 144
6.3. EXPERIMENTAL
6.3.1. The Decomposition of [Pt(SNC(Ph)NS-*S,S*)(dppe)]. 146
6.3.2. The Preparation of $[Pt_3(\mu_{S\text{-}S}SNC(Ph)NS)_2(dppe)_2]$. 146
6.3.3. The Preparation of $[PtPdPt(\mu_{S\text{-}S}SNC(Ph)NS)_2(dppe)_2]$. 147
6.3.4. Attempted Crystal Growth Reaction of $PtPdPt(\mu_{S\text{-}S}SNC(Ph)NS)_2(dppe)_2]$. 147
6.4. CONCLUSION 148
6.5. REFERENCES 150

CHAPTER SEVEN

An Oxidative Decomposition Study on Monometallic Dithiadiazolyl Complexes

7.1. INTRODUCTION 151
7.1.1. Proposed One-Electron Oxidation of Monometallic Dithiadiazolyl Complexes. 151
7.1.2. Cyclic Voltammetry. 151
7.2. RESULTS AND DISCUSSION 153
7.2.1. Cyclic Voltammetry Study of [PhCNSSN]• Based Monometallic Complexes. 153
7.2.2. Oxidative Decomposition of Monometallic Complexes. 154

Page No.

7.2.3. The ^{31}P n.m.r. Spectra of the Products of the Reaction Between Pd(SNC(Ph)NS-*S,S*)(dppe) and $NOBF_4$. 157
7.2.4. X-Ray Structure of $[Pd_2(\mu S\text{-}SSNC(Ph)N(H)S)(dppe)_2][BF_4]_2$. 159
7.2.5. A Re-evaluation of the ^{31}P n.m.r. Spectrum of the Products of the Reaction Between [Pd(SNC(Ph)NS-S,S)(dppe)] and $NOBF_4$. 164
7.2.6. The ^{31}P n.m.r. Spectrum of the Products of the Reaction Between [Pt(SNC(Ph)NS-*S,S*)(dppe)] and $NOBF_4$. 164
7.2.7. The ^{31}P n.m.r. Spectrum of the Products of the Reaction Between [Pt(SNC(Ph)NS-*S,S*)$(PPh_3)_2$] and $NOBF_4$. 166
7.3. EXPERIMENTAL 169
7.3.1. The Reaction Between [Pd(SNC(Ph)NS-*S,S*)(dppe)] and $NOBF_4$. 169
7.3.2. The Reaction Between [Pt(SNC(Ph)NS-*S,S*)(dppe)] and $NOBF_4$. 169
7.3.3. The Reaction Between [Pt(SNC(Ph)NS-*S,S*)$(PPh_3)_2$] and $NOBF_4$. 169
7.4. CONCLUSION 171
7.5 REFERENCES 172

CHAPTER EIGHT

The Preparation of Phenyl Diselenadiazolyl and its Reaction with Platinum and Palladium Complexes

8.1. INTRODUCTION 173
8.1.2. The Replacement of Sulfur with Selenium in [RCNEEN]$^\bullet$ (E = chalcogen). 173
8.1.2. The Synthesis and Properties of 1,2,3,5 Diselenadiazolyl. 173
8.1.3. Multi and Mixed Diselenadiazolyls Complexes. 174
8.1.4. The Preparation and Characterisation of of [PhCNSeSeN]$^\bullet$ and its use as a Ligand. 174
8.2. RESULTS AND DISCUSSION 175
8.2.1. The Preparation of [PhCNSeSeN]Cl. 175
8.2.2. Reduction of [PhCNSeSeN]Cl to $(PhCNSeSeN)_2$. 176
8.2.3. One Pot Synthesis of $(PhCNSeSeN)_2$. 177
8.2.4. Previous E.s.r. Spectroscopic Studies on [PhCNSeSeN]$^\bullet$. 177
8.2.5. Anisotropic 'Frozen Glass' E.s.r. spectra of [PhCNSeSeN]$^\bullet$. 178
8.2.6. Preliminary Complexation Reactions of [PhCNSeSeN]$^\bullet$ with $M(PPh_3)_4$ (where M = Pd or Pt). 184
8.2.7. Solution State E.s.r. Spectra of [Pt(SeNC(Ph)NSe-*Se,Se*)$(PPh_3)_2$]. 184
8.2.8. The Reaction of [PhCNSeSeN]$^\bullet$ with $[Pt(PPh_3)_4]$. 188

		Page No.
8.2.9.	The Reaction of [PhCNSeSeN]$^{\bullet}$ with [$Pd(PPh_3)_4$].	188
8.3.	EXPERIMENTAL	189
8.3.1.	The Preparation of [PhCNSeSeN]Cl.	189
8.3.2.	The Reduction of [PhCNSeSeN]Cl to $(PhCNSeSeN)_2$ with Zn/Cu Couple.	189
8.3.3.	The Reduction of [PhCNSeSeN]Cl to $(PhCNSeSeN)_2$ with Silver Powder.	190
8.3.4.	The Reduction of [PhCNSeSeN]Cl to $(PhCNSeSeN)_2$.by Ph_3Sb.	191
8.3.5.	The 'One-Pot' Preparation of $(PhCNSeSeN)_2$.	191
8.3.6.	The Reaction Between $(PhCNSeSeN)_2$ and [$Pt(PPh_3)_4$].	192
8.3.7.	TheReaction Between $(PhCNSeSeN)_2$ and [$Pd(PPh_3)_4$].	192
8.3.8.	Crystal Reaction Between $(PhCNSeSeN)_2$ and $Pd(PPh_3)_4$ in CH_2Cl_2.	193
8.4.	CONCLUSION	194
8.5.	REFERENCES	195
	Appendix 1	
A.1.	SUPPLEMENTARY X-RAY STRUCTURAL DATA	197
	Appendix 2	
A.2.	CONFERENCES AND LECTURES ATTENDED	200
A.2.1.	Conferences Attended.	200
A.2.2.	Lectures Attended.	200

CHAPTER ONE

GENERAL EXPERIMENTAL

1.1. INTRODUCTION

The following chapters in this thesis contain chemistry that has been undertaken using a wide range of techniques, some of which may be unfamiliar to the reader. It is appropriate therefore to begin by outlining these experimental methods. The experimental work and physical measurements were undertaken by the author after the required training. Where this is not the case the operators involved are mentioned.

1.2. GENERAL EXPERIMENTAL

Many of the reactions undertaken and the compounds prepared were air and moisture sensitive; therefore inert atmosphere techniques were applied throughout the majority of this work. All air and moisture sensitive materials were handled under dry nitrogen in a Vacuum Atmospheres HE43-2 glove box fitted with an HE493 Dri-Train and standard vacuum line techniques were used throughout. Unless stated O_2 free N_2 (BOC) was used as the inert gas (dried further through a P_4O_{10} column). All glassware was pre-dried overnight at ca.130°C prior to use.

1.3. THE STORAGE AND HANDLING OF DRY LIQUID SO_2.

Liquid SO_2 was used extensively as a solvent and was handled on a Monel vacuum line fitted with stainless steel and monel 'Whitey' taps (IK54) which are in turn fitted with Teflon compression ferrules. Sulfur dioxide was transferred from the original canister into specially designed pressurised cylinders containing P_4O_{10} or CaH_2 as a drying agent. The SO_2 handling and storage equipment was designed and built by Dr. Z.V. Hauptman formerly of the Durham University Chemistry Department.

1.4. SPECIALISED GLASSWARE

1.4.1. The Closed Soxhlet Extractor.

The closed soxhlet extractor[1] functions as a normal soxhlet extractor (figure 1.a.) except that the J.Young Teflon tap allows the use of SO_2 in a closed system as the extracting solvent. The $^1/_4$" glass tubing enables connection to the metal vacuum line via Swage lock Teflon compression fittings or the conventional vacuum line via a glass adapter and Swage lock fitting.

1.4.2. The "Dog".

The "dog" (figure 1.b.)[2] is a twin bulbed reaction vessel connected by a glass tube partitioned by a glass sinter. As with the closed extractor, Teflon vacuum taps and $^1/_4$" tubing facilitates the use of SO_2 as a solvent in this apparatus although in the course of this research it was more commonly inverted and used as a method of slow diffusion of solutions to facilitate crystal growth, a procedure described more fully in chapter four.

1.5. PHYSICAL METHODS.

1.5.1. Elemental Analysis.

Carbon, hydrogen and nitrogen analysis was undertaken by Mrs J. Dostal, Miss J. Magee and Mr. B. Coult on a Carlo Erba 1106 Elemental Analyser.

1.5.2. Infrared Spectroscopy.

Infrared (I.R.) spectra were recorded as KBr discs using a Perkin-Elmer FT 1720X spectrophotometer. Samples that were more moisture/air sensitive were run as nujol mulls using KBr plates (enclosed in a brass holder) and were made up in a glove box.

1.5.3. Differential Scanning Calorimetry.

Differential scanning calorimetry (d.s.c.) measurements were undertaken with a Mettler FP80 control unit linked to a Mettler FP85 thermal analysis cell and interfaced with an Opus PC III computer running a d.s.c. analysis program. The computer program was written by Dr.J.M. Rawson.

1.5.4. Nuclear Magnetic Resonance Spectroscopy.

Nuclear magnetic resonance (n.m.r.) spectra were recorded on a Bruker AC250MHz spectrometer. Standard n.m.r. tubes were used after oven drying.

1.5.5. Electron Spin Resonance Spectrometry.

Electron spin resonance (e.s.r. or e.p.r.) spectra were obtained in conjunction with Dr. J.M.. Rawson at the University of Edinburgh on a Bruker ER200D-SRC spectrometer with attached plotter. Oven dried standard e.s.r. tubes were used throughout. Typical errors are +/-0.002mT for hyperfine coupling and +/-0.005 for g-tensors.

1.5.6. Ultra-Violet/Visible Spectroscopy.

Ultra violet/visible (U.V./vis.) spectra were recorded on a Unicam U.V./vis. spectrophotometer (UV2) connected to an Elonex PC.

1.5.7. Mass Spectrometry.

Routine mass spectra were recorded on a V.G. Analytical 7070E spectrometer using electron impact (E I) or chemical-ionisation techniques by Dr. M. Jones and Miss L.M. Turner. F.A.B. mass spectra were obtained using a dedicated ion source fitted with a F.A.B. atom gun at the University of Manchester Institute of Science and Technology.

1.5.8. Cyclic Voltammetry.

Cyclic voltammetry (c.v.) measurements were recorded using a Bioanalytical Systems type CV-113 potential wave generator and a Linseis type LY1710Q x-y chart recorder. The cyclic voltammogram was undertaken in a 3-limbed undivided cell with a basal bulb[3] (figure 1.c.). Into different limbs were placed the reference (Ag/Ag^+), working (Pt dot) and auxiliary (Pt coil) electrodes held by tight "Swage lock" connectors. Samples (ca.20mg) and supporting electrolyte $[Bu_4N][BF_4]$ (500mg) were placed in the cell and dissolved in MeCN. The sample was agitated between scans by a magnetic flea. Further details can be found in a previous thesis submitted by this research group[4].

1.5.9. Single Crystal X-Ray Diffraction.

Single crystal x-ray crystallography was undertaken on a Stoë Stadi-4 four-circle diffractometer fitted with an Oxford Cryosystems low temperature device[5] or a Siemens SMART CCD detector, and using graphite monochromatic Mo-Kα radiation. The data were corrected for absorption by means of φ-scans[6] and a subsequent empirical absorption correction[7]. The structures were solved by Patterson or direct methods using the SHELXS 86 program[8] and were refined using a full matrix least squares method.[9]

1.5.10. Magnetic Measurements

Magnetic measurements were run by Dr. C. Gregory of the Department of Physics, University of Durham, on a Faraday Balance (Oxford Instruments) in the range 10-300K and with an applied field of 1T. Accurately weighed samples of about 50mg were loaded in sealable Teflon buckets.

1.5.11. Biological Test Measurements

Biological test measurements were undertaken by Dr. S. Fricker at the Johnson-Matthey Technology Centre (Reading) .

1.6. CHEMICALS AND SOLVENTS

1.6.1. Purification of Solvents.

Acetonitrile (Aldrich HPLC Grade) was dried by refluxing over CaH_2 under an atmosphere of dry N_2 followed by distillation (with filtration through a glass column packed with pre-dried alumina) into clean dry flasks equipped with J.Young Teflon vacuum taps. It was then degassed via a freeze-thaw cycle and stored under dry N_2.

Dichloromethane (BDH), dried by distillation from CaH_2 into clean dry flasks, was degassed and stored under N_2.

Toluene was dried by refluxing over lump sodium, followed by distillation under an atmosphere of dry N_2 onto fresh Na wire into a clean dry flask from where it was degassed and stored under N_2.

Diethyl ether, anhydrous (BDH) was stored over sodium wire and used direct from the Winchester.

Tetrahydrofuran (thf), was purified (by Mr. B. Hall of the Chemistry Department) by fractional distillation from sodium under an atmosphere of dry nitrogen. The solvent was then stored under N_2 in a Winchester equipped with a teflon tap.

$CDCl_3$ (Goss) was dried over P_4O_{10} in the back leg of a "dog" before vacuum transfer into the front limb prior to use.

1.6.2. Chemicals.

The precious metal chlorides, K_2PtCl_4, K_2PdCl_4 and $PdCl_2$ were loaned by Johnson-Matthey and used as provided.

KOH (BDH), $NaBH_4$ (Aldrich), PhCN (Aldrich), Ch_3COONa (Aldrich), dibenzylidene acetone (Aldrich & Avocado), 1,2-dichloroethane (Aldrich), $LiN(SiMe_3)_2$ (Aldrich), $SeCl_4$ (Aldrich), Se powder (various sources) and SCl_2 (BDH) were also used as provided.

PPh_3 (Fluka) and $SbPh_3$ (Aldrich) were recrystallised from EtOH prior to use.

Strip lithium metal (Aldrich) was delivered under argon and transferred to storage under mineral oil.

Figure 1.a. The Closed Extractor.

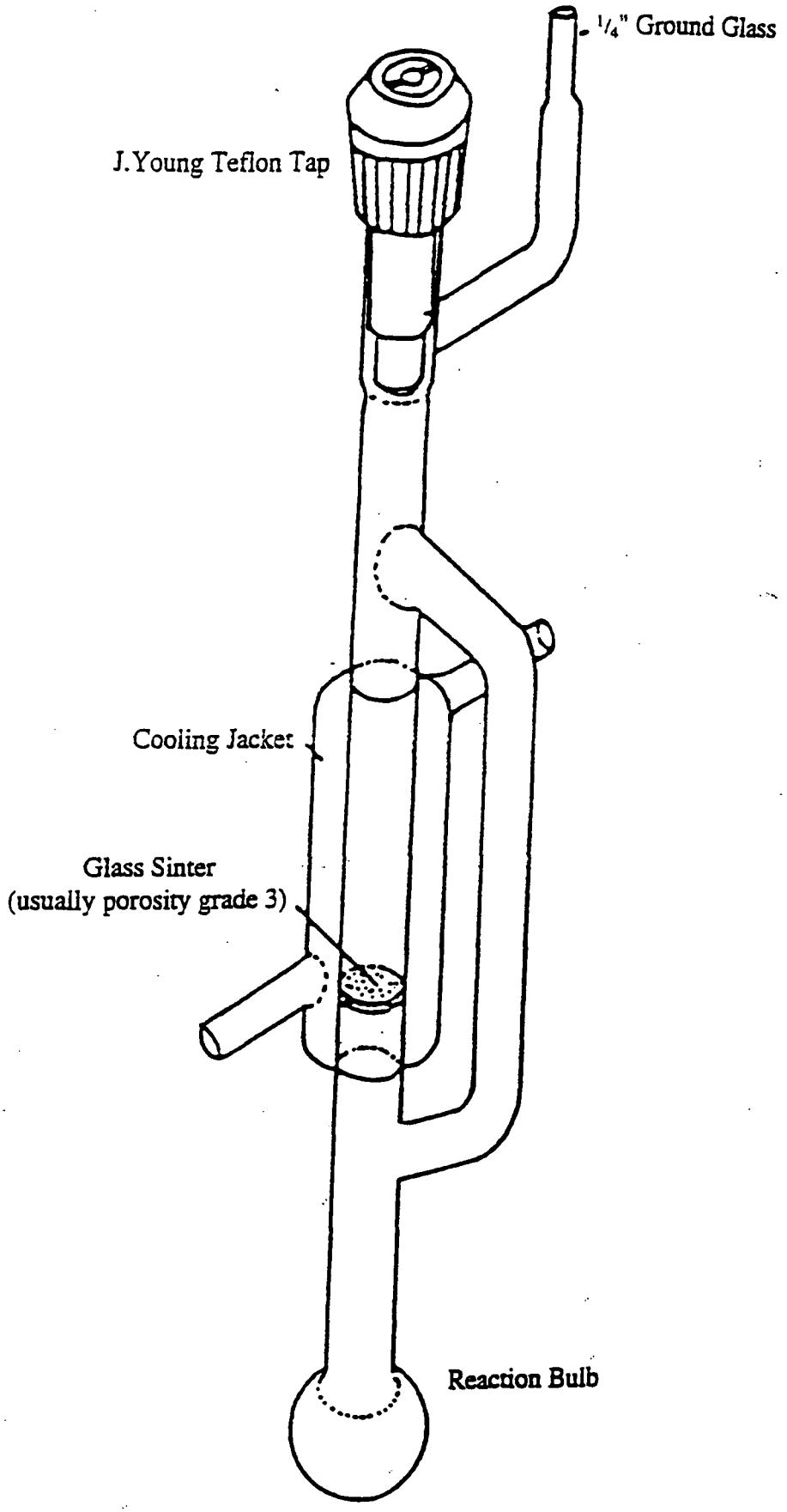

Figure 1.b. The Twin - Bulbed Reaction Vessel (The "Dog")

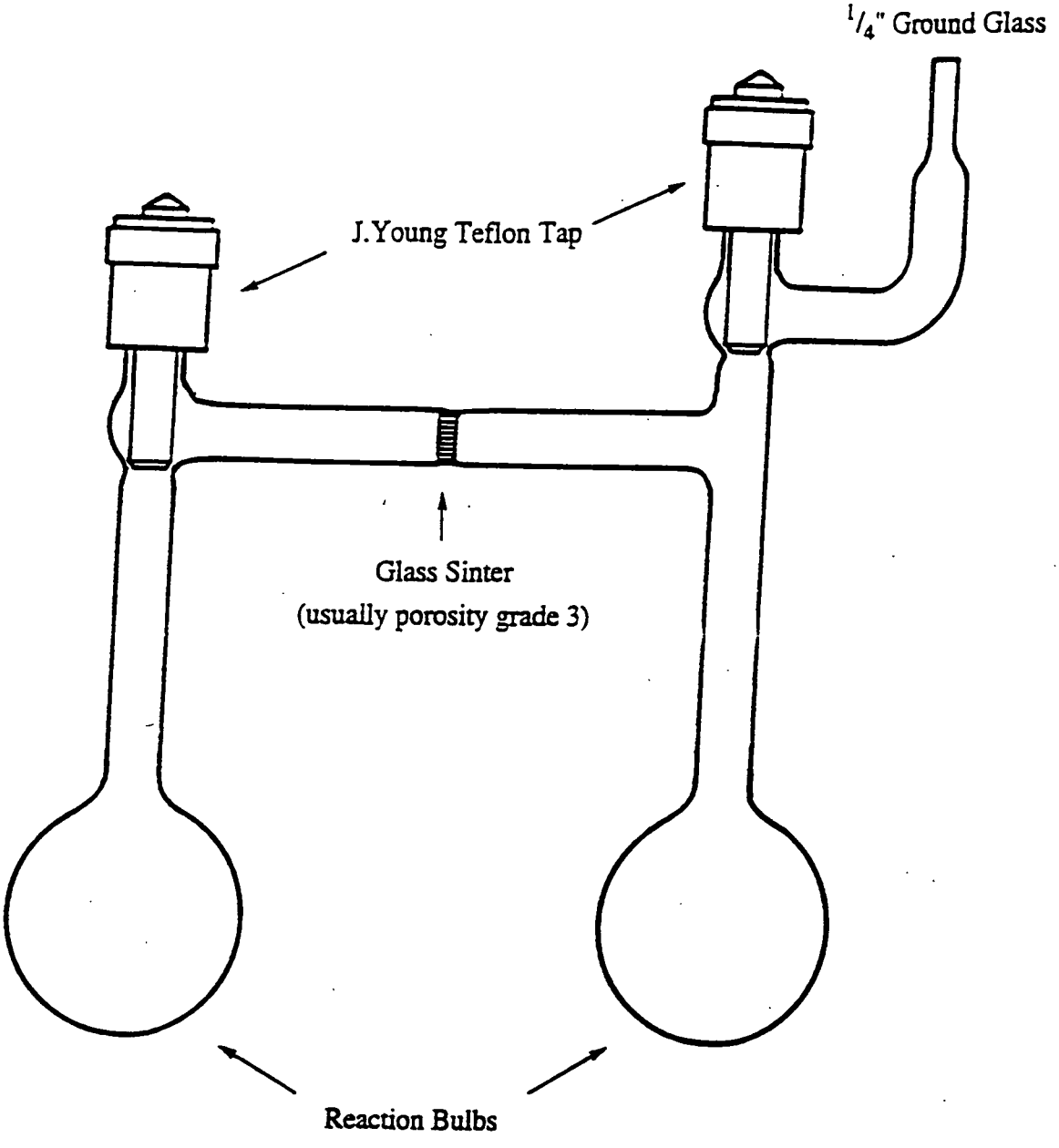

Figure 1.c. The Cyclic Voltammetry Cell (a) Illustrating the Modified Swage lock Glass to Metal Connector (b).

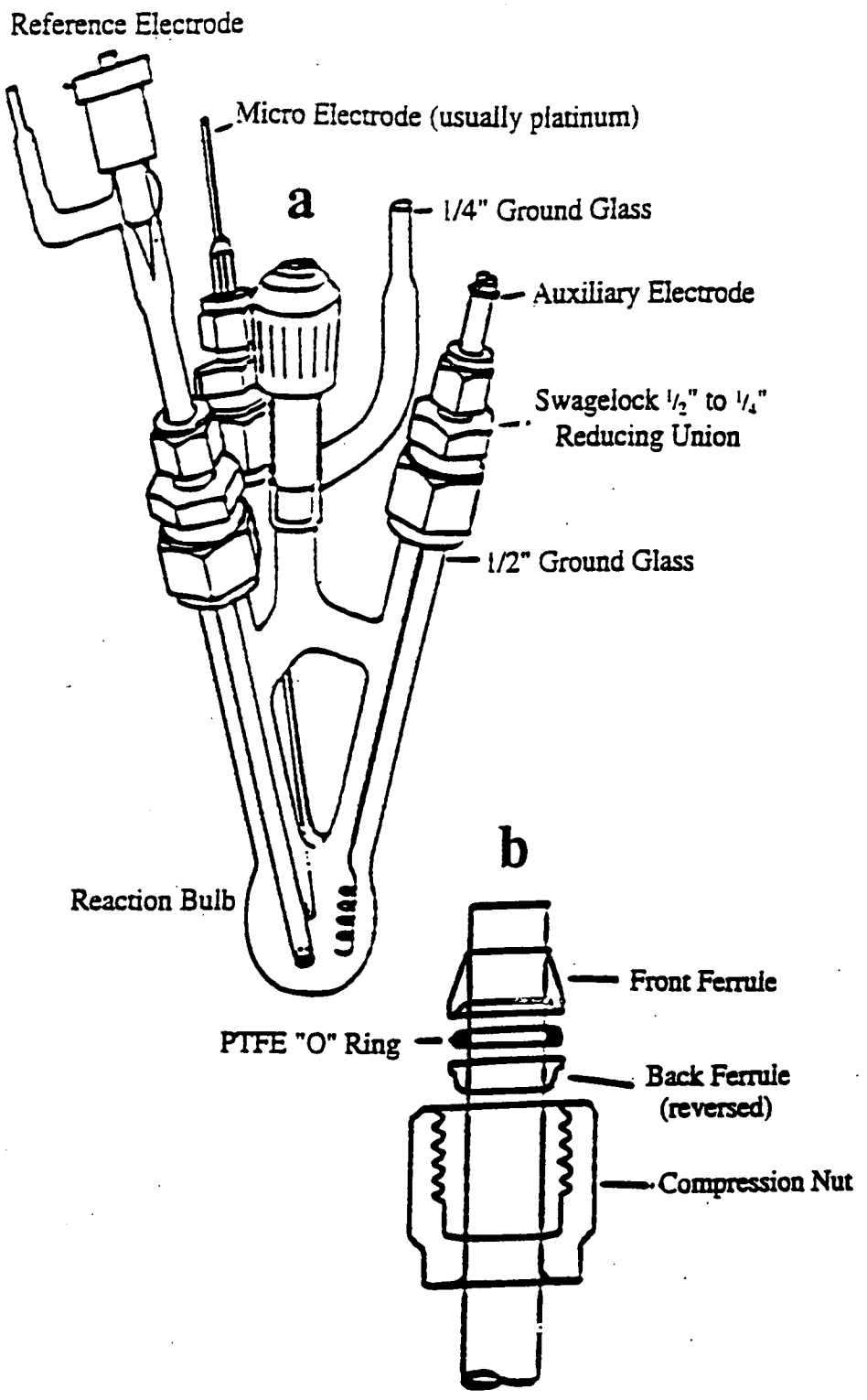

1.7. REFERENCES.

1. A.J. Banister, M.I. Hansford, and Z.V. Hauptman *J.Chem.Soc., Dalton Trans.*, 984, 1377.

2. A.J. Banister, M.I. Hansford, Z.V. Hauptman, A.W. Luke, S.T. Wait, W. Clegg and K.A. Jørgensen, *J.Chem.Soc., Dalton Trans.*, 1990, 2793.

3. A.J. Banister, M.I. Hansford and Z.V. Hauptman, *J.Chem.Soc., Dalton Trans.*, 1987, 915.

4. C.M. Aherne, *PhD.Thesis*, University of Durham, 1995.

5. J. Cosier and A.M. Glazer, *J.Appl.Crystallog.*, 1986, **19**, 105.

6. A.C.T.North, D.C. Phillips and F.S.Mathews, *Acta Cryst ., Sect. A,* 1968, **24** , 351.

7. N.Walker and D. Stuart, *Acta Cryst ., Sect. A,* 1983 **39** 158.

8. G.M. Sheldrick, *Acta Cryst ., Sect. A,* 1990, **46**, 467

9. G.M. Sheldrick, SHELXL93, University of Göttingen, Germany, 1993.

CHAPTER TWO

THE PROPERTIES OF DITHIADIAZOLYLS AND THE SYNTHESIS OF 1,2,3,5 PHENYL DITHIADIAZOLYL

2.1 INTRODUCTION

2.1.1. General Introduction.

Dithiadiazolyls are carbon, di-nitrogen, di-sulfur 7π heterocycles isoelectronic with the $[SNSSN]^{+\bullet}$, radical present in $[S_6N_4]Cl_2$. Theoretically, 4 isomers of these compounds may exist (figure 2.a.), although only the 1,2,3,5 and the 1,3,2,4 species have been isolated. The structure and chemistry of these compounds has been comprehensively reviewed[1].

Figure 2.a. Isomers of Dithiadiazolyl

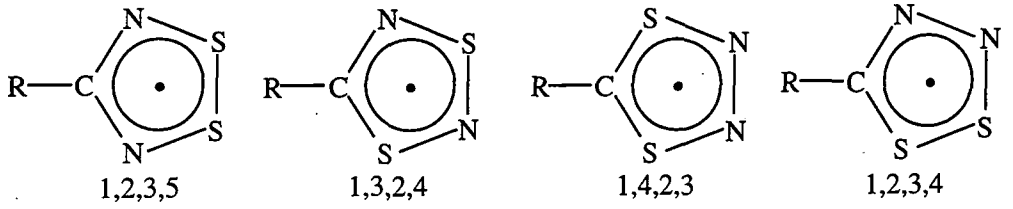

2.1.2. 1,3,2,4 Dithiadiazolyls.

1,3,2,4 radicals are prepared by the cycloaddition reaction between [SNS]X and an organic nitrile to form the 6π salts [RCNSNS]X, which can be reduced to the radical. The 1,3,2,4 radicals are inherently unstable and decompose to the thermodynamically more stable 1,2,3,5 radical. The 1,3,2,4 species, although interesting, are not directly relevant to this work and will only be mentioned briefly in later sections of this introduction. Their chemistry has been examined in great detail in another recent review article[2].

2.1.3. 1,2,3,5 Dithiadiazolyls.

Until the late 1980's much of the research of this group, and others, has concentrated on devising new and improved routes to forming the parent cation, $[RCNSSN]^+$, and its subsequent reduction to the radical. From that period on higher yielding routes (the most recent of which will be described later in this chapter) have resulted in a change of emphasis away from novel synthesis towards a better understanding of the physical and chemical properties of the species.

In the solid state the majority of [RCNSSN]• species exist as dimer pairs through weak intermolecular S-S interactions (figure 2.b.). This dimerisation process produces a remarkably stable 6π-2π-6π delocalised system and renders the compound diamagnetic i.e. $[RCNSSN]_2$. In solution these dimer pairs are almost completely dissociated producing 'free radical' [RCNSSN]• species. The strength of association in solution and solid state is dependent upon the nature of R, as described below.

Figure 2.b. Dimer pair of phenyl dithiadiazolyl.

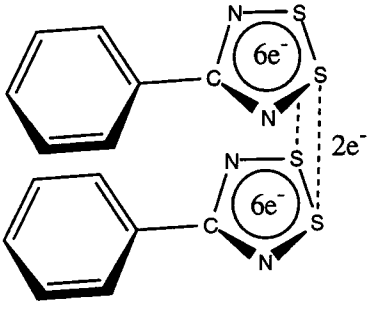

2.1.4. Potential Applications and Synthetic Aims.

There is much current interest in the use of stable free radical species as 'molecular building blocks' in the synthesis of novel materials with unusual magnetic and/or electrical properties. To induce conducting properties in dithiadiazolyls it was envisaged that the ring systems would have to stack (figure 2.c.).

Unfortunately, the dimerisation process highlighted above gives only diamagnetic insulators in the solid state although, encouragingly, the enthalpy of dimerisation (ΔH 2.52kcal/mol)[3] is very low (cf. I_2 3.65kcal/mol)[4]. One of the two S-S intermolecular bond can be broken by making the R group non-planar. (e.g. CF_3[5], Me[6]) where the interaction is now only through one sulfur atom of each ring. Unfortunately, these non-planar species will not be able to stack when fully eclipsed due to the steric hindrance of the R group and the compounds are still diamagnetic insulators in the solid state.

Figure 2.c.Idealised stacking in dithiadiazolyls.

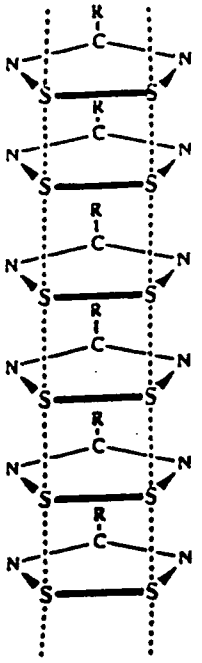

A whole range of planar dithiadiazolyls were prepared in this and other laboratories in the hope of preparing materials that can exist as segregated stacks; $[X_nC_6H_{5-n}CNSSN]^{\bullet}$, where X = halide, CN, $[CNSSN]^{\bullet}$, $[CNSNS]^{\bullet}$, $[CNSeSeN]^{\bullet}$, etc. Unfortunately this has met with only limited success, the vast majority of these compounds crystallising in dimeric pairs. The first notable success came from Oakley et al who achieved one-dimensional stacking from the difunctionalised dithiadiazolyl $[1,3(NSSNC(C_6H_4)CNSSN)]^{\bullet\bullet}$ and its selenium analogue[7]. Recently twisted stacks have also been seen in the solid state in the planar difluorinated dithiadiazolyl $[2,3,FC_6H_3CNSSN]^{\bullet}$[8] (figure 2.d.).

In another breakthrough trimer species were formed by co-sublimation of $(RCNSSN)_2$ and I_2 to produce mixed valence radicals which are semi-conductors at room temperature[9-11] (figure 2.e). Similar mixed valence species have been prepared in this research group by co-crystallisation of radicals with cations e.g. $[p\text{-}ClC_6H_4CNSSN]_3Cl$[12]. The physical solid state properties of the latter have not yet been investigated.

Figure 2.d. Packing diagram of [2,3,FC_6H_3CNSSN]$^{\bullet}$.

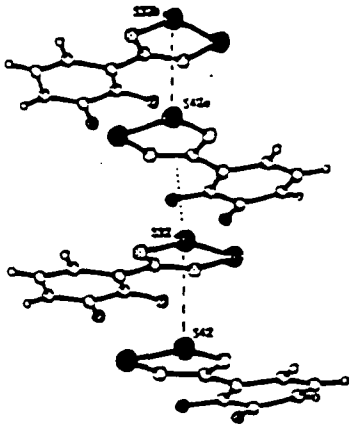

Figure 2.e. Iodine doped phenyl dithiadiazolyl.

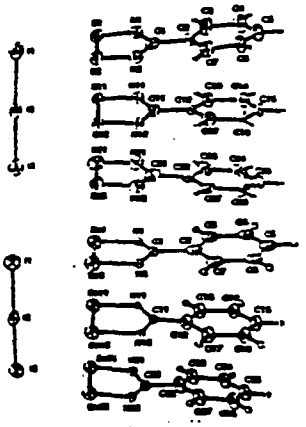

2.1.5 The Preparation and Properties of [p-NCC_6F_4CNSSN]$^{\bullet}$.

Until late 1993 no dithiadiazolyl radical had been prepared with truly novel magnetic properties. However, interest was aroused by the solid state packing of the dithiadiazolyl [*m*-NCC_6H_4CNSSN]$^{\bullet}$[13] which crystallises in two phases; the β-phase consisted of transoid dimer pairs as opposed to the cisoid pairs normally seen in $(RCNSSN)_2$, whereas the α-phase formed more conventional cisoid dimers. It was the molecular packing of the latter though that proved the more interesting with further secondary interactions occuring between the cyano group and the two sulfurs.

In this laboratory by replacing the hydrogens by fluorines, it has been possible to completely break the close intermolecular sulfur-sulfur interactions hence forming the first dithiadiazolyl radical which retains its paramagnetic nature in the solid state[14] (figure 2.f.).

Figure 2.f. Packing Diagram of the β-phase of [*p*-NCC_6F_4CNSSN]$^{\bullet}$

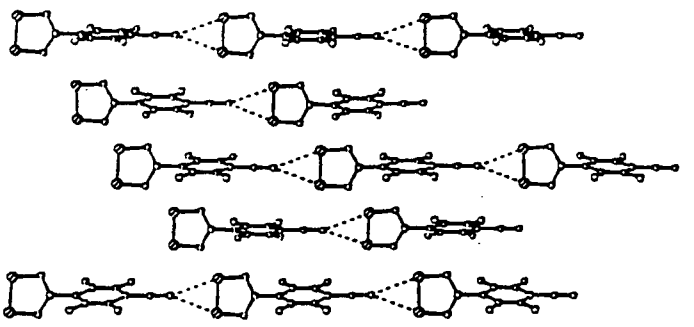

The [*p*-NCC_6F_4CNSSN]$^{\bullet}$ radical is also polymorphic with two phases. Structurally both phases are very similar consisting of chains of monomeric [*p*-NCC_6F_4CNSSN]$^{\bullet}$ radical units packed in a head to tail manner through weak CN...S interactions. In the α-phase these chains are aligned in an anti-parallel manner, whereas those in the β-phase are all aligned in the same direction. Magnetically the two phases are very different; the α-phase[14] is paramagnetic at room temperature with a magnetic moment of 1.6μB. Below 8K this phase exhibits long range anti-ferromagnetic order. The magnetic behaviour of the β-phase[15] is quite remarkable. Above 36K the material exhibits a one-dimensional antiferromagnetism. Below 36K an unprecedented transition to a weak ferromagnet occurs i.e. below 36K the material behaves like a weak classical magnet. The first organic ferromagnet was discovered in 1991 and no other compound (apart from a poorly characterised and understood fullerene charge transfer species with a transition temperature of 16K) has been observed with ferromagnetic behaviour above 3K[11].

2.1.6. Formation of Metal Complexes.

Previous investigations by I.B. Gorrell concerned the reaction of $(PhCNSSN)_2$ with a series of low-valent metal complexes, with the hope of inserting a transition metal into the ring system (probably through the S-S bond); these were mostly unsuccessful.

Reaction between $[PhCNSSN]^{\bullet}$ and a whole series of metal carbonyls resulted, on the whole, in the formation of black, insoluble, poorly characterised, powders[16]. However, reaction with $[Fe_2(CO)_9]$[17] and $[Ni(cp)CO]_2$[18] resulted in the formation of novel complexes. In both cases reaction occurred with the elimination of carbonyl to yield dimetallic complexes where the dithiadiazolyl ring bridges two metal centres via the two sulfurs of the ring system (figures 2.g and 2.h.). In the iron species one of the ring nitrogens has been protonated as will be described later.

Figure 2.g. Structure of $[Fe_2(\mu_{S\text{-}S}SNCPhN(H)S)(CO)_6]$.

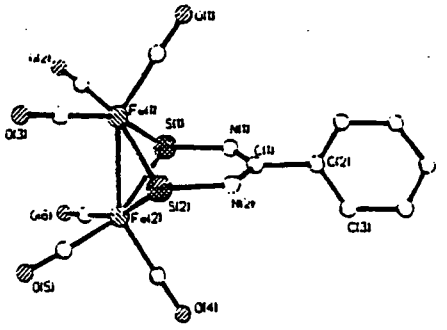

The position of the NH hydrogen is not shown

Figure 2.h. Structure of $[Ni_2(cp)_2(\mu_{S\text{-}S}SNCPhNS)]$.

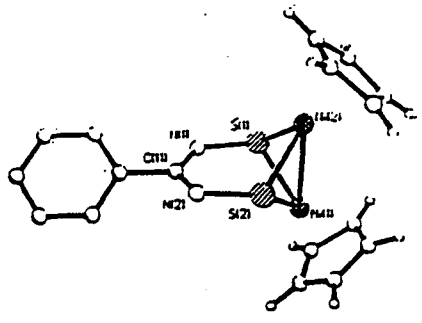

Each sulfur atom acts as a 1+2 electron donor and formally oxidises the metal by +1. As the S-S bond is now formally broken it is conventional to write the ring system as (SNCPhNS) i.e. $[Fe_2(\mu_{S\text{-}S}SNCPhN(H)S)(CO)_6]$ and $[Ni_2(\mu_{S\text{-}S}SNCPhNS)(cp)_2]$.

In both cases it was originally thought that the free radical remained delocalised throughout the ring system. A recent n.m.r. and m.o. study of the iron complex by Boeré has proved that one of the ring nitrogens on the iron species undergoes protonation rendering the ring diamagnetic[19][20]. It is perhaps an indication of the difficulty involved in the preparation and characterisation of dithiadiazolyl complexes that this has been the only other investigation into the work of Gorrell. This recent research by Boeré has only involved some modifications of known complexes; various analogues of the iron species were prepared where the dithiadiazolyl phenyl group had different substituents on the para position (see section 2.1.11) .

2.1.7. Electron Spin Resonance Spectroscopy.

E.s.r. spectroscopy is a vital tool in the study of dithiadiazolyls and is thus used extensively in our research. A good review of the technique, especially in relation to $[PhCNSSN]^{\bullet}$ and similar species, has recently been published[21].

Simple solution state measurements of $[RCNSSN]^{\bullet}$ exhibit well resolved isotropic spectra with hyperfine splitting to two equivalent ^{14}N nuclei, a_N =0.5mT to yield a 1:2:3:2:1 quintet[3,22] (see Fig 2.i.). Hyperfine coupling to the substituents on R is also sometimes observed[3,23,24].

Figure 2.i. E.S.R Spectrum of $[PhCNSSN]^{\bullet}$.

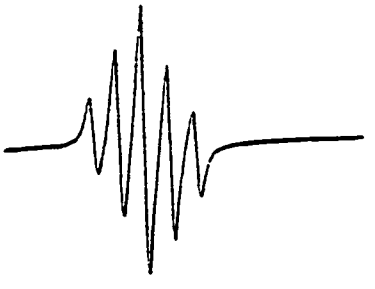

E.s.r measurements have been used to monitor the equilibrium between monomer (e.s.r. active) and dimer (e.s.r. inactive). Increased dimerisation at lower temperatures yielded

thermodynamic data on the monomer-dimer equilibrium[3,25]. They have also been used to investigate the rearrangement of 1,3,2,4 radicals (main hyperfine splitting 1:1:1 triplet, coupling to only one ring nitrogen) to 1,2,3,5 radicals[26] and to give an indication of the spin distribution of the singly occupied molecular orbitals (see section 2.1.8.).

Anisotropic spectra (frozen glass[3,27], powder[24,28] and single crystal spectra[29]) separate out the hyperfine coupling into their x,y and z axes (similar to solid state n.m.r.). This enables calculations of the percentage occupancy (spin density) of the radical on the ring atoms.

The only e.s.r. investigation of a dithiadiazolyl complex has been on $[Ni_2(\mu_S\text{-}_SSNCPhNS)(cp)_2]$, the only complex so far prepared. The spectrum consisted of a broad unresolved singlet (i.e. no hyperfine coupling is visible)[19,20].

2.1.8. Theoretical Studies

Molecular orbital calculations on dithiadiazolyls are often undertaken in conjunction with synthetic chemistry and e.s.r. spectroscopy. As stated in section 2.1.1., the 1,3,4,5 and 1,2,3,4 isomers have never been prepared. Theoretical studies (as well as chemical common sense) have shown that these two species would be the hardest to synthesise[1].

The M.O. diagram of $[PhCNSSN]^+$ (figure 2.k.) gives an indication of where the electron density is distributed in the frontier molecular orbitals.

The three highest occupied molecular orbitals in the cation form the delocalised 6π system. In the free radical the lowest unoccupied molecular orbital (the $2a_2\pi^*$) becomes the singly occupied molecular orbital which contains the unpaired electron. As correlated by e.s.r. measurements the radical electron can occupy orbitals on both nitrogens but not the carbon, which is on a node. The two sulfur atoms also make a significant contribution and ^{33}S (0.75%) hyperfine splitting can occasionally be seen in the e.s.r. spectra[3,27]. In contrast, the singly occupied molecular orbital of the 1,3,2,4 radical[1] shows a large molecular orbital contribution to the outermost ring nitrogen compared to a much smaller contribution from the nitrogen bound to carbon (hence large hyperfine e.s.r. coupling is only found on the former).

Figure 2.j. Frontier Molecular Orbitals of $[HCNSSN]^+$.

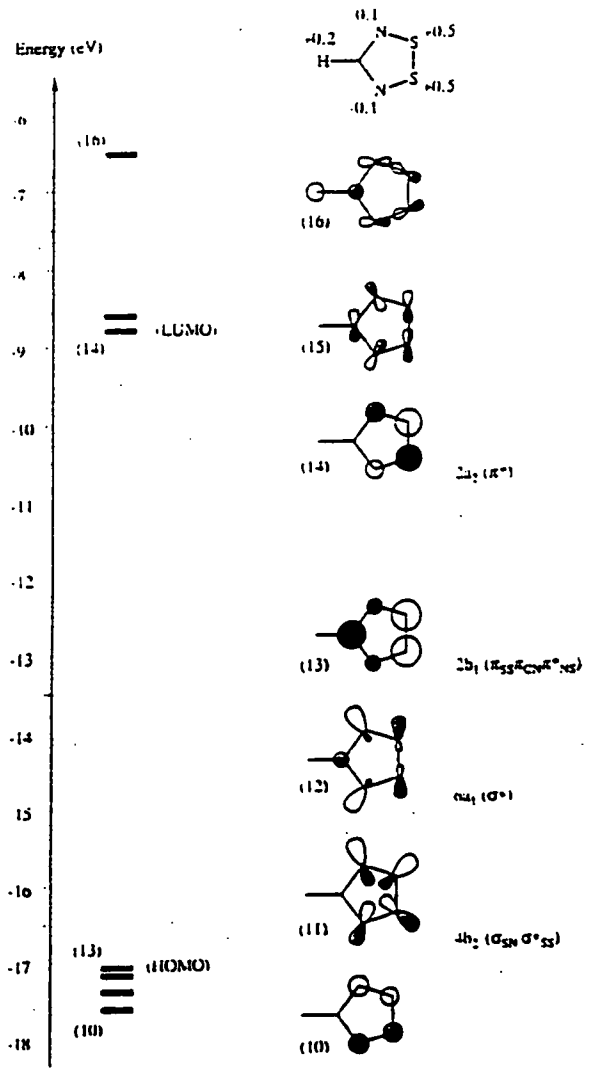

Theoretical calculations have been undertaken on both the nickel and iron transition metal complexes prepared from $[PhCNSSN]^{\bullet}$. In the nickel species[18] a satisfactory account of the bonding could be gained from the orbital diagrams (figure 2.k.) and helped to explain the splitting of the S-S bond of the ring system more thoroughly than simple bonding rules.

Figure 2.k. Molecular Orbital Diagram of $[Ni_2(\mu_{S,S}SNCPhNS)(cp)_2]$.

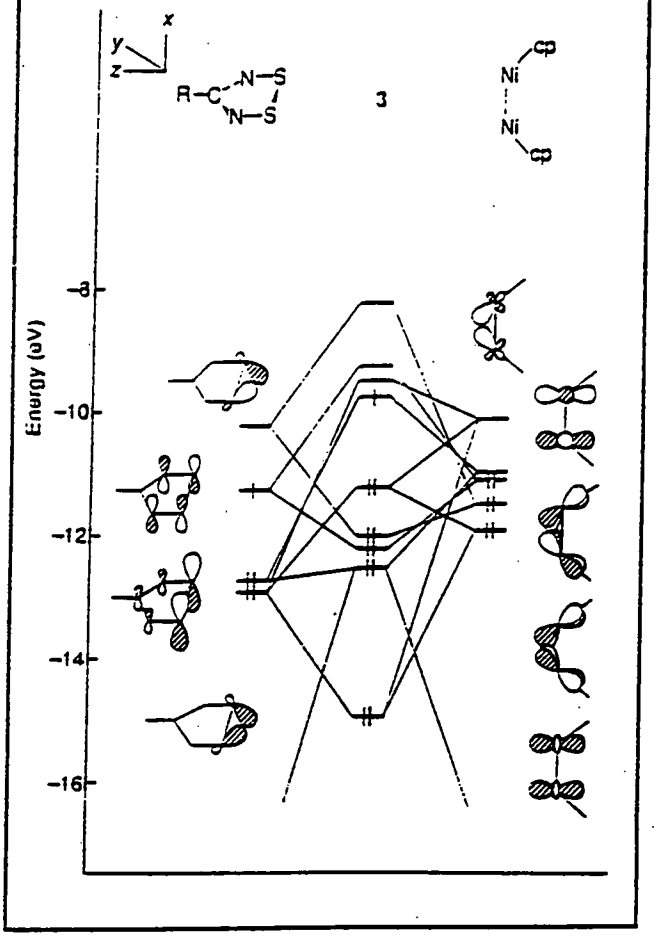

The m.o. of the iron complex[17] had proved to be misleading, the ring protonation, and susequent loss of the unpaired electron was not initially taken into account as stated previously in this chapter. Recent theoretical studies have, however, supported the experimental results which indicate that a ring nitrogen is protonated and the radical lost[20].

2.1.9. X-Ray Crystallography.

Crystallography is a vital tool for investigating the solid state properties of dithiadiazolyl radicals and their complexes, not only for structural determination but also for elucidating the intermolecular interactions and packing.

2.1.10. Magnetic Measurements.

As mentioned previously dithiadiazolyls have been studied extensively in the hope that they may yield interesting magnetic properties

In a very basic description, most materials can be classed into one of 4 main magnetic groups; diamagnetic, paramagnetic, ferromagnetic and ferrimagnetic depending apon the allignment of the spins of their electrons. All the above main magnetic types are shown below (figure 2.1. with the arrows indicating spin alignment).

Figure 2.1. Classes of Magnetism.

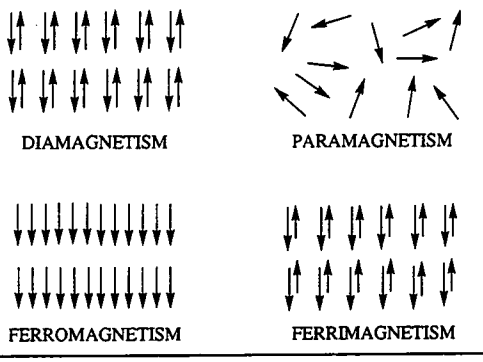

Diamagnetic compounds (most organic materials and many main group compounds and dithiadiazolyl dimer pairs) have their electron spins paired in opposite directions and thus have no net magnetic moment and in turn no magnetic properties. Anti-ferromagnetic compounds also have their spins aligned in opposite directions but in this case they are not paired. Paramagnetic compounds (mostly transition metal complexes) have their spins pointing in random directions and thus also have no overall magnetic moment.

Of more interest are ferromagnetic compounds which have their spins aligned (e.g. classical magnets) and ferrimagnetic materials which have spins pointing in opposite directions, but with unequal weighting thus yielding a slight net magnetic moment. The potential use of compounds with such properties has been discussed previously (section 2.1.4.) and in a recent review[30].

Magnetic measurements have been undertaken on poorly characterised dithiadiazolyl complexes of manganese[16] and ruthenium[31] carbonyls. They have, however, provided little firm information on the magnetic properties of such species.

2.1.11. Cyclic Voltammetry.

C.V. studies have been undertaken on a range of $[RCNSSN]^{\bullet}/[RCNSSN]^{+}$ and $[RCSNSN]^{\bullet}/[RCSNSN]^{+}$ species to determine their half wave potential, $E^{1}/_{2}$. These value have been used to measure, by the Hammett constant, the electronic effects of the R group[32-34]. The voltammogram shown below (figure 2.m.) also gives evidence for the formation of the dithiadiazolide anion.

Figure 2.m. Cyclic Voltammogram of $[PhCNSSN]^{+}$.

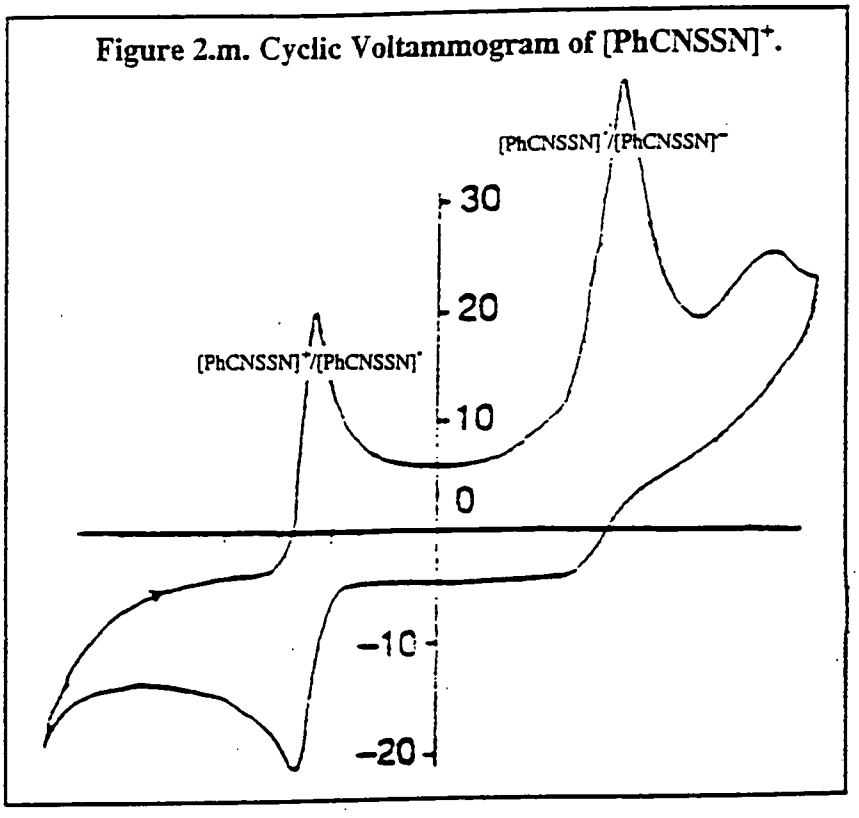

As with other techniques described previously, the $[RCNSNS]^{\bullet}$ to $[RCNSSN]^{\bullet}$ isomerisation[26] can be studied by this method. Also, a limited c.v. study has been undertaken on a range of iron dithiadiazolyl(imine) complexes $[Fe_2(\mu_S\text{-}_SSNCPhN(H)S)(CO)_6]$ (where R = H, CF_3, OCH_3) and $[Ni_2(\mu_S\text{-}_SSNCPhNS)(cp)_2]$[19,20]. The latter shows a reversible one electron oxidation.

2.1.12. Further Techniques.

Other techniques routinely used to study dithiadiazolyls include, I.R., d.s.c., elemental analysis and mass spectrometry. N.m.r.. spectroscopy is rarely used due to the presence of the free radical and subsequent paramagnetic broadening of the spectra[35].

2.2. RESULTS AND DISCUSSION

2.2.1. Synthesis of $(PhCNSSN)_2$.

If [PhCNSSN]$^{\bullet}$ were to be the chosen ligand for a series of reactions with different transition metal complexes then a high yield synthesis of this species would have to be developed. In general dithiadiazolyls have only been studied for their properties and yields have not been of paramount importance. This is obviously not the case here and many grammes of this material had to be prepared throughout this research.

The best synthetic route for preparing $(PhCNSSN)_2$ was reported by Oakley and co-workers[36][37]. The method used here is a modification of this route which gives higher yields. The key step in all synthetic routes to dithiadiazolyls is the ring formation step.

2.2.2. Original Synthetic Routes.

The salt $[RCNSSN]^+$ was first prepared by reaction between nitrile, $(NSCl)_3$ and elemental suphur[38]. Other low yielding synthetic routes have been reported and are well documented[1]. Reduction of dithiadiazolylium salts can be undertaken by many different reducing agents including zinc/copper couple (the prefered reagent), Ph_3Sb, potassium, mercury and zinc in oxygen donor solvents, t.h.f. (the prefered solvent), monoglyme or SO_2[1]. Purification is usually by sublimation to yield dark red/green dichroic crystalline material.

2.2.3. Preparation of $(PhCNSSN)_2$ - The Persilylated Amidine Route.

This preparation was reported by Oakley and co-workers. The reaction between $Li[N(SiMe_3)_2]$ and PhCN in Et_2O followed by the addition of Me_3SiCl results in the formation of $RC(=NSiMe_3)N(SiMe_3)_2$ which can be isolated as an oily solid (no yield is quoted for the benzonitrile reaction but the highest yield quoted for any other R group is 72%)[36]. This compound can then react with $2SCl_2$ in a condensation reaction to form the salt, [PhCNSSN]Cl, in 90% yield and $2Me_3SiCl$. Reduction of [PhCNSSN]Cl by Zn/Cu couple can yield pure $(PhCNSSN)_2$ after sublimation in about 50% yield. This synthetic route, although an improvement from previous reactions, still has two main disadvantages; the low overall yield (at best 30%) and the large amount of time and effort required (two intermediates have to be isolated).

2.2.4. Preparation of $[PhCNSSN]_2$ Without Isolation of Amidine .

At the start of this study this research group had managed to cut down this reaction to the isolation of just one intermediate, the dithiadiazolium salt[34]. This route is described in the experimental section (2.3.1. and 2.3.2.).

The reaction of PhCN and $Li[(N(SiMe_3)_2]$ in Et_2O yields a straw coloured solution of the salt $Li[PhC(=NSiMe_3)(NSiMe_3)]$. Instead of reacting with Me_3SiCl (as in the Oakley method) the salt is reacted with SCl_2 *'in situ'*. The solution is cooled down to 0°C and 2 equivalents of SCl_2 are added to yield [PhCNSSN]Cl, $2Me_3SiCl$ and LiCl in an exothermic reaction. Me_3SiCl and excess SCl_2 are removed by washing with Et_2O. The partial solubility of [PhCNSSN]Cl in SO_2 allows its slow extraction over several days and leaves behind the last impurity, LiCl. The dithiadiazolium salt is gained in a 70% yield.

The salt can be reacted with Zn/Cu couple in t.h.f. at room temperature. The dark red suspension formed contains $[PhCNSSN]^{\bullet}$, $(PhCNSSN)_2$, $ZnCl_2$, $CuCl_2$, CuCl and perhaps some other uncharacterised Zn and Cu containing sulfur complexes. The whole mixture is dried *in vacuo* and a cold finger is inserted into the reaction vessel. On heating to 110°C only $[PhCNSSN]_2$ is sublimed on to the finger in 47% yield. The entire reaction scheme is shown below (Reaction scheme 2.a.).

The overall yield for this simplified method is about 33% and is a slight improvement on the method highlighted previously. The one slow step is the extraction with SO_2.

Reaction Scheme 2.a. Synthesis of $(PhCNSSN)_2$

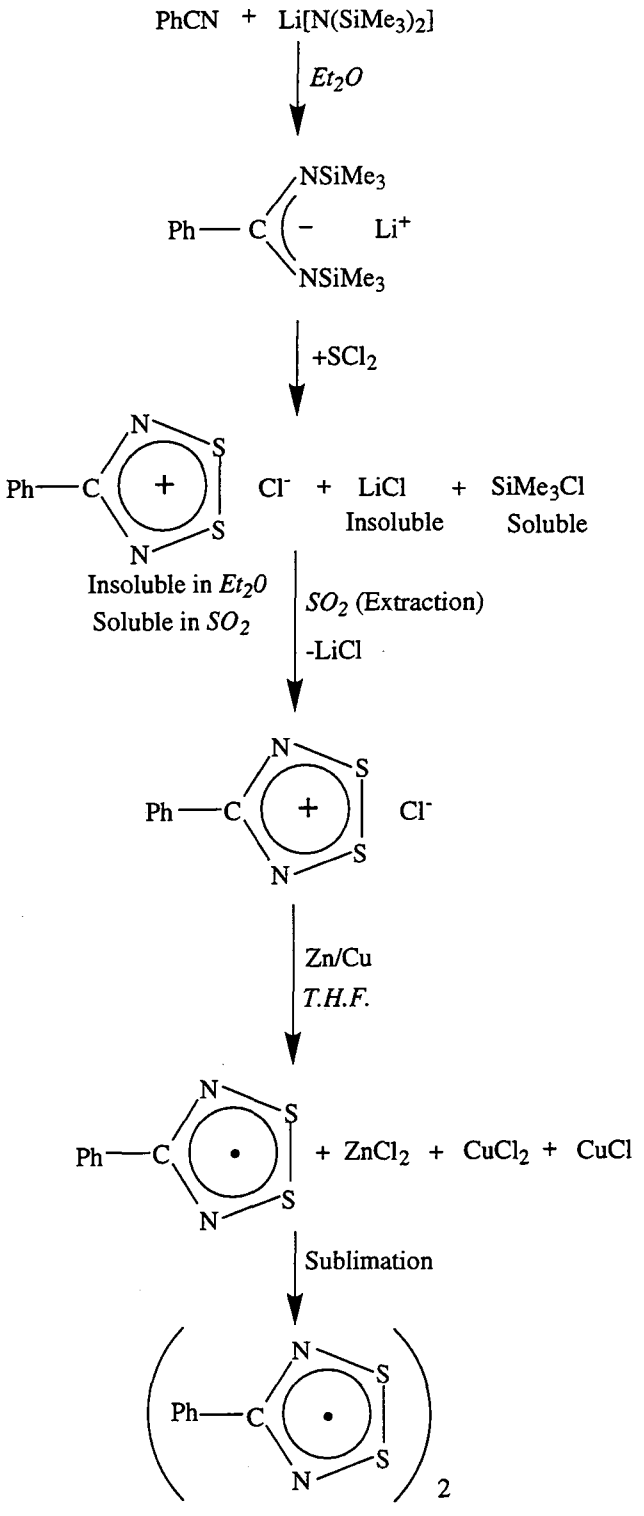

2.2.5. The Preparation of $(PhCNSSN)_2$ Avoiding SO_2 Extraction.

During this research I have developed another method for the preparation of phenyl dithiadiazolyl which eliminates the SO_2 extraction stage (section 2.3.3.).

Instead of removing LiCl from the [PhCNSSN]Cl/LiCl solid mixture obtained after the condensation step and washing with Et_2O, the solids were reduced without SO_2 purification. As lithium chloride does not effect the Zn/Cu couple reduction or the subsequent sublimation of phenyl dithiadiazolyl it does not need to be removed. Thus the whole reaction can be undertaken in one vessel and gives a yield of 47% $(PhCNSSN)_2$ in high purity (as shown by elemental analysis).

Thus in this final synthetic route a significant increase in yield and saving in time can be gained. The whole reaction can be undertaken in two days.

2.3. Experimental.

2.3.1. The Preparation of [PhCNSSN]Cl.

$Li[(N(SiMe_3)_2]$ (4.9g, 29.6mmol) was dissolved in Et_2O (100ml). PhCN (3.9ml, 38.2mmol) was added and the straw coloured solution was left stirring overnight. The solution was cooled to 0°C and SCl_2 (5ml, 65.8mmol) added dropwise, with stirring. A bright yellow solid precipitates immediately under an orange solution. This suspension was stirred for 3hr, filtered, washed with Et_2O (3x30ml) and dried *in vacuo* . The yellow solids were then extracted in a closed soxhlet extractor with SO_2 (30ml) until all the yellow [PhCNSSN]Cl had extracted leaving behind the insoluble LiCl (at least 48hr). The SO_2 was then removed and the yellow crystalline material dried *in vacuo*..

Yield 4.48g, 70%.

IR $\nu_{max}(cm^{-1})$ 1590w, 1580w, 1320w, 1295w, 1210w, 1170w, 1150w, 1135w, 1100w, 1065m, 1025m, 1000w, 940w, 920sh, 890sbr, 840s, 780s, 720w, 690sbr, 670sh, 650sh, 550ssh, 475m, 395sh, 325ssh, 310shd, 280m, 255w.

Elemental analysis, found: C, 35.41%; H,2.32%; N,12.41%, calc.: C,38.80%; H,2.32%; N12.93%)

D.s.c.. 192°C (decomposition).

Mass spec (assignable peaks) $^{m}/_{e}$, EI^+: 181 $[PhCNSSN]^+$, 78 $[SSN]^+$, CI^+: 103 $[PhCN]^+$, CI^-: 181 $[PhCNSSN]^+$, 78 $[SSN]^+$

2.3.2. The Reduction of [PhCNSSN]Cl to $[PhCNSSN]_2$.

[PhCNSSN]Cl (4.0g, 18.6mmol) and Zn/Cu couple (1.3g, 0.20mmol) were stirred in thf (30ml) overnight. The resultant dark red suspension was dried *in vacuo*. The solids were heated to 110°C and the red/green dichroic crystals of $(PhCNSSN)_2$ sublimed. The crystals were removed from the cold finger and the residues resublimed. This process was repeated until no new product could be sublimed.

Yield 1.6g, 47%.

IR $\nu_{max}(cm^{-1})$ 1265w, 1240, 1225, 1190w, 1180w, 1160w, 1145shd, 1140, 1120shd, 1095w, 1075, 1030sh, 1020, 1000w, 980wbr, 920sh, 900sh, 840shd, 830ssh, 825shd, 805ssh, 775ssh, 765ssh, 720, 690sh, 685ssh, 665shd, 655shd, 650ssh, 620shd, 510ssh, 490sh, 445w, 435w, 405w, 265wbr.

Elemental analysis, found: C, 45.75%; H,2.64%; N,15.24%, calc.: C,46.38%; H,2.78%; N15.45%)

D.s.c.. 121°C(endotherm) .

Mass spec (assignable peaks) $^{m}/_{e}$, EI^{+}: 181 $[PhCNSSN]^{+}$, 78 $[SSN]^{+}$, CI^{+}: 103 $[PhCN]^{+}$, CI^{-}: 181 $[PhCNSSN]^{+}$, 78 $[SSN]^{+}$

2.3.3. The 'Single Pot' Preparation of $[PhCNSSN]_2$.

$Li[(N(SMe_3)_2]$ (7.08g, 42.3mmol) was dissolved in Et_2O (100ml). PhCN (4.4ml, 43mmol) was added and the straw coloured solution left stirring overnight. The solution was then cooled to 0°C and SCl_2 (5.8ml, 76.3mmol) added dropwise over a period of 10min. The resultant yellow precipitate was stirred for 3h, filtered, washed (3x50ml Et_2O) and dried *in vacuo*. The bright yellow solids ([PhCNSSN]Cl and LiCl) and Zn/Cu couple were stirred in t.h.f. (50ml) overnight. The deep red suspension was pumped to dryness *in vacuo*. The solids were then heated to 110°C and sublimed to yield red/green dichroic crystals of $(PhCNSSN)_2$ on the cold finger. The crystals were removed from the cold finger and the process repeated until no new product could be sublimed.

Yield 3.45g, 49.9%.

IR $\nu_{max}(cm^{-1})$ 1265w, 1240, 1225, 1190w, 1180w, 1160w, 1145shd, 1140, 1120shd, 1095w, 1075, 1030sh, 1020, 1000w, 980wbr, 920sh, 900sh, 840shd, 830ssh, 825shd, 805ssh, 775ssh, 765ssh, 720, 690sh, 685ssh, 665shd, 655shd, 650ssh, 620shd, 510ssh, 490sh, 445w, 435w, 405w, 265wbr.,

Elemental analysis, found: C,46.04%; H,2.64%; N,15.24%, calc.:C,46.38%; H,2.78%; N15.45%).

D.s.c. 121°C(endotherm)

Mass spec (assignable peaks) $^{m}/_{e}$, EI^{+}: 181 $[PhCNSSN]^{+}$, 78 $[SSN]^{+}$, CI^{+}: 121 $[PhCN]^{+}$, CI^{+}: 181 $[PhCNSSN]^{+}$, 78 $[SSN]^{+}$

2.4. CONCLUSION.

It is hoped that this chapter will have provided a flavour of the rich and diverse chemistry of dithiadiazolyls and, in particular, 1,2,3,5-dithiadiazolyls. It was also an aim of this introductory chapter to highlight the potential magnetic and electronic properties of these unusual species and thus provide a valid reason for further study.

As indicated in this chapter, the one area of this chemistry that has been underdeveloped is the use of these heterocycles as ligands to transition metal species. It is this field that provides the basis for this thesis. As such it was important that a high yield, low effort, preparation of the ligand of choice, [PhCNSSN]$^{\bullet}$, could be, and has been, developed.

2.5. REFERENCES

1. J.M.Rawson, A.J.Banister and I.Lavender, *Adv. Hetero. Chem.*, 1995, **62**, 137.

2. S.Parsons and J.Passmore, *Acc. Chem. Res.*, 1994, **27**, 101.

3. S.A.Fairhurst, K.M.Johnson, L.H.Sutcliffe, K.F.Preston, A.J.Banister, Z.V.Hauptman and J.Passmore, *J. Chem. Soc.,Dalton Trans.*, 1986,1465.

4. *Handbook of Chemistry and Physics*, C.R.C. Press, Ed. R.C.Weast and D.R.Lide, 1989-90, **70**, B223.

5. H.U.Höffs,.J.W.Bats, R.Gleiter, G.Hartman, R.Mews, M.Eckert-Macksic, H.Oberhammer and G.M.Sheldrick, *Chem. Ber.*, 1985, **118**, 3781.

6. A.J.Banister, M.I.Hansford, Z.V.Hauptman, S.T.Wait and W.Clegg, *J. Chem. Soc., Dalton Trans.*, 1989, 1705.

7. M.P.Andrews, A.W.Cordes, D.C.Douglas, R.M.Fleming, S.H.Glarum, R.C.Haddon, P.M.Marsh, R.T.Oakley, T.T.M.Palstra, L.F.Schneemeyer, G.W.Touchs, R.Tycho, J.V.Waszcak, K.M.Young and N.M.Zimmerman, *J. Am. Chem. Soc.*, 1991, **113**, 3559.

8. O.G.Dawe, MSc. Thesis, University of Durham, 1995.

9. C.D.Bryan, A.W.Cordes, R.C.Haddon, R.G.Hicks, R.T.Oakley, T.T.M.Palstra, A.S.Perel and S.R.Scott, *Chem. Materials,* 1994, **6**, 508.

10. C.D.Bryan, A.W.Cordes, R.C.Haddon, R.G.Hicks, D.K.Kennepohl, C.D.MacKinnon, R.T.Oakley, T.T.M.Palstra, A.S.Perel, S.R.Scott, L.F.Schneemeyer, *J.Am.Chem.Soc.*,1994,**116**,1205.

11. C.D.Bryan, A.W.Cordes, R.M.Fleming, N.A.George, S.H.Glarum, R.C.Haddon, R.T.Oakley, T.T.M.Palstra, A.S.Perel, L.F.Schneemeyer and J.V.Waszak, *Nature*, 1993, **365**, 821.

12. S.E.Lawrence, PhD Thesis, University of Durham, 1994.

13. A.W.Cordes, R.C.Haddon, R.G.Hicks, R.T.Oakley and T.T.M.Palstra, *Inorg. Chem.*, 1992,**31**,1802.

14. A.J.Banister, N.Bricklebank, W.Clegg, M.F.G.Elsegood, C.I.Gregory, I.Lavender, J.M.Rawson and B.K.Tanner, *J.Chem.Soc., Chem. Commun.*, 1995, 679.

15. A.J.Banister, N.Bricklebank, W.Clegg, M.F.G.Elsegood, C.I.Gregory, I.Lavender, J.M.Rawson, B.K.Tanner, *J.Magn.Magn.Materials*, in preparation.

16. I.B.Gorrell, PhD. Thesis, University of Durham, 1989.

17. A.J.Banister, I.B.Gorrell, W.Clegg and K.A.Jørgensen, *J.Chem.Soc., Dalton Trans.*, 1989, 229.

18. A.J.Banister, I.B.Gorrell, W.Clegg and K.A.Jørgenson, *J.Chem.Soc., Dalton Trans.*, 1991, 1105.

19. V.Klassen, K.Preuss, K.H.Moock and R.T.Boeré, *Phos.Sulf. Silicon and Rltd Elem.*, 1994, **93-94**, 449.

20. R.T.Boeré, V.Klassen, D.Lentz, H.Michael, K.H.Moock and J.Weaver, *Inorg. Chem,* submitted for publication.

21. S.A.Fairhurst, K.F.Preston and L.H.Sutcliffe, *Phos.Sulf. Silicon and Rltd Elem.*, 1994, **93-94**, 105.

22. L.N.Markovski, O.M.Polumbrik, V.S.Talanov and Y.G.Shermolovich, *Tet. Letts.*, 1982, **23**, 761.

23. S.A.Fairhurst, J.M.Rawson, J.Passmore and M.J.Shriver, *Magn. Reson., Chem.*, 1992, **30**, 666.

24. Y.L.Chung, S.A.Fairhurst, D.G.Gillies, K.F.Preston and L.H.Sutcliffe, *Magn. Reson. Chem.* 1992, **30**, 666.

25. W.V.F.Brooks, N.Burford, J.Passmore, M.J.Schriver and L.H.Sutcliffe, *J.Chem.Soc., Chem. Commun.*, 1987,69.

26. C.Aherne, A.J.Banister, A.W.Luke, J.M.Rawson and R.J.Whitehead, J. Chem. Soc., Dalton Trans., 1992, 1277.

27. S.A.Fairhurst, L.H.Sutcliffe, K.F.Preston, A.J.Banister, A.S.Partington, J.M.Rawson and J.Passmore, *Magn. Reson. Chem.*, 1993, **31**, 1027.

28. A.J.Banister, N.R.M.Smith and R.G.Hey, *J.Chem.Soc., Perkin Trans.*, 1983, **1**, 1181.

29. F.L.Lee, K.F.Preston, A.J.Williams, L.H.Sutcliffe, A.J.Banister and S.T.Wait, *Magn.Reson.Chem.*, 1989, **27**, 1161.

30. J.S.Miller, A.J.Epstein, *Angew.Chem.Int.Ed.Engl.*, 1994,**33**,385.

31. A.W.Luke, Phd Thesis, University of Durham, 1995.

32. C.M.Aherne, A.J.Banister, I.B.Gorrell, M.I.Hansford, Z.V.Hauptman, A.W.Luke and J.M.Rawson, *J.Chem.Soc., Dalton Trans.*, 1993, 967.

33. C.M.Aherne, PhD Thesis, University of Durham, 1995.

34. R.T.Boeré, K.H.Moock, and M.Parvez, *Z.Anorg.Allg.Chem.*, 1994, **620**, 1589.

35. E.A.Ebsworth, D.W.H.Rankin, S.Cradock, *Structural Methods in Inorganic Chemistry*, Blackwell Scientific Publications, 1987.

36. R.T.Boére, R.T.Oakley and R.W.Reed, *J.Organomet. Chem.*, 1987, **331**, 161.

37. A.W.Cordes, R.C.Haddon, R.T.Oakley, L.F.Schneemeyer, J.V.Waszcak, K.M.Young & N.M.Zimmerman, *J.Am.Chem.Soc.*, 1991, **113**, 582.

38. G.G.Alange, A.J.Banister, B.Bell and P.W.Millen, *Inorg. Nucl. Chem. Lett.*, 1977, **13**, 143.

CHAPTER THREE

THE PROPERTIIES OF PLATINUM AND PALLADIUM CO-ORDINATION COMPOUNDS AND THE SYNTHESIS OF THEIR ZERO VALENT PHOSPHINE COMPLEXES

3.1. INTRODUCTION

3.1.1. General Introduction

Six elements form the platinum group metals, Ru, Os, Rh, Ir, Pd, and Pt. Two of these elements, platinum and palladium, have been studied throughout the course of this thesis. To the non-chemist platinum metal is most commonly associated with jewellery and hard currency. Platinum has, however, many industrial uses e.g. as electrodes, thermocouples, crucibles and as a component of glasses. Its compounds are used in medicinal drugs and as heterogeneous and homogeneous catalysts in the preparation of small organic molecules and polymers.

Palladium metal is used in the electronics industry, dentistry and its compounds are even more extensively used than platinum in heterogeneous and homogeneous catalytic processes.

The above applications[1] result in millions of pounds p.a. being spent on investigations into the chemical properties of these two elements.

3.1.2. Complexes of Platinum and Palladium

Platinum and palladium form a large number of complexes in a wide range of oxidation states (0 to IV for Pd and 0 to VI for Pt), co-ordination numbers (2 to 6) and geometries (e.g. planar, square planar, tetrahedral and octahedral)[2a]. Due to the presence of f orbitals and the subsequent lanthanide contraction[2b] between the 2nd and 3rd row transition elements the two metals have almost the same atomic radii. Consequently, there are many similarities between the chemical properties and reactivities of these two elements.

In direct contrast, the properties of nickel (the first row member of the triad) are in many ways markedly different. Nickel is a 'hard' metal and hence prefers to bond in its complexes with hard bases such as NH_3, CN^-, F^-, CO, OR^- etc. whereas Pt and Pd prefer to bond with soft bases such as PR_3, AsR_3, I^-, SR^- etc.[3]. As such it perhaps comes as no suprise that the chemistry achieved with S and Se ligands and Pt and Pd in this thesis could not be readily repeated with Ni, as mentioned in chapter four.

The Comprehensive Co-ordination Chemistry[4] and Comprehensive Organometallic Chemistry[5] series provide a good general overview of the chemistry of these two metals.

3.1.3. Zero-valent Chemistry.

The zero-valent chemistry of Pt and Pd is dominated by phosphine complexes. The metal can be bound to 2,3 or 4 phosphines, forming linear (14 electron), planar (16 electron) and tetrahedral (18 electron) complexes respectively. The tendency for 4 co-ordinate species $[M(PR_3)_4]$ to dissociate to give three or two co-ordinate species, which may be stable in the solid state and in solution, depends upon the electronic and steric effects of the phosphine ligand[6] For example, $[Pt(PMe_3)_4]$ (least bulky phosphine) forms only the 4 co-ordinate species. $[Pt(PEt_3)_4]$ (more bulky) dissociates to $[Pt(PEt_3)_3]$ on heating[7]. With the larger triphenylphosphine groups, $[Pt(PPh_3)_4]$ exists as $[Pt(PPh_3)_3].PPh_3$[8][9] in the solid state whereas in solution $[Pt(PPh_3)_2]$ is also observable by ^{31}P and ^{1}H n.m.r. spectroscopy[6]. Very bulky phosphines can produce complexes with only two phosphines in the solid state e.g. $[Pt\{P(t\text{-}Bu)_3\}_2]$[10] and $[Pd\{PPh(t\text{-}Bu)_2\}_2]$[11]. Four co-ordinate species can also be stabilised by the use of chelating phosphines such as 1,2-bis(diphenylphosphino)ethane) (dppe) i.e. $[M(dppe)_2]$ (see section 3.2.4 and 3.2.5).

Other zero-valent complexes can be prepared with ligands such as arsines (e.g. $[Pd(AsPh_3)_4)]$[12]), olefins (e.g. $M(cod)_2$[13]) and carbonyls (e.g. $Pd_4(CO)_5(PR_3)_4$ and $Pt_3(CO)_3(PR_3)_3$) [2b].

3.1.4. Chemistry and Applications of Zero-Valent Complexes.

Zero-valent complexes can react by simple ligand (L) displacement (e.g. $[Pd_2dba_3.CHCl_3]$ to $[Pd(PPh_3)_4]$[14]) maintaining the low oxidation state. However, the most important reaction is the oxidative addition of 2X (where X = Cl^-, I^-, SR^- etc.) to form, usually, square-planar M(II) complexes[2c] (equation 3a). The most widely studied example of this process is the vast oxidative addition chemistry of $[Pt(PPh_3)_3]$[2d]. When the oxidative addition involves organics and is reversible, a whole series of catalytic processes can occur e.g.$[Pd(PPh_3)_4]$ can be used as a catalyst for the oxidation of 1-3 dienes[15]. It is this potential oxidation of zero-valent Pt and Pd phosphine complexes that is employed extensively later in this thesis.

Equation 3a.

$$M^0L_A + 2X \longrightarrow M^{II}L_BX_2$$

3.1.5. Square-planar Chemistry of Platinum and Palladium.

By far the most common complexes of Pt and Pd are square-planar four co-ordinate M(II) species with zero to 4 donor ligands (L= PR_3, NR_3, SR_2, olefin etc.) and with four down to zero one electron oxidising ligands (X=. F^-, Cl^-, SR^-, OR^-, CR_3^- etc.) i.e. ML_nX_{4-n}. The formal oxidation of the metal, (II), is maintained with the appropriate counterion(s) if necessary e.g. K_2PtCl_4. It must be noted that for these and other transition metal complexes there are different, equally valid, methods of electron counting[2e]. Many properties of these complexes have been studied, including cis-trans isomerism in ligand exchange and the 'trans effect' using the Pt species $[Pt(Cl)_2(NH_3)_2]$[16] and their biological properties (see 3.1.6.)

There are many commercial applications of these square planar compounds such as the oxidation of ethylene by $[PdCl_4]^{2-}$ in the Wacker process[17][18]. Two applications in particular relate to the work described here: biological activity and low dimensional conductiviy.

3.1.6. Cis-platin and Other Square-Planar Anti-Cancer Drugs.

Until 1969 simple square-planar complexes of platinum were mainly studied for the trends in their substitution reactions highlighted above. At this time the anti-tumour activity of cis-$[PtCl_2(NH_3)_2]$[19] was discovered. The discovery of this complex, which is also known as cis-platin, has resulted in great interest in the chemistry of square-planar platinum.

Although cis-platin was an effective treatment for many cancers including testicular and lung cancer, it produced numerous side effects including nausea and vomiting[20]. More potent and less toxic platinum (II) analogous have since been discovered e.g. carboplatin[21] and spiroplatin[22]. Recently, more water soluble carboplatin analogue complexes have also been studied[23a] (see figure 3.a. for examples of anti-cancer complexes).

The most common site of attack by these complexes has been cancer cells' helical D.N.A. Removal of the X^- ligands from the complex allows the platinum to bind with the guanidine base pairs thus kinking the double stranded D.N.A. strand, preventing replication and in turn cell division. Other sites of attack have been highlighted and the mechanism of these processes has been studied in great detail[23b]. In general though it can be said that the Pt species complex to the D.N.A. and inhibits cell replication thus killing the cancerous cells.

Although cis platinum (II) complexes have been studied widely, there has been limited success with octahedral complexes of Pt(IV) e.g. oxoplatin[24]. Some of the other trends of activity have also been broken e.g. trans complexes such as trans-2-pyridine dichloride platinum(II) have shown activity against tumour lines[25].

Other limitations remain, however. The greater reactivity of analogous square planar Pd(II) complexes means that these species frequently decompose before reaching the active sites. Therefore palladium complexes show much lower activity than those of platinum[26].

Thus, despite some notable exceptions highlighted above, in the preparation of new complexes which may be cancer active, the greatest likelihood of anti-tumour activity would still be in the preparation of square planar Pt(II), in a cis geometry, with X^- groups that are removable in an aqueous medium.

Figure 3a. Some Platinum Anti-Cancer Complexes

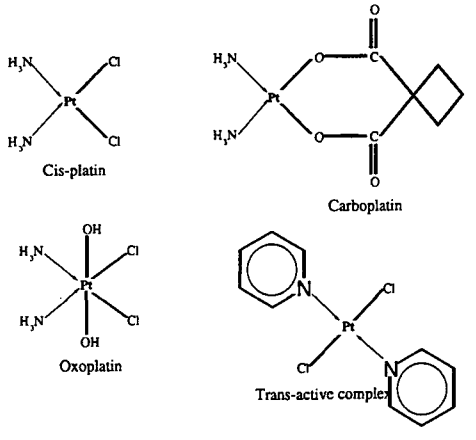

3.1.7. Linear Chain Compounds.

In 1969 a new area of one-dimensional metals was highlighted through a structural study by Krogmann et al[27] of a series of partially oxidised Pt and Ir salts e.g. $M_2[Pt(CN)_4]X_n.pH_2O$. In these salts and similar 15/16e$^-$ complexes, the partially empty $5d_z2$ orbitals can overlap to form a one dimensional stack (figure3b).

A whole series of partially oxidised cyano and bis(oxalato) (e.g. $[Pt(C_2O_4)_2]^{2-}$) salts were prepared with Pt-Pt separation down to 2.717Å in $Rb_{1.67}[Pt(C_2O_4)_2].1.5H_2O$[4] (in platinum metal the Pt-Pt bond distance is 2.775Å). These complexes had varying degrees of conductivity and were, on the whole, one-dimensional conductive materials.

Figure 3b. Idealised stacking in square-planar complexes

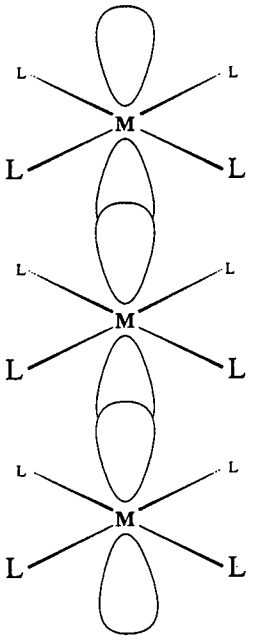

A range of other stacked square planar complexes of Pt, Pd and Ni has been studied such as partially oxidised Pt amine salts[28] and metal dithiolenes[29] (see Figure 3c. overleaf). In general, high room temperature conductivity is only obtained by partial oxidation to form 15/16e- complexes e.g. $Li_{0.82}[Pt\{S_2C_2(CN)_2\}_2].2H_2O$ has an RT conductivity of $100\Omega^{-1}$ cm^{-1} cf. $10\Omega^{-1}$ cm^{-1} for $Na[Pt\{S_2C_2(CN)_2\}_2].1.15H_2O$[30].

Figure 3c. Metal dithiolene anion

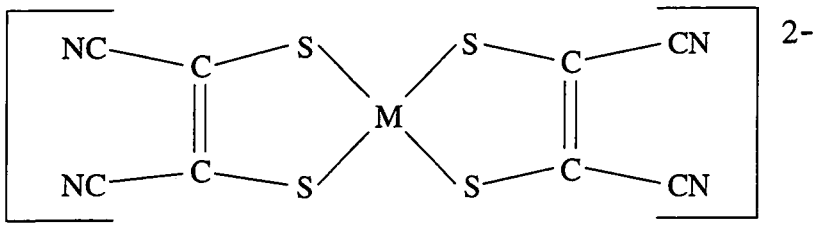

In recent years these complexes have not evoked the same level of interest compared with the 1970's and 1980's although they still attract attention because of their unusual properties e.g. the molecular conductor $[NHMe_3][Pt(dmit)_2]$ where dmit = 4,5-dimercapto-1,3-dithiole-2-thione)[31].

3.1.8. Sulphur-Nitrogen Complexes of Platinum and Palladium.

There is a large range of sulfur-nitrogen ring systems complexed to transition metals[32-34]. Many of these complexes involve Pt and Pd (see Figure 3.d.). As indicated from the examples, almost all these species have square planar co-ordination and involve the ligands in both chelating and bridging bonding modes as either 1e- oxidisers and/or two electron lone pair donors,.

Figure 3d. Some Sulfur-Nitrogen Ring Systems of Pt and Pd

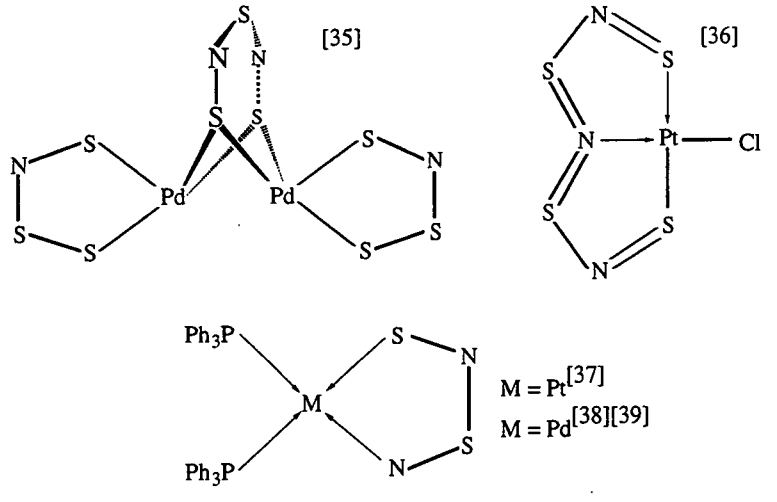

Of greatest relevance to this work, is the preparation of Pt and Pd complexes containing sulfur ligands by the oxidation of zero-valent complexes in the presence of the ring

system in question. In these reactions the metal inserts into the ring as shown below (Equations 3b.)

Equations 3b. Examples of +2 Oxidation of Zero Valent Pt and Pd Phosphine Complexes

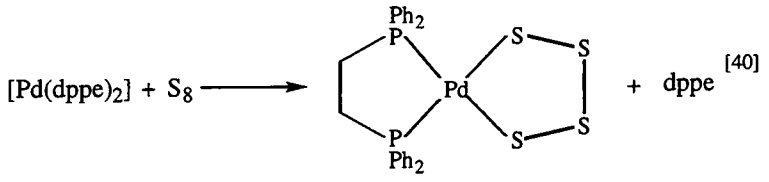

$$[Pt(PPh_3)_3] + [S_4N_4H_4] \longrightarrow [\overline{PtSNSN}(PPh_3)_2]^{[39]}$$

$$M^0 + [S_4N_4] \longrightarrow [\overline{MSNSN}] \text{ species}^{[41]}$$

$$2(Ph_3P)_2Pd(C_2H_4) + S_4N_4 \longrightarrow [(Ph_3P)_2Pd(S_2N_2)]_2 + 2PPh_3 + 2C_2H_4^{[42]}$$

3.1.9. ^{31}P N.m.r. Spectroscopy of Phosphine Complexes.

The platinum and palladium complexes which will be studied during the course of this thesis all possess phosphine ligands. ^{31}P (100% natural abundance , $I=^1/_2$), with its high relative sensitivity ($66.3x10^{-3}$), is a convenient nucleus for n.m.r. .

The range of chemical shift values is far greater for phosphorus than for proton although some general trends do emerge. In the context of this research there is a shift to higher frequency on the co-ordination of a phosphine to Pt or Pd e.g. PPh_3 (δ-5ppm)[43a], $[Pt(PPh_3)_3]$ (δ49.9ppm)[9]; dppe (δ-13.2ppm)[43b], $[Pd(dppe)_2]$ (δ30.9ppm)[44].

In platinum-phosphine complexes coupling between P and ^{195}Pt (33.8% abundant, $I=^1/_2$) results in Pt satellites. Again only a limited amount of information can be gained from the size of the $J_{P\text{-}Pt}$ coupling constant in this series of compounds. Zero-valent platinum phosphine complexes usually have values of around 4000Hz e.g. $[Pt(PPh_3)_3]$ with $J_{P\text{-}Pt}$ 4438Hz[6] and $[Pt(dppe)_2]$ with $J_{P\text{-}Pt}$ 3730Hz. Pt(II) phosphine based species usually have $J_{P\text{-}Pt}$ coupling constants of around 3000Hz e.g. $[(SNSN)Pt(PPh_3)_2]$ $J_{P\text{-}Pt}$ 2827Hz and 2994Hz[45]. It must be stated however that these are general rules only.

3.2. RESULTS AND DISCUSSION

3.2.1. Preparation of zero-valent phosphine complexes of Pt and Pd.

Four zero-valent phosphine complexes have been used extensively in this research, $[Pd(PPh_3)_4]$, $[Pt(PPh_3)_4]$, $[Pd(dppe)_2]$ and $[Pt(dppe)_2]$ and, to a lesser extent, $[Pt(PPh_3)_3]$ and $[Pt(PMe_2Ph)_4]$. The complexes were prepared either in accordance with the literature methods, sometimes with minor modifications to the literature procedures or in methods directly analogous to known procedures.

Johnson-Matthey plc. kindly loaned the research group the precious metal halides K_2PtCl_4, K_2PdCl_4 and $PdCl_2$. These compounds were reduced to the required phosphine complex via three synthetic routes;

(i) Preparation of the zero-valent dibenzylidene acetone complex of Pd, $[Pd_2dba_3.CHCl_3]$[14] and subsequent ligand exchange reaction with PPh_3 or dppe to form $[Pd(PPh_3)_4]$ and $[Pd(dppe)_2]$ respectively.

(ii) Reduction of K_2MCl_4 by $NaBH_4$ in the presence of PPh_3 or dppe to form the required complex[46].

(iii) Reaction of K_2PtCl_4 with PPh_3 or PMe_2Ph in the presence of KOH to form $[Pt(PPh_3)_4]$ and $[Pt(PMe_2Ph)_4]$[47].

3.2.2. The preparation of Dppe ($Ph_2PC_2H_4PPh_2$).

The chelating diphosphine, dppe, was prepared in accordance with the literature method,[48] producing the phosphine in high purity, as shown by elemental analysis, ^1H and ^{31}P spectroscopy, d.s.c. and I.R. spectroscopy. The white crystalline solid was used in later reactions.

3.2.3. The Preparation of $[Pd_2dba_3.CHCl_3]$.

$[Pd_2dba_3.CHCl_3]$ was also prepared in accordance with the literature procedure[14]. $PdCl_2$, dba, (dibenzylidene acetone) and $Na[CH_3COO]$ were stirred in hot MeOH (40°c) forming a red brown precipitate $[Pd(dba)_2]$. Boiling this solid in $CHCl_3$ resulted in the formation of purple crystals of the dimeric Pd complex, Pd_2dba_3. In this complex the metal is bridged by the olefinic double bonds of the dba ligand to form a 16 electron zero valent palladium complex (see figure 3e.). Again satisfactory analyses proved the purity of the species.

Figure 3e. Pd_2dba_3

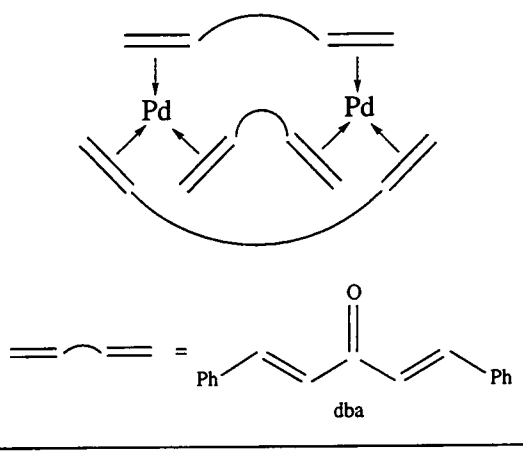

3.2.4. The Preparation of $[Pd(PPh_3)_4]$ and $[Pd(dppe)_2]$ from $[Pd_2dba_3.CHCl_3]$.

The dba ligands on $[Pd_2dba_3.CHCl_3]$ can be removed by simple ligand displacement (e.g. using bipyridine)[14]. In the same publication it was reported that $[Pd(PPh_3)_4]$ could be prepared by stirring $[Pd_2dba_3.CHCl_3]$ and PPh_3 in benzene. I discovered that this reaction also occured in toluene (see Equation 3c.). Increased yields were obtained by reducing the solvent concentration before filtering the product and washing with EtOH. The bright yellow colour of the complex and good analysis (elemental, d.s.c., and I.R.) indicated the presence of the pure palladium-phosphine species. No room temperature ^{31}P n.m.r spectra were recorded due to the ligand exchange processes that occur (i.e. exchange between $[Pd(PPh_3)_4]$, $[Pd(PPh_3)_3]$ and $[Pd(PPh_3)_2]$) which only slow to a rate below the n.m.r. timescale at -80°C[49]. This reaction avoids the use of hydrazine hydrate and dimethyl sulphoxide, reagents required in the preparation of $Pd(PPh_3)_4$ from $PdCl_2$[50].

I suggest that an analogous reaction could be used to form $[Pd(dppe)_2]$, with dppe replacing PPh_3. However, although most of the relevant analysis, and the bright yellow colour of the product indicated the presence of a pure product, the ^{31}P n.m.r spectra showed evidence for two minor impurities (at δ32.75 and δ56.25) as well as the peak for $[Pd(dppe)_2]$ at δ30.86.[50]

Equation 3d.

$$[Pd_2dba_3,ChCl_3] \xrightarrow[2dppe]{4PPh_3} \begin{matrix}[Pd(PPh_3)_4] \\ [Pd(dppe)_2]\end{matrix}$$

Other trial reactions (unrelated to the main body of this work) indicated that further substitution reactions could take place e.g. with $AsPh_3$ to form $[Pd(AsPh_3)_4]$. In fact, this reaction may prove to be a good synthetic route to a whole series of zero-valent phosphine and arsine complexes of palladium.

3.2.5. The reduction of K_2MCl_4 by $NaBH_4$ in the presence of phosphine.

This synthetic route was used to prepare $[Pd(PPh_3)_4]$, $[Pt(PPh_3)_4]$, $[Pd(dppe)_2]$, and $[Pt(dppe)_2]$ in an analogous method to the literature procedure that was used to prepare zero-valent complexes of arylated polytertiary phosphine and arsine complexes of Pt[46]. In general, an excess of phosphine was dissolved in boiling EtOH and an aqueous solution of K_2PtCl_4 or K_2PdCl_4 added. Finally, an aqueous solution of $NaBH_4$ (in excess) was carefully added to yield the yellow zero-valent phosphine complex as a precipitate with the evolution of gaseous H_2, and B_2H_6 (see Equation 3d.).

Equation 3.d.

$$K_2MCl_4 + 2NaBH_4 + \begin{matrix}4PPh_3 \\ \text{or} \\ 2dppe\end{matrix} \longrightarrow \begin{matrix}[Pd(PPh_3)_4] \\ \text{or} \\ [Pd(dppe)_2]\end{matrix} + 2NaCl + 2KCl + B_2H_6 + H_2$$

Although $[Pd(PPh_3)_4]$, and $[Pt(PPh_3)_4]$ could be prepared (as shown by spectroscopic and elemental analysis) the reaction did not always provide a pure product and other synthetic routes highlighted in this chapter were used preferentially.

For the two dppe complexes, $[Pd(dppe)_2]$ and $[Pt(dppe)_2]$, the products formed were of a higher purity. In the case of $[Pt(dppe)_2]$, producing a pure product (as indicated by analysis and spectroscopic techniques shown in the experimental section) was essential as none of the major chemical suppliers (e.g. BDH, Lancaster, Avocado, Aldrich etc.) sold this complex. As in the synthesis of $[Pd(dppe)_2]$ from $[Pd_2dba_3.CHCl_3]$, small amounts

of an impurity were highlighted (in this case there was only the one additional peak at δ32.7ppm). However [Pd(dppe)$_2$] is a light sensitive, easily oxidisable, complex which readily starts to decompose within a week even when stored under N_2 in darkness. Thus it was better to prepare fresh, slightly impure, complex than to purchase it from Aldrich from where only a brown, greatly oxidised complex could be obtained.

3.2.6. The Reaction of K_2PtCl_4 with Phosphine in the Presence of KOH.

This was by far the best method for preparing the purest samples of [Pt(PPh$_3$)$_4$][47]. An aqueous/ethanol solution of KOH was added to a boiling EtOH solution of PPh$_3$. To the resultant basic phosphine solution, an aqueous solution of K_2PtCl_4 was added dropwise producing bright yellow [Pt(PPh$_3$)$_4$] which was washed (H_2O, EtOH) and dried *in vacuo* (see Equation 3e.). As in the case of [Pd(PPh$_3$)$_4$] no room temperature ^{31}P spectra were run due to ligand exchange processes that can only be slowed down below -80°C[6].

Equation 3e.

$$K_2PtCl_4 + PPh_3 + KOH \xrightarrow{EtOH} [Pt(PPh_3)_4]$$

The above method was utilised to prepare [Pt(PMe$_2$Ph)$_4$] except that the increased solubility of the phosphine complex in EtOH created a problem. In the preparation (section 3.3.8) reducing the volume of the solvent *in vacuo* precipitated out the bright yellow solid product. However, subsequent reactions yielded only a sticky yellow brown solid of low purity. No attempt was made to prepare the analogous Pd complex.

3.2.7 The Preparation of [Pt(PPh$_3$)$_3$] from [Pt(PPh$_3$)$_4$].

It has been shown by X-ray crystallography[8][9] that Pt(PPh$_3$)$_4$ exists as the planar three co-ordinate species Pt(PPh$_3$)$_3$ with the fourth PPh$_3$ group not bonded. Thus it is not suprising that by simply boiling Pt(PPh$_3$)$_4$ in EtOH, one phosphine can be removed[46]. The yellow-orange crystalline solid formed, Pt(PPh$_3$)$_3$, is slightly more oxygen and moisture sensitive than [Pt(PPh$_3$)$_4$] and was thus used immediately after preparation and drying *in vacuo*.

3.3. EXPERIMENTAL

3.3.1. The Preparation of [$Pd_2dba_3.CHCl_3$].

$PdCl_2$ (1.08g, 6.09mmol), dba (4.70g, 20.06mmol) and Na[CH_3COO] (4.00g, 48.8mmol) were stirred at 40°C in MeOH (150ml). The reddish-purple precipitate which formed was filtered, washed with H_2O (20ml) and acetone (20ml) and pumped to dryness *in vacuo*. The precipitate was dissolved in boiling $CHCl_3$ (160ml) and the deep violet solution removed by canula filtration from the residual solids. To this solution Et_2O (250ml) was slowly added and the solution cooled to 0°C to yield deep purple needles of $Pd_2dba_3.CHCl_3$ which were filtered, washed with Et_2O (20ml) and dried *in vacuo*.

Yield 2.18g, 69.2%

IR $\nu_{max}(cm^{-1})$ 3053w, 1645w, 1615s, 1575sh, 1541s, 1486sh, 1443m, 1385(w), 1335m, 1272w, 1245w, 1185s, 1157w, 1095br, 1027w, 976m, 912w, 856w, 760s, 699ssh, 678m, 622w, 598w, 559w, 515m.

Elemental analysis, found: C,60.97%; H,4.12%; N,0.00%. Calc.:C,60.32%; H,4.19%; N,0.00%

Nm.r.; (250mHz; solvent $CDCl_3$) ^1H complex multiplets[16].

D.s.c.. 124.0°C mpt (lit. 122-124°C[14]).

3.3.2. The Preparation of [$Pd(PPh_3)_4$] from [$Pd_2dba_3.CHCl_3$].

[$Pd_2dba_3.CHCl_3$] (0.3g, 0.29mmol) and PPh_3(1.24g, 4.73mmol) were stirred at room temperature in MePh (20ml) for 1hr to yield a bright yellow precipitate [$Pd(PPh_3)_4$]. The solvent was reduced to ~5ml *in vacuo* to complete the precipitation. The solids were filtered, washed with EtOH (2x20ml) and dried *in vacuo*.

Yield 0.50g, 75%

IR $\nu_{max}(cm^{-1})$ 3052m, 1958w, 1885w, 1813w, 1153m, 1569w, 1475s, 1431ssh, 1322w, 1305w, 1263w, 1179w, 1153w, 1082m, 1068w, 1025m, 998m, 910w, 848w, 802w, 742ssh, 692ssh, 619w, 539w, 505sh, 432w, 407m,

Elemental analysis, found: C,74.35%; H,4.92%; N,0.00%.Calc.: C,74.83%; H,5.24%; N,0.00%)

D.s.c.. 115°C dec. (lit. 116°C[50]).

3.3.3. The Preparation of $[Pd(PPh_3)_4]$ from $NaBH_4$ reduction of K_2PdCl_4.

PPh_3 (3.66g, 14.0mmol) was dissolved in refluxing EtOH (100ml). An aqueous solution of K_2PdCl_4 (1.0g, 3.06mmol) was canular transferred into the phosphine solution and the mixture stirred at 60°C to yield a brown coloured solution. Excess aqueous $NaBH_4$ (>0.23g, 6.13mmol) was added producing the immediate evolution of H_2 and the formation of a bright yellow precipitate. The suspension was stirred for 20mins, filtered, washed with H_2O (10ml) and EtOH (2x10ml) and dried *in vacuo*.

Yield 2.62g, 14.0mmol.

IR $\nu_{max}(cm^{-1})$ 3052m, 1958w, 1885w, 1813w, 1153m, 1571w, 1475s, 1431ssh, 1322w, 1305w, 1263w, 1179w, 1082m, 1068w, 1025m, 998m, 910w, 848w, 802w, 742ssh, 692ssh, 619w, 539w, 505sh, 430w, 407m.

Elemental analysis, found: C,75.55%; H,4.83%; N,0.00%.Calc.:C,74.83%; H,5.24%; N,0.00%.

D.s.c. 118°C dec. (lit. 116°C[50]).

3.3.4. The Preparation of dppe.

PPh_3 (20g, 76mmol) was dissolved in T.H.F. (100ml). Thin strips of Li (1.06g, 153mmol) were added and the T.H.F. refluxed for 2hrs to yield a deep red/brown solution. The solution was cooled to 0°C and $ClCH_2CH_2Cl$ (6ml, 76.2mmol) was added dropwise over 20mins. The resultant solution was refluxed for 30mins, allowed to cool to room T and poured into cold H_2O to yield an off white solid which was filtered and recrystallised from EtOH to yield white crystalline $Ph_2PC_2H_4PPh_2$

Yield 8.94g, 62.9%

IR $\nu_{max}(cm^{-1})$ 2926s,br, 1944w, 1884w, 1583wsh, 1568w, 1464s, 1432s, 1377s, 1328m, 1304m, 1273m, 1185w, 1160sh, 1097m, 1080m, 1066sh, 1024s, 998sh, 907w, 845w, 751sh, 740sh, 726ssh, 705sh, 692ssh, 674sh, 505ssh, 474m, 446m,

Elemental analysis, found: C,78.44%; H,6.11%; N,0.00%. Calc.: C,78.37%; H,6.08%; N0.00%

N.m.r.; (250mHz; solvent $CDCl_3$) ^1H δ7.34 (m, 20, Ph), 2.14 (s, 4, CH_2), ^{31}P δ-9.47 (s).

D.s.c. 143°C mpt (lit 140-142°C[48])

3.3.5. The Preparation of [Pd(dppe)$_2$].

Dppe (1.52g, 3.81mmol) was dissolved in refluxing EtOH (100ml). An aqueous solution of K_2PdCl_4 (0.57g, 1.75mmol) was canular transferred into the phosphine solution and the mixture stirred at 60°C to yield a brown coloured solution. Excess aqueous $NaBH_4$ (>0.137g, 3.50mmol) was added to yield an immediate evolution of H_2 and the formation of a bright yellow precipitate. The suspension was stirred for 20mins, filtered, washed with H_2O (10ml) and EtOH (2x10ml) and dried *in vacuo*.

Yield 1.36g, 85.8%

IR $\nu_{max}(cm^{-1})$3047m, 1583sh, 1479s, 1431s, 1408m, 1364w, 1261m, 1190w, 1169w, 1090s, 1066m, 1025ssh, 871m, 815m, 739s, 693ssh, 660m, 522sh, 509sh, 483m, 428w, 412w.

Elemental analysis, found: C,68.75%; H,5.36%; N,0.00%. Calc.: C,69.13%; H,5.37%; N0.00%

N.m.r.; (250mHz; solvent $CDCl_3$) ^1H δ_H 7.78-7.13 (m, 20, Ph), 2.19 (s, 4, CH_2), ^{31}P δ_p30.9

D.s.c. 94°C mpt, 202°C and 226°C dec.

3.3.6. The Preparation of [Pt(PPh$_3$)$_4$] from K$_2$PtCl$_4$ and NaBH$_4$.

PPh_3 (2.08g, 7.93mmol) was dissolved in refluxing EtOH (100ml). An aqueous solution of K_2PtCl_4 (0.7g, 1.69mmol) was canular transferred into the phosphine solution and the mixture stirred at 60°C to yield a clear solution. Excess aqueous $NaBH_4$ (>0.128g, 3.38mmol) was added with an immediate evolution of H_2 and the formation of a bright yellow precipitate. The suspension was stirred for 20mins, filtered, washed with H_2O (10ml) and EtOH (2x10ml) and dried *in vacuo*.

Yield 1.40g, 66.2%)

IR $\nu_{max}(cm^{-1})$ 3053m, 1959w, 1888w, 1816w, 1583msh, 1476ssh, 1431sssh, 1305w, 1265w, 1198m, 1181m, 1154w, 1119m, 1083m, 1069wsh, 1026sh, 998w, 743s, 721m, 694s, 619w, 542m, 507ssh, 415s.

Elemental analysis, found: C,69.02%; H,4.55%; N,0.00%.Calc.:C,69.50%; H,4.86%; N,0.00%

D.s.c. 109°C (weak) exotherm and 161°C (strong) dec (lit. 159-160°C[47])

3.3.7. The Preparation of $[Pt(PPh_3)_4]$ from K_2PtCl_4/KOH.

PPh_3 (2g,7.63mmol) was dissolved in refluxing EtOH (15ml). KOH (0.2g,3.56mmol) dissolved in a mixture of EtOH (7ml) and H_2O (1ml) was canular transferred on to the phosphine solution. K_2PtCl_4 (0.7g, 1.69mmol) dissolved in H_2O (6ml) was added slowly to this alkaline triphenylphosphine solution while stirring at 65°C for 20mins. The pale yellow solid formed was filtered and washed with H_2O (10ml) and Et_2O (2x10ml) and dried *in vacuo*

Yield 1.6g, 76%.

IR $\nu_{max}(cm^{-1})$ 3053m, 1959w, 1888w, 1816w, 1583msh, 1476ssh, 1431sssh, 1305w, 1265w, 1198m, 1181m, 1154w, 1119m, 1083m, 1069wsh, 1026sh, 998w, 743s, 721m, 694s, 619w, 542m, 507ssh, 415s.

Elemental analysis, found: C,69.51%; H,4.76%; N,0.00%.Calc.:C,69.50%; H,4.86%; N,0.00%.

D.s.c. 109°C (weak) exotherm and 160°C (strong) dec (lit. 159-160°C[47])

3.3.8. The Preparation of $Pt(PPh_3)_3$ from $Pt(PPh_3)_4$.

$Pt(PPh_3)_4$ (1.0g, 0.80mmol) was suspended in EtOH (15ml) and refluxed, with stirring, for 2hrs. The hot suspension was filtered and the resultant deep yellow crystals were dried *in vacuo.*

Yield 0.33g, 42%.

IR $\nu_{max}(cm^{-1})$ 1431vs, 1302w, 1082m, 1020m, 995w, 740shd, 731m, 712m, 680s, 509ssh, 500s, 415m.

Elemental analysis, found: C,66.33%; H,4.62%; N,0.00%.Calc.:C,66.0%; H,4.59%; N,0.00%)

D.S.C.204°C dec (lit. 205-206°C[47]).

3.3.9. The Preparation of $[Pt(PMe_2Ph)_4]$.

PMe_2Ph (0.6ml, 4.20mmol) was dissolved in EtOH (20ml). KOH (0.20g, 3.56mmol) dissolved in a mixture of EtOH (7ml) and H_2O (1ml) was canular transferred onto the phosphine solution. K_2PtCl_4 (0.40g, 0.96mmol) dissolved in H_2O (5ml) was added slowly to this alkaline phosphine solution to yield a deep yellow solution. The solvent

was removed *in vacuo* until a yellow solid [$Pt(PMe_2Ph)_4$] had precipitated out of solution. This precipitate was filtered and washed with H_2O (3x10ml) and dried *in vacuo*.

Yield 0.60g, 83%.

IR $\nu_{max}(cm^{-1})$ 2955m, 2890m, 1582m, 1483m, 1431sh, 1415m, 1321w, 1283m, 1271m, 1177w, 1154w, 1091m, 1070w, 1027m, 1000w, 963w, 931ssh, 895ssh, 889ssh, 860shd, 825m, 739ssh, 717shd, 696s, 669s, 489ssh, 415ssh.

Elemental analysis, found: C,51.43%; H,5.84%; N,0.00%.Calc.:C,51.40%; H,5.93%; N,0.00%.

D.s.c. 88.7°C mpt.

3.3.10. The Preparation of [$Pt(dppe)_2$].

Dppe (1.33g, 3.33mmol) was dissolved in refluxing EtOH (60ml). An aqueous solution (4ml) of K_2PtCl_4 (0.59g, 1.42mmol) was canular transferred into the phosphine solution and the mixture stirred at 60°C to yield a colourless solution. Excess aqueous $NaBH_4$ (.0.107g, 2.84mmol) was added with a immediate evolution of H_2 and the formation of a bright yellow precipitate. The suspension was stirred for 10mins, filtered, washed with H_2O (10ml) and EtOH (2x10ml) and dried in vacuo.

Yield 1.20g, 85.4%.

IR $\nu_{max}(cm^{-1})$ 3048m, 196w, 1890w, 1813w, 1583m, 1569w, 1480m, 1432ssh, 1407w, 1304w, 1272w, 1179w, 1156w, 1089m, 1066m, 1025m, 999w, 871m, 815m, 802m, 738sh, 693ssh, 660m, 520ssh, 513ssh, 489m, 412m.

Elemental analysis, found: C,62.90%; H,4.92%; N,0.00%.Calc.:C,62.96%; H,4.88%; N,0.00%.

N.m.r.; (250mHz; solvent $CDCl_3$) ^1H δ7.88-6.91ppm (m, 20,Ph), 2.22ppm (s, 4, CH_2), ^{31}P δ30.7ppm, ($J_{P\text{-}Pt}$ 3732Hz)

D.s.c..230°C dec.

3.4. CONCLUSION

Chapter two described the chemistry of the ligand [PhCNSSN]• and its previous, limited, reaction chemistry with transition metal species. In this chapter a series of zero-valent platinum and palladium phosphine complexes has been prepared with the aim of forming interesting complexes with the above chalcogen ring system. It was hoped that these metal complexes would lose phosphine and be oxidised by the sulfur atoms of the ring; it has been shown in this chapter that these species can be oxidised by various other ligands, including sulfur based compounds.

A range of properties and industrial applications of Pt and Pd species have been highlighted. It was hoped that [PhCNSSN]• based Pt and Pd complexes might also exhibit similar properties and have similar uses.

3.5 REFERENCES

1. F.R. Hartley, *Studies in Inorganic Chemistry Chemistry of the Platinum Group Metals*, 1991, **11**, 26.

2. F.A. Cotton and G. Wilkinson, *Advanced Inorganic Chemistry 5th Edn..*, John Wiley and Sons, 1988. a)918, b)776, c)818 & d)934, e)36.

3. S.M. Owen and A.T. Brooker, *A guide to Modern Inorganic Chemistry*, Longman Scientific & technical, 1991, 27.

4. a) M.J. Russell and C.F. Barnard, *Comperehensive Co-ordination Chemistry*, Ed. G.Wilkinson, R.D. Gillard and J.A. McCleverty, Pergamon Press, 1987, **5**, 1171.

   b)A.J. Hutton, *Comprehensive Co-ordination Chemistry*, Ed. G. Wilkinson, R.D. Gillard and J.A. McCleverty, Pergamon Press, 1987, **5**, 1131.

   c) D.M. Roundhill, *Comprehensive Co-ordination Chemistry*, Ed. G.Wilkinson, R.D. Gillard and J.A. McCleverty, Pergamon Press, 1987, **5**, 351.

5. a) P.M. Maitlis and M.J. Russell in *Comprehensive Organometallic Chemistry*, Ed. G. Wilkinson, F.G.A. Stone and E.W. Abel, Pergamon Press, 1982, **38**, 233.

   b) T.R. Hartley in *Comprehensive Organometallic Chemistry*, Ed. G.Wilkinson, F.G.A.Stone and E.W.Abel, **38**, 1982, 471.

6. A. Sen and J. Halpern, *Inorg. Chem.*, 1980,**19**, 1073.

7. B.E. Mann and A. Musco, *J.Chem. Soc., Dalton Trans.*, 1980, 776.

8. V. Alabono, P.L. Bellon and V. Scallurin, *J.Chem.Soc., Chem.Commun.*, 1966, 507.

9. P.A. Chaloner, P.B. Hitchcock, G.T.L. Broadwood-Strong, *Acta Crystallogr., Sect. C*, **45**, 1989, 1309.

10. K.J. Moynihan, C. Chieb and R.G. Ciel, *Acta Crystallogr., Sect. B*, **35**, 1979, 3060.

11. T. Yoshida and S.Otsuka, *J. Am. Chem. Soc.*, 1974, **96**, 3322.

12. L. Malatesta and M. Angoletta, J. Chem. Soc., 1957, 1187.

13. M. Green, J.A.K. Howard, J.L. Spencer and F.G.A. Stone, *J.Chem.Soc., Dalton Trans.*, 1977, 271.

14. T. Ukai, H. Kawazua and Y. Ishii, *J. Organomet. Chem.*, 1974, **65**, 253.

15. M. Suzuki, Y. Oda, R. Noyori, *J.Am. Chem. Soc.*, 1979, **101**, 1623.

16. N.N. Greenwood and A. Earnshaw, *Chemistry of the Elements*, Pergamon Press, 1985, 1350.

17. P.M. Henry, J.E. Bàckvall, B. Åkermark and S.O. Ljunggren, *J.Am.Chem.Soc.*, 1979, **101**, 2411..

18. N. Gragor and P.M. Henry, *J. Am. Chem. Soc.*, 1981, **102**, 681.

19. B. Rosenberg, L. Van Camp, J.E. Trasko and V.H. Mansour, *Nature*, 1969, **222**, 385.

20. A. Rossof, R. Slayton and C. Perlia, *Cancer*, 1972, **30**, 1451.

21. Bristol-Myers Handbook, Paraplatin, Compendium of Recent Data, Ed. L. Lenaz, New York, 1987.

22. P. Levieved, *Euro. J. Cancer Clin. Oncol.*, 1984, **20**. 1087.

23. a). C.A. McAuliffe, H.L. Sharma and N.P. Tinker, *Studies in Inorganic Chemistry*, **11**, Ch16, 546.

b). C.A. McAuliffe, H.L. Sharma and N.P. Tinker, *Studies in Inorganic Chemistry*, **11**, Ch16, 579.

24. M. Presnov, A. Konovalova, A. Kozlov, V. Brovtsyn and L. Romanova, *Neoplasma*, 1985, **32**, 73.

25. M. Van Beusichem and N. Farrel, *Inorg. Chem.*, 1992, **31**, 634.

26. M. Cleare, *Recent Results in Cancer Research*, Springer-Verlag, 1974, **48**, 2.

27. K. Krogmann, *Angew. Chem. Int. Ed. Engl.*, 1969, **8**, 35.

28 J.P. Catinat, J. Robert and G. Offergeld, *J.Chem.Soc., Chem.Commun.*, 1983,1310.

29. J.A. McCleverty, *Prog. Inorg. Chem.*, 1968, **10**, 49.

30. A.E. Underhill,*Comperehensive Co-ordination Chemistry*, Ed. G. Wilkinson, R.D. Gillard and J.A. McCleverty, Pergamon Press, 1982, **5**, 147.

31. B. Garreau, B. Pomarede, P. Cassoux, *J.Mater.Chem.*, 1993, **3(3)**, 315.

32. P.F. Kelly and J.D. Woollins, *Polyhedron*, 1986, **5**, 607.

33. T. Chivers and F. Edelmann, *Polyhedron*, 1986, **5**, 1661,

34. J.D. Woollins, *Studies in Inorganic Chemistry*, Ed. F.Steudel, **18**, 1992, 349.

35. U. Thewalt, *Z.Naturforsch*, 1982, **37B**, 276.

36. H. Endres and E. Galantai, *Angew. Chem., Int. Ed. Engl.* 1980, **19**, 653.

37. P.A. Bates, M.B. Hurshouse, P.F. Kelly and J.D. Woollins, *J.Chem.Soc. Dalton Trans.*, 1986, 2367.

38. R. Jones, P.F. Kelly, D.J. Williams and J.D. Woollins, *J.Chem.Soc., Chem. Commun.*, 1985, 1321.

39. C.A Ghilardi,.S. Miollini, S. Moneti, A. Orlandi, *J.Organomet. Chem.*, 1985, **286**, 419.

40. J. Chatt and D.M.P. Mingos, *J.Chem.Soc.(A)*, 1970, 1243.

41. G. Hartmann, P.J. Jones, R. Mews, M. Nottemeyer and G.M. Sheldrick, *Angew. Chem., Int. Ed. Eng.* 1979, **18**, 231.

42. R. Jones, P.F. Kelley, D.J. Williams, J.D. Woollins, *J.Chem.Soc., Chem. Commun.*, 1985, 1325.

43. J.C. Tebby, ed., Handbook of Phosphorus - 31 Nuclear Magnetic resonance Data, C.R.C. press, 1991, a)160, b)154.

44. G.T.L. Broadwood-Strong, P.A. Chaloner and P.B. Hitchcock, *Polyhedron*, 1993, **12**, 721.

45. I.P. Parkin, J.D. Woollins, J.Chem.Soc., *Dalton Trans.*, 1990, 921.

46. R.B. King and P.N. Kapoor, *Inorg. Chem.*, 1972, **11**, 1524.

47. R. Ugo, F. Cariati and G. La Monica, *Inorg. Synth.* 1990, **28**, 123.

48. G.R. Van Hecke and W. de Horrocks, *Inorg. Chem.*, 1966, **5**, 1968.

49. B.E. Mann, A. Musco, *J.Chem.Soc., Dalton Trans.*, 1975, 1673.

50. D.R. Coulson, L.C. Satek and S.O. Grim, *Inorg. Synth.*, 1990, **28**, 107.

CHAPTER FOUR

THE SYNTHESIS AND PROPERTIES OF MONOMETALLIC PLATINUM AND PALLADIUM DITHIADIAZOLYL COMPLEXES

4.1. INTRODUCTION

4.1.1. The Chelating Bonding Mode of (SNCPhNS).

The two dithiadiazolyl based complexes discussed in chapter two, $[Ni_2(\mu_{S\text{-}S}SNCPhNS)Cp_2]$ and $[Fe_2(\mu_{S\text{-}S}SN(H)CPhNS)(CO)_6]$ both contain two metal centres bridged by the two sulfurs of one chalcogen ring system. Each sulfur atom acts as 2+1e electron donors to each metal. Therefore with two sulfurs 6 electrons from the ring are formally used for bonding.

A second type of bonding may be envisaged where the ligands open up at the S-S bond and chelate to one metal centre as a 1+1e oxidising ligand (2X ligand) i.e. 2 electrons from the ring are formally used for bonding.

The two types are shown below (figure 4.a.).

Figure 4.a. Bonding Modes of [PhCNSSN]•

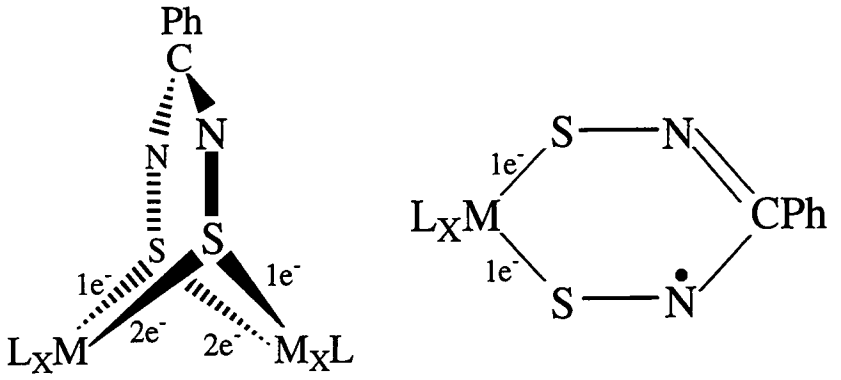

4.1.2. Requirements for Metal Complex Precursor.

[PhCNSSN]• would be a +2 oxidising ligand if it were to chelate one metal centre and remain as a radical. In order to form monometallic dithiadiazolyl species the heterocycle must be reacted with a metal complex with a low oxidation state and a +2 higher oxidation state that is readily available. Zero-valent group 10 complexes belong to one class of species that fits these requirements. The metal should also preferably be able to extend the delocalisation of the [PhCNSSN]• radical i.e. it should provide an unfilled orbital which would allow further delocalisation of the π system. It would be less likely

that the (SNC(Ph)NS) fragment could stabilise the unpaired electron on its own when the ring is broken.

4.1.3. Preliminary Reactions with Zero-Valent Group 10 Complexes.

Previous to this research several reactions were undertaken between group 10 metals and [PhCNSSN]$^{\bullet}$. The reaction of [$Ni(PPh_3)_4$] with [PhCNSSN]$^{\bullet}$ yielded only dark decomposition products and no new characterisable products[1]. This unpromising result led to the conclusion that exploring the difficult to access Ni phosphine chemistry would not be worthwhile. The reaction between [$Pt(PPh_3)_4$] and [PhCNSSN]$^{\bullet}$ in MePh did yield an initial blue solid which appeared to indicate the synthesis of a monometallic species (by elemental analysis)[2]. However, the compound decomposed when redissolved in CH_2Cl_2 making further analysis difficult.

In contrast the reaction of [PhCNSSN]$^{\bullet}$ with [$Pd(PPh_3)_4$] in MePh resulted in the formation of a novel trimetallic dithiadiazolyl species[2][3], as will be discussed in chapter 5. Finally, reaction between [$Pd(dppe)_2$] and [PhCNSSN]$^{\bullet}$ in MePh produced a green solid which was also poorly characterised again due to its decomposition in suspenion and in solution[4].

These preliminary results did give some indication that novel dithiadiazolyl complexes could be isolated but for a thorough characterisation to be undertaken the problems associated with their instability in solution would have to be overcome.

4.2. RESULTS AND DISCUSSION.

4.2.1. The Synthesis of Monometallic Dithiadiazolyl Complexes.

4.2.1.a. The Preparation of [Pt(SNCPhNS-*S,S*)(PPh_3)$_2$].MeCN.

The addition of MeCN to a mixture of [$Pt(PPh_3)_4$] and $(PhCNSSN)_2$ led to the immediate formation of a dark blue-green microcrystalline solid of [Pt(SNCPhNS-*S,S*)(PPh_3)$_2$].MeCN under a blue-green precipitate. After 20min the soluble fraction was filtered off and the precipitate washed with fresh MeCN. Elemental analysis indicated that the complex was obtained as its MeCN solvate, subsequently confirmed from structural data.

Four analogous complexes, [Pt(SNC(3,4F-C_6H_3)NS-*S,S*)(PPh_3)$_2$], [Pt(SNC(p-ClC_6H_4)NS-*S,S*)(PPh_3)$_2$], [Pt(SNC(p-BrC_6H_4)NS-*S,S*)(PPh_3)$_2$] and [Pt(SNC(p-MeC_6H_4)NS-*S,S*)(PPh_3)$_2$] were prepared by the same synthetic route from the specific substituted dithiadiazolyl and [$Pt(PPh_3)_4$] by O.G.Dawe[5] and all subsequent analysis of these species was undertaken by him. Consequently no experimental or analysis figures are quoted here.

4.2.1.b. The Preparation of [Pt(SNCPhNS-*S,S*)(dppe)].

The addition of MePh to a mixture of [$Pt(dppe)_2$] and $[PhCNSSN]_2$ led to the formation of a deep royal blue precipitate under a blue solution. The solution was heated to 70°C and after 24h the soluble fraction was filtered off and the precipitate washed with fresh MePh. Satifactory elemental analysis was achieved for the composition [Pt(SNC(Ph)NS-*S,S*)(dppe)].

The analogous complex [Pt(SNC(3,4-FC_6H_3)NS-*S,S*)(dppe)] was prepared by the same synthetic route[5].

4.2.1.c. The Preparation of [Pd(SNC(Ph)NS-*S,S*)(dppe)].

The addition of MePh to a mixture of [$Pd(dppe)_2$] and $[PhCNSSN]_2$ led to the immediate formation of a green precipitate under a green solution. After $1\frac{1}{2}$h the soluble fraction was filtered off and the precipitate was washed with fresh MePh. Satisfactory elemental analysis was achieved for the composition [Pd(SNC(Ph)NS-*S,S*)(dppe)].

4.2.1.d. The General Reaction to Form Monometallic Species.

In all the reactions to form monometallic complexes there is a loss of phosphine from the metal phosphine complex (either $2PPh_3$ or dppe) and [PhCNSSN]$^{\bullet}$ co-ordinates on to the metal through the two sulfurs, as shown in the following sections. The overall equations are shown below (equation 4.a.).

Equation 4.a. Formation of Monometallic Dithiadiazolyl Complexes.

$$[Pt(PPh_3)_4] + [RCNSSN]^{\bullet} \longrightarrow [Pt(SNC(R)NS\text{-}S,S)(PPh_3)_2] + 2PPh_3$$

$$[M(dppe)_2] + [RCNSSN]^{\bullet} \longrightarrow [M(SNC(R)NS\text{-}S,S)(dppe)] + dppe$$

M = Pt or Pd

4.2.2. Crystal Growth of Monometallic Complexes.

Growth of crystals suitable for X-ray diffraction proved to be highly problematic. Recrystallisation proved impossible as all three complexes decompose to further products in solution, as explained in the following two chapters. To overcome this problem crystals were grown directly from the reaction between [PhCNSSN]$^{\bullet}$ and the zero-valent metal phosphine.

Crystals of [Pt(SNCPhNS-*S,S*)$(PPh_3)_2$].MeCN were grown by slow transfer of [PhCNSSN]$^{\bullet}$ over excess $(PhCNSSN)_2$ through a grade 3 sinter into a solution of $[Pt(PPh_3)_3]$ over excess $[Pt(PPh_3)_3]$. Crystals started to form after 1h. The apparatus used for this reaction was an upturned 'dog' (see chapter 1 for a diagram and full description). This facilitates a diffusion controlled reaction and the monometallic species that is formed grows as crystals suitable for X-ray diffraction (see figure 4.b.). In a diffusion controlled reaction fewer micro crystals are formed and these act as nucleation sites for the growth of large crystals as the reaction proceeds.

In similar reactions crystals of [Pt(SNCPhNS-*S,S*)(dppe)] and [Pd(SNCPhNS-*S,S*)(dppe)] were grown with MeCN as the solvent overnight. This technique has been used successfully by this group in the past[1][6][7].

Figure 4.b. Crystal Growth Reaction of [Pt(SNCPhNS-*S,S*)(PPh_3)$_2$].

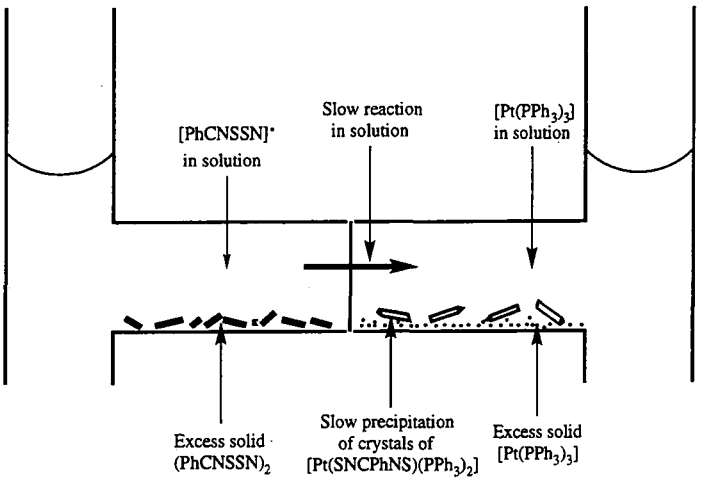

4.2.3. X-Ray Structures.

X-ray structural determinations were undertaken on [Pt(SNCPhNS-*S,S*)(PPh_3)$_2$.MeCN], [Pt(SNCPhNS-*S,S*)(dppe)] and [Pd(SNCPhNS-*S,S*)(dppe)]. All three structural solutions were undertaken by Dr. S.E.Lawrence[3].

Structural diagrams of all three complexes are shown in Figures 4.c, 4.d and 4.e. and selected bond lengths and angles are given in table 4.a. as are, for comparison, selected structural data for $(PhCNSSN)_2$[8].

The structural information gives conclusive evidence for the formation of the first monometallic dithiadiazolyl complexes, with the (SNCPhNS) group behaving as a chelating rather than a bridging ligand. The platinum complexes are also the first dithiadiazolyl species of that metal to be reported.

The two dppe complexes are essentially isostructural and are closely related to the triphenyl phosphine species. All three contain square planar $M^{(II)}$ species formed by oxidation of the $M^{(O)}$ phosphine complex by the sulfur atoms of the chelating (SNCPhNS) group. As stated in chapter two, square planar $Pt^{(II)}$ and $Pd^{(II)}$ complexes are the most common structural type in group 10 chemistry.

There is no significant difference in atomic radii between Pt and Pd (due to the lanthanide contraction[9]) and thus no significant difference in M-P and M-S bond lengths. Thus the metal-sulfur bond lengths are essentially identical for both of the dppe complexes. The

Pt-S bond distances are slightly shorter than those observed in other sulfide-bound Pt complexes (2.32-2.36Å)[10]. This indicates a slight double-bond character of the Pt-S bonds. The Pt-S bonds in the triphenylphosphine species are slightly longer than those observed for the dppe complex for a reason that will be discussed below.

The S-S bond length increases greatly from 2.089Å in $(PhCNSSN)_2$ to >3.1Å in the complexes and is thus effectively broken on insertion of the metal. The other (SNCPhNS) ring parameters, most notably bond angles, are consistent with this ring expansion and with the expected decrease in S-S and N-S bond orders. The N-S[11] and C-N[12] bond lengths are still though intermediate between the lengths associated with single and double bonds. There is thus still appreciable π delocalisation over the (SNCPhNS) framework in addition to any S-Pt π bonding and the lowest energy conformation of the six membered ring would be planar.

For a six-membered planar ring the ideal average internal angles would be 120°. However, the ideal S-M-S angle for square-planar species would be 90°. To accommodate the metal atom, the ring thus buckles at the S-S to metal interface and the metal atom sits above the planar (SNC(Ph)NS) fragment as is shown clearly in the side on view of [Pt(SNCPhNS-*SS*)(dppe)] in figure 4.d and measured by angle δ in table 4.a. The different phosphines are not simply spectator ligands that complete the co-ordination sphere: they provide the major structural differences observed in these species. The triphenyl phosphine groups in $[Pt(SNCPhNS\text{-}S,S)(PPh_3)_2]$ are sterically far bulkier i.e. (PPh_3 has a larger cone angle[13]) than $^1/_2$dppe and thus the P-M-P angle in $[Pt(SNCPhNS\text{-}S,S)(PPh_3)_2]$ is greater. This has the knock on effect of decreasing all the other metal based bond angles. The S-Pt-S angle is decreased by two effects; slight lengthening of the Pt-S bonds explained above and, more significantly by further buckling along the S-S axis thereby raising the Pt atom above the plane of the (SNC(Ph)NS) fragment. The latter effect is shown clearly in figure 4.f. in which the structure of $[Pt(SNCPhNS\text{-}S,S)(PPh_3)_2]$ is superimposed onto the structure of [Pt(SNCPhNS-*S,S*)(dppe)]. This effect also causes a slight decrease in trans annular S...S interaction in $[Pt(SNCPhNS\text{-}S,S)(PPh_3)_2]$

Finally, a curious phenomenon is the marked difference in S-M-P angles in both dppe based complexes (e.g. 93.9(2)° and 88.7(2)° in [Pd(SNCPhNS-*SS*)(dppe)]). There is no obvious single reason for this effect although it is perhaps caused by packing requirements (unlike the triphenylphosphine based complex there is no solvent of crystallisation in these two species to aid packing). Another explanation is that the bulkier triphenyl phosphine species may prevent great variation in S-M-P angle in [Pt(SNCPhNS-*S,S*)(PPh_3)$_2$]. The S-M-P angles have more potential for variation than the S-M-S and P-M-P angles which are held more rigidly by the chelating ligands. A final reason could be the trans effect[14] with opposite ligands attempting to push charge into the same metal orbitals. When at 180° d and p orbitals are in maximum competition due to charge donation in opposite directions and competition for the same orbitals

Figure 4.c. X-Ray Structure of [Pt(SNC(Ph)NS-*S*,*S*)(PPh_3)$_2$].MeCN.

(the triphenylphosphine phenyl groups, acetonitrile solvate and all the protons have been removed for clarity)

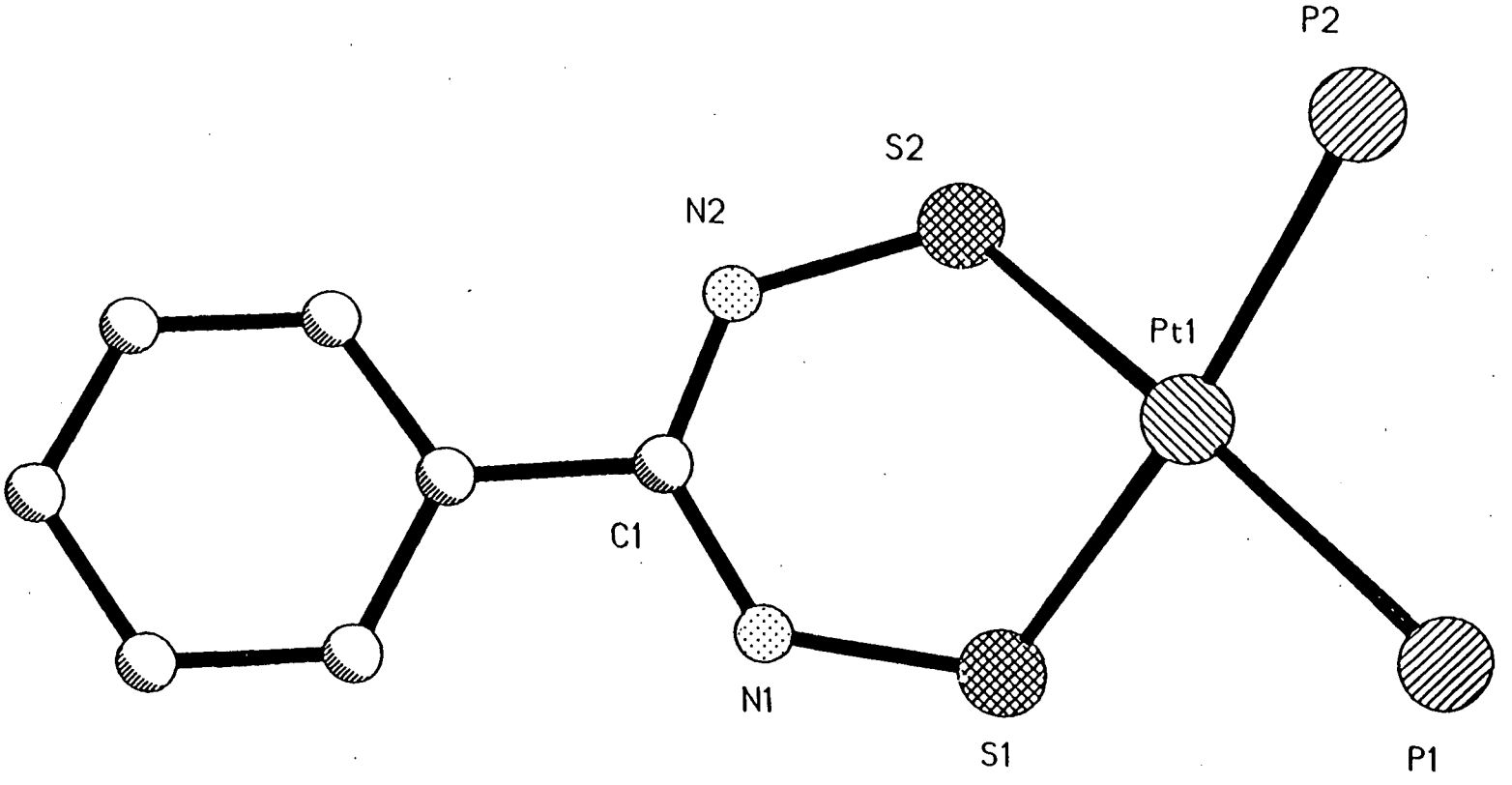

Figure 4.d. X-Ray Structure of [Pt(SNC(Ph)NS-*S,S*)(dppe)].
(the dppe phenyl groups and all the protons have been removed for clarity)

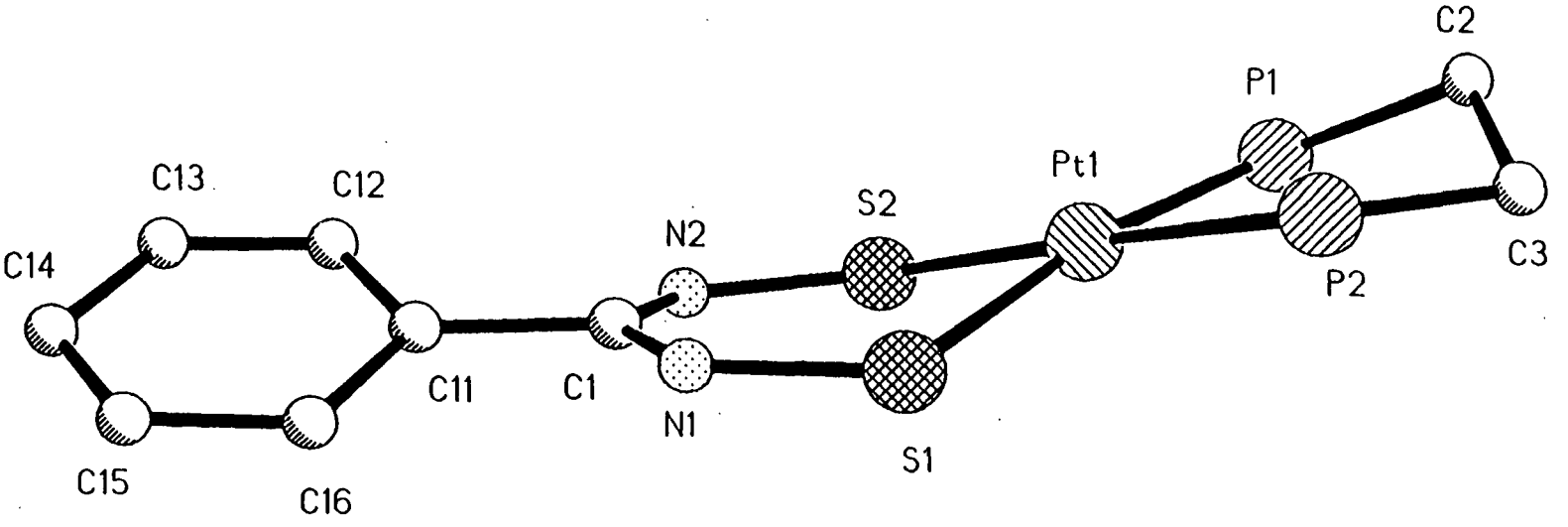

Figure 4.e. X-Ray Structure of [Pd(SNC(Ph)NS-*S*,*S*)(dppe)].

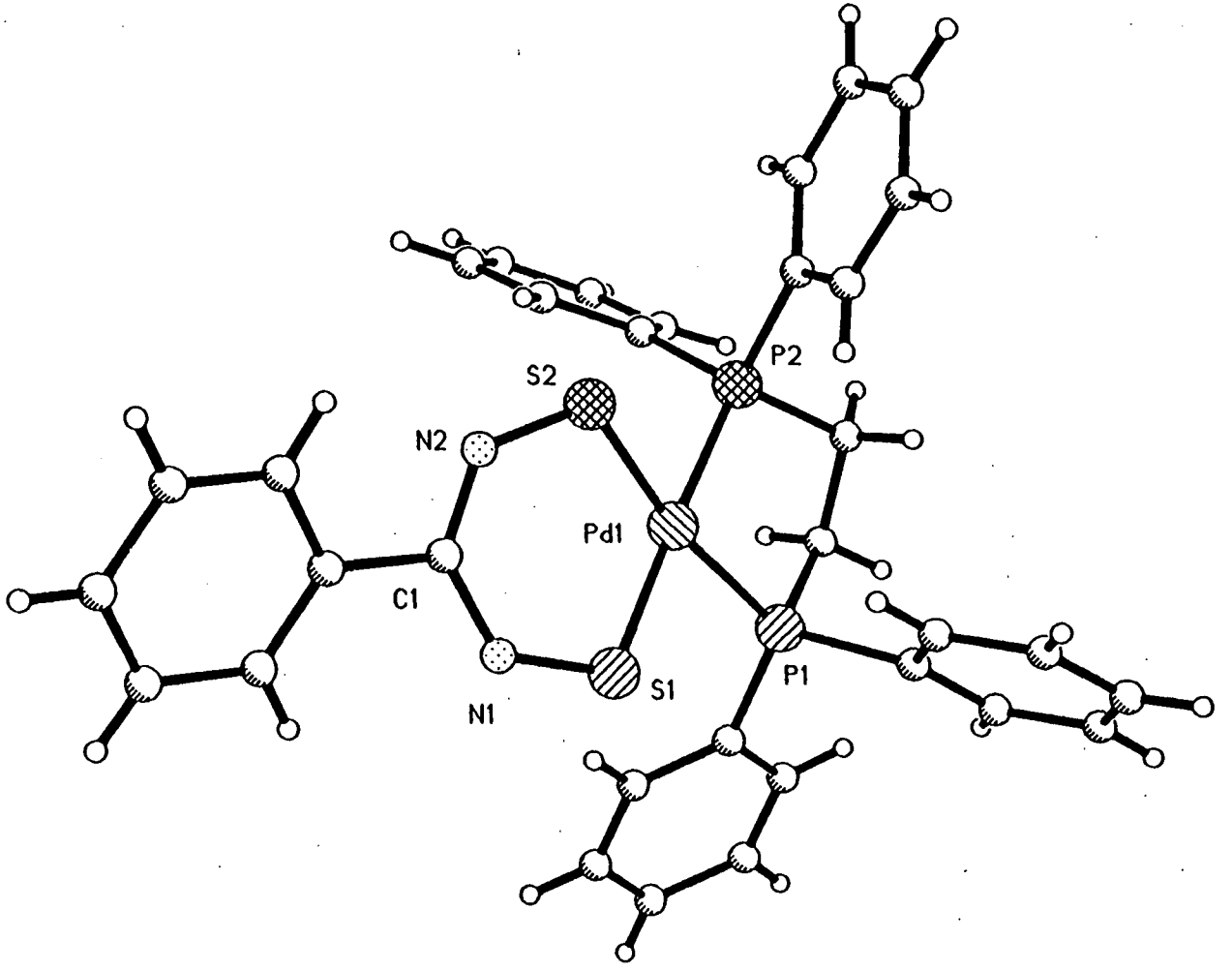

Figure 4.f. The X-Ray Structure of [Pt(SNC(Ph)NS-*S*,*S*)(PPh_3)$_2$] Superimposed On The X-Ray Structure [Pt(SNC(Ph)NS-*S*,*S*)(dppe)].

(the dppe and triphenylphosphine phenyl groups and all the protons have been removed for clarity)

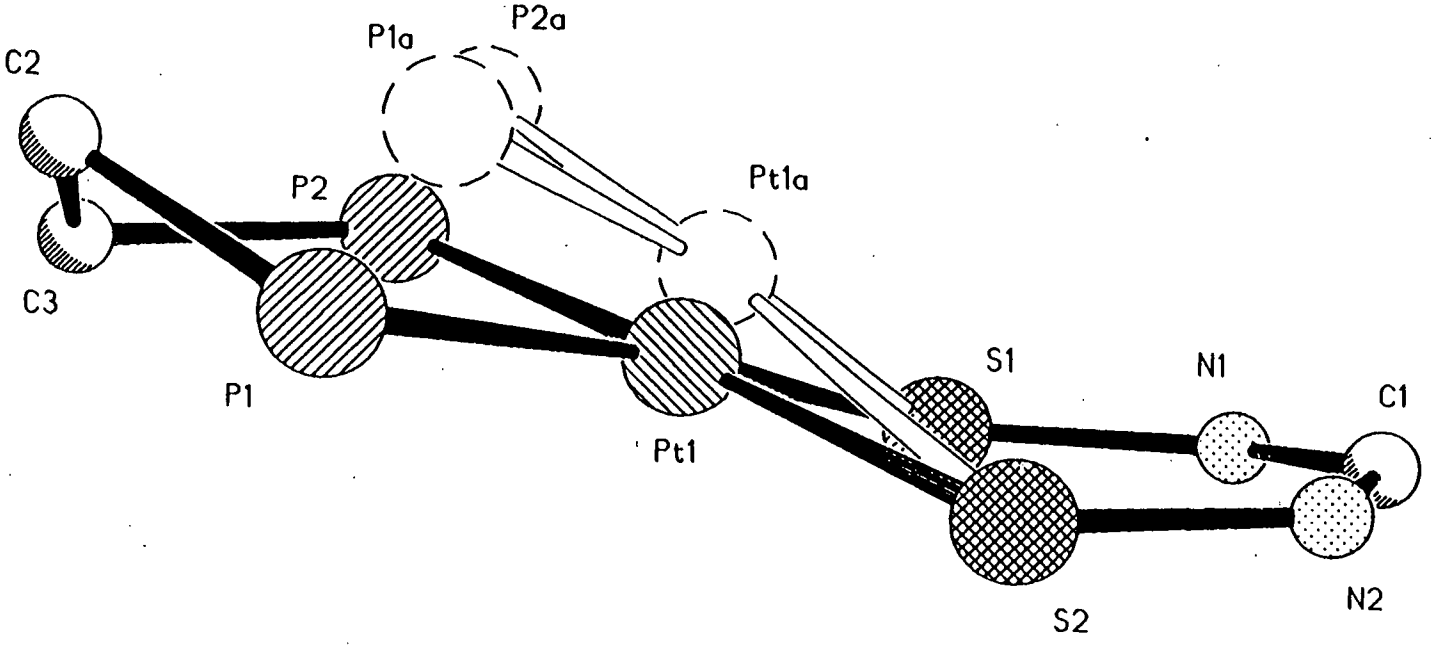

Table 4.a. Selected Bond Lengths and Angles for Monometallic Complexes.

Bond lengths (Å) and Angles (°)	[Pt(SNCPhNS*S*,*S*)(PPh3)2]	[Pt(SNCPhNS-*S*,*S*)(dppe)]	[Pd(SNCPhNS-*S*,*S*](dppe)]	[PhCNSSN]2
M - S, Å	2.294(2) 2.309(2)	2.285(6) 2.293(6)	2.285(3) 2.294(3)	------
M - P, Å	2.322(2) 2.311(2)	2.300(7) 2.308(6)	2.312(3) 2.339(3)	------
S - N, Å	1.628(7) 1.648(7)	1.64(2) 1.66(2)	1.629(9) 1.630(9)	1.62
C - N, Å	1.36(1) 1.33(1)	1.31(3) 1.34(3)	1.33(1) 1.36(1)	1.33
S(1)...S(2), Å	3.161(3)	3.281(9)	3.227(4)	2.089
S(1) - M - S(2), °	86.78(8)	91.2(2)	89.6(1)	------
P(1) - M - P(2), °	100.01(7)	85.9(2)	85.1(1)	------
S(1) - M - P(1), °	87.82(7)	93.9(2)	95.0(1)	------
S(2) - M - P(2), °	85.43(7)	88.7(2)	89.8(1)	------
M - S - N, °	115.2(2) 115.1(2)	116.5(8) 116.7(8)	117.6(3) 117.4(3)	115.5
S - N - C, °	128.4(5) 128.0(6)	130(2) 128(1)	129.0(8) 129.7(7)	------
angle δ, °	20.6(2)	10.6(4)	11.0(2)	

4.2.4. E.s.r. Spectroscopy.

From simple bonding principles there is no evidence for the unpaired electron present in [PhCNSSN]• being significantly involved in the bonding on complexation, as shown in the canonical form below figure 4.g.).

Figure 4.g. [M(SNCPhNS-*S,S*)(PR_3)$_2$].

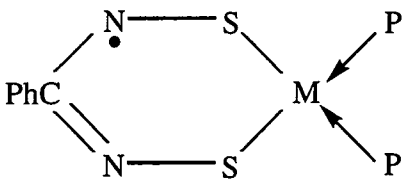

As such in solution monometallic complexes should exhibit an e.s.r. signal similar to that of the parent radical [PhCNSSN]•. All three complexes are e.s.r. active and gave signals with well resolved hyperfine splitting. Unfortunately, as previously stated, all three complexes decompose in CH_2Cl_2 liberating [PhCNSSN]• which partially obscures the signal for the complex. An example of this effect is shown for [Pt(SNCPhNS-*S,S*)(dppe)] (figure 4.h.).

To overcome this problem the complexes were prepared *'in situ'* from [PhCNSSN]• and the specific zero-valent phosphine complex. The excess phosphine complex reacts with any [PhCNSSN]• liberated during decomposition. In both Pt species (see figure 4.i. for spectrum of [Pt(SNCPhNS-*S,S*)(PPh_3)$_2$)]) there is hyperfine coupling to ^{195}Pt ($I=^1/_2$, 33%), and to the two nitrogen and two phosphorus nuclei. This indicates that the unpaired electron occupies a molecular orbital which is extensively delocalised over the whole metallo heterocyclic framework. The spectrum for [Pd(SNCPhNS-*S,S*)(dppe)] (figure 4.j.) shows even clearer resolution with hyperfine coupling to two phosphorus, two nitrogen and one palladium atom, ^{105}Pd ($I=^5/_2$, 22.23%).

The g-value, peak width (ΔB) and hyperfine splitting (a_x), for all three complexes and selected data for the fluorinated dithiadiazolyl platinum complex [Pt(SNC$_6F_5$NS-*S,S*)(PPh_3)$_2$] and [PhCNSSN]•[15] are given in table 4.b.

Table 4.b. Electron Spin Resonance Parameters for Monometallic Complexes (units in mT).

COMPOUND	PARAMETERS				
	g_{iso}	a_M	a_N	a_P	ΔB_{pp}
[PhCNSSN]$^{\bullet}$	2.0102	------	0.517	------	0.04
[Pt(SNCPhNS-S,S)(PPh_3)$_2$]	2.0386	5.385	0.553	0.280	0.20
[Pt(SNC$_6F_5$NS-S,S)(PPh_3)$_2$]	2.047	5.51	0.54	unobs	------
[Pt(SNCPhNS-S,S)(dppe)]	2.046	5.479	0.548	0.352	------
[Pd(SNCPhNS-S,S)(dppe)]	2.0310	0.372	0.573	0.383	0.10

In the case of [Pt(SNCPhNS-*S,S*)(PPh_3)$_2$] and [Pd(SNCPhNS-*S,S*)(dppe)] the values in (figure 4.b.) were used to simulate their spectra (figures 4.i. and 4.j. respectively).

A curious phenomenon in the spectra of the complexes is that the nitrogen hyperfine splitting of phenyl dithiadiazolyl actually increases on complexation despite radical electron seepage onto the metal. As hyperfine splitting is proportional to % occupancy of the free electron on any individual element, there must be gain of free radical electron density. As there is no electron density on the ring carbon (being on a node for the somo) then we must assume that free radical electron density is solely gained from the two ring sulfurs.

From the *in situ* preparation of [Pt(SNC$_6F_5$NS-S,S)(PPh_3)$_2$], from the parent radical and excess [Pt(PPh_3)$_4$] it was envisaged that hyperfine coupling to the aryl ring fluorines could be observed (as is the case for [C_6F_5CNSSN]$^{\bullet}$[16]). However, fluorine coupling only resulted in a broadening of the hyperfine interactions already observed.

Figure 4.h. E.s.r. Spectrum of [Pt(SNC(Ph)NS-*S,S*)(dppe)].

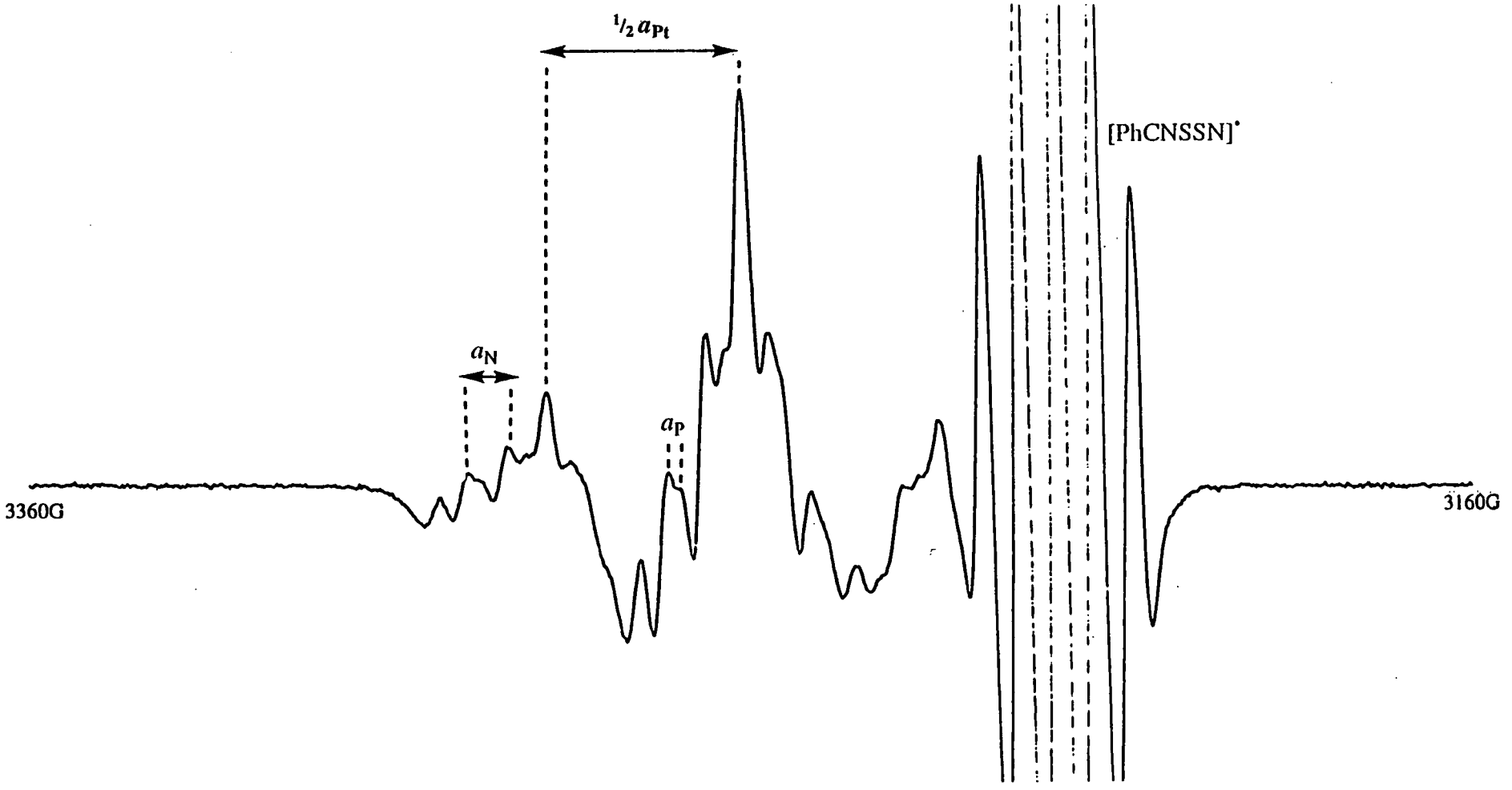

Figure 4.i. E.s.r. Spectrum of [Pt(SNC(Ph)NS-*S*,*S*)(PPh$_3$)$_2$]. Generated *'in situ'* from [PhCNSSN]$^\bullet$ and [Pt(PPh$_3$)$_4$].

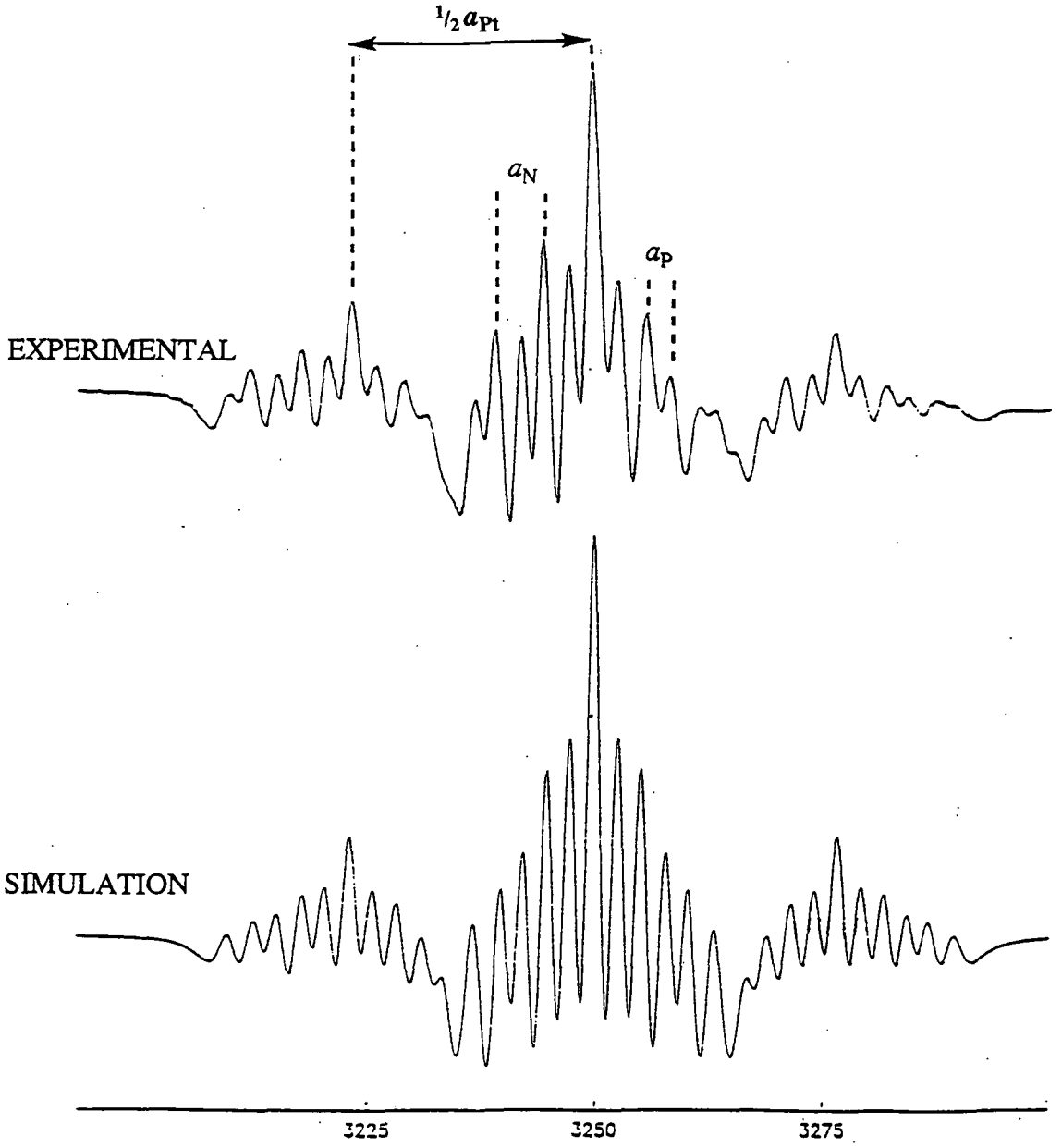

Figure 4.j. E.s.r. Spectrum of [Pd(SNC(Ph)NS-*S*,*S*)(dppe)]. Generated 'in situ' from [PhCNSSN]$^{\bullet}$ and [Pd(dppe)$_2$].

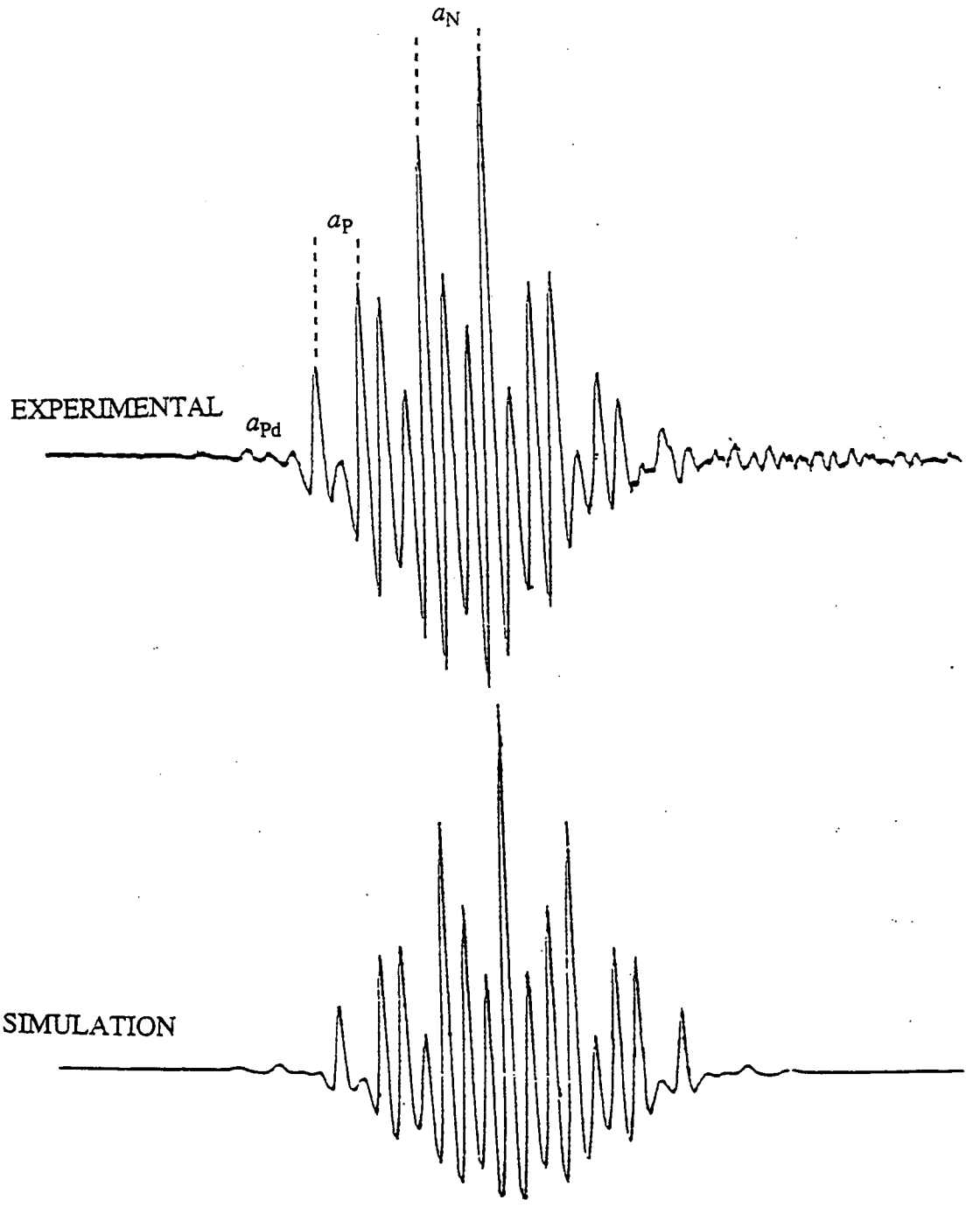

4.2.5. Molecular Orbital Studies on [Pt(SNC(H)NS-*S,S*)(PH_3)$_2$].

The e.s.r. spectroscopy measurements discussed in the previous section indicate what the singly occupied molecular orbital of monometallic dithiadiazolyl complexes would look like. EHMO calculations were undertaken by J.M.Rawson on the hypothetical 'parent' complex [Pt(SNC(HN)S-*S,S*)(PH_3)$_2$], the phenyl groups being replaced by H to simplify the calculation. The input geometry was identical to that observed in the crystallographic study apart from the phenyl groups replaced by protons at 1.08A. The HFOMO (highest fully occupied molecular orbital), SOMO (singly occupied molecular orbital) and LUMO (lowest unoccupied molecular orbital) are shown in figure 4.k.

The SOMO of the complex is formed by interaction of the Pt d_{xz} orbital with the SOMO of the [HCNSSN]$^{\bullet}$ radical and is antibonding with respect to both S-N and S-Pt. As with the dithiadiazolyl radical itself, the SOMO is nodal at carbon. Of particular interest is the fact that the SOMO has no orbital contribution from P. We must therefore assume that the P coupling observed in the e.s.r. spectrum occurs via a spin polarisation mechanism - when the coupling parameter (isotropic hyperfine interaction)[17] for P is taken into account the amount of s orbital density found on P is about fifty times that observed for N. The LUMO, some 3eV above the SOMO, is predominantly based on the NCN fragment of the dithiadiazolyl ring with less than 1% contributions from either S or Pt. The HFOMO, only 0.8eV below the SOMO, is formed by interaction of the HFOMO of [HCNSSN]$^{\bullet}$ with d orbitals based on Pt. The d_{yz} orbital contributes the greatest component (32%) of the orbital contribution, although there is also a further 15% from d_{x2-y2} and 5% from d_{z2} orbitals.

Figure 4.k. Frontier Molecular Orbitals of [Pt(SNC(H)NS-*S*,*S*)(PH_3)$_2$].

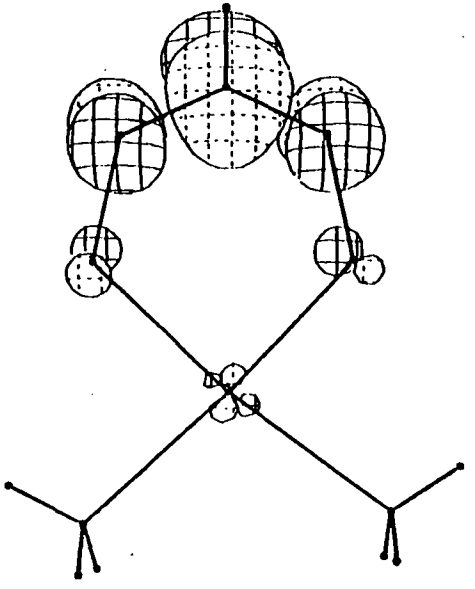

LUMO
-8.00eV

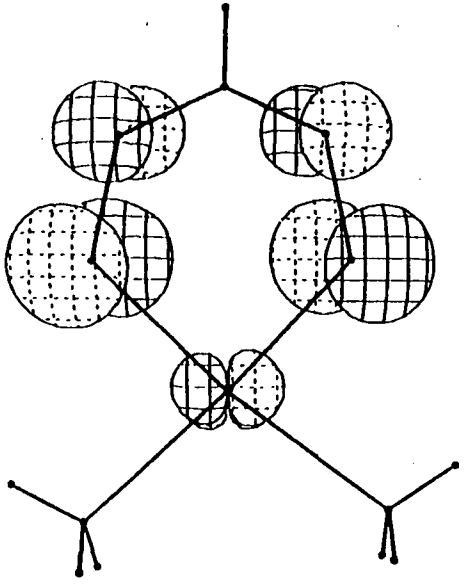

SOMO
-11.03eV

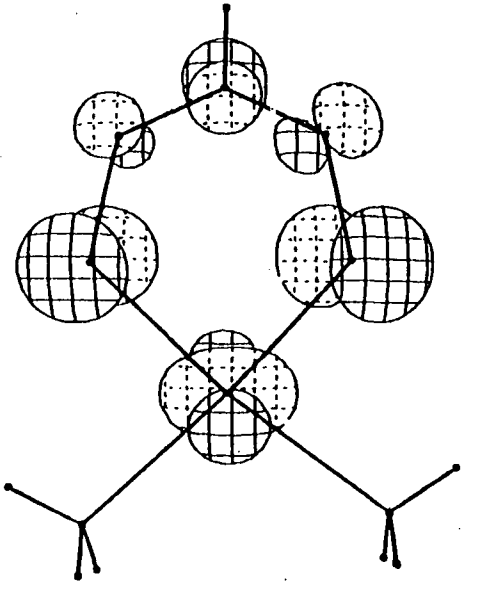

HFOMO
-11.83eV

4.2.7. Magnetic Measurements.

From e.s.r. spectroscopy and m.o. calculations there is conclusive proof for the presence of an unpaired electron in the isolated molecule and in solution. X-ray crystallography on [Pt(SNCPhNS-*S,S*)(PPh_3)$_2$], [Pt(SNCPhNS-*S,S*)(dppe)], and [Pd(SNCPhNS-*S,S*)(dppe)] have also shown that these monomeric radical complexes do not closely interact in the solid state (i.e. do not dimerise like the parent compound (PhCNSSN)$_2$). Magnetic measurements were undertaken on the three [PhCNSSN]$^{\bullet}$ complexes shown above to demonstrate the existence and magnetic effect of this free electron in the solid state and to elucidate its magnetic properties.

All the magnetic data obtained are shown in graphical form on the pages immediately after this description.

Plots of magnetic susceptibility (χ) *vs* temperature (K) for all three complexes are shown in figures 4.l., 4.p. & 4.t. As the temperature is lowered there is a gradual spin alignment of the unpaired electrons with the applied magnetic field. This results in an exponential increase in magnetic susceptibility on lowering the temperature. If the graph were extrapolated to 0K then in each case χ would reach infinity.

The plot of inverse magnetic susceptibility *vs* temperature for [Pt(SNCPhNS-*S,S*)(PPh_3)$_2$] and [Pt(SNCPhNS-*S,S*)(dppe)] (figures m & q) results in a linear dependence of $^1/_\chi$ as a function of temperature. Both compounds thus obeys the Curie-Weiss law (equation 4.b.) where θ is the temperature when $^1/_\chi = 0$. This temperature θ is 4K for both Pt species[18].

$$\chi \ \alpha \ {}^{1}/_{(T-\theta)}$$

Equation 4.a. Curie -Weiss Law

At higher temperatures there is a slight increase in $^1/_\chi$ above the line representing linear dependency. This is due to the fact that no diamagnetic correction[19] has been made for the sizeable number of paired electrons involved in bonding in these two large molecules

[note; $\chi_{obs} = \chi_{paramagnetic} + \chi_{diamagnetic}$]. At higher temperatures, and thus lower $\chi_{paramagnetic}$ this diamagnetic constant will have a larger effect.

Below 110K, [Pd(SNCPhNS-*S,S*)(dppe)] (figure 4u) also obeys the Curie-Weiss law where again $\theta = 4K$. From this temperature onwards $^1/_\chi$ increases markedly above the linear dependence value, and by too large a factor to be explained solely by the lack of a diamagnetic correction. It must be assumed that due to the poor stability of the palladium species there must be a fair proportion of the decomposition product, [$Pd_3(\mu_S$-$_S$SNCPhNS-*S,S*)$_2$(dppe)$_2$], present (this complex will be discussed further in chapter 5). The effect of this diamagnetic impurity coupled with the paired electron effect described for the two Pt species, results in a big decrease of χ at higher temperatures and thus further increases $^1/_\chi$.

The magnetic moment (μ_{eff} mol^{-1}) for [Pt(SNCPhNS-*S,S*)(PPh_3)$_2$].MeCN (figure 4.n) and [Pt(SNCPhNS-*S,S*)(dppe)] (figure 4.r.) is about 1.73BM down to 20K. This value is typical for an S=$^1/_2$ spin only paramagnet with one unpaired electron per molecule[20]. Below this temperature there is an exponential increase in magnetic moment. This is taken to be due to small amounts of [PhCNSSN]$^\bullet$ radical impurity as explained below. The magnetic moment is proportional to the square route of χT. As the temperature is lowered the value for χ becomes more influential and if the value for χ is higher than expected, then μ_{eff} will also increase. The calculations take into account the molecular weight of the complexes (i.e. 941.63g for [Pt(SNCPhNS-*S,S*)(PPh_3)$_2$].MeCN and any lower molecular weight species with unpaired electrons (i.e. [PhCNSSN]$^\bullet$, 181.26g) will artificially increase the magnetic susceptibility. The same effect is observed for [Pd(SNCPhNS-*S,S*)(dppe)] (figure 4.v.) although the magnetic moment is lower than expected at all temperatures due to the presence of the diamagnetic impurity [Pd_3(SNCPhNS-*S,S*)$_2$(dppe)$_2$] .

Finally a plot of χT *vs* temperature was made for all three complexes (figures 4.o., 4.s. & 4.w.). Again, as anticipated, at lower temperatures this value increases greatly due to [PhCNSSN]$^\bullet$ impurity and in the palladium species the value for χT is lower due to the reasons already explained in the previous paragraph.

Thus all three monometallic complexes are classical paramagnetic materials and it has been possible to prepare a series of [PhCNSSN]$^{\bullet}$ based compounds which do not dimerise in the solid state to form diamagnetic solids. Presumably the lack of interaction between neighbouring electrons is due to the bulky phenyl phosphine groups which prevent close interaction between unpaired electrons in adjacent molecules.

Magnetic Measurements on [Pt(SNC(Ph)NS-*S*,*S*)(PPh_3)$_2$]MeCN.

Figure 4.l.

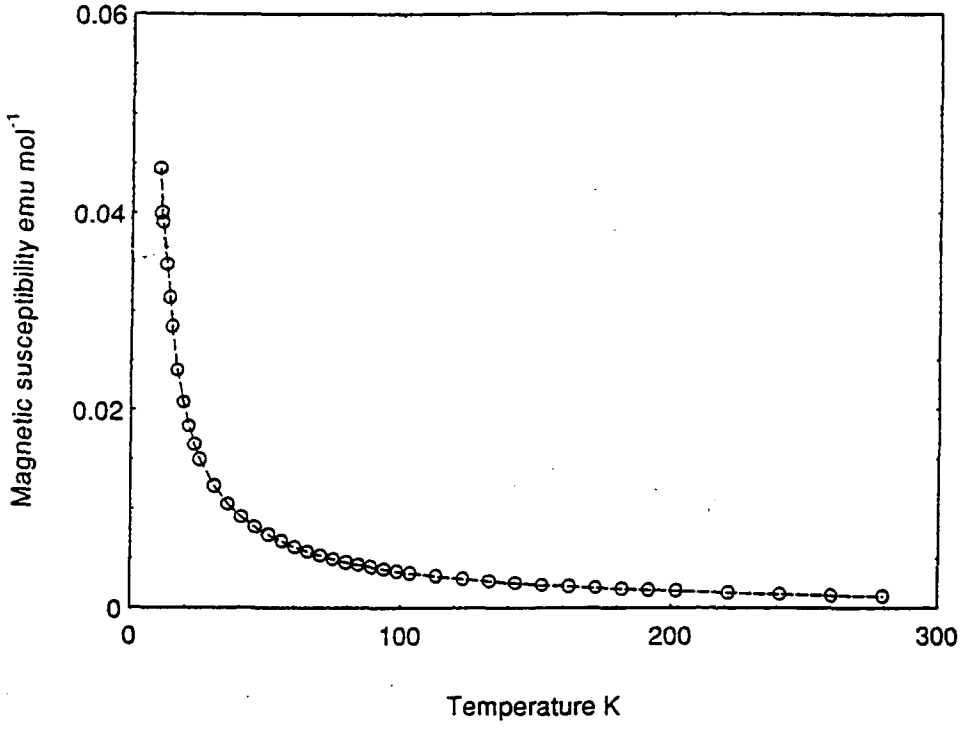

Figure 4.m.

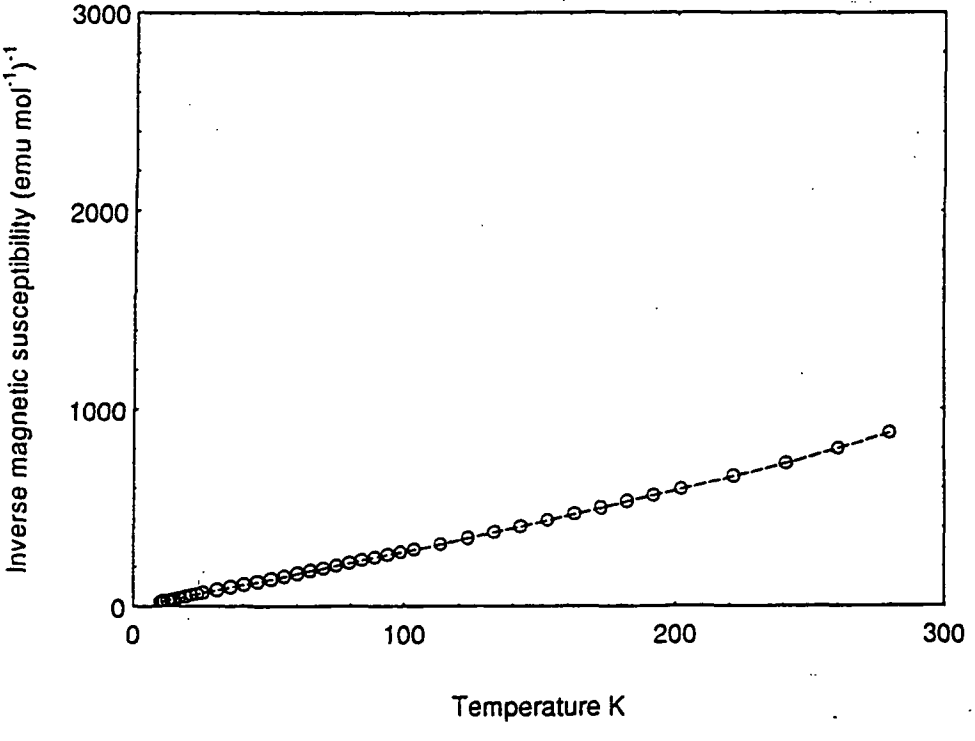

Magnetic Measurements on [Pt(SNC(Ph)NS-*S*,*S*)(PPh$_3$)$_2$].MeCN.

Figure 4.n.

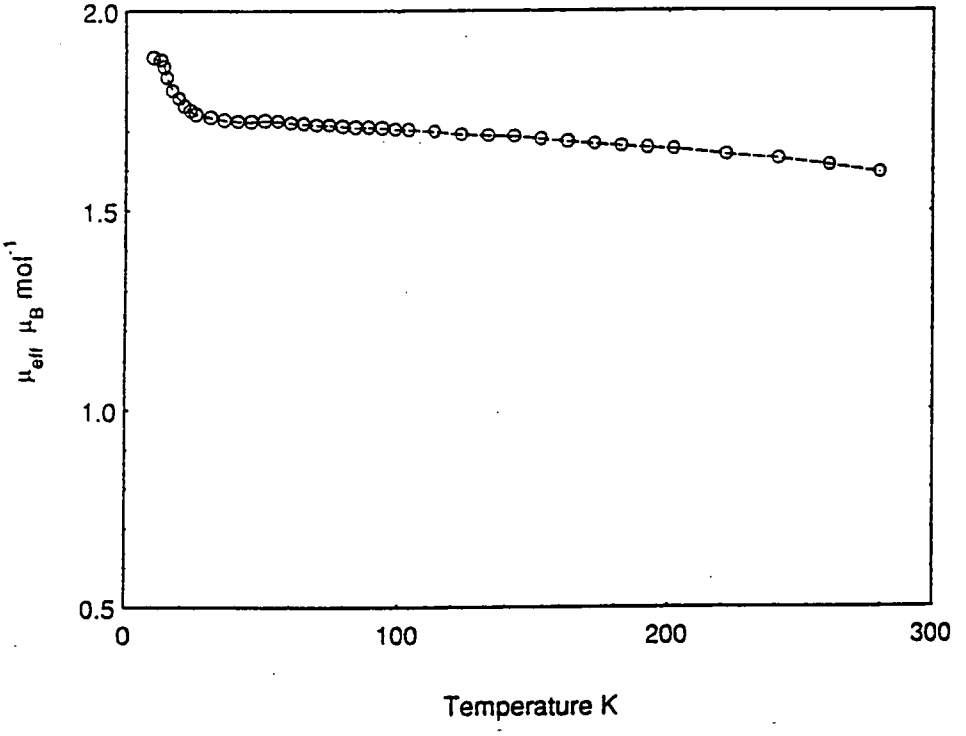

Figure 4.o.

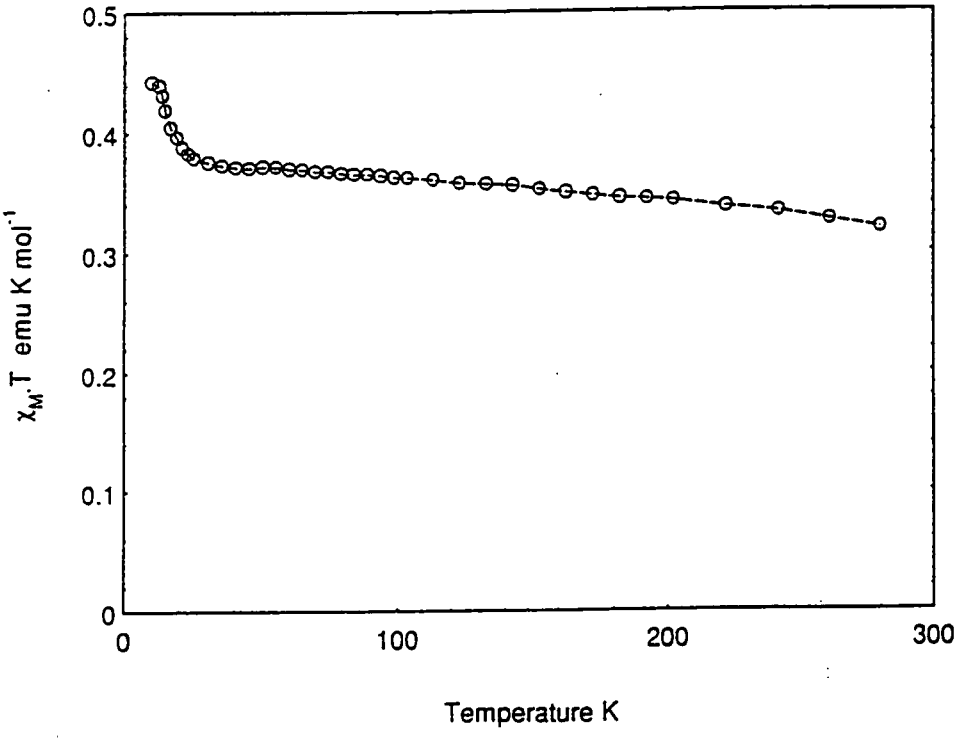

Magnetic Measurements on [Pt(SNC(Ph)NS-*S*,*S*)(dppe)].

Figure 4.p.

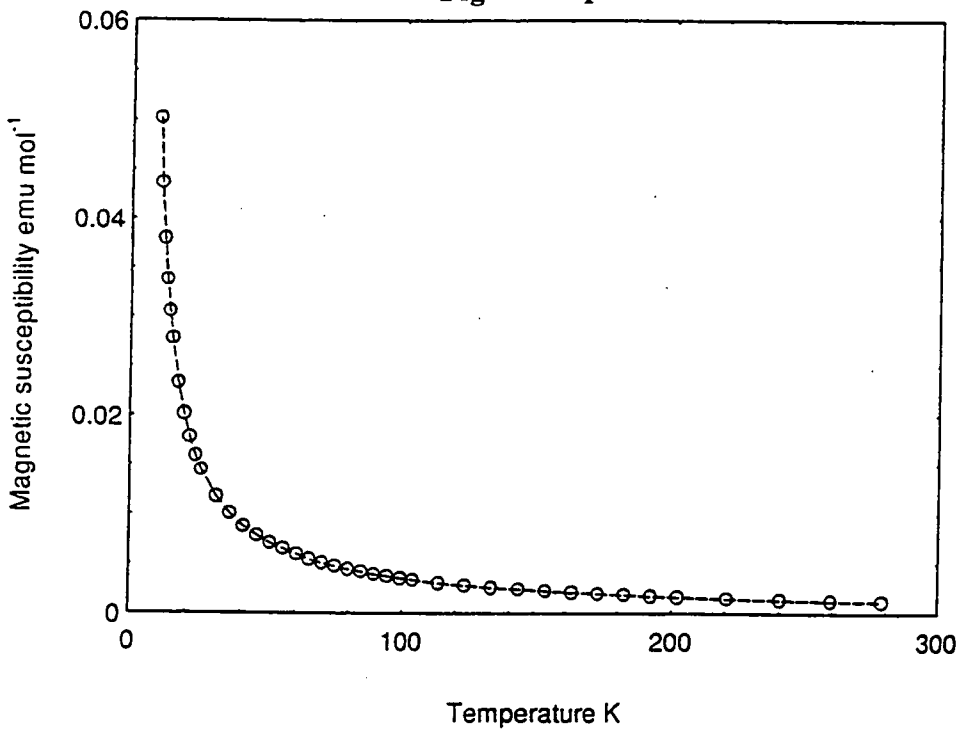

Figure 4.q.

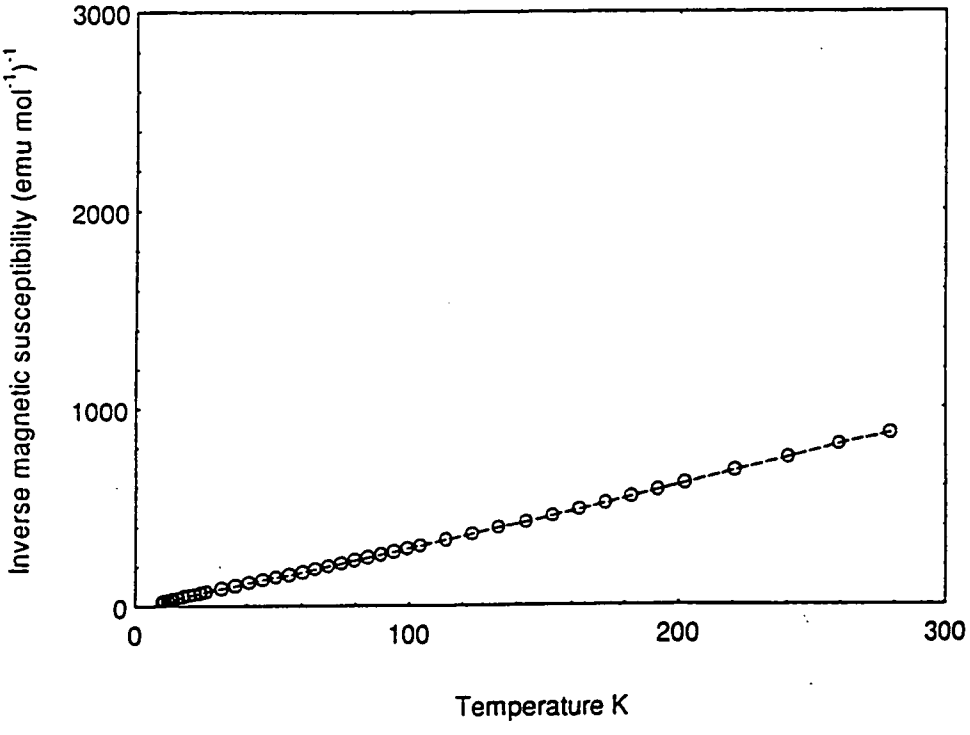

Magnetic Measurements on [Pt(SNC(Ph)NS-*S*,*S*)(dppe)].

Figure 4.r.

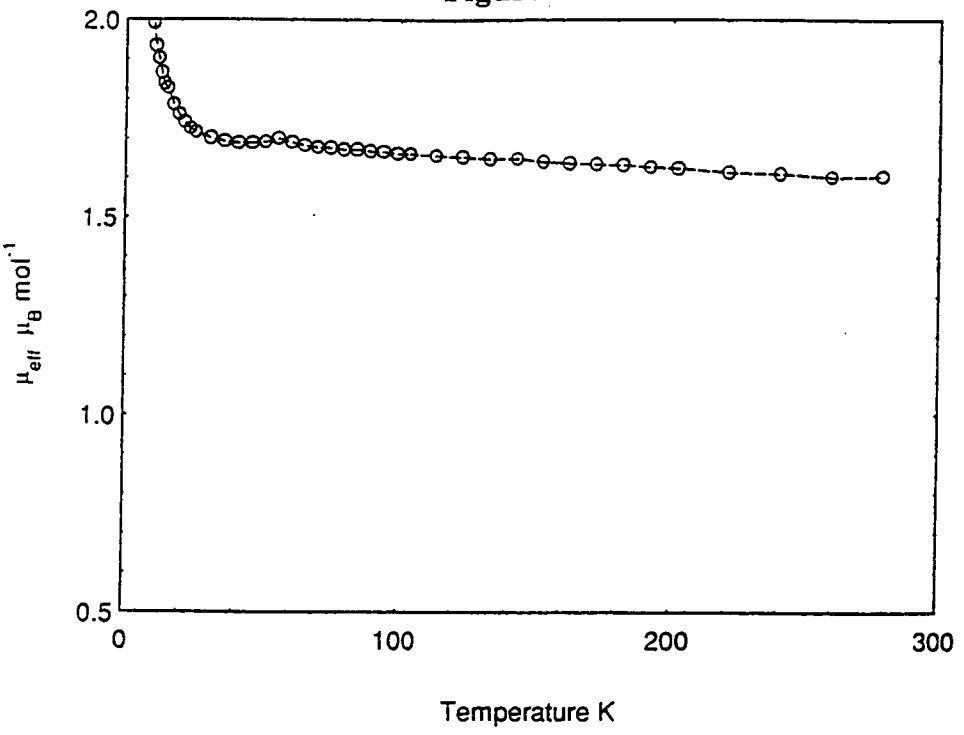

Figure 4.s.

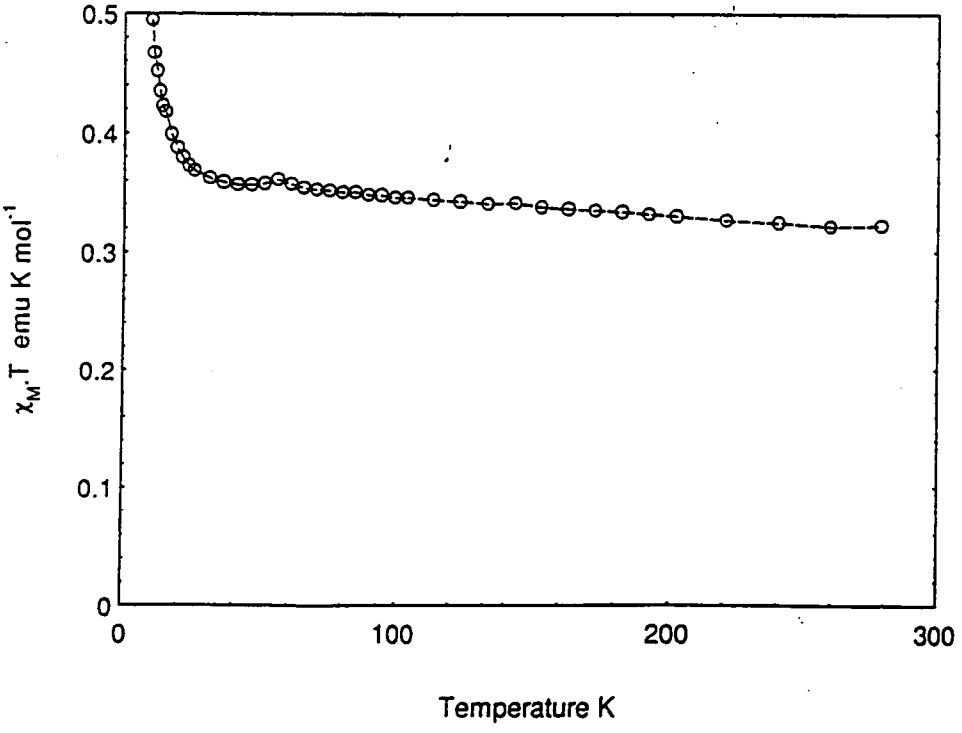

Magnetic Measurements on [Pd(SNC(Ph)NS-*S*,*S*)(dppe)].

Figure 4.t.

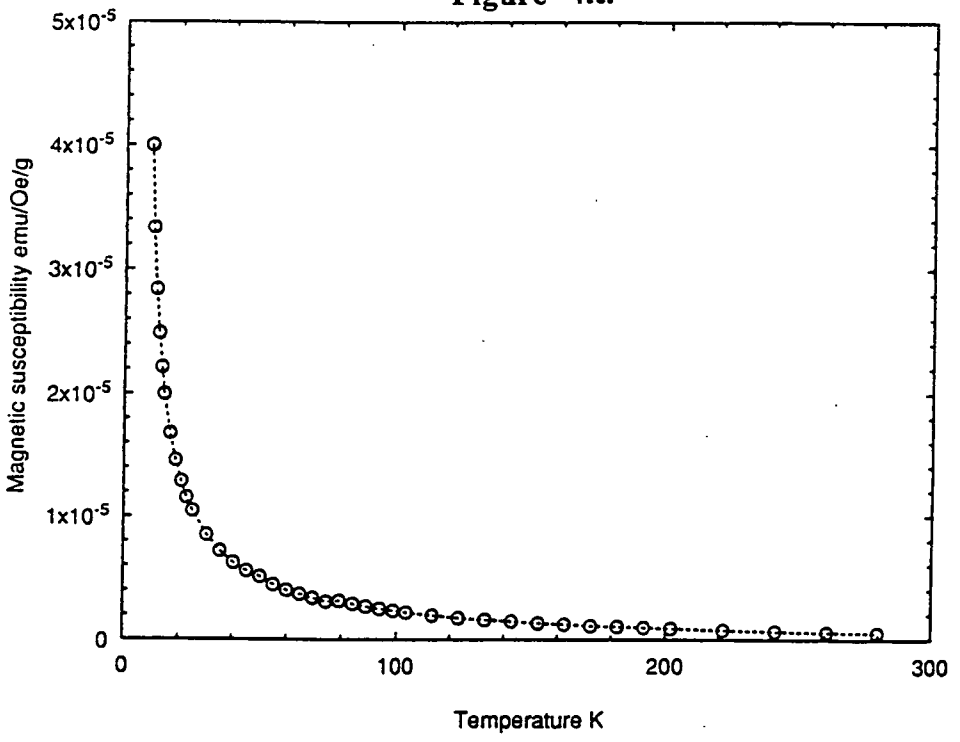

Figure 4.u.

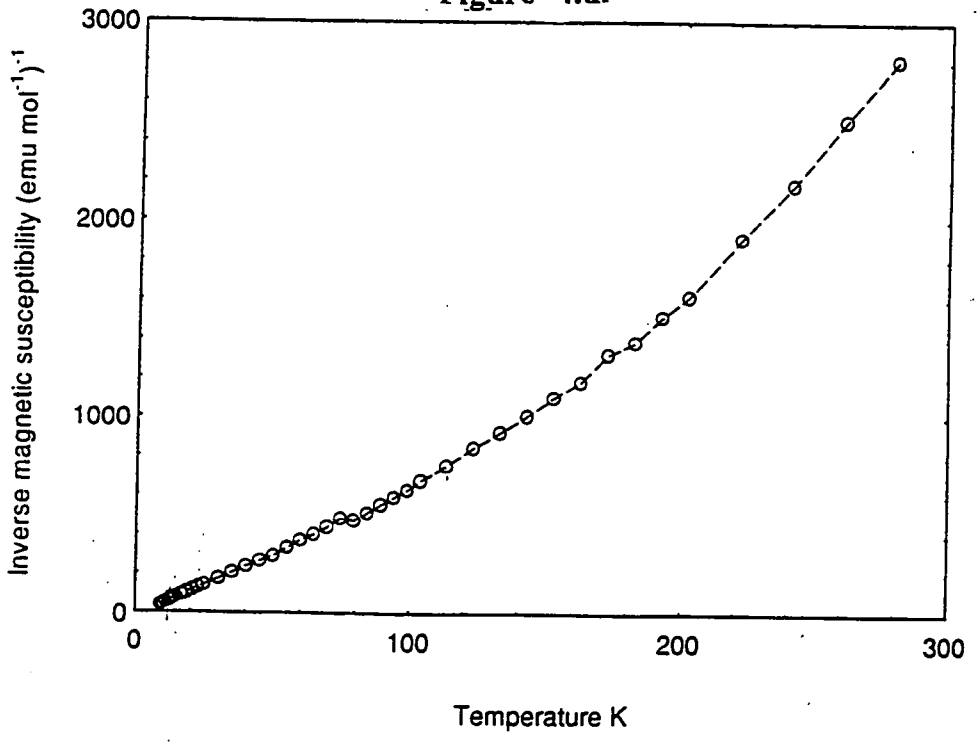

Magnetic Measurements on [Pd(SNC(Ph)NS-*S*,*S*)(dppe)].

Figure 4.v.

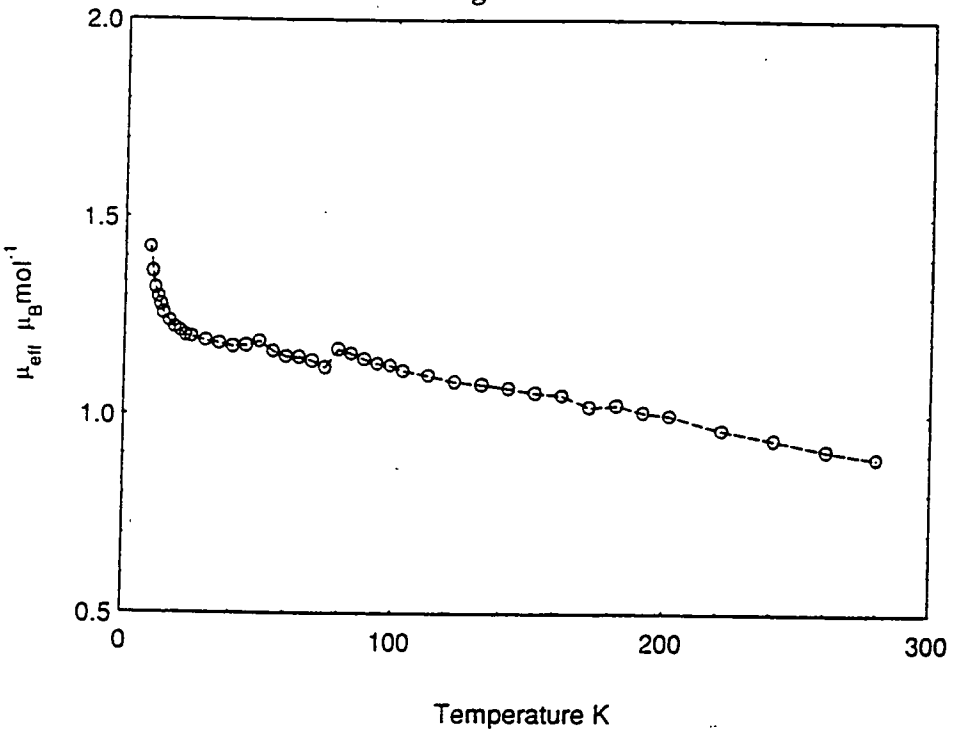

Figure 4.w.

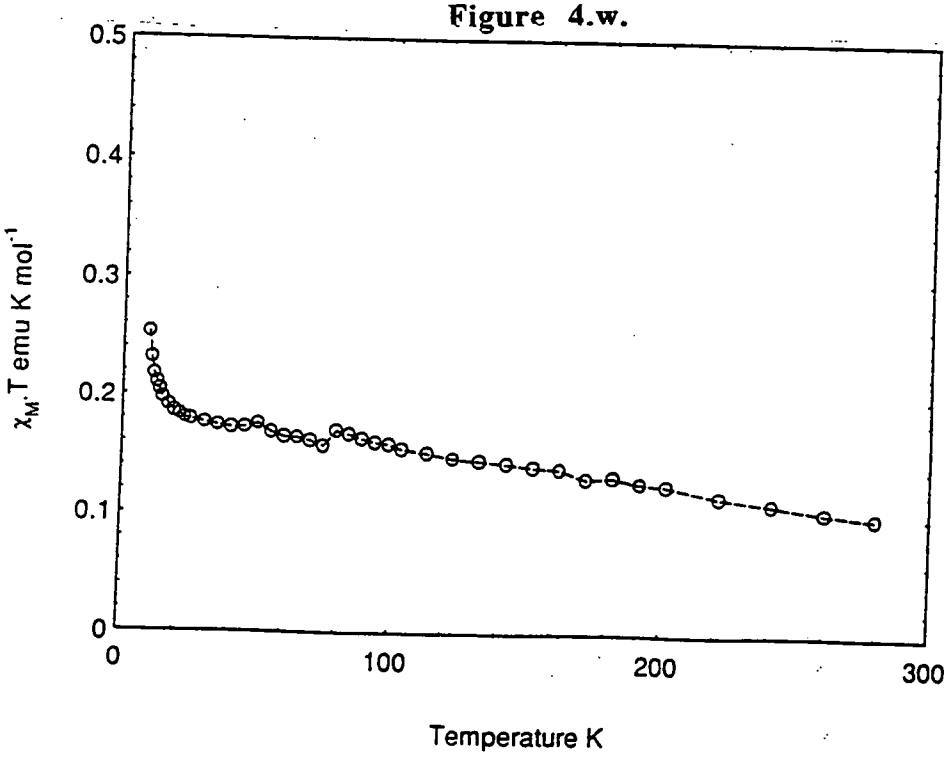

4.2.8. Ultra Violet/Visible Spectroscopy.

The U.V./visible spectra of all the monometallic dithiadiazolyl complexes prepared show an absorbance at the red end of the visible region with λ values of between 658 and 684nm e.g. see figure 4.x for spectrum of [Pt(SNC(Ph)NS-*S*,*S*)(PPh_3)$_2$]. In contrast, the parent radicals [RCNSSN]$^\bullet$ show no absorbance in this region. Due to the rapid decay of the signal caused by the decomposition of the complexes in solution, an accurate measurement of extinction coefficient was not possible[21]. It was therefore not possible to determine the particular ligand-metal transition that occurs. Values for a range of monometallic species prepared by both the author and O.G.Dawe are shown in table 4.c.

Figure 4.x. U.V./Vis Spectrum of [Pt(SNC(Ph)NS-*S*,*S*)(PPh_3)$_2$]

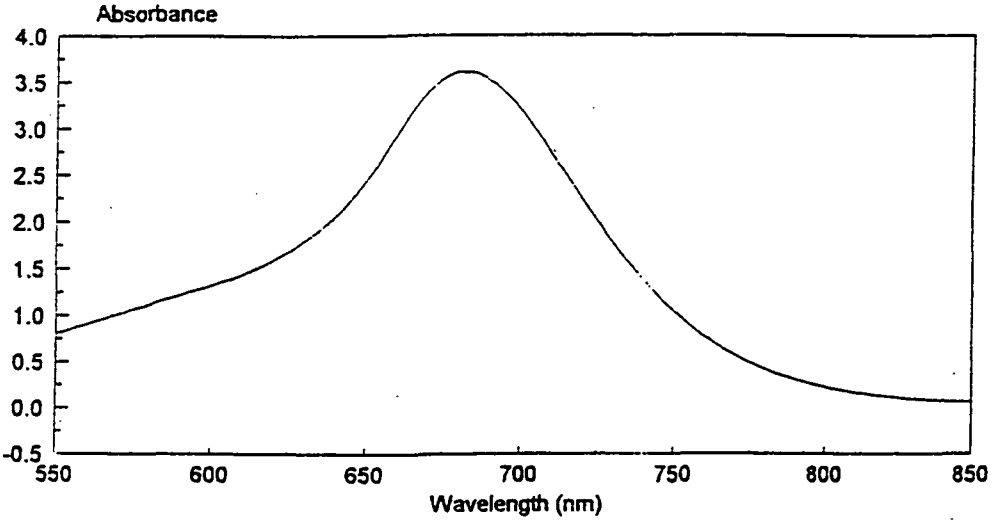

Table 4.c. U.V./Vis Spectroscopy Measurements For Monometallic Dithiadiazolyl Complexes.

COMPLEX	ABSORPTION	WAVELENGTH (λ, nm)	CONCENTRATION (Molarity x10^3)	EXTINCTION COEFFICIENT (ε)
$Pt(SNCPhNS\text{-}S,S)(PPh_3)_2$	3.606	680	3.11	1161
$Pt(SNC(p\text{-}ClC_6H_4)NS\text{-}S,S)(PPh_3)_2$	1.730	684	5.6	309
$Pt(SNC(p\text{-}BrC_6H_4)NS\text{-}S,S)(PPh_3)_2$	2.300	684	4.4	523
$Pt(SNC(3,4,FC_6H_3)NS\text{-}S,S)(PPh_3)_2$	3.505	682	5.1	687
Pt(SNCPhNS-S,S)(dppe)	2.720	658	3.10	877
$Pt(SNC(3,4,FC_6H_3)NS\text{-}S,S)$(dppe)	3.75	660	6.78	553
Pd(SNCPhNS-S,S)(dppe)	0.474	672	3.10	153

4.2.9. Biological Properties.

As highlighted in chapter 3 square-planar platinum complexes have atttracted great biomedical interest due to the anti-cancer activity that many exhibit. Johnson Matthey expressed an interest in this biological aspect of the monometallic platinum dithiadiazolyl complexes. They all contain $16e^-$ square-planar platinum and the free radical is delocalised over the extended ring system. It was hoped that this free radical would increase activity (free radical compounds are well known for their toxicity).

The triphenyl phosphine complex [Pt(SNCPhNS-*S,S*)$(PPh_3)_2$].MeCN. was extensively tested against a series of cell cultures including human tumour lines (e.g. SKOV-3)[20] and the results are shown in table 4.d. The parameter employed, IC_{50} is the concentration of compound (μg/ml) required to give 50% decrease in cell proliferation of a culture (i.e. the less compound required the higher the toxicity). The values for the parent anti-cancer drug cis platin $[Pt(NH_3)_2Cl_2]$[22] are also shown for comparison. Cis^R samples are cultures which have previously been exposed to cis-platin and have thus gained a degree of resistance. The resistance factor (R.F.) gives a measure of how active a complex is against a resistant strain of a culture as compared with the non-resistant strain.

It is evident that [Pt(SNCPhNS-*S,S*)$(PPh_3)_2$.MeCN] is more potent than cis-platin against almost all the cell strains tested. This is almost certainly mainly due to the presence of the free radical on the complex although the presence of toxic MeCN in the lattice may also be a factor.

On initial examination these results are encouraging. On closer examination, however, there is little selectivity in the activity i.e. the dithiadiazolyl complex is very toxic towards all cell cultures. This is not a useful property when only cancerous cells are to be targeted. Also, although the complex is remarkably stable in water it is very insoluble in aqueous systems (e.g. the human body). As a result of these findings no further testing was deemed worthwhile with respect to the use of [Pt(SNCPhNS-*S,S*)$(PPh_3)_2$] as an anti-cancer drug though the toxicity and solubility characteristics can be expected to change for related compounds. All monometallic dithiadiazolyl species should, though, be treated with great care.

Recently [Pt(SNC(3,4F-C_6H_3NS-*S,S*)(PPh_3)$_2$] and [Pt(SNC(3,4F-C_6H_3)NS-*S,S*)(dppe)] have been submitted for biological testing. It is hoped that the partially fluorinated species may possess more discrimination in their biological properties.

Table 4.d. Biological Test Results For [Pt(SNCPhNS-*S,S*)(PPh_3)$_2$]. IC_{50} vs. Cell Line

CELL CULTURE	[Pt(SNCPhNS-*S,S*)(PPh_3)$_2$]	CISPLATIN
A2780	0.5	8.90
A2780 cis^R	0.35	29.0
A2780 RF	0.7	3.3
CH1	0.43	0.082
CH1 cis^R	0.43	0.33
CH1 RF	1	4.0
41M	0.66	0.22
41M cis^R	0.7	1.05
41M RF	1.1	4.7
SKOV-3	1.45	14.5
HX62	1.05	2.80

$$\text{RF} = \text{Resistance factor} = \frac{\text{IC50 Resistant (cisR) Line}}{\text{IC50 Sensitve Line}}$$

4.2.10. F.A.B. Spectroscopy of [Pt(SNCPhNS-*S,S*)(PPh_3)$_2$].

The FAB mass spectrum (positive ion) of [Pt(SNCPhNS-*S,S*)(PPh_3)$_2$] shows the parent ion Pt(SNCPhNS-*S,S*)(PPh_3)$_2$ 901, and its breakdown product Pt(PPh_3)$_2$ 719. However, there are also molecular ion peaks at higher $^m/_z$ ratios which can be assigned to dimetallic species [Pt_2(μ–SNCPhNS-*S,S*)(PPh_3)$_4$] 1620, [Pt_2(μ–SNCPhNS-*S,S*)(PPh_3)$_3$ 1358 and [Pt_2(μ_2–SNCPhNS-*S,S*)(PPh_3)$_2$] 1096. It is not uncommon for monometallic species to dimerise in the FAB source[23] and gives evidence for the formation of oligomeric complexes.

4.2.11. Other Techniques.

Cyclic Voltammetry experiments were undertaken on all three main monometallic complexes and the results are discussed in Chapter 7.

Due to the presence of the unpaired electron, the ^{1}H n.m.r spectra of monometallic species are poorly resolved and are affected by paramagnetic broadening as discussed in chapter two. No peaks attributable to monometallic complexes could be observed in the ^{31}P n.m.r. between 300 and -300ppm, even when the complex is prepared *in situ* from the starting zero-valent phosphine and [PhCNSSN]$^\bullet$. This is not suprising; it is often the case that species that yield good e.s.r. spectra have n.m.r. resonances too broadened to be observable[24].

4.3. EXPERIMENTAL.

4.3.1. Preparation of [Pt(SNCPhNS-S,S)(PPh_3)$_2$].MeCN.

[$Pt(PPh_3)_4$] (0.500g, 0.402mmol) and $(PhCNSSN)_2$ (0.073g, 0.20 mmol) were stirred in MeCN (20ml) to yield, immediately, a deep green-blue, microcrystalline precipitate under a green solution. The suspension was stirred for 20min, filtered and washed with fresh MeCN (3x10ml). The pale green filtrate and washings were discarded and the microcrystalline solid dried *in vacuo*

Yield 0.288g,76%.

IR $\nu_{max}(cm^{-1})$ 3051w, 1480m, 1435ssh, 1324m, 1178w, 1160w, 1095ssh, 1070w, 1026w, 999w, 925w, 900w, 823w, 742m, 693s, 645wsh, 536s, 522s, 510s, 496m, 459w, 429w.

Elemental analysis, found: C57.61%; H3.95%; N4.19. Calc.: C57.37%; H4.07%; N4.46%).

U.v. absorption (CH_2Cl_2) λ_{max} $680nm^{-1}$ (ε= $1116dm^3mol^{-1}cm^{-1}$).

E.s.r., g= 2.0485, a_{Pt}=5.30mT, a_P=0.26mT, a_N=0.55mT.

Ds.c. 136°C (dec.).

4.3.2. Crystal growth of [Pt(SNCPhNS-*S,S*)(PPh_3)$_2$].MeCN,

Freshly prepared [$Pt(PPh_3)_3$] (0.010g, 0.08mmol) was placed in one limb of a two-limbed vessel with $(PhCNSSN)_2$ (0.100g, 0.28mmol) in the other. MeCN (10ml) was added to each. Inversion of the sealed reaction vessel allowed slow diffusion through a grade three sinter of a solution of [PhCNSSN]$^{\bullet}$ into the former limb. Within 30min dark blue-green crystals were forming over solid [$Pt(PPh_3)_3$]. After three days the solvent was removed yielding a number of well-formed crystals suitable for X-ray analysis.

4.3.3. Preparation of [Pd(SNCPhNS-*S,S*)(dppe)].

[$Pd(dppe)_2$] (0.500g, 0.55mmol) and $(PhCNSSN)_2$ (0.11g, 0.30mmol) were stirred in MePh (20ml) to yield immediately a deep green precipitate under a green solution. The suspension was stirred for $1^1/_2$h, filtered and washed with fresh MePh (3x10ml). The pale green filtrate and washings were discarded and the solid was dried *in vacuo*

Yield 0.37g, 97%.

IR $\nu_{max}(cm^{-1})$ 3053m, 1483sh, 1435ssh, 1319m, 1172w, 1103m, 1026w, 998w, 875w, 823m, 746m, 706ssh, 692ssh, 655w, 528ssh, 483m.

Elemental analysis, found: C,58.04%; H,3.72%; N,4.39%. Calc.: C,57.76%; H,4.27%; N4.08%.

U.V. absorption (CH_2Cl_2) λ_{max} 672.0nm^{-1}, (ε = 153$dm^3mol^{-1}cm^{-1}$).

E.s.r.; g= 2.03, a_{Pd}=0.63mT, a_P=0.37mT, a_N=0.56mT.

D.s.c. 154°C (dec.).

4.3.4. Crystal growth of [Pd(SNCPhNS-*S,S*)(dppe)]

Freshly prepared [$Pd(dppe)_2$] (0.069g, 0.076mmol) and $(PhCNSSN)_2$ (0.095g, 0.26mmol) were placed in separate limbs of a two bulbed vessel separated by a grade 3 sinter. MeCN (10ml) was added to each and the reaction vessel inverted. Slow diffusion of the [PhCNSSN]$^{\bullet}$ solution through the sinter occurred and within 30mins dark green crystals were forming over solid [$Pd(dppe)_2$]. After a day the solvent was removed yielding a number of well formed crystals suitable for X-ray analysis.

4.3.5. Preparation of [Pt(SNCPhNS-*S,S*)(dppe)],

[$Pt(dppe)_2$] (0.850g, 0.85mmol) and $[PhCNSSN]_2$ (0.16g, 0.44 mmol) were stirred in MePh (10ml) at 70°c to yield an immediate deep royal blue precipitate under a blue solution. The suspension was stirred for 24hrs with no colour change, filtered and the solids washed with fresh MePh (3x10ml). The pale blue filtrate plus washings were discarded and the solid was dried in vacuo.

Yield 0.41g,92%.

IR $\nu_{max}(cm^{-1})$ 2862w, 2724w, 2362w, 1654w, 1591w, 1570w, 1462s, 1377s, 1318ssh, 1225sh, 1169sh, 1098w, 1023w, 997w, 919w, 896w, 881w, 846w, 822sh, 812sh, 769w, 758w, 744sh, 710ssh, 702ssh, 689ssh, 654w.

Elemental analysis found: C,51.27%; H,3.72%; N,4.46%. Calc.:C,51.15%; H,3.78%; N3.62%).

U.V. absorption (CH_2Cl_2) λ_{max} 680.0nm^{-1}, (ε = 877$dm^3mol^{-1}cm^{-1}$).

E.s.r. g= 2.04, a_{Pt}=5.48mT, a_P=3.56mT, a_N=5.48mT.

D.s.c.218°C (dec.).

4.3.6. Crystal growth of [Pt(SNCPhNS-*S*,*S*)(dppe)].

$[Pt(dppe)_2]$ (0.050g, 0.05mmol) and $[PhCNSSN]_2$ (0.084g, 0.23mmol) were placed in separate limbs of a two bulbed vessel separated by a grade 3 sinter. MeCN (10ml) was added to each and the reaction vessel inverted. Slow diffusion of the $[PhCNSSN]^{\bullet}$ solution through the sinter occurred and within 30mins dark blue crystals were forming over solid $[Pt(dppe)_2]$. After a day the solvent was removed yielding a number of well formed crystals suitable for X-ray analysis.

4.4. CONCLUSION.

In this chapter a new range of metal dithiadiazolyl complexes has been discovered and extensively characterised. The major problem in handling these complexes, their instability in solution, has been overcome and crystalline material was isolated for structural characterisation. These monometallic platinum and palladium species ([M(SNC(R)NS)$(P)_2$] where M=Pt or Pd and P=phosphine) are the first examples of a dithiadiazolyl acting as a chelating rather than a bridging ligand and, in the case of the Pt species, the first structurally characterised Pt complexes of [RCNSSN]$^{\bullet}$.

The retention of the unpaired electron in these compounds and its delocalisation onto the metal atom (as well as within the dithiadiazolyl species) has been shown by e.s.r. spectroscopy and molecular orbital studies. The [PhCNSSN]$^{\bullet}$ based complexes have also been studied magnetically and are shown to be paramagnetic solids. Unfortunately, the bulky phosphine ligands prevent any interaction between adjacent molecules and thus inhibit any potentially useful magnetic properties. This could perhaps be overcome by using planar counter ligands. The deep blue or green colouration of these species has allowed a U.V./vis study although decomposition of these species in solution has limited the information that can be gained.

The biological properties of the Pt complex [Pt(SNC(Ph)NS-*S*,*S*)$(PPh_3)_2$].MeCN have been probed and compared to the anti-cancer drug cis-platin. Despite the high toxicity and low selectivity of this particular dithiadiazolyl complex several other analogues, with different substituents on the phenyl ring of the dithiadiazolyl have been prepared with the hope of enhanced selectivity in future tests.

4.5. REFERENCES.

1. J.M. Rawson, University of Durham, unpublished results.
2. I.B. Gorrell, PhD thesis, University of Durham, 1989.
3. J.M. Rawson, PhD Thesis, University of Durham, 1990.
4. N. Adamson, J.M. Rawson and A.J. Banister, University of Durham, unpublished results.
5. O.G. Dawe, MSc. Thesis, University of Durham, 1995.
6. A.J. Banister, M.I. Hansford, Z.V. Hauptman, A.W. Luke, S.T. Wait, W. Clegg and K.A. Jørgensen, *J.Chem. Soc. Dalton Trans.*, 1990, 2793.
7. S.E. Lawrence, PhD Thesis, University of Durham, 1994.
8. A. Vegas, A. Pérez-Salazar, A.J. Banister and R.G. Hey, *J.Chem. Soc., Dalton Trans.*, 1980, 1812.
9. F.A. Cotton and G. Wilkinson, *Advanced Inorganic Chemistry*, 5th Ed., John Wiley & Sons, New York, 1988, 955.
10. (a) S. Kuwata, Y. Mizobe and M.Hidai, *J. Am. Chem. Soc.*, 1993,**115**, 8499.

    (b) R.D. Adams and T.S.A. Hor, *Inorg. Chem.*, 1984, **23**, 4723.

    (c) C.E. Briant, C.J. Gardner, T.S.A. Hor, N.D. Howells and D.M.P. Mingos, *J. Chem. Soc., Dalton Trans.*, 1984, 2645.

    (d) N. Hadj-Bagheri, R-J. Puddephatt, L. Manojlovic-Muir and A. Stedanovic, *J. Chem. Soc., Dalton Trans.*, 1990, 535.
11. A.J.Banister and I.B.Gorrell, *J.Chem. Soc., Faraday Trans. II*, 1985, 81, 1783.
12. Revised Nuffield Advanced Science, Book of data, Ed. H.Ellis, Longman Group Ltd, 4th Ed., 1986, **51**, No.3, 314.
13. C.A.Tolman, *Chem. Revs.*, 1977, Vol.77, No.3, 314.
14. F.A. Cotton and G. Wilkinson, *Advanced Inorganic Chemistry*, 5th Ed., John Wiley & Sons, New York, 1988, 1299.
15. S.A. Fairhurst, K.M. Johnson, L.H. Sutcliffe, K.F. Preston, A.J. Banister, Z.V. Hauptman and J. Passmore, *J.Chem. Soc., Dalton Trans.*, 1986, 1465.
16. S.A. Fairhurst, L.H. Sutcliffe, K.F. Preston, A.J. Banister, A.S. Partington, J.M. Rawson and J. Passmore, *Magn.Reson. in Chem.*, 1993, 31, 1027.
17. J.R. Morton and K.F. Preston, *J.Magn.Reson.*, 1978, **30**, 577.
18. J.R. Bowser, Inorganic Chemistry, Brooks/Cole, 1993, 720.

19. W.W. Porterfield, Inorganic Chemistry - a Unified Approach, 2nd Ed., Academic Press, 1993, 581.

20. F.A. Cotton, G. Wilkinson and P.L. Gaus, Basic Inorganic Chemistry, 2nd Ed., John Wiley and Sons, 1987, 64.

21. H.H.Jaffé and M. Orchin, Theory and Applications of Ultra-Violet Spectroscopy, John Wiley and Sons, 1962, 526.

22. S. Fricker, Johnson Matthey Tech. Centre, private communication to Dr. A.J. Banister, 1994.

23. R. Davis, I.F. Groves, J.L.A. Durrant, P. Brooks, and I. Lewis, *J.Organomet. Chem.*, 1983, **241**, C27.

24. E.A.V. Ebsworth, D.W.H. Rankin, S. Cradock, *Structural Methods in Inorganic Chemistry*, Blackwell Scientific Publications, 1987, 239.

CHAPTER FIVE

THE SYNTHESIS AND PROPERTIES OF TRIMETALLIC PLATINUM AND PALLADIUM DITHIADIAZOLYL COMPLEXES

5.1. INTRODUCTION

5.1.1. Decomposition of Monometallic Dithiadiazolyl Complexes.

As previously stated in chapter four, solutions of [Pt(SNCPhNS-*S,S*)(PPh_3)$_2$] and [Pd(SNCPhNS-*S,S*)(dppe)] decompose to yield orange precipitates under orange solutions. Previous studies[1] on the platinum based orange species gave little indication about the nature of the species formed. There was, however, analytical evidence (C,H and N) to suggest that dithiadiazolyl remained bonded to the metal. E.s.r. studies on the monometallic species (chapter four) indicated that some [PhCNSSN]$^{\bullet}$ was lost during this decomposition. It was thus inferred that the new compound formed contained a greater ratio of metal to chalcogen ring system.

5.1.2. Reaction Between [$Pd(PPh_3)_4$] and ($PhCNSSN)_2$.

The reaction between [$Pd(PPh_3)_4$] and ($PhCNSSN)_2$ in toluene did not yield a monometallic species but instead a red solid was formed[1]. Crystals of this species were grown from CH_2Cl_2 and a preliminary X-ray determination yielded a trimetallic dithiadiazolyl species[2]. This complex, along with the compounds described above, will be discussed in the following sections.

5.2. RESULTS AND DISCUSSION.

5.2.1. Preparation of Trimetallic Complexes.

When $[Pt(PPh_3)_4]$ and $(PhCNSSN)_2$ were stirred in MePh an immediate blue precipitate $[Pt(SNCPhNS\text{-}S,S)(PPh_3)_2]$ formed. On heating to 70°C this species started to decompose, firstly to a brown precipitate under a brown solution and finally to a bright orange solid under an orange solution. The solid was washed with fresh MePh and the solution (mainly PPh_3) and washings discarded. Satisfactory analysis was obtained for the composition, $[Pt_3(\mu_{S\text{-}S}SNCPhNS\text{-}S,S)_2(PPh_3)_4]$.

In a similar reaction $[Pd(dppe)_2]$ and $(PhCNSSN)_2$ were stirred in MePh to yield an immediate green precipitate [Pd(SNCPhNS-*S,S*)(dppe)]. On heating to 70°C this complex also started to break down via a brown suspension until again an orange solid had formed under an orange solution. In this case the reaction went to completion faster than in the analogous Pt reaction described above. Thus the monometallic Pd intermediate, [Pd(SNCPhNS-*S,S*)(dppe)], is less stable than the Pt species $[Pt(SNCPhNS\text{-}S,S)(PPh_3)_2]$. Again the solid was washed with fresh MePh and the solution and washings discarded. Satisfactory analysis was obtained for the composition, $[Pd_3(\mu_{S\text{-}S}SNCPhNS)_2(dppe)_2]$.

Toluene was also the solvent of choice for the reaction between $[Pd(PPh_3)_4]$ and $(PhCNSSN)_2$. In this case, however, the sole product was a deep red precipitate under a red solution: from the visible colour change (and e.s.r. inactivity) no unstable intermediate was observed. The red solids (presumably $[Pd_3(\mu_{S\text{-}S}SNCPhNS)_2(PPh_3)_4]$) were filtered and washed with fresh toluene. The solids were then refluxed in CH_2Cl_2 to further purify and yield a microcrystalline material which was fitered and dried. This crystalline solid satisfied the analysis for the composition $[Pd_3(\mu_{S\text{-}S}SNCPhNS\text{-})_2(PPh_3)_4].2CH_2Cl_2$.

5.2.2. Crystal Growth of Trimetallic Complexes.

Crystals of $[Pt_3(\mu_{S\text{-}S}\text{-}SNCPhNS)_2(PPh_3)_4].2MePh$ suitable for X-ray diffraction were grown by slow diffusion of a toluene solution of $[PhCNSSN]^{\bullet}$ through a grade three sinter into a saturated solution of $[Pt(PPh_3)_3]$ over excess $[Pt(PPh_3)_3]$. Crystals of $[Pd_3(\mu\text{-}SNCPhNS\text{-}S,S)_2(PPh_3)_4].2CH_2Cl_2$ suitable for X-ray analysis were grown by

slow diffusion of a CH_2Cl_2 solution of [PhCNSSN]$^{\bullet}$ into a saturated solution of $[Pd(PPh_3)_4]$ over excess $[Pd(PPh_3)_4]$. The crystal growth method employed in both cases was described fully in chapter four.

Crystals of the analogous Pt species with the difluoro ligand, ($SNC(3,4FC_6H_3)NS$), (i.e. $[Pt_3(\mu_{S\text{-}S}SNC(3,4FC_6H_3)NS)_2(PPh_3)_4]$) were grown in conjunction with O.G.Dawe[3] from the decomposition of a solution of [Pt(SNC(3,4FC$_6$H$_3$)NS-*S,S*)(PPh$_3$)$_2$] in $CDCl_3$. This solution decomposed to the trimetallic species which crystallised out of solution as its $CDCl_3$ solvate.

In all three cases the crystals were suitable for X-ray diffraction studies.

5.2.3. X-Ray Structures of Trimetallic Species.

The X-ray structural studies of these trimetallic species (figures 5.c., 5.d. and 5.e.) reveal a novel type of group 10 complex. They are composed of linear M_3 chains bridged by two 'trans' (SNC(Ph)NS) ligands. All the metals possess square planar gometries; the terminal metal atoms have an MP_2S_2 environment whereas the central metal is bonded only to the dithiadiazolyl S atoms thus producing a MS_4 co-ordination geometry. This structural type can thus be envisaged as two monometallic species, [Pt(SNCPhNS-*S,S*)(PPh$_3$)$_2$], sandwiching a bare metal atom in a trans fashion.

The two Pt species (Figures 5.c. and 5.d.) have a crystallographic inversion centre. Selected bond lengths and angles are shown in table 5.a. There is little significant difference between the bond lengths and angles in both Pt complexes. The minor differences (e.g. the P-Pt-P bond angle) can probably be attributed to the packing requirements of two different solvents of crystallisation, MePh and $CDCl_3$ respectively.

In comparing $[Pt_3(\mu_{S\text{-}S}SNCPhNS)_2(PPh_3)_4]$ to [Pt(SNCPhNS-*S,S*)(PPh$_3$)$_2$] (structural details in chapter four) the major structural difference for the dithiadiazolyl ring is that in $[Pt_3(\mu_{S\text{-}S}SNCPhNS)_2(PPh_3)_4]$ it now bridges between a PtP_2 unit and a central Pt atom. Neither Pt atom can thus insert as closely into the S-S bond as can occur in the monometallic chelating species. This results in a decrease in S-S distance (3.019(6)Å from 3.168(4)Å) and a decrease in S-Pt-S angle (78.8(2)Å and 80.4(2)Å from 86.78(8)Å) as the chalcogen system contracts slightly at the S-S interface. There is also an accompanying increases in S-M bond distance (e.g. 2.332(5)Å & 2.387(4)Å from

2.294(2)Å & 2.309(2)Å). As the chalcogen ring now takes up less space around the metal the triphenylphosphine groups are able to take up more space (P-Pt-P 103.3(2)° from 100.01(7)°), and are more strongly bound to platinum (2.297(2)Å and 2.305(2)Å from 2.311(2)Å and 2.322(2)Å) .

A feature of the 3,4, di-fluoro complex is that only the 'trans' di-fluoro species is present in the crystal. There is no obvious reason why a cis species should not be formed. It could be the case that both isomers were formed and that the trans species crystallised preferentially.

The structure of $[Pd_3(\mu_{S\text{-}S}SNCPhNS)_2(PPh_3)_4]$ is shown in figure 5.e. and, unlike the two Pt based species, does not possess a crystallographic inversion centre. Selected bond lengths and angles are shown in table 5.b. The palladium complex has no immediate monometallic analogue for comparison. In an indirect comparison with the dppe species [Pd(SNCPhNS-*S,S*)(dppe)] a similar trend to that observed for the two platinum species described above can be seen i.e. the metals in the trimetallic complex do not insert into the S-S bond as effectively as in the monometallic species resulting in longer S-Pd bond lengths and a smaller Pd-S-N angle.

These trimetallic species are unusual since Pt and Pd based complexes more often form mono or di-nuclear species or long chains or clusters[4a]. However, there are examples of trimetallic and higher oligomeric species with bridging ligands e.g. the Pt blues (see section 5.7.). In recent years there has also been a series of tri and tetra, homo and hetero metallic Pd(II) and Pt(II) species prepared with bridging double halides or thiolate ligands e.g. $[NBu_4]_2[(C_6F_5)_2Pt(\mu Cl)_2Pt(\mu Cl)_2Pt(C_6F_5)_2]$[5] (shown in figure 5.a.) and $[P(CH_2Ph)Ph_3]_2[(C_6F_5)_2Pd(\mu SC_6F_5)_2Pt(\mu SC_6F_5)_2Pt(\mu SC_6F_5)_2Pd(C_6F_5)_2]$[6].

Figure 5.a. Pt chain species.

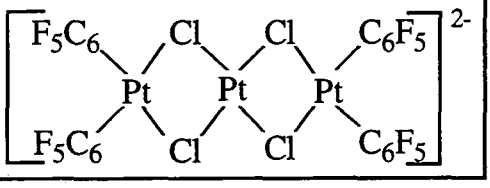

An interesting feature of these trimetallic dithiadiazolyl complexes is their close metal-metal interactions ranging between 2.8499(11)Å and 2.9026(4)Å. Though these are close interactions (the covalent radii of Pt and Pd are 1.28 and 1.31Å respectively[7]) they are longer than those observed for genuine Pt-Pt and Pd-Pd bonded species, e.g. Pt-Pt clusters usually have Pt-Pt bonds of between 2.61 and 2.79Å[8]. Some examples of such metal-metal bonded species for Pt and Pd are shown in figure 5.b.

From this evidence I would conclude that the metal-metal interaction in the trimetallic species is not a full single bond but it still represents a significant bonding interaction.

Figure 5.b. Selected M-M Bonded Complexes.

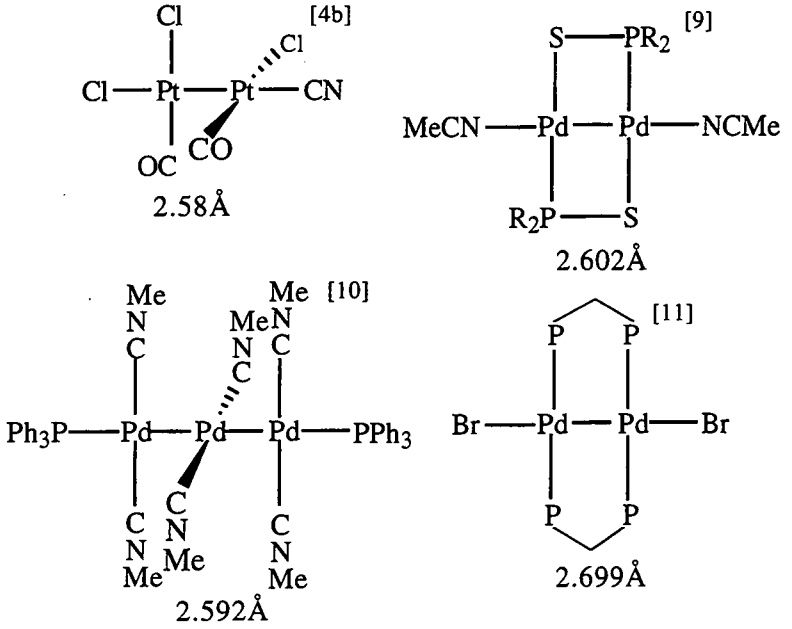

Figure 5.c. X-Ray Structure of $[Pt_3(\mu_{S,S}SNC(Ph)NS)_2(PPh_3)_4].2MePh$.

The triphenylphosphine phenyl groups, toluene solvate and all the protons have been removed for clarity.

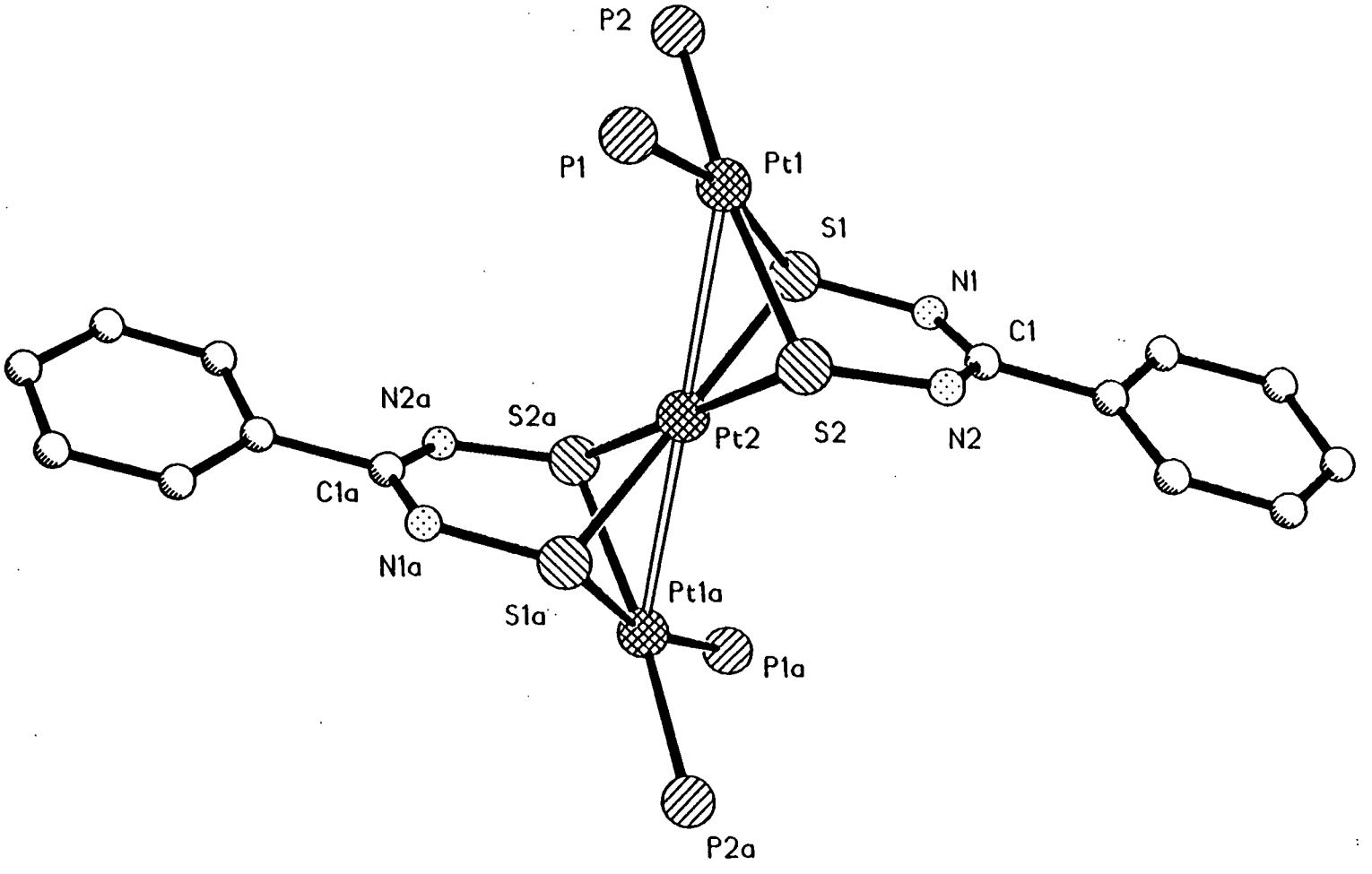

Figure 5.d. X-Ray Structure of
$[Pt_3(\mu_{S,S}SNC(3,4FC_6H_3)NS)_2(PPh_3)_4].4CDCl_3$.

The triphenylphosphine phenyl groups (except the carbon atoms bound to phosphorus), deuterochloroform solvate and all the protons have been removed for claritv.

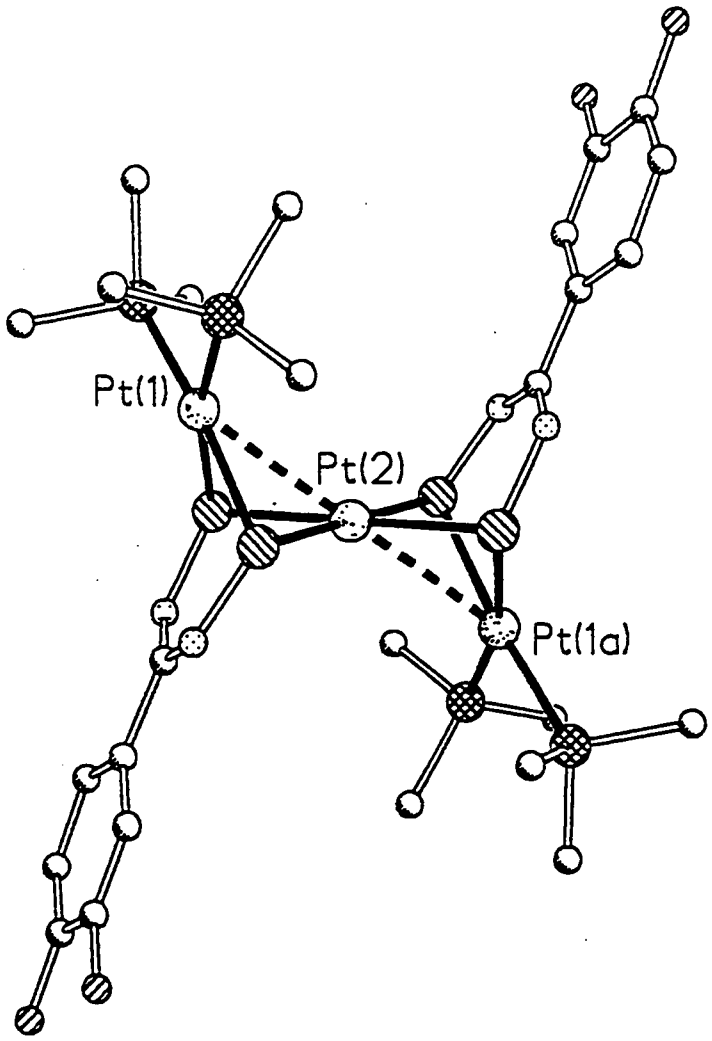

Table 5.a. Selected bond lengths and angles for both trimetallic platinum complexes.

	TRIMETALLIC PLATINUM COMPLEX	3,4 F TRIMETALLIC PLATINUM COMPLEX
Bond Length (Å)		
M(1)-S(1)	2.367(4)	2.383(2)
M(1)-S(2)	2.387(4)	2.380(7)
M(1)-P(1)	2.300(5)	2.297(2)
M(1)-P(2)	2.301(4)	2.305(2)
M(2)-S(1)	2.332(5)	2.344(2)
M(2)-S(2)	2.344(4)	2.340(2)
S(1)-N(1)	1.66(1)	1.669(7)
S(2)-N(2)	1.64(1)	1.667(7)
Pt(1)-Pt(2)	2.865(1)	2.9026(4)
S(1)....S(2)	3.019(6)	------
C(1)-N(1)	1.31(2)	1.315(12)
C(1)-N(2)	1.34(2)	1.325(12)
Bond Angle(°)		
S(1)-M(1)-S(2)	78.8(2)	79.29(8)
S(1)-M(2)-S(2)	80.4(2)	80.90(8)
P(1)-Pt(1)-P(2)	103.3(2)	99.06(8)
P(1)-M(1)-S(2)	87.8(2)	91.37(8)
M(1)-S(1)-N(1)	113.2(5)	113.3(3)
M(1)-S(2)-N(2)	111.1(5)	107.4(3)
M(2)-S(1)-N(1)	109.3(5)	107.4(3)
M(2)-S(2)-N(2)	107.4(6)	107.4(3)
S(1)-N(1)-C(1)	122.5(13)	123.9(6)
S(2)-N(2)-C(1)	126.1(13)	123.9(7)
M(1)-M(2)-M(1')	180.0	180.0

Figure 5.e. X-Ray Structure of $[Pd_3(\mu_{S,S}SNC(Ph)NS)_2(PPh_3)_4].2CH_2Cl_2$.

Th carbon atoms of triphenyl phosphine, dichloromethane solvate and all the protons have been removed for clarity.

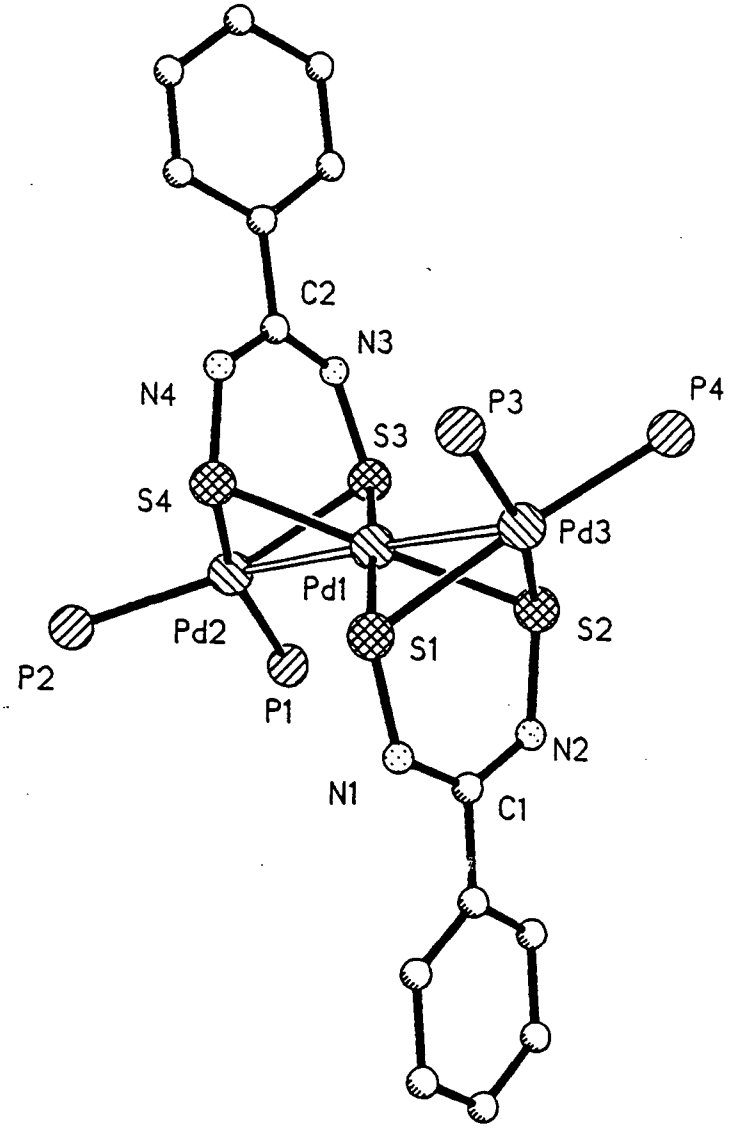

Table 5.b. Selectted Bond Lengths and Angles for $[Pd_3(\mu_{S\text{-}S}SNC(Ph)NS)(PPh_3)_4]$.

$[Pd_3(\mu_{S\text{-}S}SNC(Ph)NS)_2(PPh_3)_4]$			
Bond Length (Å)		**Bond Angle (°)**	
Pd(1)-S(1)	2.332(2)	S(1)-Pd(1)-S(2)	80.20(8)
Pd(1)-S(2)	2.346(2)	S(3)-Pd(1)-S(4)	81.34(8)
Pd(1)-S(3)	2.356(2)	S(1)-Pd(1)-S(4)	98.74(9)
Pd(1)-S(4)	2.361(2)	S(2)-Pd(1)-S(3)	99.86(9)
Pd(2)-S(3)	2.359(2)	P(1)-Pd(2)-P(2)	102.25(10)
Pd(2)-S(4)	2.402(3)	S(3)-Pd(2)-S(4)	79.64(8)
Pd(2)-P(1)	2.323(3)	P(1)-Pd(2)-S(3)	90.37(9)
Pd(2)-P(2)	2.345(3)	P(2)-Pd(2)-S(4)	89.83(9)
Pd(3)-S(1)	2.371(2)	P(3)-Pd(3)-P(4)	101.43(9)
Pd(3)-S(2)	2.374(2)	S(1)-Pd(3)-S(2)	79.62(8)
Pd(3)-P(3)	2.334(3)	P(3)-Pd(3)-S(1)	90.93(9)
Pd(3)-P(4)	2.351(3)	P(4)-Pd(3)-S(2)	87.35(9)
S(1)-N(1)	1.643(8)	Pd(1)-S(1)-N(1)	106.5(3)
S(2)-N(2)	1.648(7)	Pd(1)-S(2)-N(2)	107.9(3)
S(3)-N(3)	1.631(8)	Pd(1)-S(3)-N(3)	111.9(3)
S(4)-N(4)	1.649(7)	Pd(1)-S(4)-N(4)	108.6(3)
Pd(1)-Pd(3)	2.8499(11)	Pd(2)-S(3)-N(3)	105.0(3)
Pd(1)-Pd(2)	2.8693(12)	Pd(2)-S(4)-N(4)	109.1(3)
C(1)-N(1)	1.330(11)	Pd(3)-S(1)-N(1)	112.4(3)
C(1)-N(2)	1.304(11)	Pd(3)-S(2)-N(2)	111.4(3)
C(2)-N(3)	1.328(11)	S(1)-N(1)-C(1)	127.1(6)
C(2)-N(4)	1.310(11)	S(2)-N(2)-C(1)	126.9(7)
S(1)....S(2)	3.038	S(3)-N(3)-C(2)	127.1(7)
S(3)....S(4)	3.049	S(4)-N(4)-C(2)	125.6(7)

5.2.4. Rationalisation of Bonding in Trimetallic Complexes.

The X-ray structural determinations leave many questions unanswered about the bonding in this type of complex. Magnetic measurements conducted on the Faraday Balance indicate that the bulk material in the three [PhCNSSN]$^{\bullet}$ based trimetallic species is diamagnetic, thus the unpaired electron on each dithiadiazolyl unit must have somehow 'paired up' with another electron.

Another interesting phenomena is highlighted when you attempt to apply conventional electron counting principles. If the (SNCPhNS) acyclic fragment is thought of as a 5e$^-$ donor (see figure 5.g. overleaf) then each metal atom can gain the 16e$^-$ electron count required for square planar group 10 metal complexes i.e. the terminal Pt or Pd can obtain 2e$^-$ from each phosphine and 1e$^-$ from each sulfur of the chalcogen ring system. The central metal atom can gain 3e$^-$ each from each (SNC(Ph)NS) fragment to gain 16e$^-$ (again see figure 5.g. overleaf). This contrasts with a classical bridging di-sulfur ligand which can only donate 6e$^-$ and not 5e$^-$[4c] (figure 5.f.).

Figure 5.f. Bridging Di-sulfur Ligand.

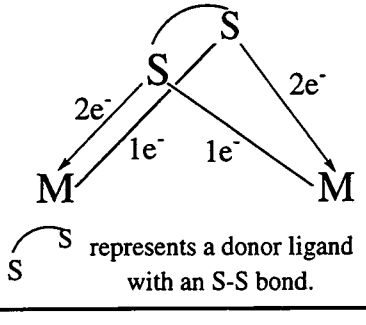

A simplified view of this bonding is given in the valence bonding view in figure 5.g. This view shows one S-N and one C-N π bond in each chalcogen ring. More conventional bridging RS$^-$ species do not have the potential to undertake this type of bonding.

Finally, the close M-M contacts can occur through partial overlap of full d_{z2} and empty p_z orbitals on the metal.

The formation of longer chain complexes can be envisaged. For example a tatrametallic complex would be composed of four terminal phosphine ligands, two 'trimetallic' type

ligands (i.e. no unpaired electrons, donating $5e^-$ to the bonding) and a central 'dimetallic' type ligand (as found in $[Ni(\mu_{S\text{-}S}SNC(Ph)NS)Cp_2]$, donating $6e^-$).

Figure 5.g. Electron Counting in $[M_3(\mu_{S\text{-}S}SNCPhNS)_2(PR_3)_4]$.

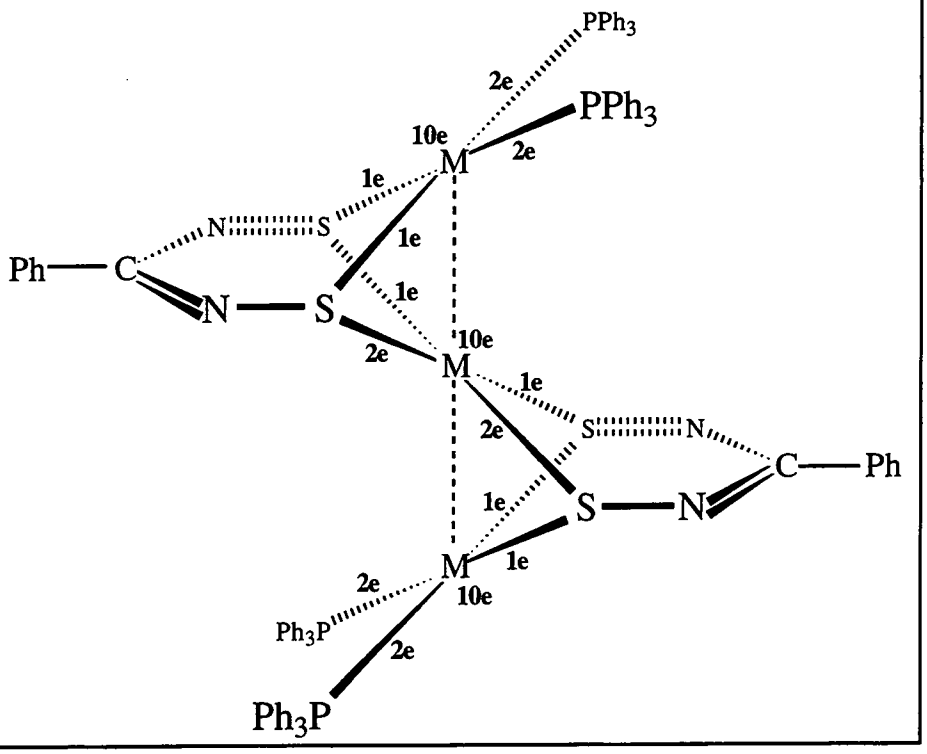

5.2.5. Molecular Orbital Study of $Pt_3(\mu_{S,S}SNCHNS)_2(PH_3)_4$.

The above bonding description gives a satisfactory, simplified, explanation of the bonding in this type of complex. However, for such a novel system a more thorough interpretation of the bonding is required. Thus EHMO calculations on the parent analogue $[Pt_3[\mu_{s,s}SNCHNS\text{-}S,S][PH_3]_4]$ were undertaken using the CACAO program[12]. The Frontier Molecular Orbitals are illustrated in Figure 5.h. and indicate that they are extensively delocalised over the whole of the core structure. Note that in the following discussion, the metal orbitals are described in terms of their own internal geometries in which the z axis is perpendicular to the square plane given by atoms S_2PtP_2.

The LUMO is formed by interaction of the [HCNSSN] SOMO with d-orbitals on the metal atoms. For the central Pt, this is predominantly d_{xy}, 20%, with the terminal atoms also predominantly d_{xy}, 8%. All four P atoms also make a contribution to the orbital. There are then two orbitals close in energy (within 0.05eV) which constitute the highest occupied molecular orbitals. The higher of these (the HOMO) is mostly metal based (although each sulfur has 2% spin density) and the central Pt atom has d_{x2-y2}, 19%, d_{z2}, 5% and d_{yz}, 22% character. The terminal Pt atoms have predominantly d_{yz} 10% and d_{z2} 4% contributions. The metal-metal interactions in this orbital are anti-bonding. The lower energy orbital of this pair (HOMO-1) is mostly S-N based, with no central platinum contribution.

Figure 5.h. The Frontier Molecular Orbitals of $[Pt_3(\mu_{S,S}SNC(H)NS)(PH_3)_4]$

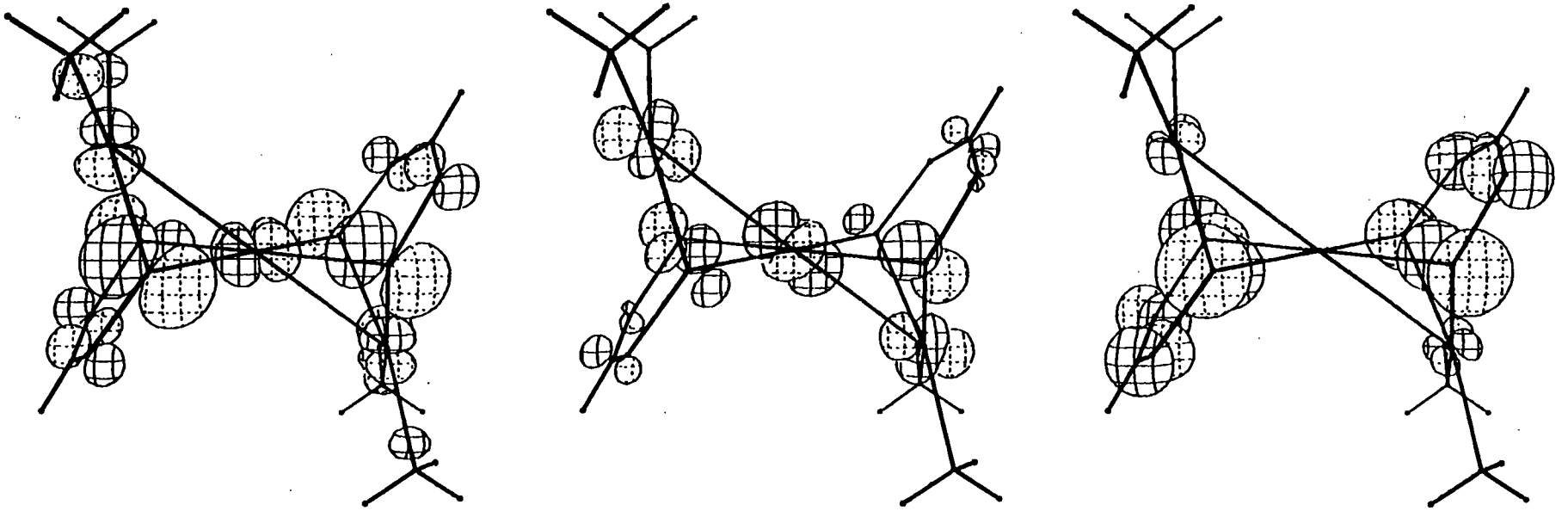

LUMO
-8.51eV

HOMO
-11.41eV

HOMO-1
-11.46eV

5.2.6. N.m.r. Studies.

Since the four trimetallic species described above have no unpaired electrons, they are e.s.r. inactive and all have well resolved ^{1}H and ^{31}P n.m.r. spectra (unlike the monometallic complexes discussed in chapter four). All the species were insoluble in most common solvents and only partially soluble in the solvent ($CDCl_3$) used for n.m.r. studies easily precipitating back out of solution. This made interpretation of intensities of different species meaningless. In the case of ^{31}P n.m.r. the low solubilities of these species results in a requirement of a large number of scans to yield spectra with a good signal to noise ratio.

The ^{1}H n.m.r. spectra of $[Pt_3(\mu_{S\text{-}S}SNCPhNS)_2(PPh_3)_4]$ and $[Pd_3(\mu_{S\text{-}S}SNCPhNS)_2(PPh_3)_4].2CH_2Cl_2$ consist of aromatic proton multiplets at δ7.51–6.99ppm and δ 7.34-6.94ppm respectively; in the latter CH_2Cl_2 (δ5.35ppm) is also observed[13]. There is no ^{1}H n.m.r. signal between δ6-7ppm and thus indicative of no N-H bound proton in a chemical environment similar to those found in $[Fe_2(\mu_{S\text{-}S}SNCPhN(H)S)(CO)_6]$[14]. The dppe complex $[Pd_3(\mu_{S\text{-}S}SNC(Ph)NS)_2(dppe)_2]$ gives a ^{1}H n.m.r. spectrum with the dppe and (SNC(Ph)NS) aromatic protons (δ7.69–7.26ppm) and dppe aliphatic protons (δ2.13ppm) clearly visible.

As expected the ^{31}P n.m.r. of the Pd triphenylphosphine species consists of a single peak at δ24.81ppm i.e. only one type of phosphorus is present (figure 5.j.). The ^{31}P n.m.r. of the platinum species also consists of a single peak (δ18.5ppm) with platinum satellites [$J_{P\text{-}Pt}$ = 3282Hz]. A much less intense peak can also be observed (δ 15.36ppm) with Pt satellites[$J_{P\text{-}Pt}$ = 3551Hz] and the nature of this second species will be discussed in chapter 6, as well as other decomposition products observed. The ^{31}P n.m.r. spectrum of the fluoro complex $[Pt_3(\mu_{S\text{-}S}SNC(3,4FC_6H_3)NS)_2(PPh_3)_4]$ is very similar [δ18.0, $J_{P\text{-}Pt}$=2805Hz]. All the phosphorus atoms are in an equivalent chemical environment due to the free rotation of the carbon-carbon bond of the (SNCNS) fragment and the partially fluorinated aromatic ring ($3,4FC_6H_3$). Again a second major species is observed; this will also be discussed in chapter six.

The ^{31}P n.m.r. spectra of all three triphenyl phosphine species give peaks with very similar values to those for four similar sulfur based complexes, $[M(PPh_3)_2(1,5\text{-}$

$Ph_4P_2N_4S_2)]$[15] and [M(PhSN{4-$CH_3C_6H_4$}CN-NC{4-$CH_3C_6H_4$}NSPh(PPh_3)][16] where M = Pt or Pd (figure 5.i. and table 5.c.).

Figure 5.i.

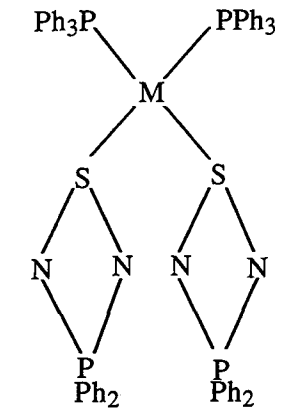

$[M(PPh_3)_2(1,5\text{-}Ph_4P_2N_4S_2)]$

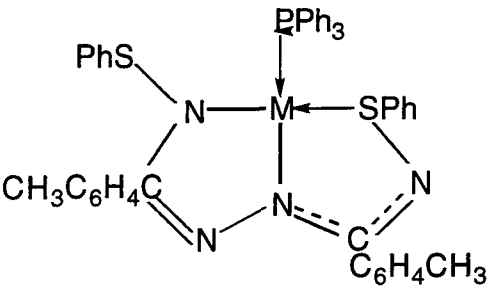

[M(PhSN[4-$CH_3C_6H_4$]CN-NC[4-$CH_3C_6H_4$]NSPh(PPh_3)]

M = Pt or Pd

Table 5.c. ^{31}P n.m.r. of trimetallic species.

COMPLEX	δ (ppm)	$J_{Pt\text{-}P}$ (Hz)
[Pt_3(μ-SNC(Ph)NS-*S,S*)$_2$(PPh_3)$_4$]	18.5	3282
[Pt_3(μ-SNC(3,4FC_6H_3)NS-*S,S*)$_2$(PPh_3)$_4$]	18.0	2805
[Pt(PPh_3)$_2$(1,5-$Ph_4P_2N_4S_2$)]	18.3	2861
[Pt(PhSN{4-$CH_3C_6H_4$}CN-NC{4-$CH_3C_6H_4$}NSPh(PPh_3)]	19.1	3651
[Pd_3(μ-SNC(Ph)NS-*S,S*)$_2$(PPh_3)$_4$]	24.8	-----
[Pd(PPh_3)$_2$(1,5-$Ph_4P_2N_4S_2$)]	25.4	-----
[Pd(PhSN{4-$CH_3C_6H_4$}CN-NC{4-$CH_3C_6H_4$}NSPh(PPh_3)	25.7	-----

The ^{31}P spectrum of [Pd_3($\mu_{S\text{-}S}$SNC(Ph)NS)$_2$(dppe)$_2$] consists of a singlet (δ41.14) and a trace of $(Ph)_2P(S)C_2H_4(S)P(Ph)_2$ (δ43.13)[17] (figure 5.k.).formed during extraction of sulfur from free [PhCNSSN]•, as will be explained in chapter six.

Figure 5.j. ^{31}P n.m.r. Spectrum of $[Pd_3(\mu_{S,S}SNC(Ph)NS)(PPh_3)_4]$.

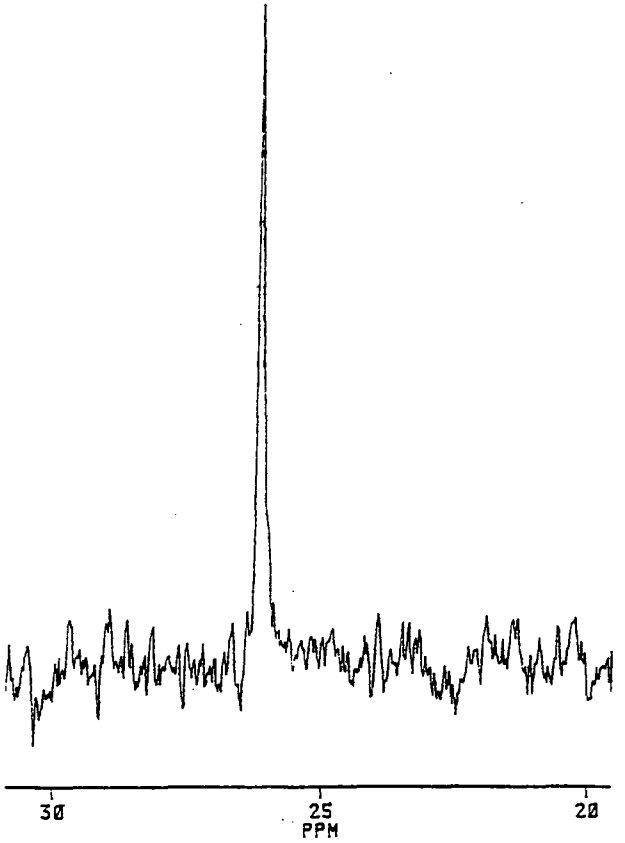

Figure 5.k. ^{31}P n.m.r. Spectrum of $[Pd_3(\mu_{S,S}SNC(Ph)NS)(dppe)_2]$.

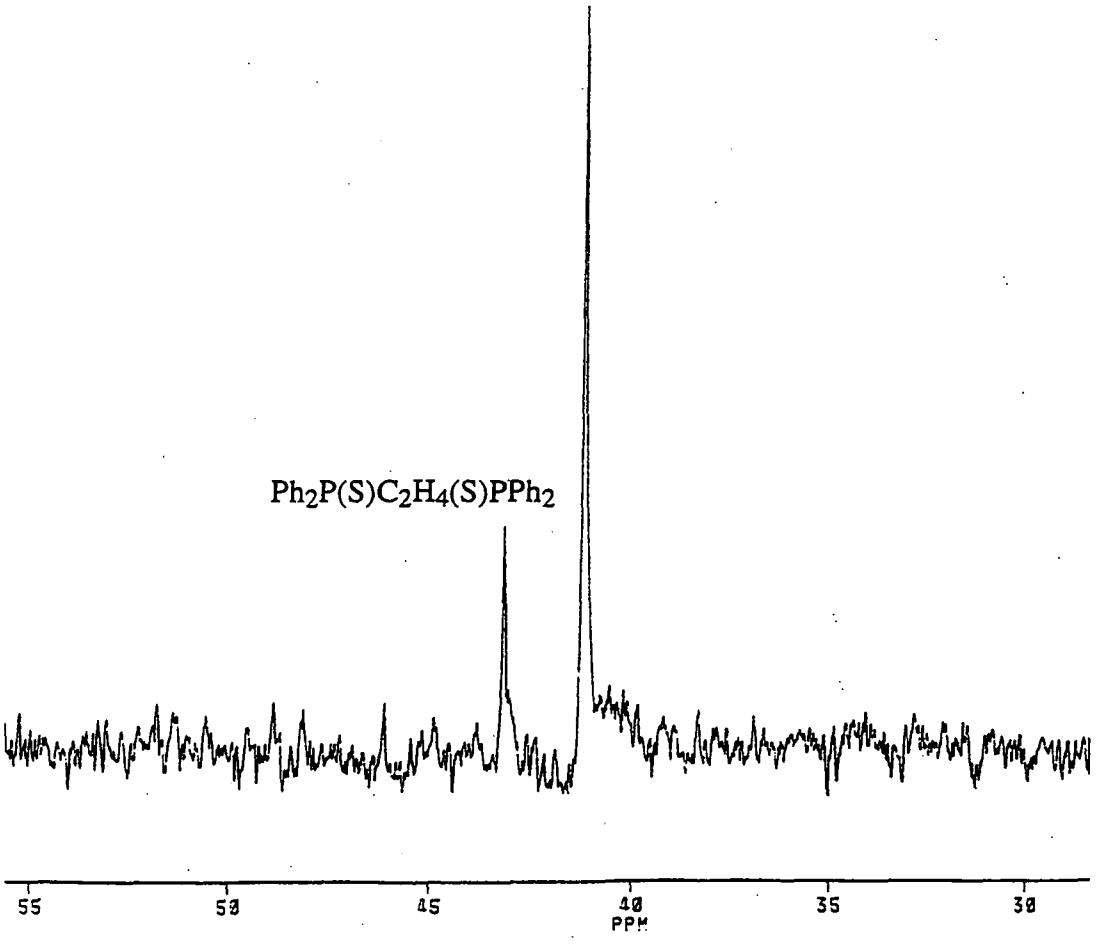

5.2.7. Biological Test Results For $Pt_3(\mu_{S,S}SNC(Ph)NS)_2(PPh_3)_4$.

As discussed in chapter four, [Pt(SNC(Ph)NS-*S,S*)$(PPh_3)_2$] was tested extensively for its activity against different cancer cells, due to its structural resemblance to cis-platin and other anti-cancer drugs. The trimetallic species also have a structural similarity to another series of anti-tumour active chemicals, the platinum blues. These species are oligomeric Pt(II)-Pt(IV) chains (usually with four Pt atoms in the chain), bridged by uracil, uridine and thymine ligands[4d]. These compounds still attract interest because of their biological properties e.g. $[Pt_4(NH_3)_8L_4]^{5+}$ where L= 3,5 dimethylglutarimidate or glutarimidate[18]. Consequently $[Pt_3(\mu_{S,S}SNC(Ph)NS)_2(PPh_3)_4]$ was also tested in preliminary studies. Three mammalian cell lines were used in the cytotoxicity measurements, SW620 (colon adenocarcinoma) and SKOV-3 (ovarian carcinoma), which are both human tumour lines, and CHO rodent fibroblast. The last is used for routine cytotoxicity testing.

The results are shown in table 5.d. As in chapter four, IC_{50} is the concentration of compound required to give 50% decrease in cell proliferation in a set sample of the culture. As can clearly be seen much higher concentrations of the trimetallic complex were required to kill 50% of cell cultures compared with the monometallic species. This complex was thus much less active and no further test measurements were undertaken. The low activity was almost certainly a combination of the lack of free radical nature of the complex, the high stability of the species and its low water solubility.

Table 5.d. Preliminary Cytotoxicity Measurements For the Monometallic and Trimetallic Species Prepared From [PhCNSSN]• and $Pt(PPh_3)_4$.

I.C.50 (μg/ml)	TRIMETALLIC COMPLEX	MONOMETALLIC COMPLEX
SW 620	125	63
SKOV-3	110	26
CHO	225	55

5.3. EXPERIMENTAL.

5.3.1. Preparation of $[Pt_3(\mu_{S\text{-}S}SNCPhNS)_2(PPh_3)_4]$.

$[Pt(PPh_3)_4]$ (2.5g, 2.0mmol) and $(PhCNSSN)_2$ (0.36g, 1.00mmol) were stirred at 80°C in 40ml MePh to yield an immediate blue precipitate. After 4h a bright orange solid was present which was filtered, washed with fresh MePh (3x 15ml) and dried *in vacuo*

Yield 1.03g, 85%.

IR ν_{max} (cm^{-1}) 3051w, 2363w, 1594w, 1571w, 1480m, 1456m, 1434ssh, 1405w, 1303s, 1182m, 1166m, 1143m, 1095s, 1026m, 998m, 844w, 801w, 741m, 695m, 693s, 676m, 644w, 618w, 536ssh, 523ssh, 511ssh, 497sh, 459w, 434w,

Elemental analysis, found: C51.88%; H3.50%; N2.77%; Calc. C51.72%; H3.54%, N2.82%.

N.m.r.; (250MHz; solvent $CDCl_3$) ^1H δ7.51-7.00 (m), ^{31}P δ 18.53 [$J_{Pt\text{-}P}$ 3282.3Hz].

D.s.c. broad exotherm centred at 225°C.

5.3.2. Crystal growth of $[Pt_3(\mu_{S\text{-}S}SNCPhNS)_2(PPh_3)_4].2MePh$..

Freshly prepared $[Pt(PPh_3)_3]$ (0.10g, 0.80mmol) was placed in one limb of a two-limbed reaction vessel with $(PhCNSSN)_2$ (0.10g, 0.28mmol) placed in the other. MePh was added to each side. Inversion of the sealed reaction vessel resulted in the slow diffusion of $[PhCNSSN]^{\bullet}$ into a saturated solution of $[Pt(PPh_3)_3]$. Within 48h red crystals suitable for X-ray analysis had formed.

5.3.3. Preparation of $[Pd_3(\mu_{S\text{-}S}SNCPhNS)_2(PPh_3)_4].2CH_2Cl_2$.

$[Pd(PPh_3)_4]$ (0.5g,0.43mmol) and $(PhCNSSN)_2$ (0.072g, 0.20mmol) were stirred in MePh (10ml) for 5h at ambient temperature. The resultant deep red precipitate was filtered, washed with toluene (3x5ml) and dried *in vacuo*. CH_2Cl_2 (5ml) was added and the mixture refluxed for 10m to yield a red microcrystalline solid which was filtered and dried *in vacuo* .

Yield 0.20g, 75%.

IR ν_{max} (cm^{-1}) 3051w, 1959w, 1890w, 1811w, 1594w, 1479sh, 1451w, 1434ssh, 1381w, 1309ssh, 1181w, 1168m, 1148w, 1094m, 1069w, 1026m, 998m, 920w, 902w, 845w, 822w, 739m, 714ssh, 692s, 669ssh, 650w, 618w, 527ssh, 519ssh, 506ssh, 492m, 449w, 440w.

Elemental analysis, found: C55.62%; H3.91%, N2.95%, Calc.: C55.60%, H3.90%, N2.95%.

Nm.r., (250MHz; solvent $CDCl_3$) ^1H δ7.34-6.94 (m), 5.30 (singlet-CH_2Cl_2), ^{31}P δ26.22 (s).

D.s.c. 270°C (dec.).

5.3.4. Crystal growth of $[Pd_3(\mu_{S\text{-}S}SNCPhNS)_2(PPh_3)_4].2CH_2Cl_2$.

$[Pd(PPh_3)_4$ (0.35g, 0.31mmol) was placed in one limb of a two-limbed reaction vessel with $(PhCNSSN)_2$ (0.08g, 0.22mmol) placed in the other limb. CH_2Cl_2 (10ml) was added to each side. Inversion of the sealed reaction vessel resulted in the slow diffusion through the separating grade three sinter of a solution of [PhCNSSN]• into the former limb. Within 3h deep red crystals had formed. The solvent was removed and a number of crystals suitable for X-ray diffraction were selected.

5.3.5. Preparation of $[Pd_3(\mu_{S\text{-}S}SNCPhNS)_2(dppe)_2]$.

$[Pd(dppe)_2]$ (0.52g, 0.41mmol) and $(PhCNSSN)_2$ (0.075g, 0.21mmol) were stirred at 70°C in 20ml MePh to yield an immediate green precipitate. After $2^1/_2$h a bright orange precipitate had formed under a yellow/orange solution. The solid was filtered off, washed with fresh MePh (3x 10ml) and dried *in vacuo* .

Yield 0.20g, 65%.

IR ν_{max} (cm^{-1}) 3049m, 2365w, 1483m, 1450wsh, 1434ssh, 1384w, 1299sh, 1261w, 1186w, 1167msh, 1140m, 1102sh, 1067w, 1027sh, 998wsh, 868m, 817m, 745m, 707ssh, 695ssh, 670ssh, 646w, 525sh, 476m, 451w, 434w, 419w.

Elemental analysis, Found: C,54.06%; H,4.00%; N,3.57%; Calc.: C,53.61%; H,3.92%, N,3.79%.

NMR; (250mHz; solvent $CDCl_3$) ^1H δ7.69-7.26 (40H,m), ^{31}P δp41.17ppm(s).

D.S.C.278°C (dec.).

5.4. CONCLUSION.

In this chapter the properties of a new class of dithiadiazolyl complex have been studied. These species are the major product from the solution decomposition of the monometallic dithiadiazolyl complexes discussed in chapter four. They are novel trimetallic complexes, $[M_3(\mu_{S,S}SNC(Ph)NS)_2(P)_4]$ (where M=Pt or Pd and P=PPh_3 or dppe) and are composed of linear three metal chains bridged by the sulfur atoms of two dithiadiazolyl groups and capped by terminal phosphines. They have an unusual bonding system that has been probed during the course of this chapter by crystallography, electron counting rules and M.O. calculations. These measurements have provided complementary evidence for a rationalisation of the highly unusual bonding found in these species which renders all the complexes diamagnetic.

5.5. REFERENCES

1. I.B. Gorrell, *PhD. Thesis*, University of Durham, 1989.
2. J.M. Rawson, *PhD. Thesis*, University of Durham, 1990.
3. O.G. Dawe, *MSc. Thesis*, University of Durham, 1995.
4. F.A. Cotton and G.Wilkinson, *Advanced Inorganic Chemistry 5th Edn..*, John Wiley and Sons, 1988, a)917, b)932, c)531 & d)929.
5. R. Uson, J. Fornies, M. Tomas, B. Menjon, J. Carnicer and A.J. Welch, *J.Chem. Soc., Dalton Trans.*, 1990, 151.
6. R. Uson, J. Fornies, M.A. Uson, M. Tomas, M.A. Ibanez and A.J. Welch, *J.Chem. Soc., Dalton Trans.*, 1994, 401.
7. W.W. Porterfield, Inorganic Chemistry - a Unified Approach, Addison-Wesley, 1984, 168.
8. L. Manojlovic-Muir and K.W. Muir, J. Chem. Soc., Chem. Commun., 1982, 1155.
9. B. Messbauer, H. Meyer, B. Walther, M.J. Heeg, A.F.M. Maqsudor Rahman, & J.P. Oliver, *Inorg. Chem.*, 1983, **22**, 272.
10. A.L. Balch, J.R. Boehm, H. Hope and M. Olmstead, *J. Am. Chem. Soc.*, 1976, **98**, 743.
11. R.G. Holloway, B.R. Penfold, R. Colton and M.J. McCormick, *J. Chem. Soc., Chem. Commun.*, 1976, 485.
12. CACAO programme for M.O. Calculations.
13. D.H. Williams and I. Fleming, *Specroscopic Methods in Organic Chemistry*, McGraw-Hill Book Company, 4th Ed., 1989, 142.
14. V. Klassen, K. Preuss, K.H. Moock and R.T. Boeré, *Phos.Sulf. Silicon and Rltd Elem.*, 1994, **93-94**, 449.
15. T. Chivers, M. Edwards, A. Meetsma and J.C. van der Lee, Inorg. Chem., 1992, **31**, 11.
16. T. Chivers, K. McGregor and M. Parvez, *Inorg. Chem.*, 1994, **33**, 2364.
17. G.M. Kosolapoff and L. Maier, Organic Phosphorus Compounds, Vol. 4, Eds. Wiley Interscience, New York, 1972, Ch7, 391.
18. J.Matsunami, H.Urata and K.Matsumoto, *Inorg. Chem.*, 1995, **34**, 202.
19. S.Fricker, Johnson Matthey Tech. Centre, private communication to Dr. A.J. Banister, 1994.

CHAPTER SIX

A STUDY OF THE DECOMPOSITION OF MONOMETALLIC PLATINUM AND PALLADIUM DITHIADIAZOLYL COMPLEXES

6.1. INTRODUCTION.

6.1.1. The Stability of Monometallic Dithiadiazolyl Complexes.

The previous two chapters have discussed, in depth, the physical and chemical properties of two new series of dithiadiazolyl complexes [M(SNCPhNS-*S,S*)(P)$_2$] and [M$_3$($\mu_{S\text{-}S}$SNCPhNS)$_2$(P)$_4$] where M = Pt or Pd and P = PPh_3 or $^1/_2$dppe. However, the research undertaken in these two chapters has left many questions unanswered.

Both [Pt(SNCPhNS-*S,S*)(PPh_3)$_2$] and [Pd(SNCPhNS-*S,S*)(dppe)] decompose to their respective trimetallic species [Pt$_3$($\mu_{S\text{-}S}$SNCPhNS)$_2$(PPh_3)$_4$] and Pd$_3$($\mu_{S\text{-}S}$SNCPhNS)$_2$(dppe)$_2$ but I have not yet given an explanation as to why these reactions take place. Also I have not mentioned why the monometallic Pt species [Pt(SNCPhNS-*S,S*)(dppe)] does not decompose to the analogous trimetallic species under the same conditions. Finally, the reaction between [Pd(PPh_3)$_4$] and [PhCNSSN]$^\bullet$ results in the formation of the trimetallic species only. For some reason the monometallic complex is not formed. One aim of this chapter is to consider the reasons behind these different stabilities.

6.1.2. Studying the Monometallic To Trimetallic Decomposition.

As indicated above the formation of [M$_3$($\mu_{S\text{-}S}$SNCPhNS)$_2$(P)$_4$] from [M(SNCPhNS-*S,S*)(P)$_2$] is a very novel reaction and no direct comparison can be found in the literature. It was thus of some interest to attempt to elucidate the mechanism of this reaction. This was attempted by studying a) the stability of different derivatives and b) by monitoring the decomposition of the monometallic species *via* U.V./vis and e.s.r. spectroscopic kinetic studies.

Further information was gained in the study of reactive intermediates and side products using multi-nuclear n.m.r. (to examine those species without an unpaired electron) and e.s.r. experiments (for studying species with an unpaired electron). In particular, the slow decomposition of [Pt(SNCPhNS-*S,S*)(PPh_3)$_2$] and the slower still decomposition of [Pt(SNCPhNS-*S,S*)(dppe)] provide ideal candidates for these studies.

6.2. RESULTS AND DISCUSSION.

6.2.1. A Rationalisation of the Various Stabilities of [PhCNSSN]• Monometallic Complexes.

The effect of the nature of the R group on the chalcogen ring system has not yet been studied but there are two other factors which affect the stability of monometallic dithiadiazolyl complexes, the phosphine and the metal.

There are only four phosphorus atoms per three metal centres compared to 2 phosphorus atoms per one metal centre in monometallic species, thus phosphine must be lost on decomposition. Since 1,2 bisdiphenylphosphinoethane (dppe), a chelating phosphine, is more strongly bound than two unidentate triphenylphosphine (PPh_3) groups[1] the dppe complexes are more stable than the PPh_3 species. As such [Pt(SNCPhNS-S,S)(dppe)] is far more stable in solution than [Pt(SNCPhNS-S,S)$(PPh_3)_2$], and [Pd(SNCPhNS-S,S)(dppe)] can be isolated whereas [Pd(SNCPhNS-S,S)$(PPh_3)_2$] cannot.

In general square-planar Pt(II) complexes are known to be kinetically more stable than their Pd counterparts[2], a point highlighted in chapter two. Consequently monometallic Pt species are less likely to decompose than the analogous Pd species e.g. [Pt(SNCPhNS-S,S)(dppe)] is far more stable in solution than [Pd(SNCPhNS-S,S)(dppe) and [Pt(SNCPhNS-S,S)$(PPh_3)_2$] can be isolated whereas [Pd(SNCPhNS-S,S)$(PPh_3)_2$] has not been observed even as an unstable intermediate.

The above rationalisation is condensed in the following table (table 6.a.); all the complexes shown are discussed in chapters four and five and in this chapter.

The decomposition of monometallic to trimetallic complexes would appear to be thermodynamically favoured but the monometallic species can be stabilised as kinetic products[3]. In the case of the reaction between [$Pd(PPh_3)_4$] and [PhCNSSN]• the trimetallic complex [$Pd_3(\mu_{S\text{-}S}SNCPhNS)_2(PPh_3)_4$] is formed directly and so we conclude that the "intermediate" monometallic complex [Pd(SNCPhNS-S,S)$(PPh_3)_2$] is kinetically too unstable and thus no e.s.r. signal is observed from the reaction. As stated in chapter five the ^{31}P n.m.r. of the complex indicates only the presence of the trimetallic complex. No noticeable side products or other reactions are observed.

Table 6.a. 1,2,3,5, Phenyl Dithiadiazolyl Complexes.

MONOMETALLIC COMPLEXES		TRIMETALLIC COMPLEXES	
[Pd(SNCPhNS-S,S)(PPh_3)$_2$]	increased stability ↓	[Pd_3(μ_{S-S}SNCPhNS)$_2$(PPh_3)$_4$]	↑ increased ease of formation
[Pd(SNCPhNS-S,S)(dppe)]		[Pd_3(μ_{S-S}SNCPhNS)$_2$(dppe)$_2$]	
[Pt(SNCPhNS-S,S)(PPh_3)$_2$]		[Pt_3(μ_{S-S}SNCPhNS)$_2$(PPh_3)$_4$]	
[Pt(SNCPhNS-S,S)(dppe)]		[Pt_3(μ_{S-S}SNCPhNS)$_2$(dppe)$_2$]	

6.2.2. The Monometallic to Trimetallic Conversion, a Mechanistic Study by E.s.r. Spectroscopy.

6.2.2.1. E.s.r. Spectroscopy of the Decomposition of [Pd(SNCPhNS-S,S)(dppe)].

Whilst studying the e.s.r. spectrum of [Pd(SNC(Ph)NS-*S,S*)(dppe)] formed from the *in situ* reaction in CH_2Cl_2 between [PhCNSSN]$^{\bullet}$ and excess Pd(dppe)$_2$, a second high field spectrum of low intensity was observed (figure 6.a.). When instead the [Pd(SNC(Ph)NS-S,S)(dppe)] product and [Pd(dppe)$_2$] were reacted in CH_2Cl_2 and the spectrum run after an hour, the reaction had proceeded to such an extent that only this signal was present. The spectrum consists of a doublet of pentets, corresponding to hyperfine coupling to two equivalent nitrogen atoms but only one phosphorus atom (see figure 6.b. for first derivative experimental and the simulation spectra). This second signal was too weak to see Pd coupling but we assume this to be due to a monometallic intermediate in the formation of [Pd_3(μ_{S-S}SNC(Ph)NS)$_2$(dppe)$_2$]. The dppe group of the monometallic species is now coordinated through only one P atom i.e. [Pd(SNC(Ph)NS-*S,S*)(η^1-dppe)]. A formal electron count on this complex shows the Pd to be electron-deficient with 15/16e$^-$. Presumably the process is reversible, with the labile P atom able to coordinate again re-forming the 16/17e$^-$ complex. Nevertheless, this electron deficient complex may prove to be a key intermediate in the decomposition process. The larger value of *a* for P and smaller value of *a* for N compared with [Pd(SNC(Ph)NS-*S,S*)(dppe)] indicates a drift of spin density from the N to the P in this species, consistent with abstraction of electron density from the metallocycle to the metal and hence to the metal bonded phosphines. The shift of the signal to higher field is

consistent with more electron density on the metal (since [PhCNSSN]• based free electrons have lower field g values[4]).

6.2.2.2. E.s.r. Spectrum of a Decomposition Product of [Pt(SNC(Ph)NS-*S,S*)(dppe)].

As described in chapter four the e.s.r spectra of [Pt(SNC(Ph)NS-*S,S*)(dppe)] indicated the decomposition of the complex by the presence of released [PhCNSSN]• which swamped the highfield portion of the [Pt(SNC(Ph)NS-*S,S*)(dppe)] spectrum. When excess [Pt(dppe)$_2$] was added (mopping up [PhCNSSN]• by forming fresh monometallic complex) the dithiadiazolyl radical signal disappeared to be replaced by a new signal highfield of the main complex spectrum. This new signal consisted of a doublet of doublets (probably due to two inequivalent phosphorus atoms) with Pt satellites; the lower field satellites are swamped by the main complex signal for [Pt(SNC(Ph)NS-*S,S*(dppe)]. This spectrum is shown in figure 6.c.

A similar signal (doublet of doublets) was observed for the decomposition product of [Pt(SNC(C_6F_5)NS-*S,S*)(PPh_3)$_2$] (see table 6.b.). As there is no observable coupling to nitrogen in either case then the free electron cannot be well delocalised over an (SNC(Ph)NS) framework in such a species, if indeed the Pt based radical is still attatched to the chalcogen ring at all.

Table 6.b. E.s.r. Spectra of Intermediates from the Decomposition of Two Pt Dithiadiazolyl Complexes..

E.s.r. Parameters	g	a_{P1}	a_{P2}	a_{Pt}
[Pt(SNC(Ph)NS-*S,S*)(dppe)]	2.007	1.30	0.85	5.85
[Pt(SNC(C_6F_5)NS-*S,S*)(PPh_3)$_2$]	2.0097	2.57	~1	5.13

Figure 6.a. Second Derivative E.s.r. Spectra Showing the Decomposition of [Pd(SNC(Ph)NS-*S,S*)(dppe)] to [Pd(SNC(Ph)NS-*S,S*)(μ_1-dppe)]

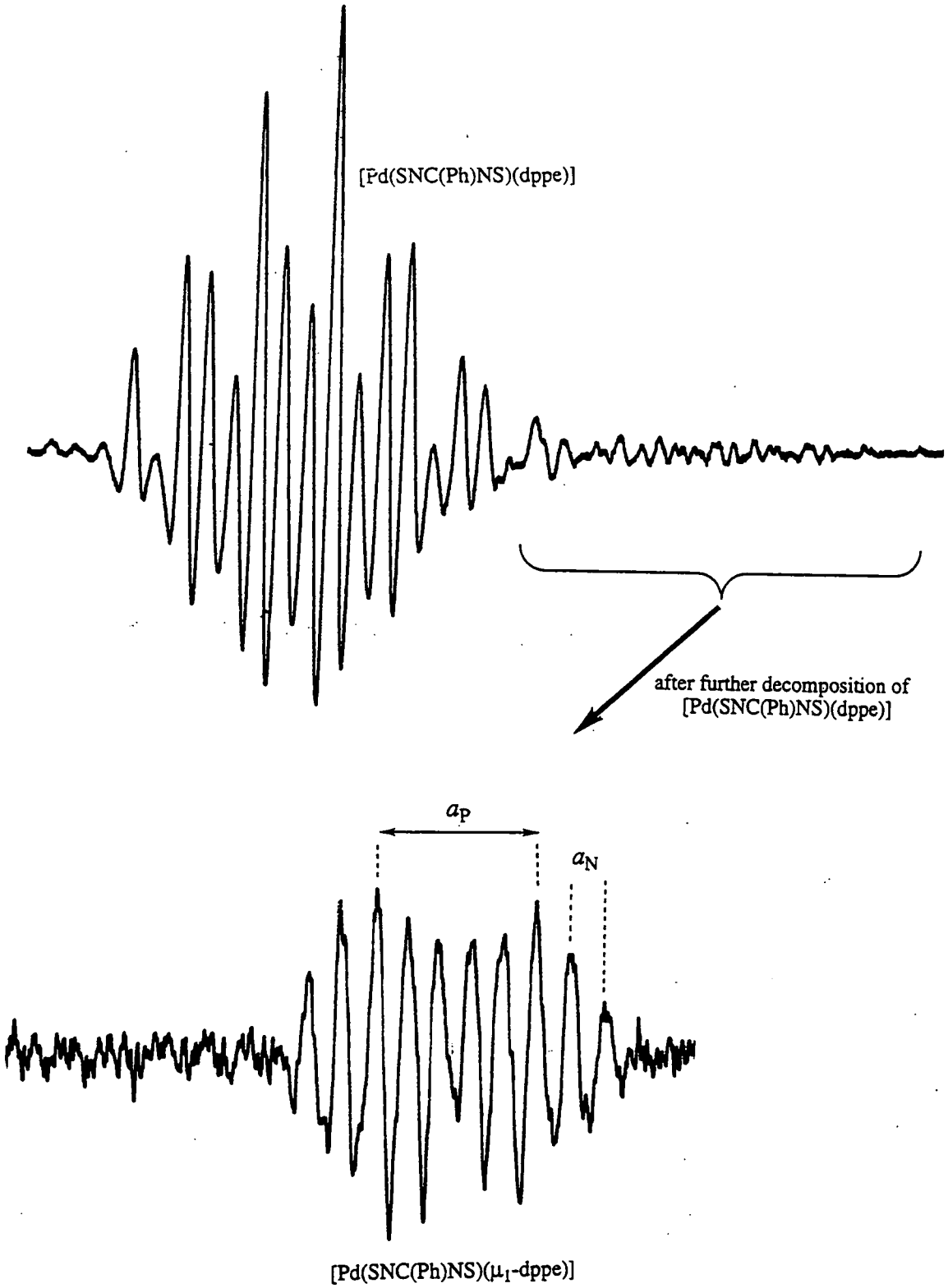

Figure 6.b. First Derivative Experimental and Simulation Spectra of [Pd(SNC(Ph)NS)(μ_1-dppe)].

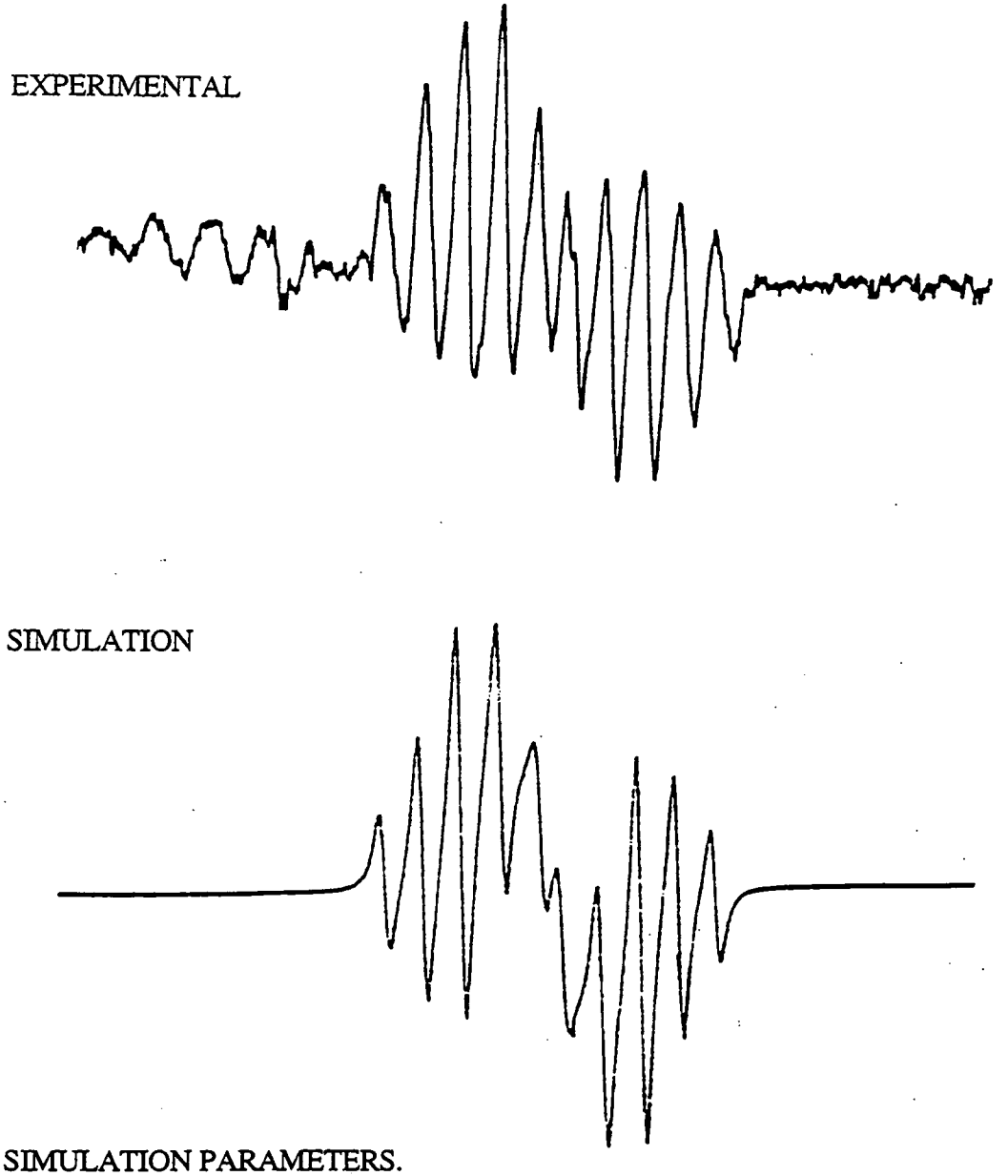

SIMULATION PARAMETERS.

$g$iso	2.0028
aN	0.429mT
aP	1.962mT
ΔHpp	0.12mT

(also 35% Gaussian ΔHpp=10.0G)

Figure 6.c. E.s.r. Spectrum of Decomposition Product of [Pt(SNC(Ph)NS)(dppe)].

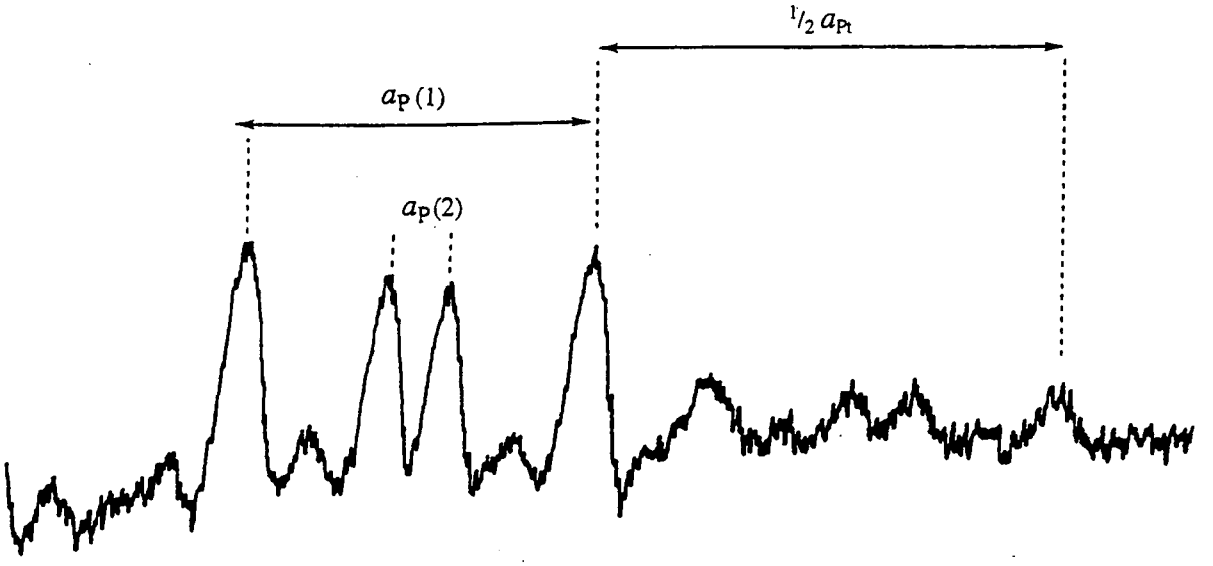

6.2.2.3. A rationalisation of e.s.r. spectroscopic results and propossed intermediates in the monometallic to trimetallic conversion.

The above e.s.r. discussion and previous e.s.r. studies in chapter five have shown two different ways that these electron rich , formally 17e$^-$ species can shed electron density. The first method, and the one that stabilises the monometallic species (as discussed in chapter four), is to shed electron density back into the ring system; hence hyperfine coupling to the ring two nitrogens is observed. This method maintains the structure of the complex and is shown in figure 6.d. The two canonical forms shown are only two of the many resonance structures that combine to form the delocalised π system of the species.

Figure 6.d. Two Resonance Forms of Monometallic Dithiadiazolyl Complexes.

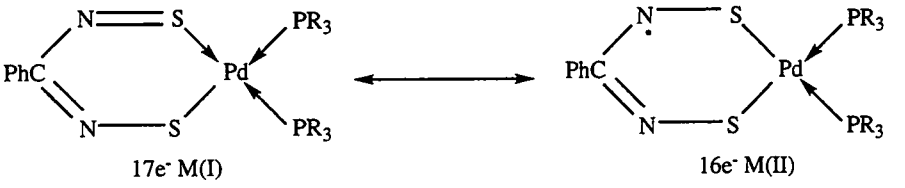

The second method involves breaking a metal phosphine bond to form an electron deficient 15e$^-$ complex (figure 6.e). This intermediate species was observed (section 6.2.2.1.) in the e.s.r. spectra of the decomposition of [Pd(SNC(Ph)NS-*S,S*)(dppe)] to [Pd(SNC(Ph)NS-*S,S*)(η^1-dppe)]. However, the delocalised metallocycle remains intact; thus a degree of stability remains and the unstable species survive long enough to be observable by e.s.r. spectroscopy. The loss of phosphine is a logical link to oligomerisation to the trimetallic species which requires the loss of phosphine and [PhCNSSN]$^\bullet$.

Figure 6.e. Unco-ordination of One Phosphine of [Pd(SNC(Ph)NS-*S,S*)(dppe)]

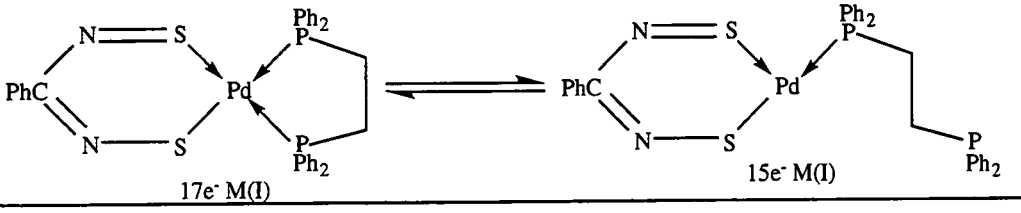

A third method of the metal shedding electron density can be envisaged (although this method was not indicated by e.s.r. spectroscopy) and involves breaking a bond to sulfur (figure 6.f.). This way of breaking up the monometallic complex will be more unlikely than the previous method as it involves partially uncoupling the [RCNSSN]• group. The chalcogen ring is chelating and provides delocalisation energy through the π framework. However, as stated previously in forming trimetallic species, [RCNSSN]• must be lost and a process such as this must take place at some stage.

Figure 6.f. Loss of phosphine from Monometallic Dithiadiazolyl Complexes.

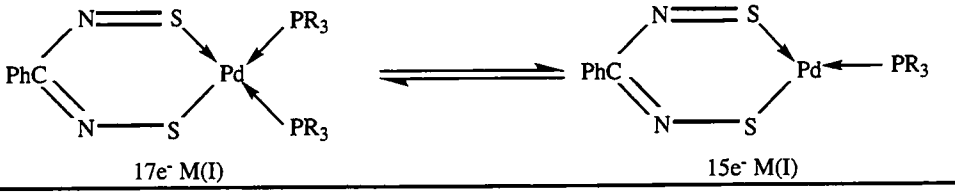

6.2.3. The Monomer to Trimer Conversion; a Kinetic Study.

6.2.3.1. Kinetic Study of the Decomposition of [Pt(SNC(Ph)NS-*S,S*)(PPh_3)$_2$] by E.s.r. and U.V./Vis Spectroscopy.

A preliminary kinetic study was undertaken to measure the rate of decay of [Pt(SNC(Ph)NS-*S,S*)(PPh_3)$_2$] by measuring both the loss of unpaired electron signal (e.s.r. spectroscopy) and loss of blue colouration (U.V./Vis). The discrepancy in T=0 for both experiments and other variables, such as temperature and differences in baseline calculation, made accurate measurement impossible from these initial studies. Despite these provisos an indication of the kinetics of the decomposition of this Pt species can be gleaned.

The decay in intensity of the e.s.r. signal is shown in graph 6.a. and of the absorption at the red end of the visible spectra (680nm) in graph 6.b. Both reactions were undertaken in CH_2Cl_2 solution and show logarithmic decay. Plots of $\ln[A]_t/[A]_0$ and $\ln[A]_t/[A]_0$ *vs* time gives a straight line where the negative gradient is the rate constant k, as shown in graphs 6.c. and 6.d. The decomposition obeys the first-order law for the consumption of the reactant [Pt(SNC(Ph)NS-*S,S*)(PPh_3)$_2$] (see equation 6.a.)[5a]. There is a discrepancy over the measurement of the rate constant using both techniques $4.58 \times 10^{-3} s^{-1}$, by e.s.r. measurements and $1.21 \times 10^{-3} s^{-1}$ by U.V./Vis spectroscopy which is undoubtably due to the errors mentioned previously e.g. temperature[5b]. However, the figures are of the same magnitude.

Equation 6.a. First-order Rate Law

$$\ln \frac{[X]_t}{[X]_o} = -kt$$

Where [X] is intensity [I] or absorbance [A], k is the rate constant and t is time

These results would indicate that the first step in the decomposition is the simple loss of PPh_3 and this is the sole method of the decomposition of [Pt(SNC(Ph)NS-*S,S*)$(PPh_3)_2$] (see equation 6.b.).

Equation 6.b. Decomposition of Pt(SNC(Ph)NS-S,S)$(PPh_3)_2$.

$$[Pt(SNC(Ph)NS\text{-}S,S)(PPh_3)_2] \longrightarrow [Pt(SNC(Ph)NS\text{-}S,S)(PPh_3)] + PPh_3$$

$$\text{Rate} = k[Pt(SNC(Ph)NS\text{-}S,S)(PPh_3)_2]$$

However, at lower concentrations of [Pt(SNC(Ph)NS-*S,S*)$(PPh_3)_2$] (after 3500sec. in the U.V. study) decomposition occurs more rapidly than expected. First-order kinetics no longer apply and [Pt(SNC(Ph)NS-*S,S*)$(PPh_3)_2$] decomposes via other routes, as well as by the simple loss of phosphine. These other routes will be described in section 6.2.9.

6.2.3.2. U.V./Vis. Kinetic Measurements of [Pd(SNC(Ph)NS-*S,S*)(dppe)].

A similar kinetic study was undertaken on the decomposition of [Pd(SNC(Ph)NS-*S,S*)(dppe)]. This reaction also followed first order kinetics as shown in graph 6.e.; thus loss of phosphine is again the rate determining step (in this case the first decomposition product is probably the same one as observed by e.s.r. spectroscopy, [Pd(SNC(Ph)NS-*S,S*)(η^1-dppe)]. On this occasion the reaction proceeded more quickly, was thus more difficult to measure accurately and first-order kinetics were only obeyed for 800sec. As a result a higher value for the rate constant 2.36×10^{-3} was observed compared to the U.V./vis value for the previously discussed Pt species, $1.21 \times 10^{-3} s^{-1}$.

Graph 6.a. Decay of [Pt(SNCPhNS-S,S)(PPh3)2] measured by E.s.r. Spectroscopy.

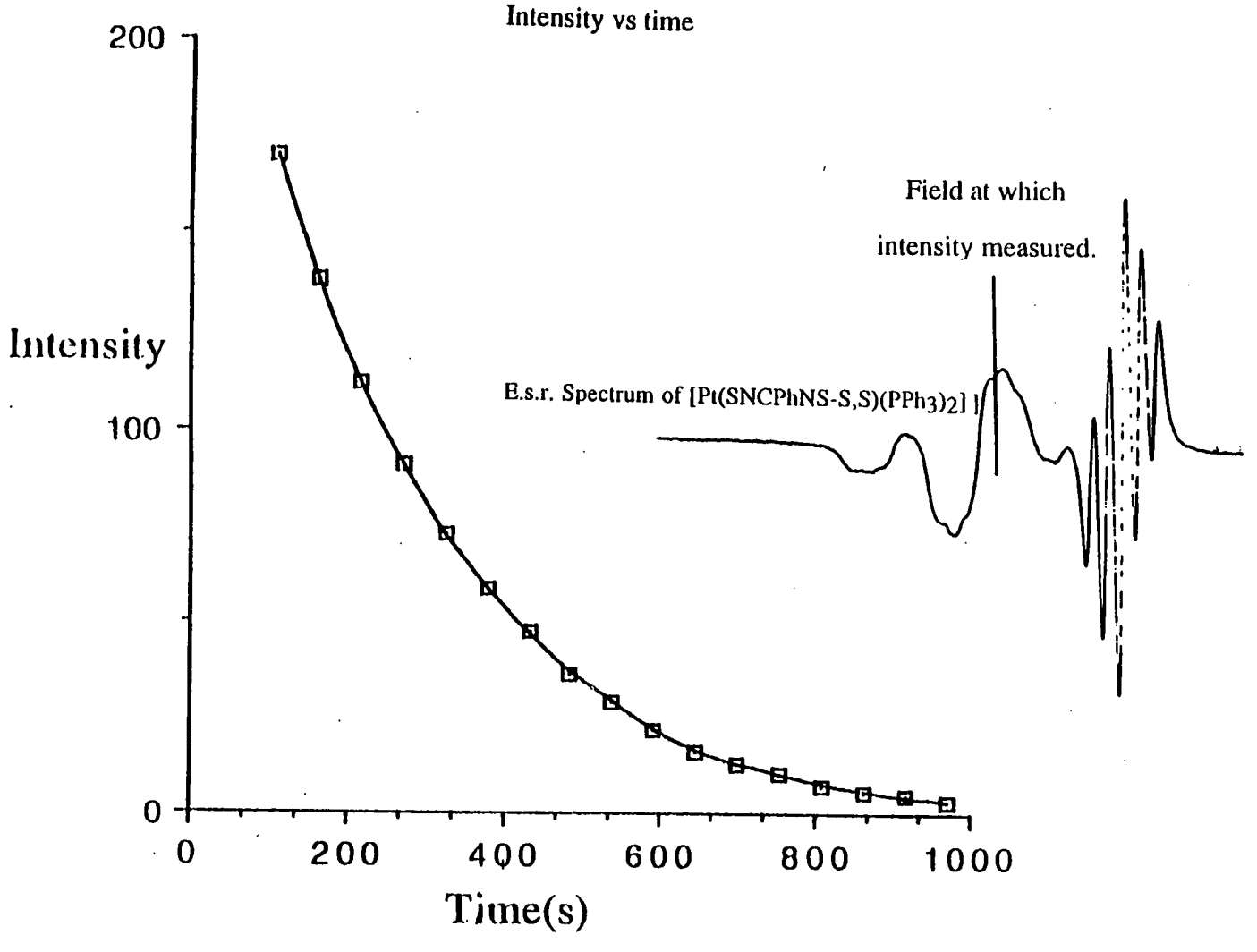

Graph 6.b. Decay of [Pt(SNCPhNS-S,S)(PPh3)2] measured by U.V /Visible Spectroscopy.

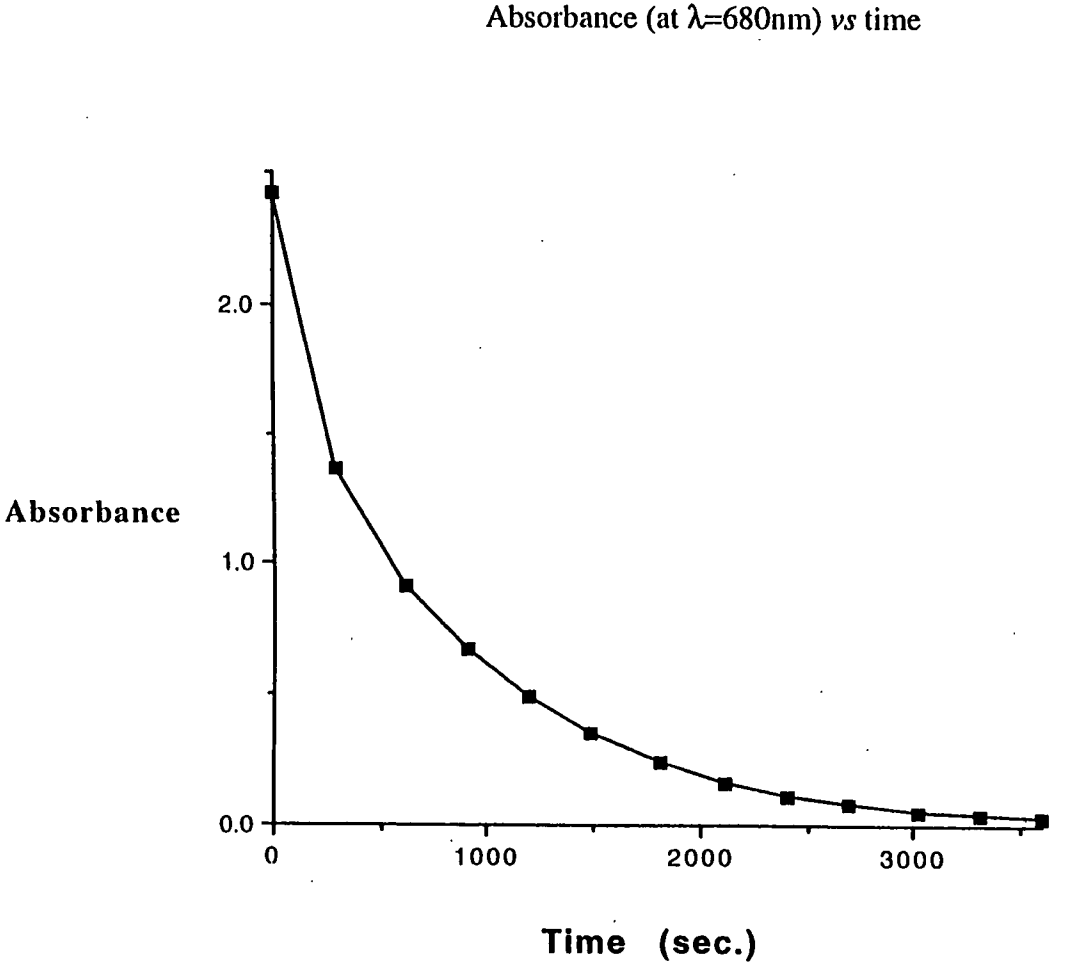

Graph 6.c. E.s.r. Kinetic Measurements of [Pt(SNCPhNS-*S*,*S*)(PPh_3)$_2$] .

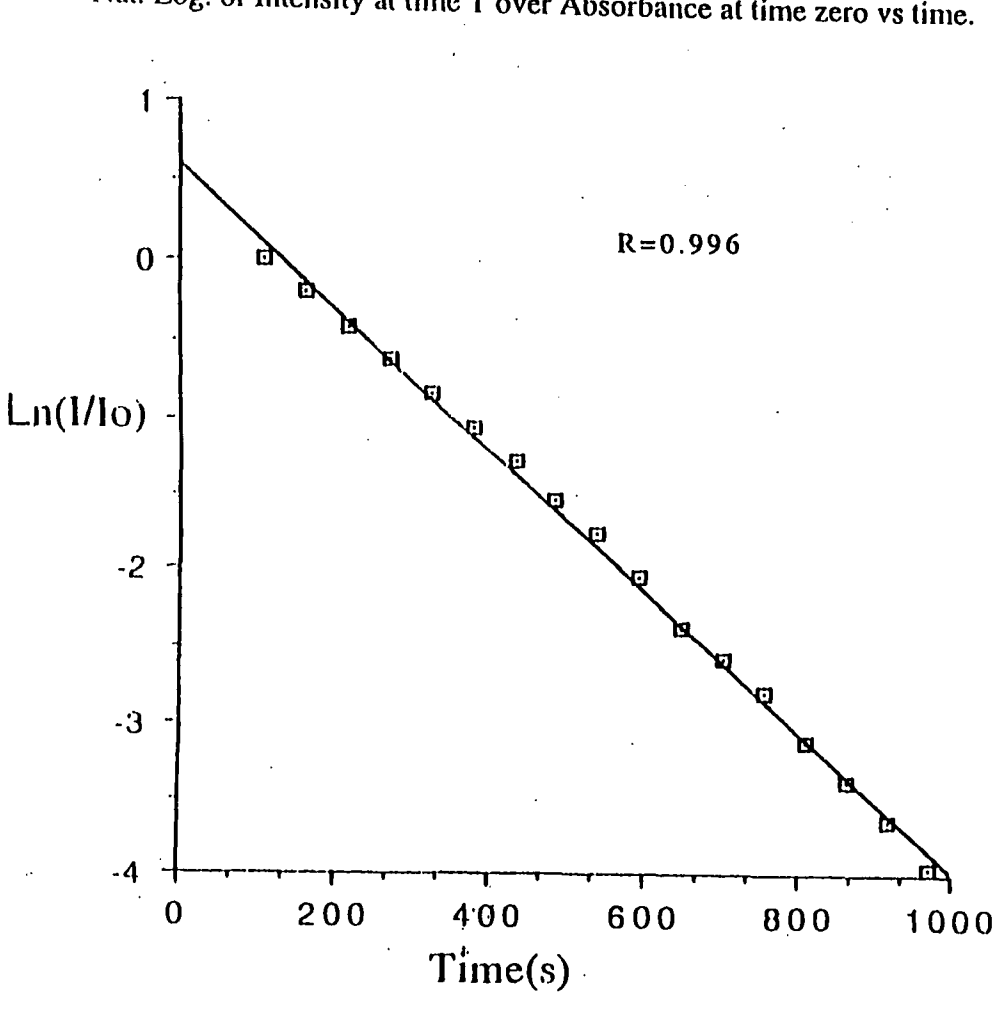

Graph 6.d. U.V /Visible Kinetic Measurements of [Pt(SNCPhNS-*S*,*S*)(PPh_3)$_2$] .

Nat. Log. of Absorbance at time T over Absorbance at time zero *vs* time.

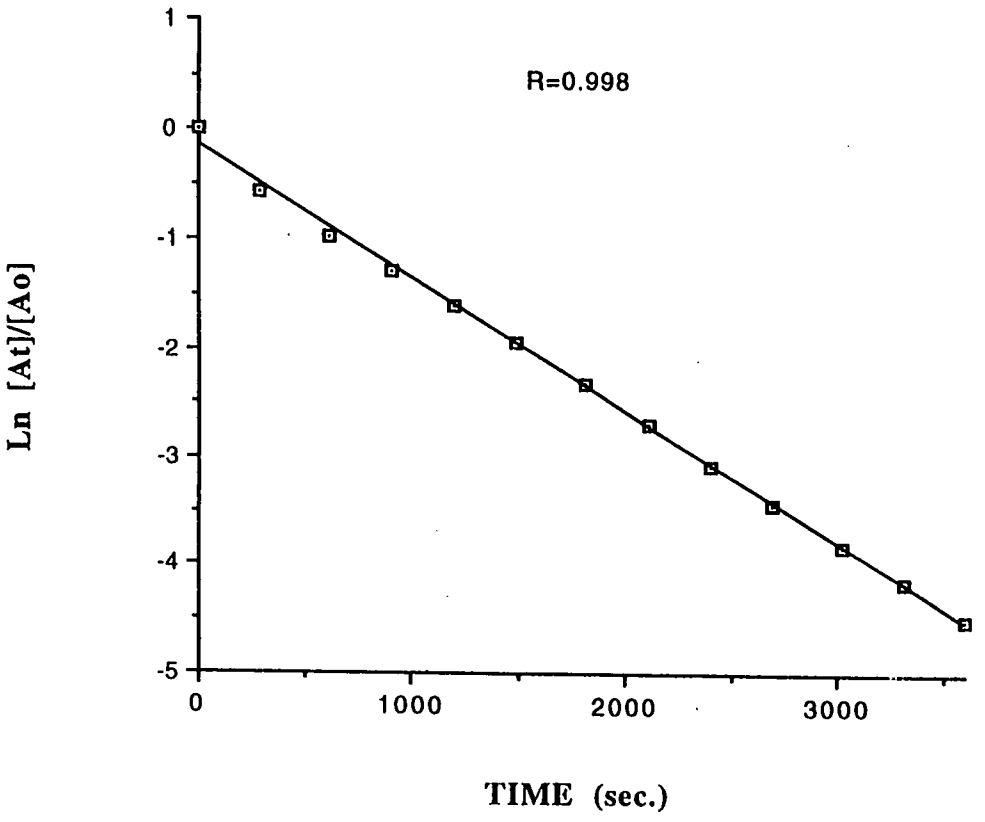

Graph 6.e. U.V /Visible Spectra Kinetic Measurements of [Pd(SNCPhNS-S,S)(dppe)].

Nat. Log. of Absorbance at time T over Absorbance at time zero *vs* time.

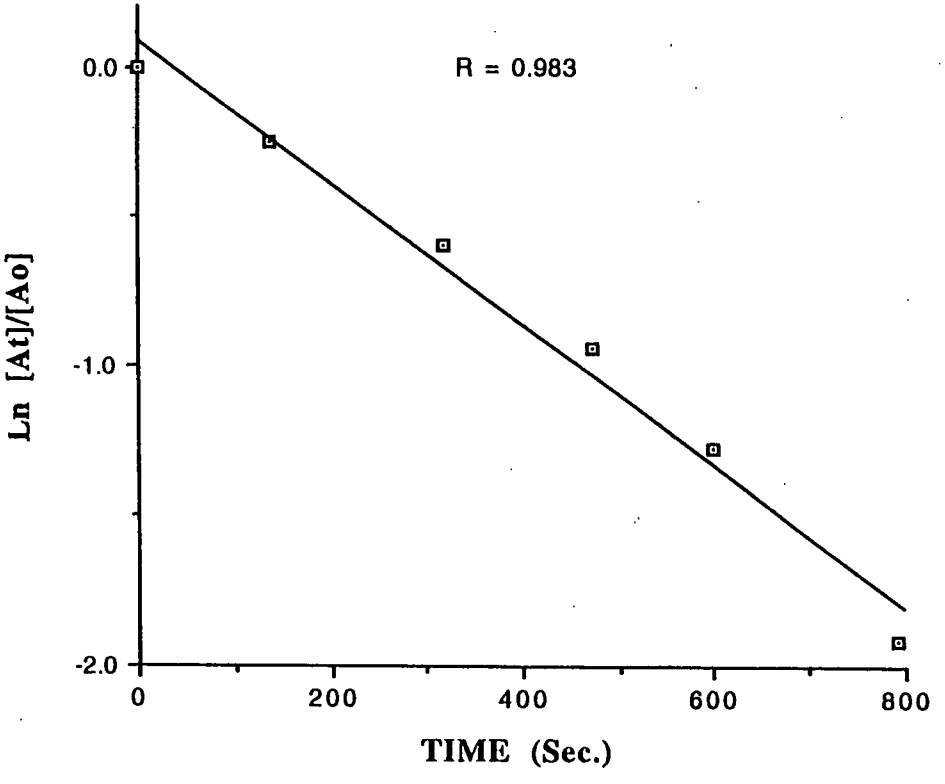

6.2.4. Other Decomposition Pathways of Monometallic Complexes.

6.2.4.1. ^{31}P N.M.R. Study of Decomposition of [Pd(SNCPhNS-*S,S*)(dppe)].

As explained previously in chapter five no signal is observed for [Pd(SNCPhNS-*S,S*)(dppe)]. This spectrum (figure 6.h.) thus shows only decomposition products. As the species decomposes, dppe extracts sulfur from the heterocycle to form $Ph_2P(S)(CH_2)_2P(S)Ph_2$ (δ43.35)[6] which is the major peak. There is no $[Pd_3(\mu_S\text{-}_SSNCPhNS)_2(dppe)_2]$ (δ41.17, see chapter 5) present even when the sample was rerun 3h later. The solution had, however, changed colour by this time to orange over an orange precipitate. The precipitate could perhaps have included some $[Pd_3(\mu_S\text{-}_SSNCPhNS)_2(dppe)_2]$ but the solution contained another species which produced a doublet of doublets (δ55.0 and 45.20ppm, $J_{P\text{-}P}$34.4Hz). This species may contain a protonated ring nitrogen in a monometallic complex (as in $[Fe_2(\mu_S\text{-}_SSN(H)CPhNS)(CO)_6]$[7] which would render both P atoms inequivalent (figure 6.g.). Similar ^{31}P values are found in the dppe complex [Pd{NS(SO_2NH_2)NSN)}(dppe)], δ54.3 &48.4, $J_{P\text{-}P}$40Hz[8].

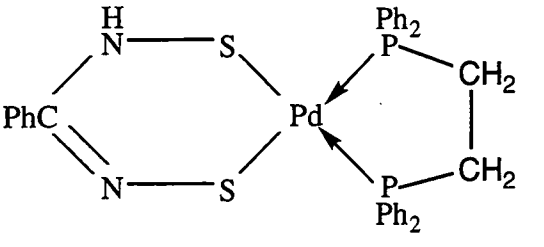

Figure 6.g. Pd(SN(H)CPhNS-*S,S*)(dppe)

Further evidence for this structure is found in a poorly resolved ^{1}H n.m.r. spectra which contains a weak, broad singlet at 6ppm (N bound protons on $[Fe_2(\mu_S\text{-}_SSN(H)C(R)NS)(CO)_6]$ are found between 6 and 7ppm[7]).

Figure 6.h. ^{31}P N.m.r. Spectrum of the Decomposition Products of [Pd(SNC(Ph)NS-*S*,*S*)(dppe)]

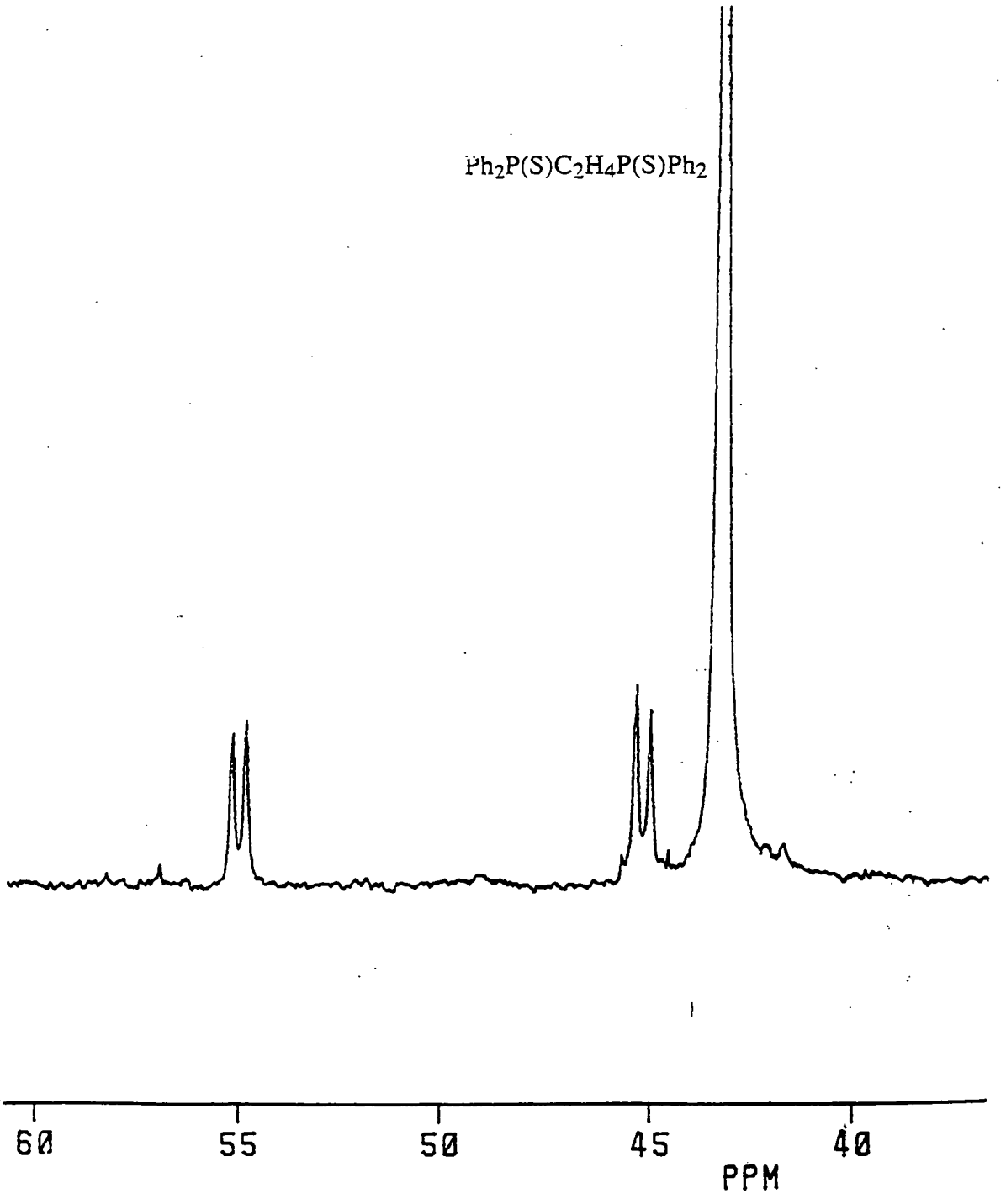

6.2.4.2. ^{31}P n.m.r. Study of the Decomposition of [Pt(SNC(PhNS-*S,S*)(PPh$_3$)$_2$].

The ^{31}P n.m.r. spectrum of a solution of [Pt(SNC(PhNS-*S,S*)(PPh$_3$)$_2$] was run at hourly intervals for 5h. Figure 6.i. shows the first spectrum run of [Pt(SNC(PhNS-*S,S*)(PPh$_3$)$_2$] and the spectrum of [Pt$_3$($\mu_{S\text{-}S}$SNC(Ph)NS)$_2$(PPh$_3$)$_4$] for comparison. Figure 6.j. shows spectra run after 1,2,3 & 4hrs.

As anticipated, the main peak observed at t=0 is for [Pt$_3$($\mu_{S\text{-}S}$SNC(Ph)NS)$_2$(PPh$_3$)$_4$] (singlet δ18.02ppm, $J_{Pt\text{-}P}$3288Hz), with PPh$_3$ (δ–5.15ppm)[9a] also observed from the decomposition of monometallic species.

There are also four sets of what initially appear to be doublets at δ26.26 &26.06ppm, δ21.65 & 21.41, δ19.45 &19.19ppm and also at δ15.40 and 15.36ppm. These peaks are marked A,B,C,and D on figures 6.g. and 6.h. Over time these signals decay at differing rates and after 4h only the two peaks at δ19.45 & 19.19ppm remain. Thus there is no evidence for a doublet of doublets and protonated dithiadiazolyl nitrogen complex as proposed for the palladium species discussed previously. It is not known what these intermediate species are.

In contrast though, the decomposition of the partially fluorinated analogue [Pt(SNC(3,4FC$_6$H$_4$)NS-*S,S*)(PPh$_3$)$_2$][10] does yield, amongst its products, a doublet of doublets as viewed by ^{31}P at δ19.45ppm & 14.64ppm, $J_{P\text{-}P}$22.6Hz (c.f. a similar species [Pt(SNSN)(PPh$_3$)$_2$] δ23.6ppm & 11.4ppm, $J_{P\text{-}P}$22Hz)[11]. As in the decomposition products previously described for [Pd(SNC(Ph)NS-*S,S*)(dppe)] this may be a ring nitrogen protonated monometallic species, the doublet of doublets indicating two phosphorus atoms in inequivalent chemical envirnoments coupled through Pt (although the signal is too week to observe Pt satellites)

Over time PPh$_3$S (δ43.57)[12] is formed from the reaction of PPh$_3$ and [PhCNSSN]$^{\bullet}$ (and any sulfur impurities) and as this peak increases in intensity so the peak for PPh$_3$ decreases.

Of greater interest is the emergence of a singlet at δ15.43ppm with Pt satellites ($J_{Pt\text{-}P}$3552Hz) which increases with intensity at the expense of [Pt$_3$($\mu_{S\text{-}S}$SNC(Ph)NS)(PPh$_3$)$_4$]. This unknown (marked X on the spectra) is also found when the spectrum of [Pt$_3$($\mu_{S\text{-}S}$SNC(Ph)NS)(PPh$_3$)$_4$] is run and may be evidence for a longer

chain complex where Pt>3. A similar species is observed in the decomposition of $[Pt(SNC(3,4FC_6H_4)NS\text{-}S,S)(PPh_3)_2]$[10], δ 15.33ppm, ($J_{Pt\text{-}P}$3555Hz) .

Figure 6.i.

Initial ^{31}P N.m.r. Spectrum of the Decomposition of $[Pt(SNC(Ph)NS\text{-}S,S)(PPh_3)_2]$.

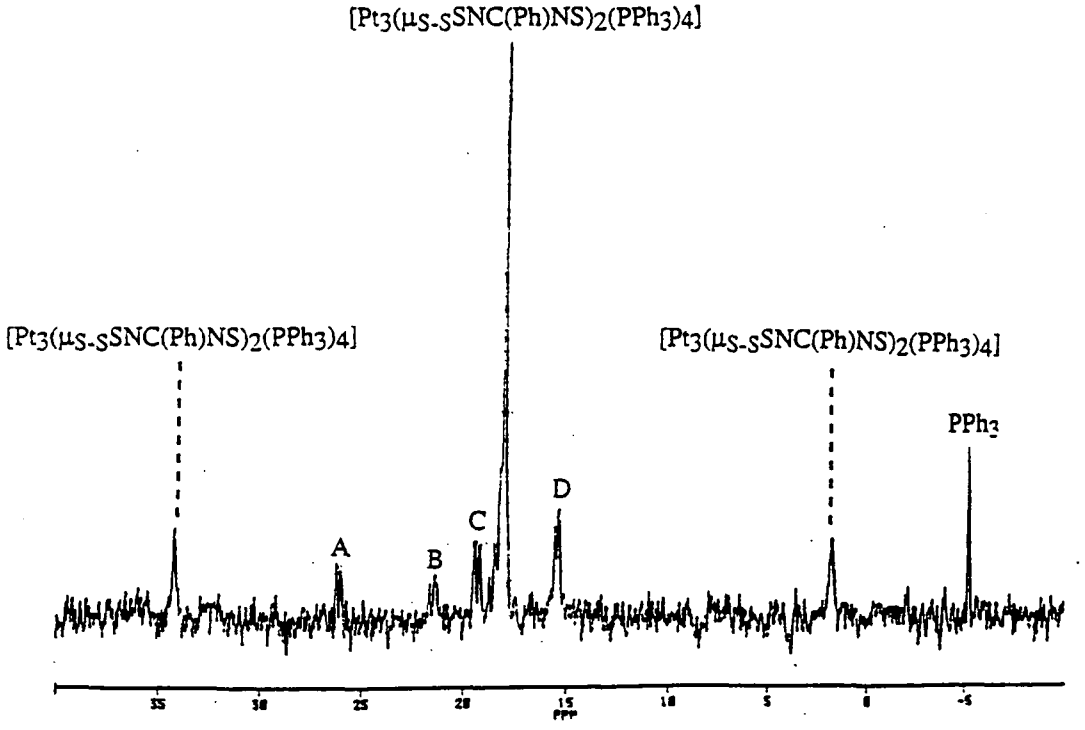

31p N.m.r. Spectrum of $[Pt_3(\mu_{S\text{-}S}SNC(Ph)NS)_2(PPh_3)_4]$ and its Decomposition Products.

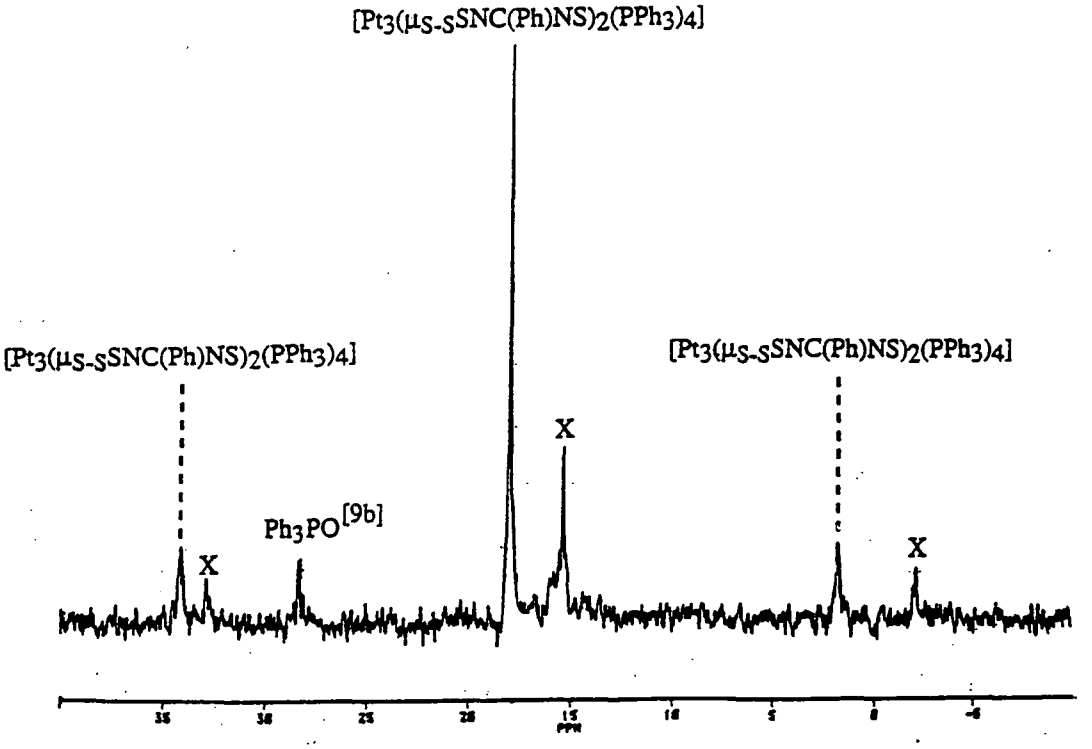

Figure 6.j. ^{31}P N.m.r. Spectra of the Decomposition of $[Pt(SNC(Ph)NS)(PPh_3)_2]$ after 1,2,3 & 4 hours.

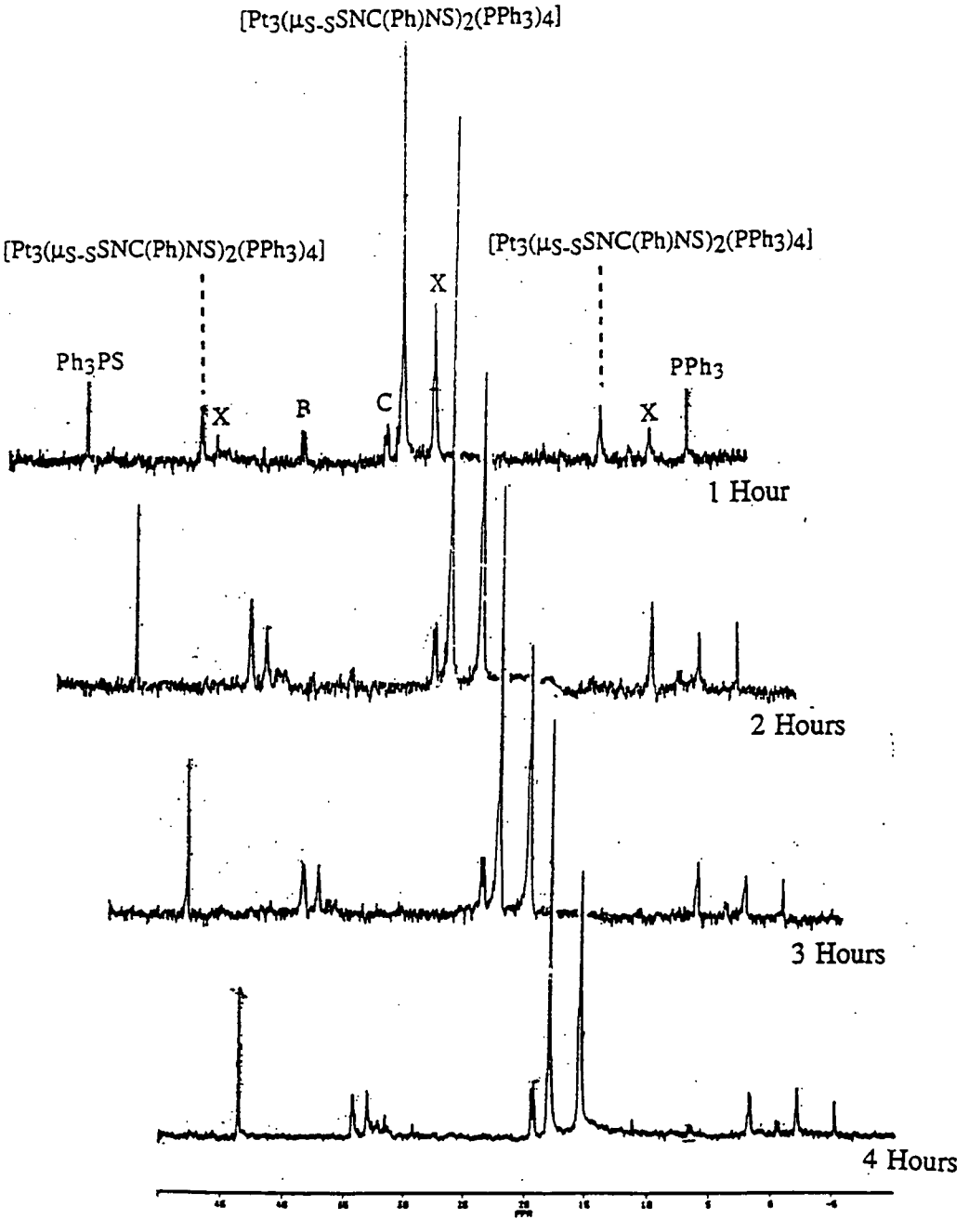

6.2.4.3. The Decomposition of [Pt(SNC(Ph)NS-*S,S*)(dppe)].

As stated previously [Pt(SNC(Ph)NS-*S,S*)(dppe)] does not decompose as readily as its Pt, triphenylphosphine analogue. However, during n.m.r. and the previously described e.s.r. experiments it was noted that CH_2Cl_2, $CDCl_3$ and MePh solutions of the complex lose their intense blue colour over a period of days to yield yellow solutions.

A suspension of [Pt(SNC(Ph)NS-*S,S*)(dppe)] was therefore stirred in CH_2Cl_2 for 2 days to yield a yellow solution. The solvent was removed *in vacuo* and the solids washed with MePh. Elemental analysis indicated that pure [$Pt_3(\mu_{S\text{-}S}$SNC(Ph)NS-*S,S*)$_2$(dppe)$_2$] (the most likely product) had not been obtained. Spectroscopic evidence discussed in section 6.2.4.4.. was to give some indication of the products formed.

6.2.4.4. ^{31}P n.m.r. Study of [Pt(SNC(Ph)NS-*S,S*)(dppe)].

The ^{31}P n.m.r. spectra were recorded of [Pt(SNC(Ph)NS-*S,S*)(dppe)] (figure 6.k.) and of the yellow solids discussed in the previous paragraph (figure 6.l.). Data for the species observed are shown below in table 6.c. There are two species present with two equivalent dppe phosphorus atoms bound to platinum. The most intense peak at δ37.50, $J_{Pt\text{-}P}$3234.0Hz (compound A), probably corresponds to the trimetallic species [$Pt_3(\mu_{S\text{-}S}$SNC(Ph)NS)$_2$(dppe)$_2$] (i.e. with equivalent dppe phosphine atoms) while the latter, unknown compound B (δ36.41ppm, $J_{Pt\text{-}P}$2457.4Hz) may be of a higher molecular mass where Pt=4 or greater or some other Pt bound dppe species with equivalent phosphines. Two signals with Pt satellites are further split into doublets (unknown A). This may be due to the presence of inequivalent P atoms (of dppe) coupling with each other in a metal complex in which one ring nitrogen is protonated (as proposed in section 6.2.4.1 for the Pd analogue). The ^{31}P n.m.r. data of two related complexes [Pt(SNSN)(dppe)] and [Pt(SeNSN)(dppe)] are included for comparison[11]. The chemical shift values and coupling constants are very similar to this unknown species. ^{1}H n.m.r. spectroscopy shows the presence of a broad peak at δ6.81ppm which may be attributed to an N bound proton in an (SN(H)C(Ph)NS) ligand system.

Two further peaks at δ48.55 & 34.17ppm can also be observed but are of too small an intensity to view any Pt satellite, no firm attempts have been made to elucidate the possible species that may give rise to these peaks due to their low intensity.

The ^{31}P n.m.r. spectra of the yellow solids indicate that as the reaction proceeds the signal proposed to be the trimetallic complex increases in intensity with respect to all the other signals and some $Ph_2P(S)C_2H_4P(S)PPh_2$ (δ43.35)[6] is also formed.

Table 6.c. ^{31}P Decomposition products of Pt(SNC(Ph)NS-*S,S*)(dppe).

COMPLEX	δ	J_{Pt-P} Hz	J_{P-P} Hz
$[Pt_3(\mu_{S-S}SNC(Ph)NS)_2(dppe)_2]$	37.50	3234.0	------
Unknown B	36.41	2457.4	------
Unknown A P(1)	44.61	2576.4	7.9-8.6
Unknown A P(2)	41.32	3070.9	8.6
[Pt(SNSN)(dppe)] P(1)	43.7	2756	12
[Pt(SNSN)(dppe)] P(2)	41.1	2784	12
[Pt(SeNSN)(dppe)] P(1)	42.7	2868	12
[Pt(SeNSN)(dppe)] P(2)	40.0	2787	12
Unknown C	34.17	------	------
Unknown D	47.56	------	------

Figure 6.k. ^{31}P N.m.r. Spectrum of the Decomposition of [Pt(SNC(Ph)NS-*S*,*S*)(dppe)]

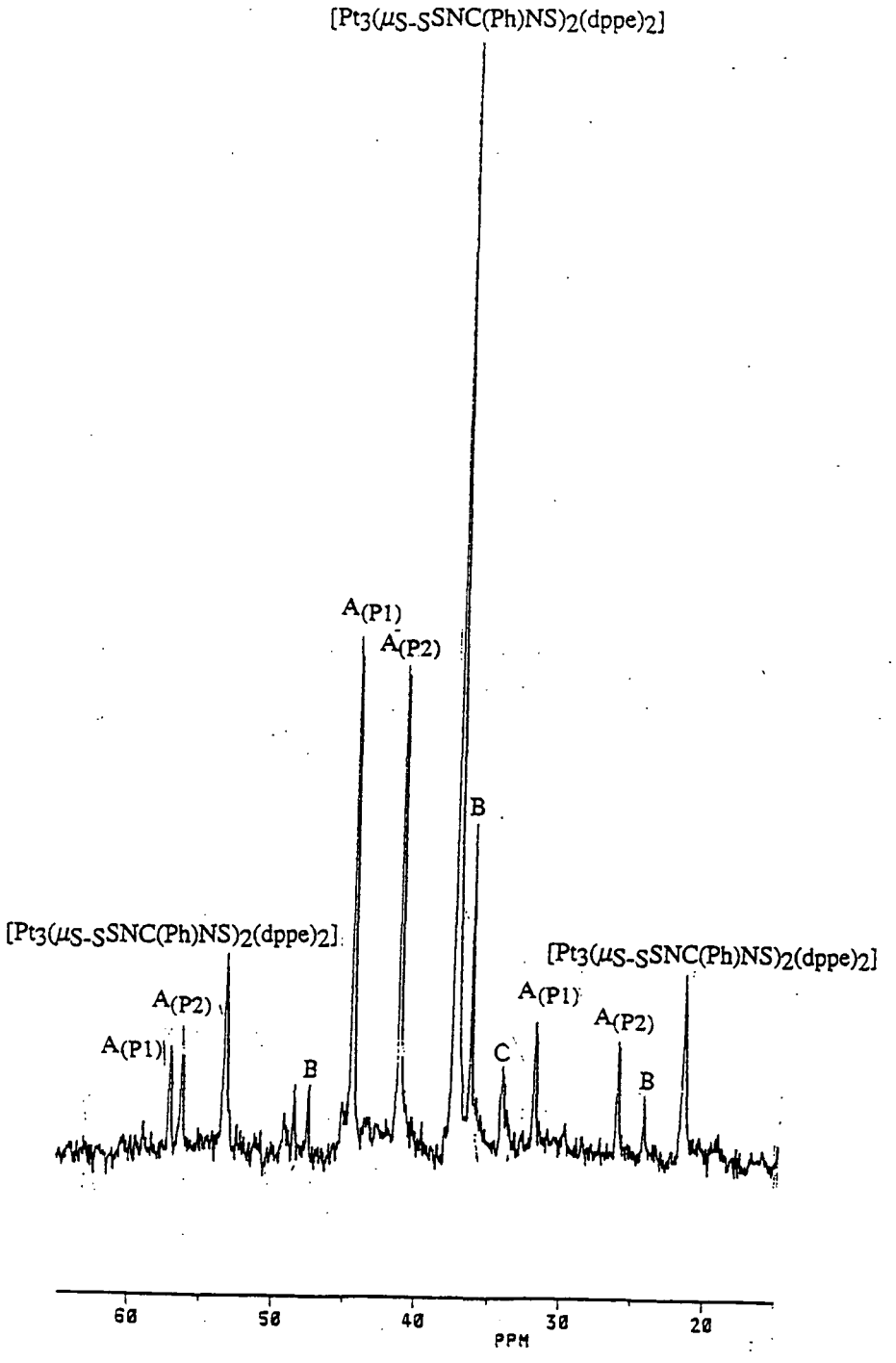

Figure 6.j. 31P N.m.r. Spectrum of the Yellow Solids Formed from the Decomposition of [Pt(SNC(Ph)NS-*S,S*)(dppe)].

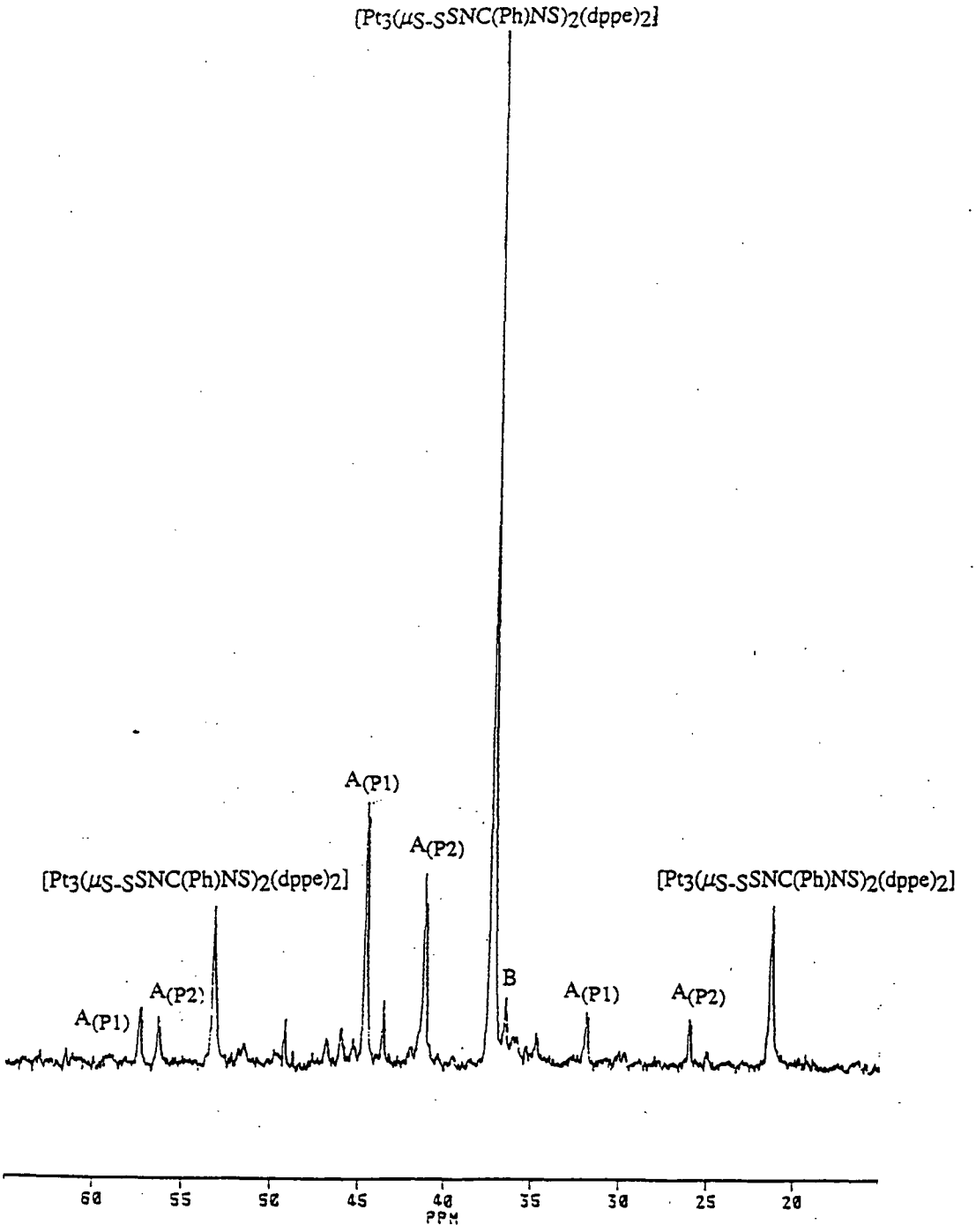

6.2.4.5. The Reaction Between [Pt(SNC(Ph)NS-*S,S*)(dppe)] and [$Pt(PPh_3)_4$].

The previous discussion has highlighted the difficulties in forming [$Pt_3(\mu_S$-$_S$SNC(Ph)NS)$_2$(dppe)$_2$] by attempting to decompose [Pt(SNC(Ph)NS-*S,S*)(dppe)] dissolved in CH_2Cl_2. The dppe ligand has proved to be too strongly bound to allow a quick relatively clean decomposition as observed for [Pt(SNC(Ph)NS-*S,S*)(PPh_3)$_2$.]. In fact, all that is required to form a trimetallic species is the insertion of a bare metal atom between two [Pt(SNC(Ph)NS-*S,S*)(dppe) units. It was hoped that [$Pt(PPh_3)_4$] could provide this metal atom.

[Pt(SNC(Ph)NS-*S,S*)(dppe)] and [$Pt(PPh_3)_4$] were stirred in MePh for two weeks at 70°C. During this time there was a gradual colour change from blue through brown to an orange solid under an orange solution. This solid was washed with fresh MePh, filtered and dried *in vacuo*. Unfortunately the compound formed, probably [$Pt_3(\mu_S$-$_S$SNC(Ph)NS)$_2$(dppe)$_2$], was not formed in great purity (as indicated by elemental analysis) and due to its insolubility in common solvents it could not be recrystallised. Low solubility also made ^{31}P n.m.r. difficult but the spectrum did yield a peak at δ37.31ppm, corresponding to the major product in the decomposition of [Pt(SNC(Ph)NS-*S,S*)(dppe)] as described and assigned to [$Pt_3(\mu_S$-$_S$SNC(Ph)NS)$_2$(dppe)$_2$] (δ37.50ppm).

6.2.4.6. The Reaction Between [Pt(SNC(Ph)NS-*S,S*)(dppe)] and [$Pd(PPh_3)_4$].

If indeed Pt from [$Pt(PPh_3)_4$] inserted into a trans sandwich of [Pt(SNC(Ph)NS-*S,S*)(dppe)] then it may be possible to insert another metal, the most obvious being Pd. As such [Pt(SNC(Ph)NS-*S,S*)(dppe)] and [$Pd(PPh_3)_4$] were stirred in MePh at 70°C for 10 days to yield an orange solid under an orange solution. This solid was washed with fresh MePh, filtered and dried *in vacuo*. Elemental analysis satisfied the composition [PtPdPt(μ_S-$_S$SNC(Ph)NS)$_2$(dppe)$_2$]. Poor solubility resulted in difficulties running the ^{31}P n.m.r. spectra. Two peaks were observed at δ37.34ppm, some [$Pt_3(\mu_S$-$_S$SNC(Ph)NS)$_2$(dppe)$_2$] had formed, and at δ38.13ppm. The second value is very close to the former and is almost certainly due to [PtPdPt(μ_S-$_S$SNC(Ph)NS)$_2$(dppe)$_2$]. Unfortunately, the peaks were too small in intensity for Pt satellites to be observed.

An x-ray structural determination was required to prove that this complex had indeed been formed. Failure of previously utilised crystal growth techniques and poor solubility in common solvents meant that crystals of the required quality could not be prepared. However there are many complexes which contain both Pt and Pd atoms e.g. (mixedPt-Pd A-frame species[13] and the linear chain species discussed in chapter five[14]. There is therefore a precedent for mixed metal compounds being formed.

6.2.4.7. ^{1}H n.m.r. of decomposition products and the decomposition of [PhCNSSN]$^\bullet$

As indicated in chapter five the ^{1}H n.m.r. spectra of the three trimetallic species $[Pt_3(\mu_S\text{-}_SSNC(Ph)NS)_2(PPh_3)_4]$, $[Pd_3(\mu_S\text{-}_SSNC(Ph)NS)_2(PPh_3)_4]$ and $[Pd_3(\mu_S\text{-}_SSNC(Ph)NS)_2(dppe)_2]$ contained various impurities. The ^{1}H n.m.r. spectra of $[Pt_3(\mu_S\text{-}_SSNC(Ph)NS)_2(PPh_3)_4]$ and $[Pd_3(\mu_S\text{-}_SSNC(Ph)NS)_2(PPh_3)_4]$ are shown (figures n & o) and show the expected peaks in the phenyl region (as previously discussed in chapter five) and various higher and lower field impurities. As stated before, the trimetallic species precipitate out of solution so these impurities may be of lower intensity than indicated. The peaks at δ5.30ppm in $[Pd_3(\mu_S\text{-}_SSNC(Ph)NS)_2(PPh_3)_4]$ and δ2.29ppm in $[Pt_3(\mu_S\text{-}_SSNC(Ph)NS)_2(PPh_3)_4]$ may be attributed to solvent of crystallisation (CH_2Cl_2[15] & MePh[16a] respectively). The other peaks can not be so readily explained away although the most obvious cause would be products from the decomposition of [PhCNSSN]$^\bullet$]. There has already been ^{31}P n.m.r. evidence (see previous sections) for the extraction of sulfur from the chalcogen ring system (forming Ph_3PS or $Ph_2P(S)C_2H_4(S)PPh_2$) and an attempt to rationalise any decomposition pathways (with or without trace H_2O) are shown in figure m).

The only way the chalcogen ring system can be protonated is by attack from trace amounts of water. The oxygen from water is more likely to attack the more electropositive ring sulfur with protons attacking the ring nitrogens. As can be seen the major source of protons in these species is amine groups (NH) which usually have a chemical shift range of between 3-5ppm[16b]. There are no peaks found in this region for $[Pd_3(\mu_S\text{-}_SSNC(Ph)NS)_2(PPh_3)_4]$ or $[Pt_3(\mu_S\text{-}_SSNC(Ph)NS)_2(PPh_3)_4]$. Interestingly there are two sharp peaks found at about 8.3ppm in both triphenyl phosphine species (δ8.27ppm & 8.30ppm in the Pd species and δ8.32ppm & 8.29ppm in the Pt species). A

similar set of values was found for the decomposition products of the reaction between [PhCNSNS][AsF_6] and H_2O[17] (figures δ8.31 & 8.32ppm). They could be attributed to amide species (RC(O)N(H)R δ5-8.5) although the signal is usually broad[16b]. It is a possibility that the low field signals at δ1.25 & 1.55ppm in [$Pd_3(\mu_{S\text{-}S}SNC(Ph)NS)_2(PPh_3)_4$], 2.46ppm in [$Pt_3(\mu_{S\text{-}S}SNC(Ph)NS)_2(dppe)$] and 1.57ppm in [$Pd_3(\mu_{S\text{-}S}SNC(Ph)NS)_2(dppe)_2$] (the only impurity found in this proton n.m.r. spectrum) could just be trace aliphatic impurities e.g. from the solvent.

Finally, as shown above, decomposition products are seen in the ^1H n.m.r. spectrum of [$Pd_3(\mu_{S\text{-}S}SNC(Ph)NS)_2(PPh_3)_4$] but, as stated in chapter five, not the ^{31}P n.m.r. spectrum. It is possible that in the purification (recrystallisation with CH_2Cl_2) any phosphorus based impurities have all been removed.

Figure 6.m. Proposed Decomposition of [PhCNSSN]$^\bullet$

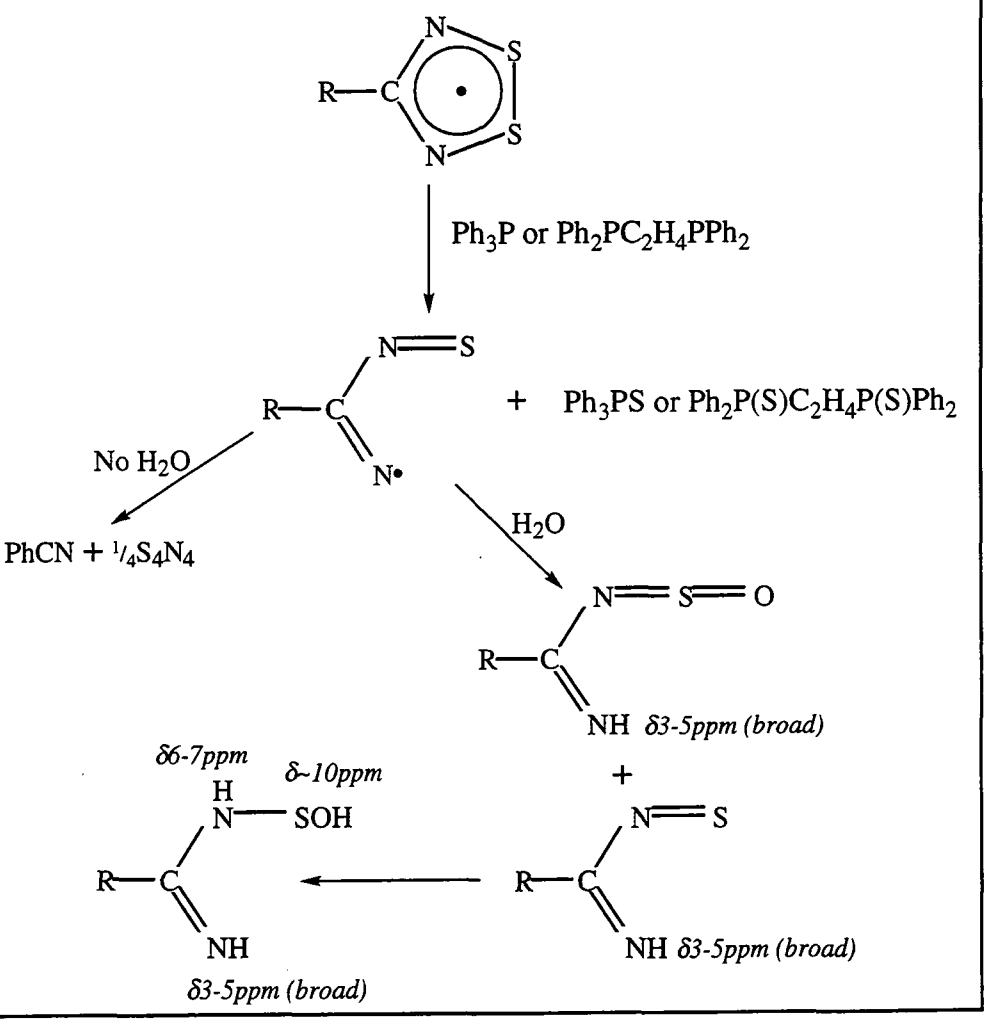

Figure 6.n. ^1H N.m.r. of $[Pt_3(\mu_{S\text{-}S}SNC(Ph)NS)_2(PPh_3)_4]$ and Unknown Side Products.

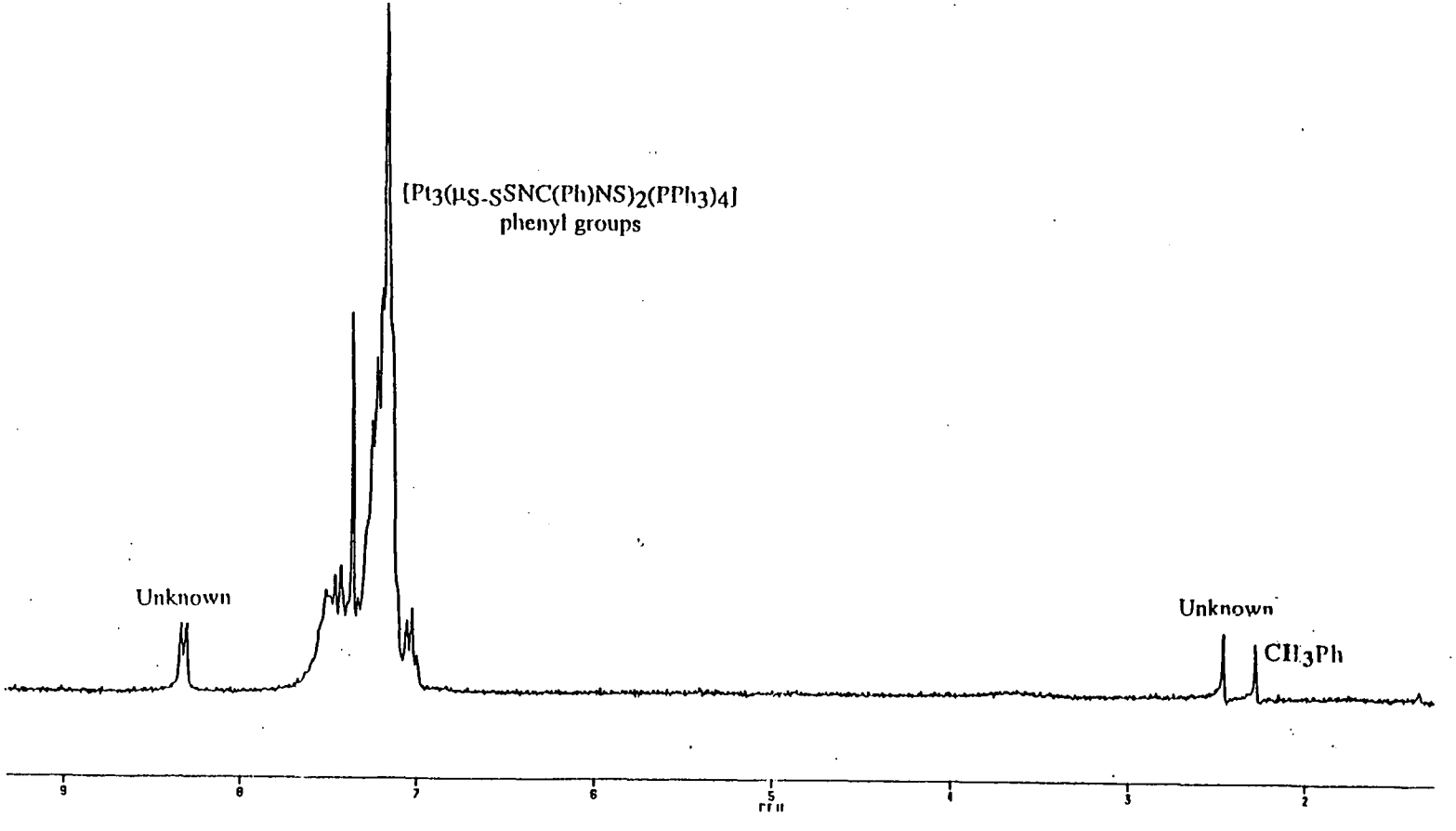

Figure 6.o. ^{1}H N.m.r. of $[Pd_3(\mu_{S,S}SNC(Ph)NS)_2(PPh_3)_4]$ and Unknown Side Products.

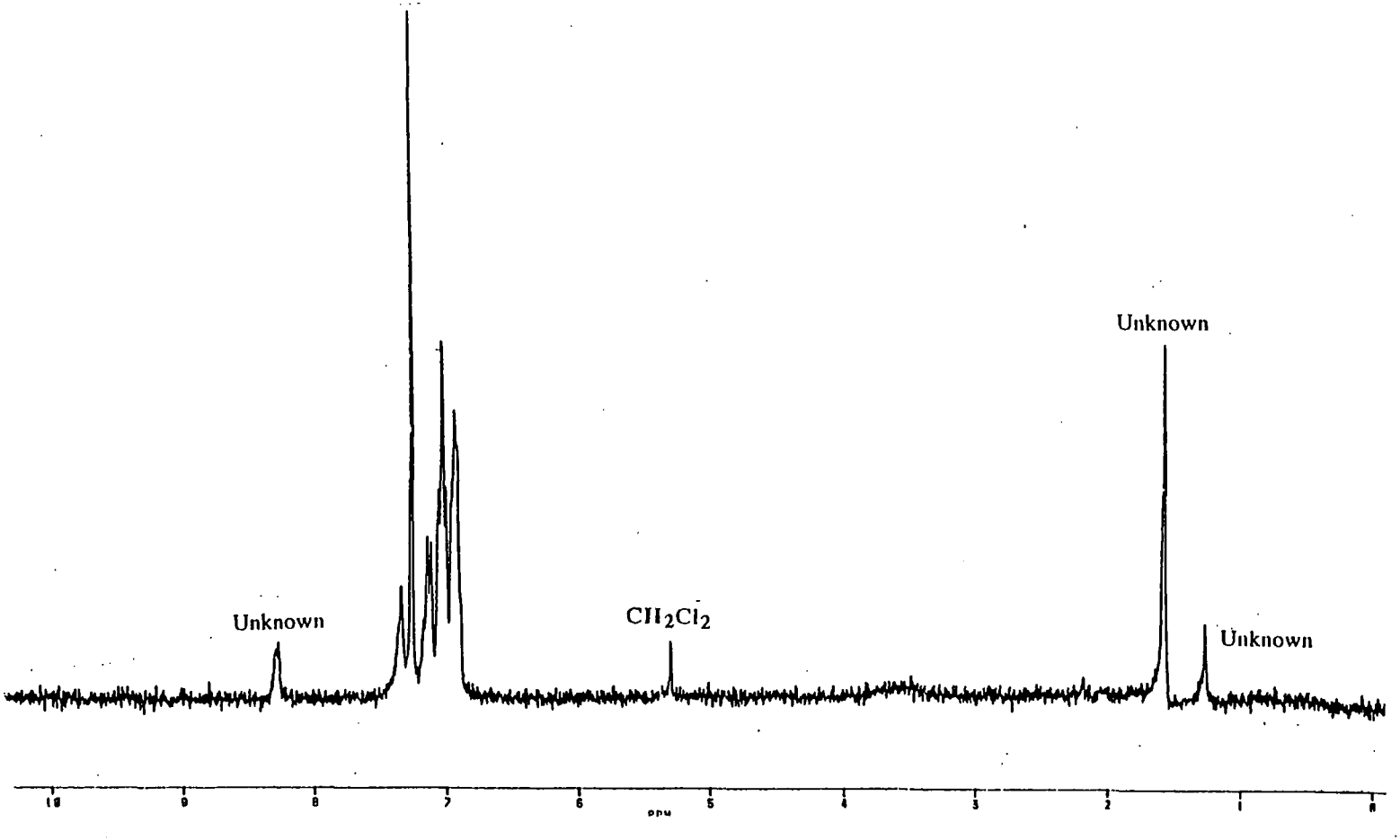

6.2.5. Attempted Rationalisation of the Decomposition Of Monometallic to Trimetallic Species.

The spectroscopic studies so far undertaken have indicated that the first step in the decomposition is the loss of phosphine (in the case of the dppe complexes e.s.r. evidence indicates that one P atom may become detatched from the metal). A reaction scheme can be postulated from this starting point. Loss of one phosphine effectively makes the metal centre electron poor (a 14-15 electron species from a 16-17e species). It is thus susceptible to attack from the two sulfur atoms of a second monometallic species to form a dimetallic complex, $[M_2(\mu_{S\text{-}S}SNC(Ph)NS)(SNC(Ph)NS\text{-}S,S)(P)_2]$ with loss of a second phosphine molecule. The sulfurs of the chelating dithiadiazolyl ring can now attack a second monometallic species displacing the (SNC(Ph)NS) radical already bound and forming the trimetallic species. As can be seen these later two reactions also consume monometallic complexes and result in loss of first order kinetics as time progresses (as indicated in section 6.2.3.). i.e. as the reaction progresses, the loss of phosphine is no longer the main method of reacting monometallic species. This reaction pathway is shown in reaction scheme 6.a.

Reaction Scheme 6.a. Proposed Mechanism for the Decomposition of Monometallic to Trimetallic dithiadiazolyl Complexes

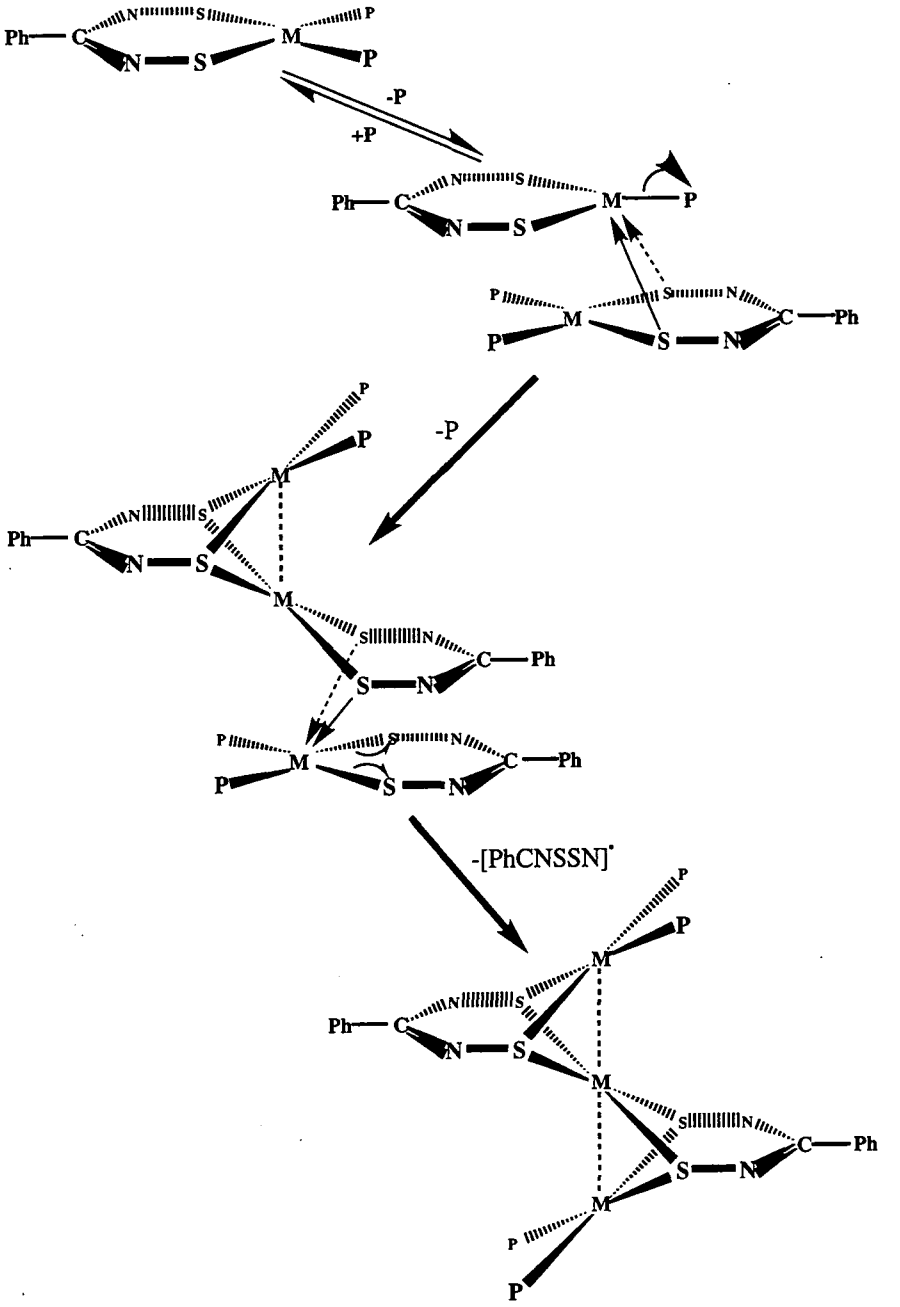

6.3. EXPERIMENTAL

6.3.1. The Decomposition of [Pt(SNC(Ph)NS-*S,S*)(dppe)].

[Pt(SNC(Ph)NS-S,S)(dppe)] (0.380g, 0.490mmol) was stirred in CH_2Cl_2 for 2 days to yield a yellow solution. The solvent was removed *in vacuo* and the solids washed with MePh (3x5ml) and dried *in vacuo*. The product is assumed to be mainly [$Pt_3(\mu_S$-$_S$SNC(Ph)NS)$_2$(dppe)$_2$]

Yield 0.163g, 60.15%.

IR ν_{max} (cm^{-1}) 3019w, 2372w, 2314w, 1637br, 1481m, 1434ssh, 1409m, 1379m, 1305m, 1215m, 1187m, 1160w, 1142w, 1102m, 1069m, 1009m, 997m, 877m, 821m, 790w, 717m, 703ssh, 691ssh, 615m, 576w, 531s, 483m, 419w.

Elemental Analysis, found: C49.91%; H3.97%; N3.58%; Calc.: C45.43%; H3.35%, N3.21%).

N.m.r.; (250MHz; solvent $CDCl_3$) ^1H δ7.10ppm (40H, m), 2.17ppm (8H, s), ^{31}P δ37.25ppm [J_{Pt-P}) 3233.5Hz].

DSC 271.3mpt.

6.3.2. The Preparation of [$Pt_3(\mu_{S-S}$SNC(Ph)NS)$_2$(dppe)$_2$].

[Pt(SNC(Ph)NS-S,S)(dppe)] (0.173g, 0.223mmol) and [$Pt(PPh_3)_4$] (0.145g, 0.117mmol) were stirred in MePh at 70°c for two weeks to yield a bright orange solid under an orange solution. The solid was filtered, washed with fresh MePh (3x5ml) and dried *in vacuo* .

Yield 0.105g, 56.8%.

IR ν_{max} (cm^{-1}) 3021w, 2371w, 1632br, 1480m, 1432s, 1411m, 1377w, 1304m, 1215w, 1186m, 1159w, 1101m, 1070m, 1006m, 996m, 875m, 819m, 788w, 715m, 701ssh, 690s, 613m, 577w, 531s, 483m, 409w.

Elemental analysis, found: C47.95%; H3.56%; N2.16%; Calc:. C45.43%; H3.35%, N3.21%).

NMR; ^1H (250MHz; solvent $CDCl_3$) δ_H 7.62-7.25 (40H, m), 2.17 (8H, s), ^{31}P (250MHz; solvent $CDCl_3$) δ_P 37.31 [J_{Pt-P}) unobserved Hz].

D.s.c. 250°C (very broad exotherm).

6.3.3. The Preparation of [PtPdPt($\mu_{S,S}$SNC(Ph)NS)$_2$(dppe)$_2$].

[Pt(SNC(Ph)NS-S,S)(dppe)] (0.389g, 0.502mmol) and [Pd(PPh_3)$_4$] (0.350g, 0.303mmol) were stirred in MePh at 70°c for 10days to yield a bright orange solid under an orange solution. The solid was filtered, washed with fresh MePh (3x5ml) and dried *in vacuo* .

Yield 0.105g, 56.8%.

IR ν_{max} (cm^{-1}) 3422br, 3051w, 2622w, 1636w, 1570w, 1482m, 1435ssh, 1409m, 1307m, 1304m, 1261w, 1180m, 1168m, 1138m, 1103s, 1026sh, 998sh, 878m, 819m, 746sh, 700shd, 693ssh, 674sh, 640w, 581m, 530s, 490m.

Elemental analysis, found: C48.31%; H3.36%; N2.94%; cal.: C47.87%; H3.54%, N3.38%.

N.m.r.; (250MHz; solvent $CDCl_3$) ^1H δ7.41-7.24ppm(40H, m), 2.17ppm (8H, s), ^{31}P δ38.13ppm [J_{Pt-P} unobserved Hz].

D.s.c. 259.7°Cdec.

6.3.4. Attempted Crystal Growth Reaction of [PtPdPt($\mu_{S,S}$SNC(Ph)NS)$_2$(dppe)$_2$].

[Pt(SNC(Ph)NS-*S,S*)(dppe)] (0.148g, 0.191mmol) and [Pd(PPh_3)$_4$] (0.100g, 0.087mmol) were placed in separate limbs of a two bulbed reaction vessel separated by a grade three sinter. MePh (10ml) was added to each side and the reaction vessel inverted. Slow diffusion of [Pd(PPh_3)$_4$] through the sinter occurred and after 4-5 days orange-red crystals had formed over solid [Pt(SNC(Ph)NS-*S,S*)(dppe)]. After 14 days the solvent was removed to yield small brittle crystals unsuitable for x-ray analysis.

6.4. CONCLUSION.

Chapters four and five outlined two new classes of dithiadiazolyl complex, the monometallic [M(SNC(Ph)N(H)S-*S,S*)(P)$_2$] and trimetallic species [$M_3(\mu_{S\text{-}S}SNC(Ph)NS)_2(P)_4$] (where M=Pt or Pd and P= PPh_3or $^1/_2$dppe). This chapter has, by experimental measurements and theoretical hypothesis, outlined chemical pathways taken by the monometallic complex in its decomposition to trimetallic and other species.

The varying stabilities of monometallic dithiadiazolyl complexes have been studied and rationalised through the effects of the metal (Pt or Pd) and phosphine (dppe or $2PPh_3$).

E.s.r. spectroscopy has highlighted some of the reactive intermediates in the monometallic decomposition and , in conjunction with U.V./vis spectroscopy, kinetic measurements have elucidated the first step in the decomposition i.e. loss of phosphine. It has thus been possible to make an attempt at describing the mechanism of mono to trimer conversion. Further kinetic studies at various temperatures could give an indication of the thermodynamics of the initial first order decomposition and more detailed study over longer time periods may indicate what rate order(s) the reaction follows after the loss of first-order characteristics.

When studying the decomposition through ^{31}P n.m.r. spectroscopy various species have been observed which are neither intermediates in the 'trimerisation' process nor M_3 species themselves. It has been possible to make informed guesses as to what these species may be, the most likely being dithiadiazolyl ring nitrogen protonated complexes or higher chain length bridging dithiadiazolyl compounds. Obviously isolation of pure solid material would make characterisation easier.

Proton n.m.r. studies have also highlighted the formation of various protonated decomposition products, either protonation of dithiadiazolyl ring nitrogen on complexes prepared or products from the decomposition of the free ligand [PhCNSSN]$^{\bullet}$, probably from reaction with trace water.

Lastly, [Pt(SNC(Ph)NS-*S,S*)(dppe)], though more stable than other monometallic species, does decompose to [$Pt_3(\mu_{S\text{-}S}SNC(Ph)NS)_2(dppe)_2$] among other products. Reaction with $Pt(PPh_3)_4$ to form [$Pt_3(\mu_{S\text{-}S}SNC(Ph)NS)_2(dppe)_2$] is potentially interesting, repeating with [$Pd(PPh_3)_4$] to form [(PtPdPt)($\mu_{S\text{-}S}SNC(Ph)NS)_2(dppe)_2$].

A full x-ray structural characterisation is required to conclusively prove that these reactions have taken place and the problem of low solubility of these species must also be surmounted (perhaps by changing the R group on the [PhCNSSN]$^{\bullet}$). At a later stage perhaps other metals (e.g. Ir, Ag) can be inserted into this square-planar 'trans sandwich' of two Pt(SNC(Ph)NS-*S,S)*(dppe) units.

6.5. REFERENCES.

1. J.E.Huheey, E.A.Keiter and R.L.Keiter, Inorganic Chemistry, 4th Ed.Harper Collins College publishers, 1993, 522.
2. F.A.Cotton, G.Wilkinson, P.L.Gaus, *Basic Inorganic Chemistry*, 2nd Ed., John Wiley & Sons, 1987, 536.
3. W.H.Slabaugh and T.D.Parsons, General Chemistry, John Wiley and Sons, 1966, 356.
4. J.M.Rawson, A.J.Banister & I.Lavender, *Advances in Heterocyclic Chemistry*, 1995, **62**, 137.
5. P.W.Atkins, Physical Chemistry, 4th Ed., Oxford English press, 1990, a)785, b)792.
6. G.M. Kosolapoff and L.Maier, Organic Phosphorus Compounds, Vol. 4, Eds. Wiley Interscience, New York, 1972, Ch7, 391.
7. V.Klassen, K.Preuss, K.H.Moock & R.T.Boeré, *Phos.Sulf. & Silicon*, 1994, **93-94**, 449.
8. I.P.Parkin and J.D.Woollins, *J.Chem.Soc., Dalton Trans.*, 1990, 519..
9. M.H. Crutchfield, C.H.Dungan, J.H.Letcher, V.Mark and J.R.van Wazer, Topics in Phosphorus Chemistry, Vol 5, ^{31}P Nuclear magnetic Resonance, Wiley, New York, 1967, a)250 and b)285.
10. O.G.Dawe, *MSc. Thesis*, University of Durham, 1995.
11. I.P.Parkin &J.D.Woollins, J.Chem.Soc., Dalton Trans., 1990, 925.
12. M.H. Crutchfield, C.H.Dungan, J.H.Letcher, V.Mark and J.R.van Wazer, Topics in Phosphorus Chemistry, Vol 5, ^{31}P Nuclear magnetic Resonance, Wiley, New York, 1967, 363.
13. P.G.Pringle & B.L.Shaw, *J.Chem.Soc., Chem.Commun.*, 1982, 81.
14. R.Uson, J.Fornies, M.Tomas, B.Menjon, J.Carnicer & A.J.Welch, *J.Chem.Soc., Dalton Trans.*, 1990, 151.
15. D.H.Williams and I.Fleming, *Spectroscopic Methods in Organic Chemistry*, McGraw-Hill, 4th Ed., 1989, 142.
16. R.M.Silverstein, G.C.Clayton Bassler and T.C.Morrill, *Spectrometric Identification of Organic Compounds*, John Wiley and Sons Ltd., 5th Ed., a)208, b)185.
17. A.W.Luke, PhD. Thesis, 1992.

CHAPTER SEVEN

AN OXIDATIVE DECOMPOSITION STUDY ON MONOMETALLIC DITHIADIAZOLYL COMPLEXES

7.1. INTRODUCTION.

7.1.1. Proposed One-Electron Oxidation of Monometallic Dithiadiazolyl Complexes.

In the previous two chapters the decomposition of monometallic dithiadiazolyl species in solution, and the subsequent compounds formed, have been discussed. It is almost certainly the unpaired electron on monometallic complexes that destablilises them (cf. the comparitive stability of other square-planar Pt and Pd species). As stated in chapter two, uncomplexed 1,2,3,5 dithiadiazolyls also have an unpaired electron. This ring system can be readily oxidised to form the cation and again, as previous mentioned in chapter two the cation is formed as one of the stable intermediates in the synthetic pathway to forming the radical.

In the monometallic complexes if this electron can be removed by oxidation (e.g. figure 7.a.) there is a good chance that the salts would be far more stable in solution. In the case of Pt species, for biological properties, the salts may be less toxic and more soluble in polar solvents (H_2O in particular).

Figure 7.a. Proposed One-Electron Oxidation of Monometallic Dithiadiazolyl Complexes

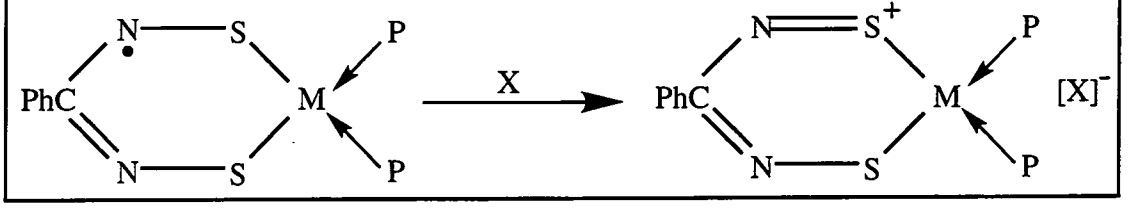

7.1.2. Cyclic Voltammetry.

Before undertaking any chemical oxidation or reduction an electrochemical study (in particular cyclic voltammetry) can indicate the possibility of oxidising the monometallic complexes, as envisaged above. Previous C.V. studies on the [RCNSSN]• radical have shown that the species can undergo a reversible oxidation to form a cation and a reversible reduction to form an anion[1][2]. The oxidation can be readily achieved (e,g, by Cl_2 or Br_2). The reduction is much harder to achieve and there is only limited evidence

for the formation of the anionic salt [Na(18-crown-6)][PhCNSSN][2] and this has involved very strong reduction by alkali metal.

Interestingly, the C.V. of the nickel dithiadiazolyl species, $[Ni_2(\mu_{S,S}SNC(Ph)NS)(cp)_2]$, shows a reversible one electron oxidation[3][4] (as described in chapter 2) and it should perhaps be possible to prepare an oxidised nickel species.

There have also been electrochemistry studies undertaken on group 10 complexes e.g. the Pt(II) to Pt(III) oxidative decomposition of $[Pt_2(NH_3)_4(C_5H_4N\text{-}O)_2](NO_3)_5$[5]. Of more relevance are the electrochemical studies of Pt(II) and Pd(II) dithiolene complexes. These complexes, previously discussed in chapter three undergo reversible oxidation and reduction processes[6].

7.2. RESULTS AND DISCUSSION.

7.2.1. Cyclic Voltammetry Study of [PhCNSSN]• Based Monometallic Complexes.

As stated in the introduction an electrochemical study on the monometallic species formed should give an indication as to whether a clean chemical oxidation can be achieved and thus cyclic voltammograms of [Pt(SNC(Ph)NS-*S,S*)(PPh_3)$_2$] [Pt(SNC(Ph)NS-*S,S*)(dppe)] and [Pd(SNC(Ph)NS-*S,S*)(dppe)] were run. C.V. studies of the known decomposition products of monometallic species i.e. [RCNSSN]•, PPh_3 and dppe were also run for comparison. All cyclic voltammograms were run referenced to Ag/Ag^+ and then calibrated to the standard calomel electrode (S.C.E.) at +0.34V, the x-axis in amps (A) and the y-axis in volts (V) .

The C.V. of [Pt(SNC(Ph)NS-*S,S*)(PPh_3)$_2$] (figure 7b.) consists of two reversible reductions at $E^1/_2$ +0.01V and -1.04V and an irreversible oxidation at $E^1/_2$ 0.42V. The reversible reductions probably involve the the ring system taking on another electron to become anionic and then the metal centre taking on an electron to become a 17 electron species. In Pt dithiolene complexes the reductive process was observed to be mainly ligand based as shown by e.s.r. spectroscopy. A second reduction was not observed[5] in these dithiolene species.

The C.V. of [Pd(SNC(Ph)NS-*S,S*)(dppe)] (figure 7.c.) consists of one reversible reduction at $E^1/_2$ -1.44V and three irreversible oxidations at $E^1/_2$ -0.10v, +0.30V and +1.12V. As with the dithiolene based complexes the reduction is probably a ligand (i.e. SNC(Ph)NS) based process.

Finally the C.V. of [Pt(SNC(Ph)NS-*S,S*)(dppe)] consists of one reversible reduction at $E1/_2$ +0.10V and one irreversible reduction at -1.66V. No oxidation attributable to the complex was observed. An oxidative decomposition may occur but the low solubility of the complex in MeCN (the solvent of choice for this C.V. study) resulted in only limited information being obtainable from the cyclic voltammogram

In conclusion, the absence of a reversible oxidation indicates that it is unlikely that an oxidised monometallic complex can be formed, or at least not as a major product. However, the irreversible oxidations found for [Pt(SNC(Ph)NS-*S,S*)(PPh_3)$_2$] and

[Pd(SNC(Ph)NS-*S,S*)(dppe)] show that on oxidation these species decompose on to further products which in turn may be interesting and novel species.

7.2.2. Oxidative Decomposition of Monometallic Complexes.

The oxidising agent chosen was $NOBF_4$. On oxidation NO^+ abstracts an.electron to form NO gas which is liberated and $[BF_4]^-$ remains as the counterion. The liberation of gas both gives an indication that the reaction has proceeded and cleanly removes a side product.

Molar equivalents of complex and oxidising agent were stirred in MeCN to yield the immediate evolution of NO and a colour change from blue (for the Pt species) or green (for the Pd complex) to an orange solution. In all three cases there was a further colour change after 3h to form yellow solutions, indicating further reaction. Elemental analysis and infra-red spectroscopy gave a further indication that reaction(s) had taken place. No d.s.c. measurements were made as no reaction yielded only one clean product as will be shown in the following sections.

Figure 7.b. Cyclic Voltammogram of [Pt(SNC(Ph)NS-*S*,*S*)(PPh_3)$_2$].

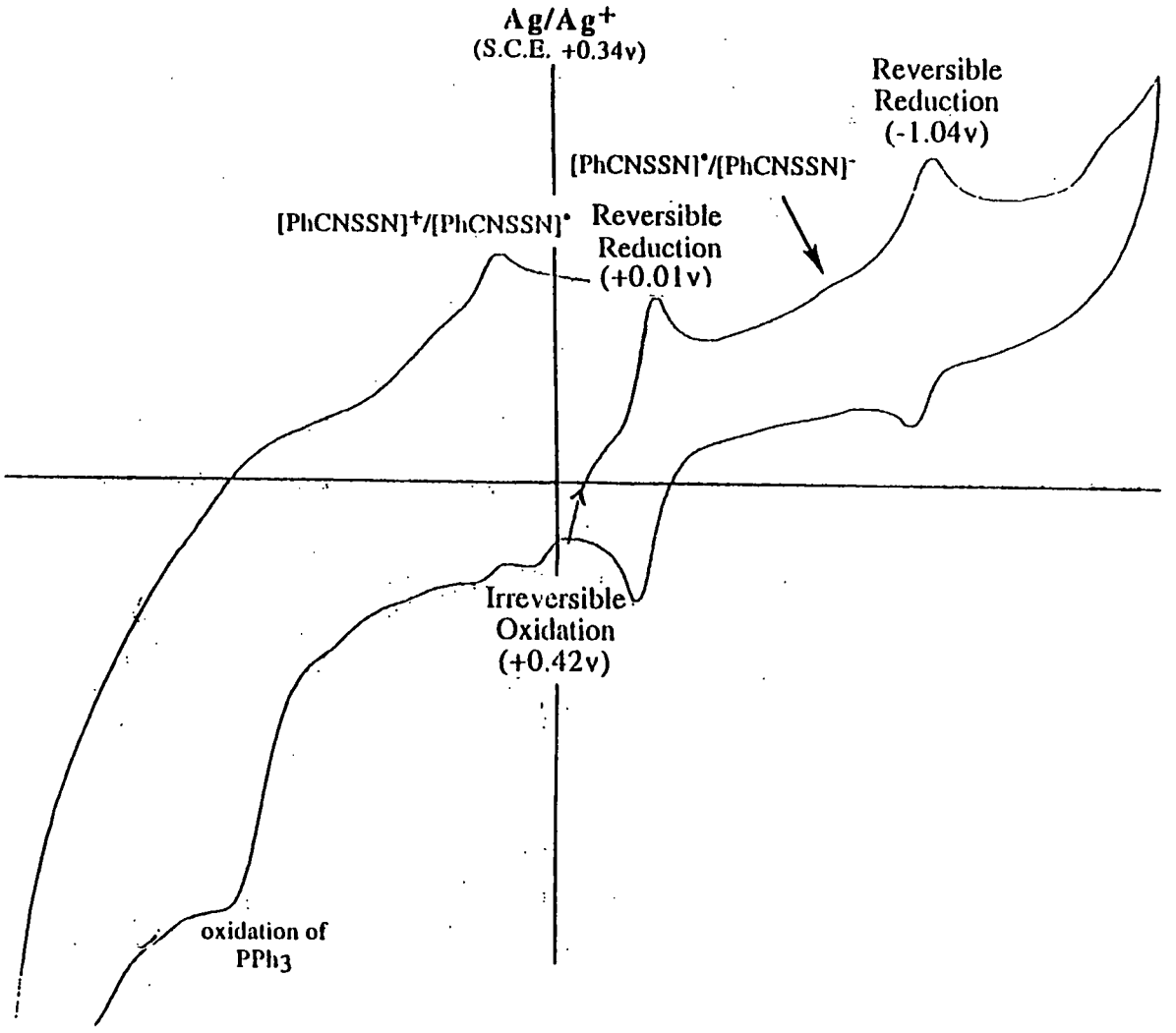

Figure 7.c. Cyclic Voltammogram of [Pd(SNC(Ph)NS-*S*,*S*)(dppe)].

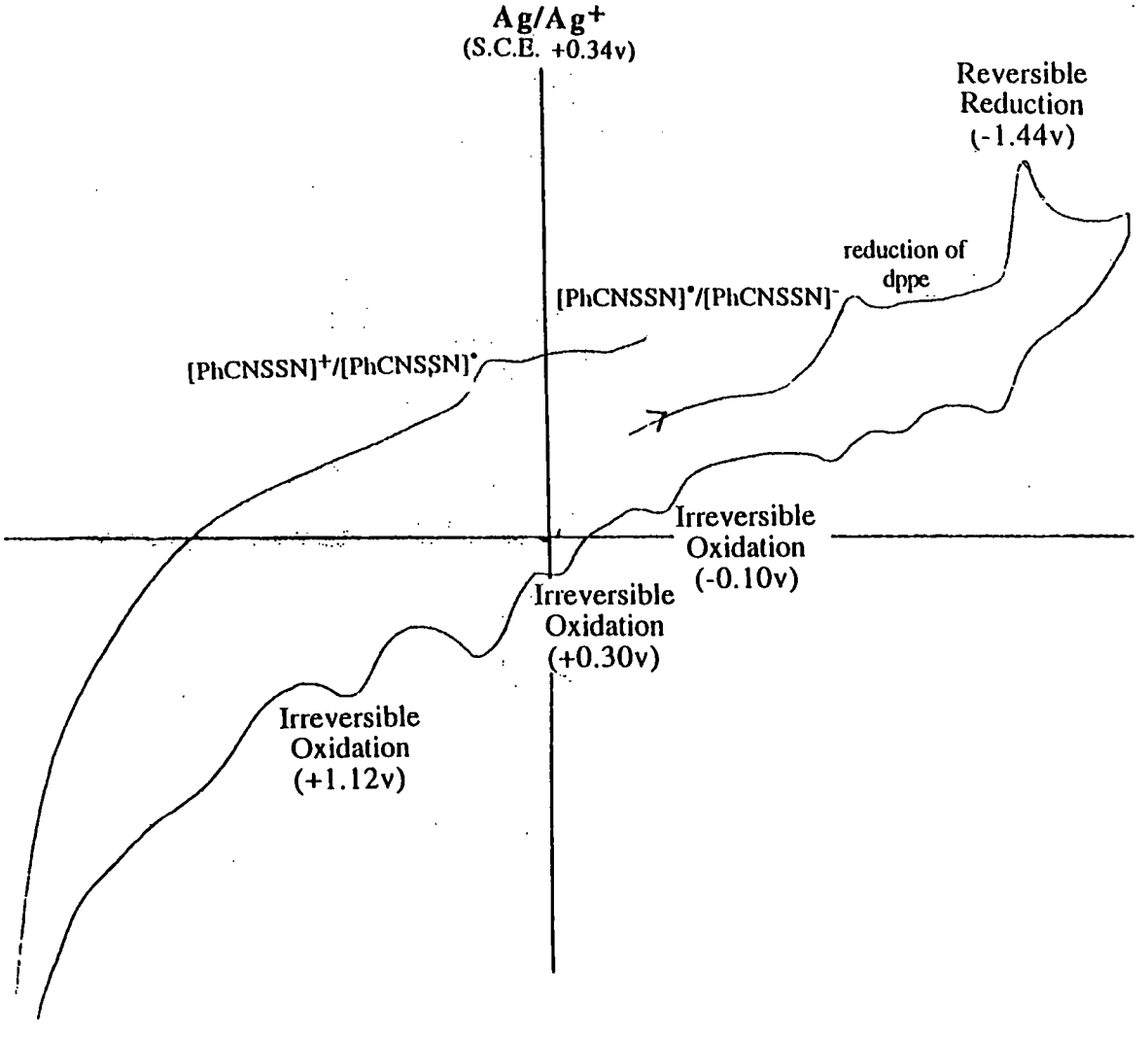

7.2.3. The ^{31}P n.m.r. Spectra of the Products of the Reaction Between [Pd(SNC(Ph)NS-*S,S*)(dppe)] and $NOBF_4$.

The ^{31}P n.m.r. spectra (in $CDCl_3$) (figure 7.d.) indicated that two products had formed, the minor product, a singlet (δ 59.6), indicating a complex where both dppe phosphines were equivalent and the major product with a doublet of doublets at δ56.6 and 52.9ppm indicating a complex where both dppe phosphines are inequivalent and couple to each other (J_{P-P} 27.8Hz). Paramagnetic broadening of the ^{1}H n.m.r. spectra indicates that some [Pd(SNC(Ph)NS-*S,S*)(dppe)] remains i.e. that there may not have been a complete 1:1 reaction between the complex and $NOBF_4$.

On standing in $CDCl_3$ crystals, of what was presumably one of the two species described above, started to slowly precipitate out of solution. A crystal of suitable quality was submitted for an x-ray structural analysis.

Figure 7.d. ^{31}P N.m.r. Spectrum of the Products from the Reaction Between [Pd(SNC(Ph)NS-*S*,*S*)(dppe)] and $NOBF_4$

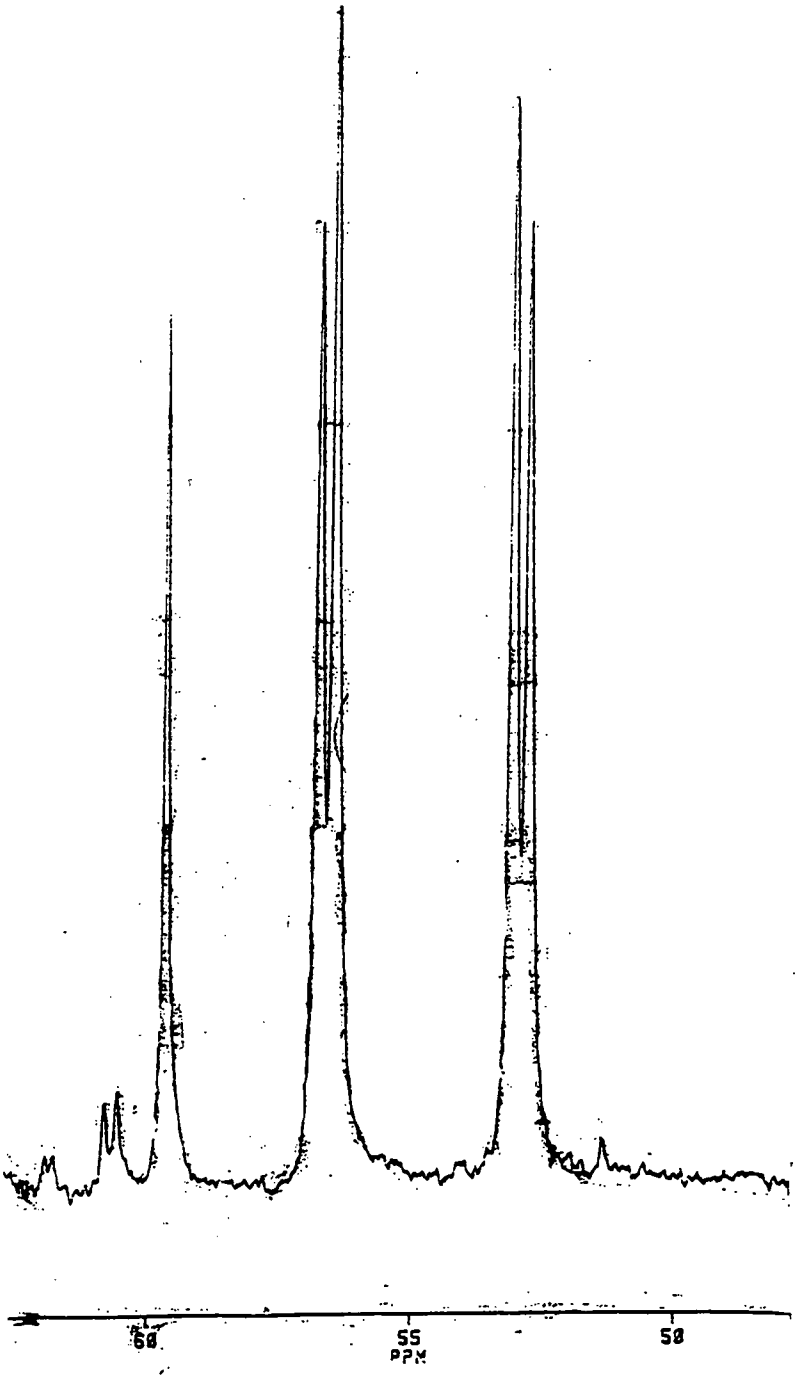

7.2.4. X-Ray Structure of $[Pd_2(\mu_{S,S}SNC(Ph)N(H)S)(dppe)_2][BF_4]_2$.

The structure of the species that was crystallised (see the previous section) was $[Pd_2(\mu_{S,S}SNC(Ph)N(H)S)(dppe)_2][BF_4]_2$ (see figure 7.g. for diagrams and table 7.b. for selected bond lengths and angles). The structure is both suprising and highly unusual. It consists of a dimetallic compound bridged by the sulfurs of the chalcogen ring with each Pd atom also bonded to a dppe group. The complex is a dicationic salt (with two BF_4^- counterions) which formally oxidises both metals from 17 to 16 electron square-planar species. Finally, the (SNC(Ph)NS) ligand has picked up a proton on a ring nitrogen to become diamagnetic i.e. (SNC(Ph)N(H)S). A schematic bonding diagram is shown below (figure 7.e.).

Figure 7.e. $[Pd_2(\mu_{S,S}SNC(Ph)N(H)S)(dppe)_2]^{2+}$

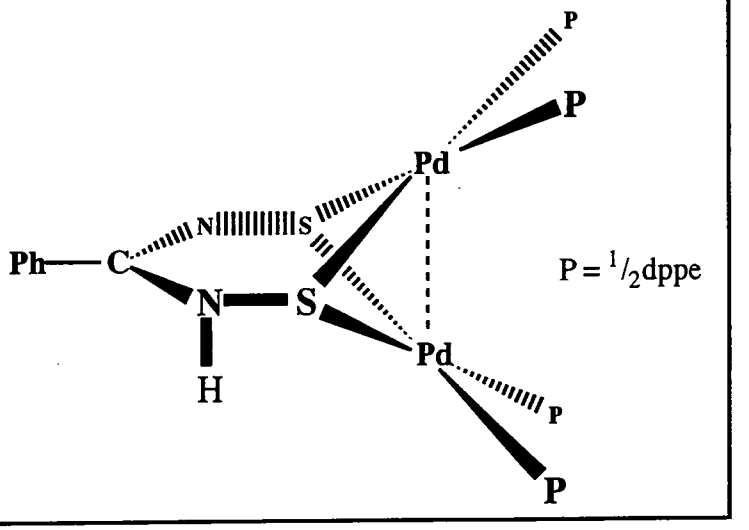

On reaction with [Pd(SNC(Ph)NS-*S*,*S*)(dppe)] and $NOBF_4$ (and trace H_20 or solvent, MeCN to provide the proton) to form $[Pd_2(\mu_{S,S}SNC(Ph)N(H)S)(dppe)]$ the ring system now bridges two metal centres in a bonding mode similar to that described in chapter five for the trimetallic species. The two sulfur atoms are pulled further away from each metal centre (between 2.351(2)Å and 2.384(2)Å in $[Pd_2(\mu_{S,S}SNC(Ph)N(H)S)(dppe)]$ compared with 2.285(3) and 2.294(3)Å in [Pd(SNC(Ph)NS-*S*,*S*)(dppe)] and the SPdS bond angle is subsequently smaller (82.66(6)° and 81.91(6)° in $[Pd_2(\mu_{S,S}SNC(Ph)N(H)S)(dppe)]$ compared with 89.6° in [Pd(SNC(Ph)NS-*S*,*S*)(dppe)]. The

ring strain described in chapter four for monometallic species is also relieved to a certain extent and the internal chalcogen ring angles are thus larger - closer to those observed for the uncomplexed ligand. Finally, as with other bridging dithiadiazolyl ligands the S-S bond interaction is shorter (3.106Å) than that found for the chelating species (c.f. 3.227(7)Å for the original monometallic complex). The metal is now bridging two (SNC(PhNS) units and cannot therefore insert as fully into the S-S bond of the ring.

In the ring itself the proton on the nitrogen prevents ring delocalisation in contrast with the (SNC(Ph)NS) ring complex that we have discussed previously (figure 7.f.). Thus in (SNC(Ph)N(H)S) complexes there will be one CN bond with predominantly double bond character and one with predominantly single bond character (in the CN(H) fragment). In (SNC(Ph)N(H)S) both CN bond lengths will be very similar and intermediate between single and double bond character.

Figure f. Comparison of the two ligands (SNC(Ph)NS) (1) and (SNC(Ph)N(H)S) (2).

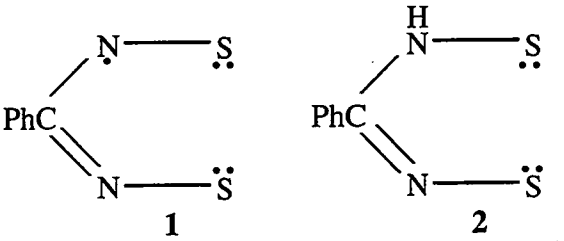

The following (table 7.a.) shows the CN bond lengths of various complexes discussed in this thesis. In the dimetallic nickel species and the monometallic palladium complex the CN bond lengths are equal and thus acyclic (SNC(Ph)NS) is the ligand while in the dimetallic Pd salt and the Fe complex both CN bond lengths are definitely inequivalent. This is yet more evidence, along with the c.v. and ^{1}H n.m.r. studies undertaken by Boeré et al that the ligand in the Fe species is in fact the dithiadiazolyl imine species (SNC(Ph)N(H)S)[3][4].

Table 7.a. CN Bond Lengths of Selected [RCNSSN]$^{\bullet}$ Based Species.

COMPOUND	C-N Bond Length (Å)	REFERENCE
$(PhCNSSN)_2$	1.33 & 1.34	[8]
$Ni_2(\mu_{S\text{-}S}SNC(PhNS)(cp)_2$	1.324(4) & 1.336(4)	[9]
Pd(SNC(Ph)NS-*S,S*)(dppe)	1.33(1) &1.36(1)	chapter four
$Pd_2(\mu_{S\text{-}S}SNC(Ph)N(H)S)(dppe)$	1.305(9) &1.359(9)	this chapter
$Fe_2(\mu_{S\text{-}S}SNC(Ph)N(H)S)(CO)_6$	1.295(8) &1.348(7)	[10]

The Pd-Pd bond interaction (3.0686(7)Å) is longer than that found in the trimetallic species $[Pd_3(\mu_{S\text{-}S}SNC(Ph)NS)_2(PPh_3)_4]$ (2.8499(11)Å & 2.8693(12)Å) and complexes with genuine Pd-Pd bonds eg.$[(\eta^3\eta^2\text{-cp})(\mu\text{-Br})(Pd)_2(P\text{-}iPr_3)_2]$ (Pd-Pd 2.61Å)[11] and many A-frame complexes[12] such as $[Pd_2(dppm)_2(OCOCF_3)]$ (Pd-Pd 2.594Å)[13]. This is not surprising as a Pd-Pd bond is not required to satisfy the bonding requirements of either metal i.e. each metal has the 16e$^-$ required for stability in the square -planar geometry. There are many examples of dipalladium complexes without a formal Pd-Pd bond e.g. trans-$[(PPh_3)(C_6F_5S)Pd(\mu\text{-}SC_6F_5)_2Pd(SC_6F_5)(PPh_3)]$[14] $[Pd_2(\mu\text{-}MeCO_2)_2Cl_2(PPhMe_2)_2]$[15] and $[PdCl_2\{Bu^t{}_2P(CH_2)_{10}PBu^t\}]_2$[16].

Figure 7.g. X-Ray Structure of

$[Pd_2(\mu_{S,S}SNC(Ph)N(H)S)(dppe)_2][BF_4]_2.3CDCl_3$.

(the dppe phenyl groups, deuterochloroform solvate and all the protons have been removed for clarity).

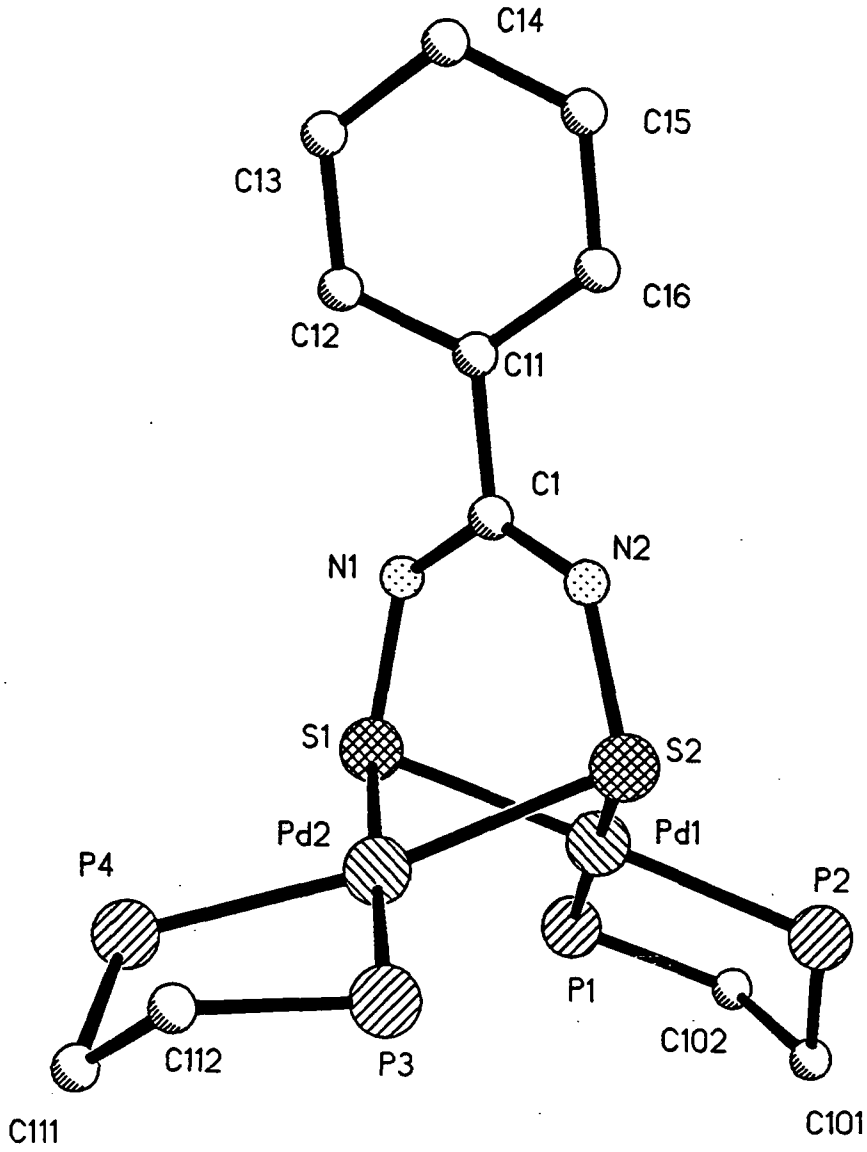

Table 7.b. Selected Bond Lengths and Angles for [Pd_2(μ-SNC(Ph)N(H)S-*S*,*S*)$_2$(dppe)].

Pd_2(μ-SNC(Ph)N(H)S-*S*,*S*)$_2$(dppe)			
Bond Length (Å)		**Bond Angle (°)**	
Pd(1)-P(2)	2.283(2)	P(2)-Pd(1)-P(1)	85.66(7)
Pd(1)-P(1)	2.305(2)	P(2)-Pd(1)-S(1)	175.93(6)
Pd(1)-S(1)	2.351(2)	P(1)-Pd(1)-S(1)	97.85(6)
Pd(1)-S(2)	2.352(2)	P(2)-Pd(1)-S(2)	93.67(6)
Pd(1)-Pd(2)	3.0686(7)	P(1)-Pd(1)-S(2)	175.23(7)
Pd(2)-P(3)	2.283(2)	S(1)-Pd(1)-S(2)	82.66(6)
Pd(2)-P(4)	2.296(2)	P(3)-Pd(2)-P(4)	85.00(7)
Pd(2)-S(1)	2.354(2)	P(3)-Pd(2)-S(1)	178.94(7)
Pd(2)-S(2)	2.384(2)	P(4)-Pd(2)-S(1)	95.59(7)
C(1)-N(2)	1.305(9)	P(4)-Pd(2)-S(2)	171.22(7)
C(1)-N(1)	1.356(9)	S(1)-Pd(2)-S(2)	81.91(6)
N(1)-S(1)	1.690(6)	N(2)-C(1)-N(1)	128.7(6)
N(2)-S(2)	1.687(6)	C(1)-N(1)-S(1)	129.4(5)
S(1)....S(2)	3.106	N(2)-S(2)-Pd(1)	109.1(2)
		N(2)-S(2)-Pd(2)	100.5(2)
		Pd(1)-S(1)-Pd(2)	81.41(6)
		C(1)-N(2)-S(2)	125.7(5)
		N(2)-S(2)-Pd(1)	109.1(2)
		N(2)-S(2)-Pd(2)	100.5(2)
		Pd(1)-S(2)-Pd(2)	80.77(6)

7.2.5. A Re-evaluation of the ^{31}P n.m.r. Spectra of the Products of the Reaction Between [Pd(SNC(Ph)NS-S,S)(dppe)] and $NOBF_4$.

The ^{31}P n.m.r. spectrum of the crystalline product $[Pd_2(\mu_{S-S}SNC(Ph)N(H)S)(dppe)]$ was in accordance with the crystal structure, the proton rendering the dppe phosphines inequivalent, as such a doublet of doublets at δ56.6 and 52.9ppm (J_{P-P} 27.8Hz) was observed. The unidentified minor peak previously observed at δ59.6ppm was now absent although a further minor peak at δ51.4 was now observed. This latter peak (or perhaps the one at δ59.6ppm) may be due to the oxidised monometallic species or a dimetallic species with a non protonated dithiadiazolyl but with a further BF_4 oxidation to form a di-positive species.

7.2.6. The ^{31}P n.m.r. Spectra of the Products of the Reaction Between [Pt(SNC(Ph)NS-*S,S*)(dppe)] and $NOBF_4$.

The ^{31}P n.m.r. spectra (in $CDCl_3$) of the orange solids from the reaction between [Pt(SNC(Ph)NS-*S,S*)(dppe)] and $NOBF_4$ (figure 7.h.) show that many different products have formed and the reaction was not as straightforward as that found previously in the Pd analogue. The chemical shift and coupling constant values are shown in the table below as well as the values for the related species $[Pt(SNS(H)N)(dppe)]BF_4$[17] (which has very similar ^{31}P n.m.r. values to complex B discussed more fully below)

There are two main species present (A & B), which provide a doublet of doublets (inequivalent phosphorus atoms in dppe coupling through a Pt atom) with Pt satellites (i.e. coupling to one phosphorus bound Pt). Either one could be the Pt analogue of the Pd species $[Pd_2(\mu_{S-S}SNC(Ph)N(H)S\text{-}S,S)(dppe)_2]$. The other could simply be a monometallic complex with a ring nitrogen protonated. The other major product, complex C, has a ^{31}P n.m.r. signal which consists of a singlet with Pt satellites and thus the dppe phosphorus atoms bound to the Pt are equivalent. This could be the monometallic oxidised species [Pt(SNC(Ph)N(H)S-*S,S*)(dppe)]. Three other peaks were present (D,E, & F), of too low an intensity to view any coupling. There is insufficient evidence to identify these.

Figure 7.h.The ^{31}P N.m.r. Spectra of the Products of the Reaction Between [Pt(SNC(Ph)NS-*S*,*S*)(dppe)] and $NOBF_4$.

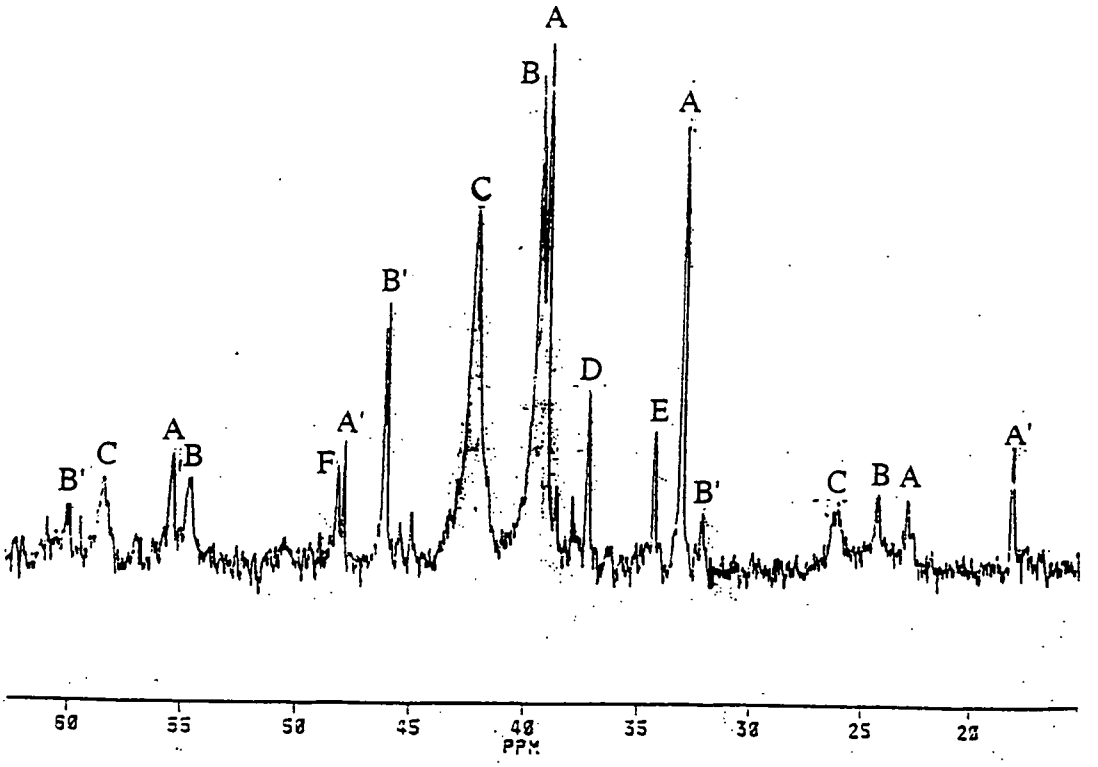

Table 7.c. ^{31}P n.m.r. peaks of the products from the reaction between [Pt(SNC(Ph)NS-*S,S*)(dppe)] and $NOBF_4$.

COMPOUND	δ (ppm)	J_{Pt-P} (Hz)	J_{P-P} (Hz)
A	39.2	3291.1	poorly resolved
	33.1	3030.1	5.4
B	39.5	3075.3	11.1
	46.15	2848.0	11.1
[Pt(SNS(H)N)(dppe)]BF_4	38.6	2734	10
	44.6	3162	10
D	37.3	unobserved	unobserved
E	34.3	unobserved	unobserved
F	48.3	unobserved	unobserved

7.2.7. The ^{31}P n.m.r. Spectrum of the Products of the Reaction Between [Pt(SNC(Ph)NS-*S,S*)(PPh_3)$_2$] and $NOBF_4$.

The orange solids from the reaction between [Pt(SNC(Ph)NS-*S,S*)(PPh_3)$_2$] and $NOBF_4$ were dissolved in $CDCl_3$ and their ^{31}P n.m.r. spectra recorded (figure 7.i.). Again as in the previous two reactions the major species is a doublet of doublets (with Pt satellites) which could again be a Pt analogue of the Pd species [$Pd_2(\mu_{S-S}$SNC(Ph)N(H)S-S,S)(dppe)$_2$] (i.e. [$Pt_2(\mu_{S-S}$SNC(Ph)N(H)S-S,S)(PPh_3)$_2$]. The ^{31}P data of this proposed species and a similar complex [Pt(SN(H)SN)(PPh_3)$_2$]BF_4[13] (for comparison) are shown in table 7.c.

Figure 7.i. The ^{31}P N.m.r. Spectra of the Products of the Reaction Between $[Pt(SNC(Ph)NS\text{-}S,S)(PPh_3)_2]$ and $NOBF_4$.

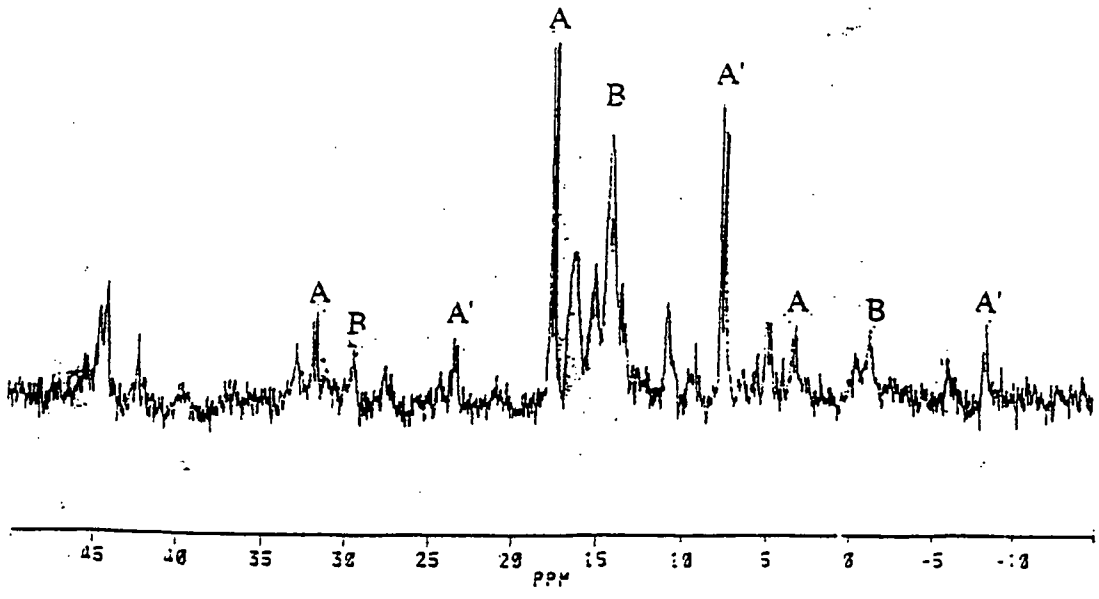

Table 7.c. ^{31}P n.m.r. of Species A and $[Pt(SNS(H)N)(PPh_3)_2]BF_4$.

COMPLEX	δ (ppm)	J_{Pt-P} (Hz)	J_{P-P} (Hz)
A	17.6	2883.4	23.3
	7.65	3227.6	23.3
$[Pt(SNS(H)N)(dppe)]BF_4$	12.9	2683	22
	6.0	3433	22

Another major species (B) δ15.15ppm, J_{Pt-P} 3110Hz, may be the monometallic oxidised species $[Pt(SNC(Ph)NS\text{-}S,S)(PPh_3)_2]$. There are many other peaks of lower intensity which are further unknown products in what was obviously a very complex reaction with many products.

7.3. EXPERIMENTAL

7.3.1. The Reaction Between [Pd(SNC(Ph)NS-*S,S*)(dppe)] and $NOBF_4$.

[Pd(SNC(Ph)NS-*S,S*)(dppe)] (0.228g, 0.33mmol) and NOBF4 (0.039g, 0.33mmol) were stirred in MeCN (10ml) to yield an immediate evolution of gas and the formation of a red solution. The solution was stirred for 3h during, which time a yellow solution had formed. This solution was filtered and solvent removed in vacuo to yield an orange solid initially assumed to be [Pd(SNC(Ph)NS-*S,S*)(dppe)]BF_4.

Yield 0.170g.

IR $\nu_{max}(cm^{-1})$ 3054w, 2366w, 2344w, 1637w, 1654w, 1540m, 1523m, 1482sh, 1435ssh, 1413m, 1331w, 1307m, 1281m, 1188m, 1163m, 1101s, 1059sh, 1083sh, 997ssh, 928m, 876sh, 848w, 819m, 747sh, 715ssh, 705ssh, 691ssh, 615w, 530s, 479m, 426w.

Elemental Analysis, found: C,51.10%; H,3.90%; N,3.49%. Calc.: C,51.28%; H,3.79%; N3.63%).

7.3.2. The Reaction Between [Pt(SNC(Ph)NS-*S,S*)(dppe)] and $NOBF_4$.

Pt(SNC(Ph)NS-*S,S*)(dppe) (0.246g, 0.318mmol) and NOBF4 (0.042g, 0.325mmol) were stirred in MeCN (10ml) to yield an immediate evolution of gas and the formation of a red solution. The solution was stirred for 3h to yield a yellow solution which was filtered and the solvent removed *in vacuo*. Initially assumed to be [Pt(SNC(Ph)NS-*S,S*)(dppe)]BF4.

Yield 0.169mg.

IR $\nu_{max}(cm^{-1})$ 3053w, 2365w, 2343w, 1637w, 1540m, 1524m, 1482sh, 1435ssh, 1413m, 1307m, 1283s, 1188m, 1162m, 1100s, 1059sh, 1081sh, 995ssh, 928m, 874ssh, 848w, 820m, 748sh, 715ssh, 705ssh, 689s, 532s, 479m, 427w

Elemental analysis, found: C,45.34%; H, 3.28%; N3.10,%. Calc.:C,46.00%;H,3.40%; N,3.25%)

7.3.3. The Reaction Between [Pt(SNC(Ph)NS-*S,S*)(PPh_3)$_2$] and $NOBF_4$.

[Pt(SNC(Ph)NS-*S,S*)(PPh_3)$_2$] (0.130g, 0.137mmol) and NOBF4 (0.0016g, 0.137mmol) were stirred in MeCN (8ml) to yield an immediate evolution of gas and the

formation of a red solution. This solution was stirred for 3h during which time a yellow solution had formed. This solution was filtered and dried *in vacuo*.

Initially assumed to be $[Pt(SNC(Ph)NS\text{-}S,S)(PPh_3)_2]BF_4$ formed.

Yield 0. 120mg

IR $\nu_{max}(cm^{-1})$ 3379w, 3240w, 3055w, 1974w, 1909w, 1817w, 1685w, 1627m, 1585sh, 1543m, 1527m, 1481ssh, 1436s, 1332w, 1312m, 1283w, 1187m, 1163m, 1095s, 1058s, 997s, 894w, 874w, 745s, 692s, 618w, 587w, 545ssh, 525s, 513s, 497s, 443w.

Elemental analysis, found: C, 51.58%; H,3.26%; N,2.54%. Calc.:C,52.28%;H,3.58%; N,2.84%)

7.4. CONCLUSION

Before undertaking the research included in this chapter it was hoped that a clean oxidation of [M(SNC(Ph)NS-*S,S*)(P)$_2$] (where M=Pt or Pd and P= PPh$_3$or $^1/_2$dppe) could be achieved to form the corresponding monometallic salt [M(SNC(Ph)NS-*S,S*)(P)$_2$][BF$_4$]. A preliminary cyclic voltammetry study had indicated that this would not be the case (at least not as a single major product) and that oxidative decomposition products could be formed instead or, indeed, as well as. On reaction of [Pt(SNC(Ph)NS-*S,S*)(PPh$_3$)$_2$] and [Pt(SNC(Ph)NS-*S,S*)(dppe)] with the oxidising agent NOBF$_4$ this theory held true with a whole series of decomposition products being formed (as shown by ^{31}P n.m.r. spectroscopy). To isolate out pure products further purification would be required e.g. separation by column chromatography. The main advantage about the species formed is their ready solubility in common solvents (e.g. MeCN and CH_2Cl_2) and extracting crystalline material should be possible, with perhaps Pt analogues of the following Pd species being isolated.

The oxidative decomposition of [Pd(SNC(Ph)NS-*S,S*)(dppe)] provided a much cleaner, simpler reaction with one major product. This species was crystallised and structurally characterised as [Pd$_2$(SNC(Ph)N(H)S-*S,S*)(dppe)$_2$]; from the oxidation of [Pd(SNC(Ph)NS-*S,S*)(dppe)] with two equivalents of NOBF$_4$ and a ring nitrogen protonation. This highly unusual species is further concrete evidence for the existence of (SNC(Ph)N(H)S) as a ligand. If (RCNSSN(H)) could be prepared as the starting reagent then a new area of chemistry could be opened up. With the loss of free radical nature this species may prove to be easier to handle and react more cleanly with more transition metals compared with [PhCNSSN]$^{\bullet}$.

Finally, from this and the previous two chapters, a pattern is emerging in the ^{31}P n.m.r. spectra of the decomposition products of [M(SNC(Ph)NS-*S,S*)(P)$_2$]. In complexes derived from [Pt(SNC(Ph)NS-*S,S*)(PPh$_3$)$_2$] the chemical shifts come between 5 and 35ppm, from Pt(SNC(Ph)NS-*S,S*)(dppe) δ35–50ppm and Pd(SNC(Ph)NS-*S,S*)(dppe) δ40-60ppm. A trend is thus emerging in the chemical shift patterns of these species.

7.5 REFERENCES

1. R.T. Boeré, K.H. Moock and M. Parvez, *Z. anorg. all. Chem.*, 1994, **620**, 1589.
2. C.M. Aherne, A.J. Banister, I.B. Gorrell, M.I. Hansford, Z.V. Hauptman, A.W. Luke and J.M. Rawson, *J.Chem.Soc., Dalton Trans.*, 1993 , 967.
3. V. Klassen, K. Preuss, K.H. Moock and R.T. Boeré, *Phos.Sulf. & Silicon*, 1994, **93-94**, 449.
4. V. Klassen, K. Preuss, K.H. Moock and R.T. Boeré, private communication to Dr. A.J. Banister, 1994.
5. L.S. Hollis and S.J. Lippard, *J.Am.Chem.Soc.*, 1981, **103**, 6761.
6. R.P. Burns and C.A. McAuliffe, *Adv.Inorg.Chem. & Radiochem.*, 1979, **22**, 303.
7. G.A. Bowmaker, P.D.W. Boyd and G.K. Campbell, *Inorg.Chem.*, 1983, **22**, 1208.
8. A.J. Banister, N.R. M.Smith and R.G. Hey, *J.Chem.Soc., Perkin Trans.*, 1983, **1**, 1181.
9. A.J. Banister, I.B. Gorrell, W. Clegg and K.A. Jørgenson, *J.Chem.Soc., Dalton Trans.*, 1991, 1105.
10. A.J. Banister, I.B. Gorrell, W. Clegg and K.A. Jørgensen, *J.Chem.Soc., Dalton Trans.*, 1989, 229.
11. T.E. Kraft, C.I. Hejna and J.S. Smith, *Inorg. Chem.*, 1990, 29, 2682.
12. B. Chaudret, B. Delavaux and R. Poilbanc, Co-ord.Chem.Revs., 1988, **86**, 191.
13. A. Ducroix, H. Felkin, C. Pascard & G.K. Turner, *J.Chem.Soc., Chem. Commun.*,1975, 615.
14. R.H. Fenn & G.R. Segrott, *J. Chem. Soc. (A)*, 1970, **31**, 97.
15. J.Powell and T.Jack, *Inorg. Chem.*, 1972, **11**, 1039.
16. A.J.Pryde, B.L.Shaw and B.Weeks, *J. Chem. Soc., Dalton Trans.*, 1976, 322.
17. I.P.Parkin and J.D.Woollins, J.Chem.Soc., Dalton Trans., 1990, 925.

CHAPTER EIGHT

THE PREPARATION OF PHENYL DISELENADIAZOLYL AND ITS REACTION WITH PLATINUM AND PALLADIUM COMPLEXES

8.1. INTRODUCTION

8.1.1. The Replacement of Sulfur with Selenium in [RCNEEN]• (E = chalcogen).

So far in this thesis only the properties of 1,2,3,5, dithiadiazolyls and their complexes have been discussed. However, it is only recently that any [RCNSSN]• species have shown any interesting magnetic or electronic properties (see chapter 2). As such the attention of this research group and Oakley et al in Canada has turned to selenium as a direct replacement for sulfur i.e. diselenadiazolyls (figure 8.a.)

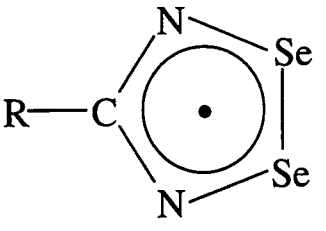

Figure 8.a. 1,2,3,5 diselenadiazolyl.

It was hoped that selenium based compounds, with more diffuse p and d orbitals, would provide stronger intermolecular interactions that would result in one dimensional stacking and, hopefully, interesting conducting properties.

8.1.2. The Synthesis and Properties of 1,2,3,5 Diselenadiazolyl.

In 1989 the first diselenadiazolyl radical, [PhCNSeSeN]•, was reported by Oakley et al.[1] The salt, [PhCNSeSeN]Cl, was synthesised in an analogous manner to their method of preparing [PhCNSSN]Cl except that Ph_3Sb and $SeCl_4$ (yielding $SeCl_2$ 'in situ' and Ph_3SbCl_2) were used instead of SCl_2. The cation was reduced to the radical with Ph_3Sb. Unfortunately, as for the sulfur species, the radical crystallised in diamagnetic dimer pairs (i.e. $(PhCNSeSeN)_2$) with some dissociation to the monomer, [PhCNSeSeN]•, in solution. Further studies have been undertaken on similar species i.e. [RCNSeSeN]• where R = H[2] and para substituted phenylene derivatives[3] e.g. [p-$ClC_6H_4CNSeSeN$]•. Recently iodine doping of [PhCNSeSeN]•[4] has resulted in the formation of a charge transfer species analogous to that described in chapter two for phenyl dithiadiazolyl.

8.1.3. Multi and Mixed Diselenadiazolyls Complexes.

The greatest interest in diselenadiazolyl research to date has been in the preparation of difunctional diselenadiazolyl and mixed diselenadiazolyl and dithiadiazolyl radicals (and radical cations); in character a continuation of the solely sulfur based research[5-8]. The most interesting of these compounds prepared was the β-phase of 1,3-[NSeSeNC (C_6H_4)CNSeSeN]$^{\bullet\bullet}$[7] (see figure 8.b.) which forms chains of discrete dimers in the solid state with semi-conducting properties (the band gap is 0.77eV).

Figure 8.b. 1,3-[NSeSeNC(C_6H_4)CNSeSeN]$^{\bullet\bullet}$

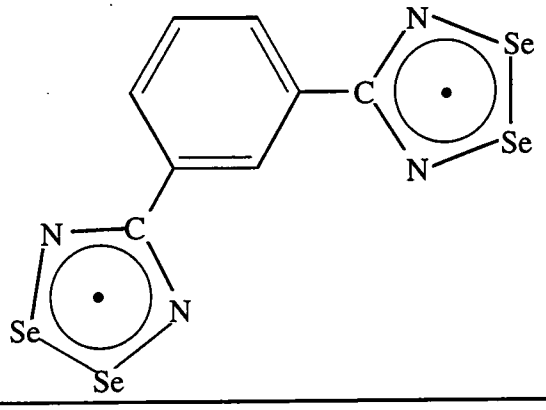

8.1.4. The Preparation and Characterisation of [PhCNSeSeN]$^{\bullet}$ and its use as a Ligand.

As previously stated there has only been limited research undertaken on [PhCNSeSeN]$^{\bullet}$ complexes compared to their sulfur analogues. As a result there is no convenient high yielding route for the preparation of [PhCNSeSeN]$^{\bullet}$ and only a limited physical study has been undertaken e.g. only a cursory e.s.r. study as discussed in the latter sections. Finally, attempts to use [PhCNSeSeN]$^{\bullet}$ as ligand have been very limited with only a few failed attempts to repeat work previously undertaken with [PhCNSSN]$^{\bullet}$[9]. Thus there are many areas of this field of chemistry to be developed, some of which will be included in the following chapter.

8.2. Results and Discussion.

8.2.1. The Preparation of [PhCNSeSeN]Cl.

If [PhCNSeSeN]$^{\bullet}$ is to be used as a ligand a high yielding preparation with the minimum of experimental work would be a great advantage. Oakley et al used the same method to prepare [PhCNSeSeN]Cl as they did to prepare [PhCNSSN]Cl i.e. starting with the previously synthesised persilylated benzamidine but instead of condensation with SCl_2, two reagents, $SeCl_4$ and Ph_3Sb are used to generate $SeCl_2$ *'in situ'* and prepare [PhCNSeSeN]Cl in 90% yield (see figure 8.c.)[1].

Figure 8.c. Condensation Reaction to form [PhCNSeSeN]Cl

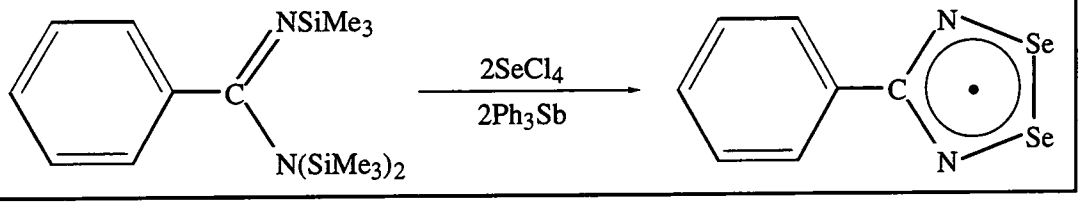

As with the sulfur system the initial preparation of the benzamidine is time consuming and leads to lower yields from basic starting material (benzonitrile and lithium bistrimethyl silylamide see chapter 2). Also, with this method only the comparatively expensive compound $SeCl_4$ is used as a source of selenium.

In this laboratory, the salt $Li[(SiMe_3)_2NC(Ph)(SiMe_3)]$ was prepared 'in situ' from PhCN and $Li[N(SiMe_3)_2]$ (as in the preparation of [PhCNSSN]Cl) in Et_2O and the ethereal solution canula transferred onto a 1:1 mixture of $SeCl_4$/Se (another 'in situ' prep of $SeCl_2$[8]) to yield [PhCNSeSeN]Cl, LiCl and $SiMe_3Cl$. As in the sulfur system Et_2O soluble $SiMe_3Cl$ is removed by filtration and LiCl is removed by exhaustive extraction of [PhCNSeSeN]Cl with SO_2 (see figure 8.d.). The use of Se (the cheapest source of selenium) with $SeCl_4$ is a more cost effective method of preparing $SeCl_2$. Satisfactory analysis was obtained for the salt [PhCNSeSeN]Cl.

Figure 8.d. Preparation of [PhCNSeSeN]Cl

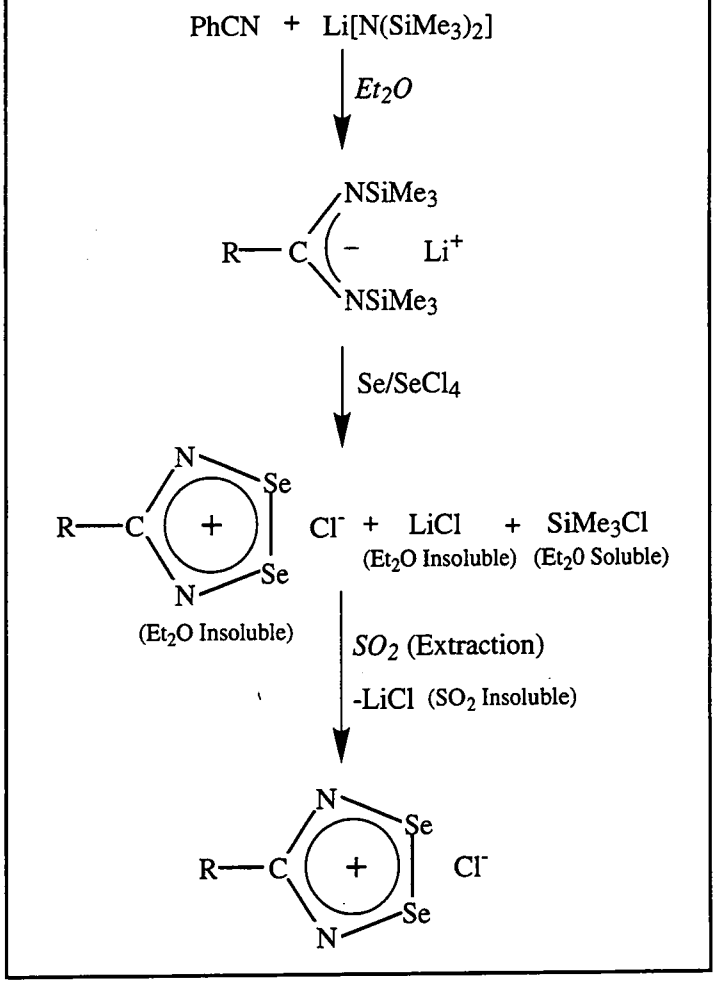

8.2.2. Reduction of [PhCNSeSeN]Cl to $(PhCNSeSeN)_2$.

Three reducing agents, Zn/Cu couple, Ag powder and Ph_3Sb, were tried to remove the chloride ion from [PhCNSeSeN]Cl to yield $(PhCNSeSeN)_2$. Reduction of [PhCNSSN]Cl by Zn/Cu couple and subsequent vacuum sublimation yields good quality crystalline $(PhCNSSN)_2$ in around 50% yields. Preparation of the selenium analogue under similar conditions yielded only 10%,of a powdered material. Better yields were achieved with other reducing agents: in an analogous reaction silver powder was used as the reducing agent and resulted in an improved yield after sublimation, 52.3% (see equation 8.a.) .

Equation 8.a. Reduction of PhCNSeSeNCl by Metal Powders.

$$[PhCNSeSeN]Cl \xrightarrow{Zn/Cu \text{ or } Ag} [PhCNSeSeN]^{\bullet} + ZnCl_2/CuCl_2 \text{ or } AgCl$$

Finally, Ph_3Sb was used as the reductant,the method employed by Oakley et al. Ph_3Sb and PhCNSeSeNCl were refluxed in MeCN. Ph_3SbCl_2 was washed out to leave behind $(PhCNSeSeN)_2$ (86% yield) which was further purified by sublimation (yield 30.8%).

8.2.3. One Pot Synthesis of $(PhCNSeSeN)_2$.

As in the case of $(PhCNSSN)_2$ the development of the preparation of $(PhCNSeSeN)_2$ has reached the stage where pure [PhCNSeSeN]Cl need not be isolated. After the condensation reaction and washing with Et_2O (to remove Me_3SiCl) Ph_3Sb is added to the [PhCNSeSeN]Cl/LiCl mixture with MeCN as the solvent. The mixture is refluxed, filtered to remove Ph_3SbCl_2 and the residue sublimed to yield pure crystalline $(PhCNSeSeN)_2$ (LiCl is left behind). Higher temperature sublimation (170°C) increases the speed of sublimation and produces crystalline product. The yield (30.8%) from starting materials is acceptable for pure crystalline $(PhCNSeSeN)_2$.

8.2.4. Previous E.s.r. Spectroscopic Studies on [PhCNSeSeN]•.

In many respects the physical properties of [PhCNSeSeN]• and related species have been thoroughly examined e.g. structural and theoretical studies and infra red spectroscopy[10]. However, e.s.r. spectroscopy has not been used extensively. In chapter two it was shown that [RCNSSN]• species have been extensively studied by e.s.r. spectroscopy with well resolved hyperfine splitting in solution (isotropic spectra) and in the solid state, powder and single crystal (anisotropic spectra). In comparison [PhCNSeSeN]• shows only a broad unresolved singlet even at low temperatures[1]. Consequently a direct comparison of the nature of the SOMOs in [PhCNEEN]• (where E = S or Se) has not been possible (although an extensive physical study using other techniques (e.g. m.o. studies and infra red spectroscopy) of a homologous pair, [HCNEEN]•, has been reported[10] recently). Chapters 2 and 4 highlight the compatibility of M.O. calculations and e.s.r. studies. Room temperature solution e.s.r. spectra of

[PhCNSeSeN]$^{\bullet}$ in CH_2Cl_2, t.h.f. and diglyme all showed broad singlets in first derivative spectra (g_{iso} = 2.0376 in t.h.f., peak-to-peak line width, ΔH_{pp}= 32G), similar to the data previously reported[1] (g_{iso} = 2.0394, CH_2Cl_2 at 295K). We have found that powdered samples of this material also exhibited broad singlets at room temperature (g = 2.0386) whilst crystalline samples were found to be e.s.r. inactive. No attempt had yet been made to record a frozen glass spectrum of this radical to attempt to separate out the hyperfine interactions of the species.

8.2.5. Anisotropic 'Frozen Glass' E.s.r. spectra of [PhCNSeSeN]$^{\bullet}$.

Despite the absence of hyperfine coupling in isotropic spectra, we found that hyperfine tensors to both N and Se could be determined from frozen glass spectra of [PhCNSeSeN]$^{\bullet}$ i.e. by freezing a solution of [PhCNSeSeN]$^{\bullet}$ in t.h.f.in an e.s.r. tube (using liquid N_2). The anisotropic spectrum obtained (figure 8.e.) shows a strong similarity to that observed[6] for [PhCNSSN]$^{\bullet}$, although replacement of S by Se has two effects; firstly, we observe a greater anisotropy in the spectra of [PhCNSeSeN]$^{\bullet}$ i.e. the x,y, and z contributions are spread further apart and secondly, the higher natural abundance of ^{77}Se (*c.f.* ^{33}S) has also allowed us to clearly observe and calculate the anisotropic hyperfine interactions with the chalcogen. The anisotropic data for [PhCNSeSeN]$^{\bullet}$ (frozen glass, t.h.f.), PhCNSSN$^{\bullet}$ (frozen glass d^8-toluene[11]), [SNSSN]$^{+\bullet}$ (frozen glass D_2SO_4[11]) and [SNSeSeN]$^{+\bullet}$ (frozen glass SO_2[12]) are listed in table 8.a. The values obtained for [PhCNSeSeN]$^{\bullet}$ have been used to simulate the spectrum (figure 8.f.). The anisotropic data were also used to simulate the frozen glass spectrum of [PhCNSeSeN]$^{\bullet}$ (figure 8.g.).

Figure 8.e. Frozen Glass E.s.r. Spectrum of [PhCNSeSeN]•.

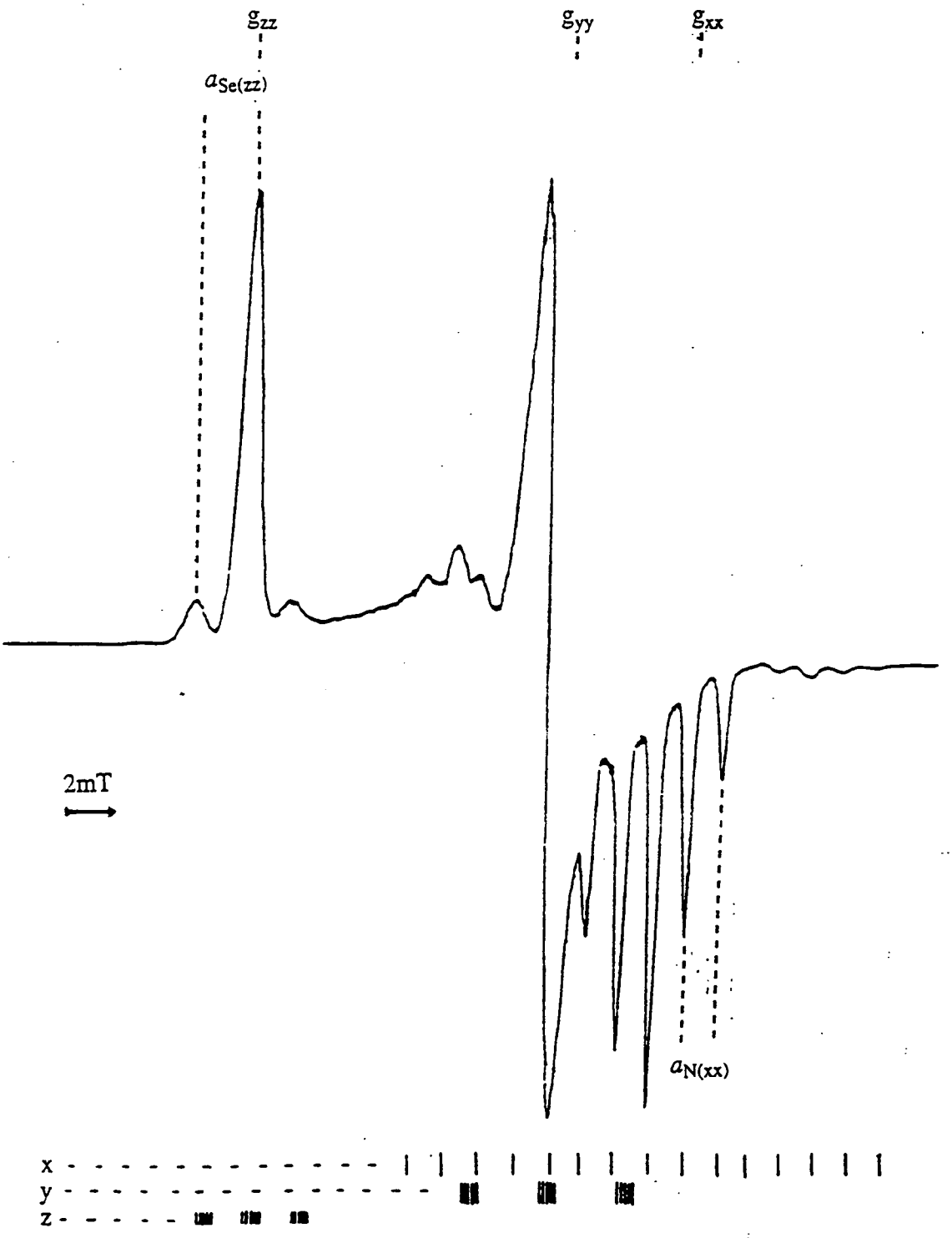

Figure 8.f. Frozen Glass Experimental and Simulation E.s.r. Spectra of [PhCNSeSeN]•.

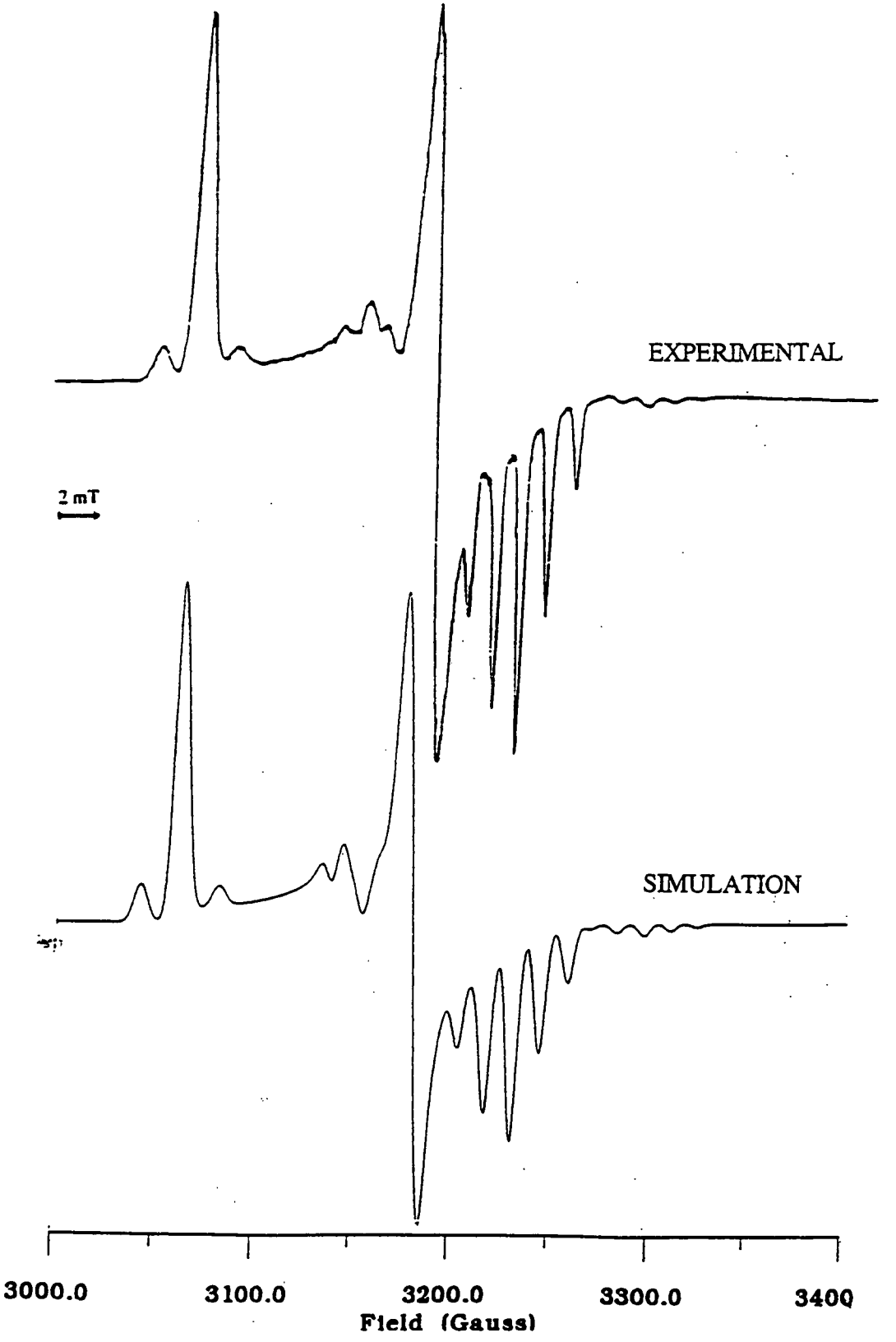

Table 8.a. E.s.r. spectral parameters[a] for 4-phenyl-1,2,3,5-diselenadiazolyl and 4-phenyl-1,2,3,5-dithiadiazolyl radicals.

	[SNSSN]$^{+\bullet}$[b]	[SNSeSeN]$^{+}$[c]	[PhCNSeSeN]$^{\bullet}$[d]	[PhCNSSN]$^{\bullet}$
Temperature (K)	77	77	77	77
g_{xx}	2.0013	1.9941	1.9828	2.0021
g_{yy}	2.0062	2.0108	2.0214	2.0078
g_{zz}	2.0250	2.1355	2.1001	2.0218
$\langle g \rangle$	2.0108	2.0468	2.0346	2.0106
g_{iso}	2.01112	2.0464	2.0376	2.0102
a[N]+A_{xx}[N]	0.918	0.692	1.367	1.410
a[N]+A_{yy}[N]	~0	~0	0.200	0.107
a[N]+A_{zz}[N]	~0	~0	0.133	0.035
$\langle a$[N]$\rangle$	0.306	0.243	0.567	0.517
a_N	0.319	--.---	--.---	0.519
a[E]+A_{xx}[E]	0.3784	~18.0	13.066	--.---
a[E]+A_{yy}[E]	~0	~7.0	5.600	--.-----
a[E]+A_{zz}[E]	-0.0882	5.0	3.866	--.-----
$\langle a$[E]$\rangle$	0.0967	2.0	1.200	--.-----
a_E	0.0861	--.-----	--.-----	0.616
ΔH_{pp}(iso)	0.1	3.4	3.2	0.04

a: hyperfine interactions in mT.
b: taken from reference [11]
c: taken from reference [12]
d: this work

As stated above, solution (first and second derivative) and solid state spectra (powders and crystalline samples) of samples of [PhCNSeSeN]$^{\bullet}$ failed to provide any hyperfine interactions a_N and a_{Se} , which we hoped to compare to the isostructural [PhCNSSN]$^{\bullet}$. This arose through the large line width of these spectra, masking the hyperfine interactions. However, frozen glass spectra provided a significant quantity of information. We have assigned g_{xx}, g_{yy} and g_{zz} in [PhCNSeSeN]$^{\bullet}$ by direct comparison with the frozen glass spectra[11] of [PhCNSSN]$^{\bullet}$ and single crystal spectra[13] of [PhCNSSN][S_3N_3] (PhCNSSN$^{\bullet}$ trapped in lattice). The relative orientations of the tensors are thus; g_{xx} perpendicular to the ring plane, g_{yy} along the C_2 axis and g_{zz} parallel to the E-E bond vector in the ring plane (Figure 8.g.).

Figure 8.g. The $^2A_2$ SOMO of [RCNEEN]$^\bullet$ and the relative orientations of the tensors

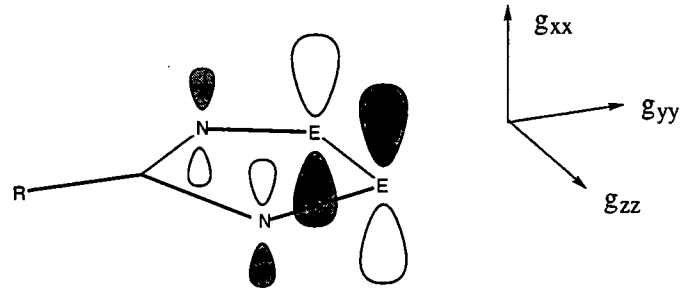

From Table 8.a. we can see that replacement of sulfur by selenium in [RCNEEN]$^\bullet$, leads to a wider spread of anisotropic g-factors producing a greater separation of the component line shapes. The larger values of g_{iso} for [PhCNSeSeN]$^\bullet$ is consistent with previous observations; [SNEEN]$^{+\bullet}$ radicals (isoelectronic with [RCNSeSeN]$^\bullet$) produce a shift in g-factor from 2.01112 (E=S)[11] to 2.0472 (E=Se)[12], and this has been attributed[12] to greater spin-orbit coupling in selenium compared with sulfur based radicals (the ratio of spin-orbit coupling constants[14] Se:S is 4.4:1).

The anomalously large line width observed in the solution spectra (in comparison to the frozen glass spectra) on substituting S by Se, is similar to that observed for the isoelectronic [SNEEN]$^{+\bullet}$ radicals[12]. In these systems, the variation in line-width (as expressed by McConnell[15]) has been found to be dependent on the extent of anisotropy in g. It has already been noted above that replacement of S by Se leads to a greater anisotropy, and hence a greater line-width in the isotropic spectrum, masking all hyperfine structure in the solution spectrum of [PhCNSeSeN]$^\bullet$.

The mean anisotropic nitrogen hyperfine coupling constants ($<a_N>$) show that there is a modest increase in s-electron density at nitrogen on replacing sulfur by selenium (in agreement with prediction[10]), increasing from 0.517mT to 0.567mT. Since the average of the anisotropic Se hyperfine couplings (~7.5mT) is significantly larger than the line-width of the first and second derivative solution spectra (3.2mT at room temperature), we must assume that the signs of two of the anisotropic hyperfine interactions are opposite with respect to the third. Preston, Sutcliffe *et al.* have shown[11][12][16] that this is the

case for the isoelectronic systems [RCNSSN]•, [SNSSN]• and [SNSeSeN]•. In all cases they observed a_{xx}(E) to oppose a_{yy}(E) and a_{zz}(E). Assuming a similar pattern for [PhCNSeSeN]•, we have determined <a(Se)> to be 1.200mT - approximately double the values of a_S in [PhCNSSN]•.

When the hyperfine coupling constants (in MHz) (Table 8.a.) are converted into unpaired spin populations using theoretical one-electron parameters[17], the change in unpaired spin density on replacing S by Se in [RCNEEN]• radicals can be estimated. These data are presented in Table 8.b..

Table 8.b.Estimated unpaired spin populations[a] of valence atomic s and p orbitals in [PhCNSSN]• and [PhCNSeSeN]•

	[PhCNSSN]•[b]	[PhCNSeSeN]•	[SNSSN]+•[c]	[SNSeSeN]+•[c]
N_S	0.8	0.9	0.5	0.4
N_{Px}	22.5	19.9	15.7	11.6
E_S	0.5	0.2	0.7	0.3
E_{Px}	--.--	33.8	42.0	45.3

a: Percentage unpaired spin populations were estimated using the experimental hyperfine tensors in Table 1 and equations given in reference [17].
b: Determined from data given in reference [11].
c: Taken from reference [12].

The unpaired electron density in [PhCNSeSeN]• is distributed primarily over the NSeSeN fragment in a π-type orbital, indicating that this radical has a π-SOMO of $^2A_2$ symmetry, analogous to that found[10][12][18] for [PhCNSSN]•, [SNSSN]• and [SNSeSeN]•. The total electron density on the (NSeSeN) fragment is calculated at 1.096e⁻ in excellent agreement wth previous work[12] and indicates a slight residual negative electron density at the nodal atom (S for [SNSSN]+• and [SNSeSeN]+•, C for [PhCNSSN]• and [PhCNSeSeN]•). Of the four radical systems discussed, the spin densities in the two [RCNEEN]• based species are the most evenly distributed and consequently we believe these to be the more delocalised π-systems. The increased π-

character arises from the lack of positive charge (in $[SNEEN]^{+\bullet}$ the electropositive chalcogen atoms bear the greater positive charge and this tends to localise the spin density on E).

Although the isotropic data indicate a marginal increase (+0.1%) in s-electron density at N (on replacing S by Se), consistent with previous proposals[10], the story is more complex; in fact, there is a net increase in π-electron density at the chalcogen, on moving from $[PhCNSSN]^{\bullet}$ to $[PhCNSeSeN]^{\bullet}$, and a corresponding decrease in π-electron density at N(-2.6%). Substitution of sulfur by selenium in the isoelectronic $[SNEEN]^{+\bullet}$ analogues also leads to an increase in π-electron density[12] at E(+3.3%). Thus replacement of S by Se would appear to have a similar electronic effect to using fluorinated substituents[19] i.e. producing an increase in unpaired spin density at the electropositive ring atoms. Such an increase in π-electron density at the chalcogen may help explain the stronger bonding interactions in both $(C_6F_5CNSSN)_2$ and $(PhCNSeSeN)_2$ compared to $(PhCNSSN)_2$. Sulfur^{33} labelling experiments on $[PhCNSSN]^{\bullet}$ would facilitate a complete evaluation of the two related radicals, $[RCNEEN]^{\bullet}$.

8.2.6. Preliminary Complexation Reactions of $[PhCNSeSeN]^{\bullet}$ with $M(PPh_3)_4$ (where M = Pd or Pt).

A preliminary reaction between $[PhCNSeSeN]^{\bullet}$ and $[Pd(PPh_3)_4]$ in CH_2Cl_2 led only to the formation of a deep red e.s.r. inactive solution. Further studies were undertaken (see section 8.2.9.). In contrast the preliminary reaction between $[PhCNSeSeN]^{\bullet}$ and $[Pt(PPh_3)_4]$ led to the initial formation of a lime green solution which proved to be e.s.r. active.

8.2.7. Solution State E.s.r. Spectra of $[Pt(SeNC(Ph)NSe\text{-}Se,Se)(PPh_3)_2]$.

Addition of a small quantity of $(PhCNSeSeN)_2$ to $[Pt(PPh_3)_4]$ in an e.s.r. tube in CH_2Cl_2 led to an immediate lime-green coloration of an e.s.r. active material, which turned orange on standing over a period of *ca.* 10 minutes. A rapid decrease in intensity of the e.s.r. spectrum accompanied this colour change. We postulate that $(PhCNSeSeN)_2$ reacts with $[Pt(PPh_3)_4]$ in a manner analogous to that previously

described in chapter four for [PhCNSSN]$^{\bullet}$, i.e. an unstable monomeric complex, [Pt(SeNC(Ph)NSe-*Se,Se*)(PPh_3)$_2$], is formed first which rapidly decomposes to a diamagnetic species, possibly [$Pt_3(\mu_{Se\text{-}Se}SeNC(Ph)NSe)_2(PPh_3)_4$] and $(PhCNSeSeN)_2$. By carrying out the reaction in the presence of a large excess of [Pt[PPh_3]$_4$], the spectra were not obscured by the contaminant [PhCNSeSeN]$^{\bullet}$ (the technique which is also used to analyse the sulfur based species discussed in chapter four).

Although the first derivative spectrum of the initial solution was poorly resolved, the second derivative spectrum and simulation (figure 8.h) clearly shows a complex consistent with the proposed formulation, [Pt(SeNC(Ph)NSe-*Se,Se*)(PPh_3)$_2$]. The spectrum shows hyperfine coupling to ^{195}Pt and two equivalent ^{14}N nuclei and shoulders attributed to ^{31}P. Although coupling to ^{77}Se was not directly observable, we have estimated (from the simulation) a magnitude of *ca.* 0.4mT. The data used to simulate the spectrum are listed in Table 8.c., along with those reported for the sulfur analogue [Pt(SNC(Ph)NS-*S,S*)(PPh_3)$_2$]. The resonances in this complex are significantly broader (ΔH_{pp} = 0.6mT) than those observed for the sulfur analogue (ΔH_{pp} = 0.2mT). The spectrum is highly asymmetric and this has made satisfactory simulation difficult. We believe this asymmetry arises primarily through the rapid loss of signal intensity caused by sample decomposition, although second order line-broadening effects may also be contributing factors. To date we have been unable to determine anisotropic hyperfine couplings for this complex from frozen glass spectra; the latter are observed as broad unresolved singlets.

Figure 8.h. Second Derivative E.s.r. Experimental and Simulation Spectra of $[Pt(SeNC(Ph)NSe\text{-}Se,Se)(PPh_3)_2]$.

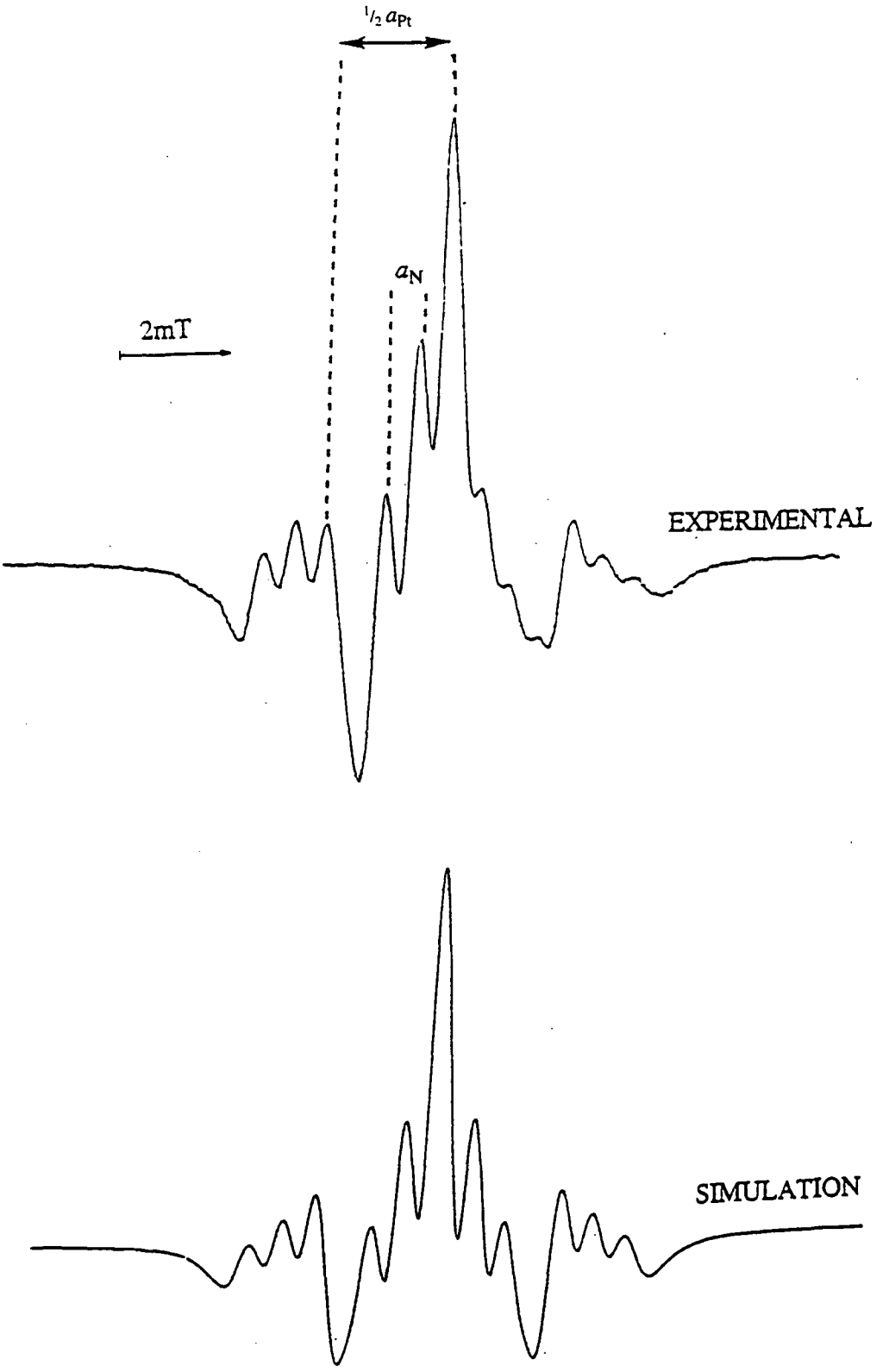

Table 8.c. ESR spectral parameters for [Pt(SeNC(Ph)NSe-*Se,Se*)(PPh$_3$)$_2$] and [Pt(SNC(Ph)NS-*S,S*)(PPh$_3$)$_2$].

	Pt(SeNC(Ph)NSe-*Se,Se*)(PPh$_3$)$_2$	Pt(SNC(Ph)NS-*S,S*)(PPh$_3$)$_2$
g_{iso}	2.0615	2.0386
a_{Pt}	4.405	5.385
a_N	0.587	0.553
a_P	~0.16	0.280
a_E	~0.40	-.-
ΔB_{pp}	0.60	0.20

Hyperfine interactions in mT.

Metal complexation would appear to lead to a drift of electron density from the chalcogen to the metal centre, producing a smaller value for a_E and strong coupling to the metal centre, whilst leaving a_N virtually unchanged. Thus we have been able to verify the estimate of a_N in the uncomplexed radical [RCNSeSeN]$^\bullet$ by comparison with this complex. Moreover, by losing electron density at Se, the line-width is substantially decreased (from 32G to 6G) allowing us to observe much of the hyperfine coupling to the heteroatoms. Notably, a_N in the metal complex (0.587mT) is in good agreement with that predicted from the anisotropic data for [Pt(SNC(Ph)NS-*S,S*)(PPh$_3$)$_2$] (0.553mT). The hyperfine-coupling to both Pt and P is significantly less than in the analogous [Pt(SNC(Ph)NS-*S,S*)(PPh$_3$)$_2$] and this must be attributed to retention of a greater proportion of the electron density on the [PhCNSeSeN]$^\bullet$ ligand. The greater residual electron density at selenium presumably makes [Pt(SeNC(Ph)NSe-*Se,Se*)(PPh$_3$)$_2$] significantly more reactive than [Pt(SNC(Ph)NS-*S,S*)(PPh$_3$)$_2$] - as indicated by the rapid decay of signal intensity in the e.s.r. experiment.

8.2.8. The Reaction of [PhCNSeSeN]• with [Pt(PPh$_3$)$_4$].

It was hoped that the reaction between [PhCNSeSeN]• and [Pt(PPh$_3$)$_4$], although not producing [Pt(SeNC(Ph)NSe-Se,Se)(PPh$_3$)$_2$] as a stable product, would decompose to the trimetallic species [Pt$_3$($\mu_{Se\text{-}Se}$SeNC(Ph)NSe)$_2$(PPh$_3$)$_4$]. The reaction between [PhCNSeSeN]• and [Pt(PPh$_3$)$_4$] in MeCN led to the formation of a yellow solid which was filtered, washed with fresh MeCN and dried *in vacuo*. The elemental analysis did not seem to indicate that this was the case. The ^{31}P n.m.r. showed that there was more than one species present with 4 major peaks at δ19.1, 18.9, 12.7 & 12.5ppm. The first two values are similar to that observed for Pt$_3$($\mu_{S\text{-}S}$SNC(Ph)NS)$_2$(PPh$_3$)$_4$ (δ18.5ppm), although due to the lack of solubility no satellites were observed. Either of these last two peaks may be due to the selenium analogue. The ^{1}H n.m.r. spectrum shows the phenyl protons of the complexes formed (δ7.63-7.29) and also MeCN protons (δ2.27), thus indicating that some solvent of crystallisation may be present.

8.2.9. The Reaction of [PhCNSeSeN]• with [Pd(PPh$_3$)$_4$].

As in the [PhCNSSN]• case, the reaction between [Pd(PPh$_3$)$_4$] in MePh results in the formation of a deep red solid. Elemental analysis and a comparison of infra red spectra with [Pd$_3$($\mu_{S\text{-}S}$SNC(Ph)NS)$_2$(PPh$_3$)$_4$] indicate that [Pd$_3$($\mu_{Se\text{-}Se}$SeNC(Ph)NSe)$_2$(PPh$_3$)$_4$] has been formed. As in the sulfur based complex the ^{31}P n.m.r. spectra showed only one peak at δ20.4 (c.f.[Pd$_3$($\mu_{S\text{-}S}$SNC(Ph)NS)$_2$(PPh$_3$)$_4$] δ18.5ppm and [Pd(PPh$_3$)$_2$(1,5-Ph$_4$P$_2$N$_4$Se$_2$)] δ24.8ppm[20]). Also the ^{1}H n.m.r. spectra showed the phenyl protons at δ7.36-6.95. The low solubility of the complex (it readily precipitates out of CDCl$_3$ solution) highlighted the presence of more soluble impurities at δ1.29, 1.61, 2.39 & 8.25ppm (again as in the sulfur case, reported in chapter six)

Any attempt to recrystallise was hampered by the low solubility of the species in common solvents. An attempt was made to grow crystals by the method used to prepare crystalline samples of [Pd$_3$($\mu_{S\text{-}S}$SNC(Ph)NS)$_2$(PPh$_3$)$_4$] i.e. slow diffusion of a solution of [PhCNSeSeN]• in CH$_2$Cl$_2$ onto a solution of Pd(PPh$_3$)$_4$ in CH$_2$Cl$_2$. This led only to the formation of yellow crystals of cis-(PPh$_3$)$_2$PdCl$_2$, as shown by a preliminary x-ray structural determination.

8.3. Experimental.

8.3.1. The Preparation of [PhCNSeSeN]Cl.

$Li[(N(SiMe_3)_2]$ (2.17g, 12.97mmol) was dissolved in Et_2O (150ml). PhCN (1.6ml, 13mmol) was added and the straw coloured solution left stirring overnight. Selenium (1g, 12.66mmol) and $SeCl_4$ (2.8g, 12.68mmol) were charged into a second flask which was cooled to 0°C. The ethereal solution was canula transfered onto these solids with stirring to yield immediately a red-brown precipitate under an orange solution. This suspension was stirred for 3hr, filtered, washed with Et_2O (3x30ml) and dried *in vacuo* . The red-brown solids were then extracted in a closed soxhlet extractor with SO_2 (30ml) until all the deep red crystalline [PhCNSeSeN]Cl had extracted leaving behind the insoluble LiCl (at least 48hr). The SO_2 was then removed and the deep red crystalline material dried in *vacuo*..

Yield 2.36g, 60.1%.

IR $\nu_{max}(cm^{-1})$ 2924br, 1592w, 1570w, 1463sh, 1433sh, 1408w, 1377s, 1297m, 1167m, 1140m, 1100m, 1064m, 1027w, 996w, 897sh, 866sh, 848m, 817m, 758m, 744m, 706ssh, 693ssh, 646m, 526ssh, 518m, 482m, 474m, 450m, 434w, 419w.

Elemental analysis, found: C,27.34%; H,1.81%; N,8.92%.Calc.: C,27.07%; H,1.62%; N9.02%).

Mass spec. $(^m/_e)$EI+ 277(PhCNSeSeN)+, 174(SeSeN)+, 103(PhCN)+.CI+ 275(PhCNSeSeN)+.

D.s.c.186°C (dec.).

8.3.2. The Reduction of [PhCNSeSeN]Cl to $(PhCNSeSeN)_2$ with Zn/Cu Couple.

[PhCNSeSeN]Cl (0.60g, 2mmol) and Zn/Cu couple (0.10g, 1.55mmol) were stirred in thf (20ml) overnight. The resultant dark purple suspension was dried *in vacuo*. The solids were heated to 110°C and the sublimed purple powder of $(PhCNSeSeN)_2$ collected on a cold finger. The solids were removed from the cold finger and the residues resublimed. This process was repeated until no new product could be sublimed.

Yield 0.058g, 10.9%.

IR $\nu_{max}(cm^{-1})$ 2860sbr, 2100br, 1450s, 1380ssh, 1305, 1265w, 1170w, 1155w, 1115, 1070wbr, 1025m, 1000w, 970wbr, 920w, 860w, 820w, 780w, 770sh, 740, 725, 715sh, 700ssh, 685ssh, 650sh, 610m.

Elemental analysis, found: C,30.64%; H,1.77%; N,10.15%. Calc.:C,30.55%; H,1.81%; 10.18N%).

Mass spec ($^m/_e$) EI+ 277(PhCNSeSeN)+, 174(SeSeN)+, 103(PhCN)+, CI+ 278(PhCNSeSeN)+.

D.s.c. 176°C (dec.).

8.3.3. The Reduction of [PhCNSeSeN]Cl to $(PhCNSeSeN)_2$ with Silver Powder.

[PhCNSeSeN]Cl (3.6g, 11.59mmol) and Ag powder (1.2g, 11.17mmol) were placed together with a stirring bar in a 250ml round bottomed flask. T.h.f. (40ml) was added and the mixture left to stir overnight, yielding a deep purple suspension. The reaction was then pumped to dryness, a cold finger attatchment was inserted into the flask and the remaining solid was sublimed at around 130°C on two occasions for around 2-3hrs each. After each sublimation the dark purple solid collected on the cold finger was harvested and the two crops combined.

Yield 1.195g,37.5%.

Infra red (CsI nujol mull) (v max cm^{-1}) 1670br, 1600w, 1330s, 1310s, 1270s, 1180, 1160, 1120s, 1070, 1030, 920w, 860w, 790sshd, 780w, 770ssh, 745, 715ssh, 700, 690shd, 650ssh, 610, 450br, 420ssh.

Elemental analysis, found: C,31.40%; H,1.98%; N,9.80%. Calc.:C,30.55%; H,1.81%; 10.18N%).

Mass spec. ($^m/_e$) EI^+ $277(PhCN_2Se_2)^+$, $174(SeNSe)^+$, $160(SeSe)^+$, $103(PhCN)^+$ CI^+ $275(PhCN_2Se_2)^+$, $121(CNNSe)^+$.

D.s.c. 175°C (dec.).

8.3.4. The Reduction of [PhCNSeSeN]Cl to $(PhCNSeSeN)_2$.by Ph_3Sb.

[PhCNSeSeN]Cl (1.5g, 5.4mmol) and Ph_3Sb (0.75g, 2.1mmol) were placed in one bulb of a two bulbed reaction vessel together with a stirring bar. CH_2Cl_2(8ml) was syringed into the other limb and back transferred onto the reactants. The reaction was left stirring overnight before the soluble fraction was filtered over into the other bulb leaving a dark purple solid. These two materials were then pumped to dryness and the insoluble fraction analysed.

Yield before sublimation 1.15g (86%), after sublimation 0.70g (52.3%)

Infra red (v max cm^{-1}) 1675br, 1610w, 1525br, 1330ssh, 1310s, 1285w, 1270, 1180, 1130ssh, 1120ssh, 1065w, 1060w, 1025, 1000w, 970w, 940w, 920sh, 870w, 860w, 840w, 780, 770ssh, 735sh, 720ssh, 700ssh, 690ssh, 650ssh, 610ssh, 470w, 450w, 430ssh.

Elemental analysis, found: C,30.38%; H,1.59%; N,10.01%. Calc.:C,30.55%; H,1.81%; 10.18N%).

Mass spec ($^m/_e$) EI^+ 277$(PhCN_2Se_2)^+$, 174$(SeSeN)^+$, 160$(SeSe)^+$, 103$(PhCN)^+$

D.s.c. 176°C (dec.).

8.3.5. The 'One-Pot' Preparation of $(PhCNSeSeN)_2$.

$Li[(N(SMe_3)_2]$ (3.05g, 18.2mmol) was dissolved in Et_2O (100ml). PhCN (2ml, 19.6mmol) was added and the straw coloured solution left stirring overnight. Selenium (1.4g, 17.8mmol) and $SeCl_4$ (4.0g, 18.1mmol) were charged to a second flask which was cooled to 0°C. The ethereal solution was canula transfered onto these solids with stirring to yield immediately a red-brown precipitate under an orange solution. This suspension was stirred for 3hr, filtered, washed with Et_2O (3x30ml) and dried *in vacuo* . The deep red solid mixture (PhCNSeSeN and LiCl) and Ph_3Sb (3.26g, 9.23mmol) were refluxed in MeCN. (30ml) for 1h. The deep purple suspension was filtered, washed (3x10ml MeCN) and dried *in vacuo*. The filtrate (mainly Ph_3SbCl_2) was discarded. The solids were then heated to 170°C and sublimed to yield dark green-purple dichroic crystals of $(PhCNSeSeN)_2$ in the sublimation tube. The crystals were removed from the tube and the process repeated until no new product could be sublimed.

Yield 1.53g 30.8%.

IR $\nu_{max}(cm^{-1})$ 3025w, 2922m, 1670w, 1601m, 1491sh, 1449m, 1311m, 1262m, 1175m, 1156br, 1116m, 1027s, 922w, 906w, 803m, 768m, 697s, 652ssh, 612m, 538m, 464m, 424ssh.

Elemental analysis, Found: C,30.68%; H,1.74%; N,10.23%. Calc.: C,30.55%; H1.81,%; 10.18N%.

Mass spec. ($^{m}/_{e}$) EI+ 277(PhCNSeSeN)+, 174(SeSeN)+, 103(PhCN)+.CI+ 278(PhCNSeSeN)+,.

D.s.c. 175°C (dec.).

8.3.6. The Reaction Between $(PhCNSeSeN)_2$ and $[Pt(PPh_3)_4]$.

$[Pt(PPh_3)_4]$ (0.78g, 0.62mmol) and $[PhCNSeSeN]^{\bullet}$ (0.112g, 0.44mmol) were stirred in MeCN (10ml) for 5h to yield a yellow solid which was filtered, washed and dried in vacuo. Assume product to be $[Pt_3(\mu_{Se\text{-}Se}SeNC(Ph)NSe)_2(PPh_3)_4]$.

Yield 0.174g, 40.0%.

N.m.r., (250MHz; solvent $CDCl_3$) ^1H δ7.63-7.29ppm (m), δ2.27ppm (MeCN).

I.R $\nu_{max}(cm^{-1})$ 3051w, 2347w, 1597w, 1584w, 1570w, 1544w, 1491sh, 1479ssh, 1434s, 1379s, 1311w, 1183m, 1157m, 1095s, 1071w, 1027m, 998m, 917w, 868w, 846w, 778w, 743s, 693s, 665m, 618w, 560w, 545ssh, 527s, 513s, 497s, 448w.

Elemental analysis, found: C,54.03%; H,3.80%; N,1,24%. Calc.: C, 47.28%; H,2.48%; N, 2.57%).

D.s.c. 276°C (dec.).

8.3.7. The Reaction Between $(PhCNSeSeN)_2$ and $[Pd(PPh_3)_4]$.

$Pd(PPh_3)_4$ (0.504g, 0.43mmol) and $[PhCNSeSeN]^{\bullet}$ (0.087g, 0.32mmol) were stirred in MePh (10ml) for 5h at ambient temperature. The resultant deep red precipitate was filtered, washed with toluene (3x5ml) and dried *in vacuo*.. Assume product to be $[Pd_3(\mu_{Se\text{-}Se}SeNC(Ph)NSe)_2(PPh_3)_4]$.

Yield 0.23g, 74%.

IR ν_{max} (cm^{-1}) 3049m, 2347m, 1571w, 1479m, 1450sh, 1433s, 1309w, 1278m, 1161w, 1128w, 1093m, 1025w, 998w, 868w, 739m, 691s, 666sh, 618w, 578w, 528s, 519ssh, 506ssh, 492m, 452w.

Elemental Analysis; found: C54.17%; H3.53%, N2.91%, Calc: C53.84%, H3.69%, N2.92%).

N.m.r., (250MHz; solvent $CDCl_3$) ^1H δ_H 7.36-6.95 (m), ^{31}P δ_P 20.4 (s).

D.s.c. 219.7°C (dec.).

8.3.8. Crystal Reaction Between $(PhCNSeSeN)_2$ and $Pd(PPh_3)_4$ in CH_2Cl_2.

$Pd(PPh_3)_4$ (1.00g, 0.865mmol) was placed in one limb of a two-limbed reaction vessel with $(PhCNSeSeN)_2$ (0.20g, 0.719mmol) placed in the other limb. CH_2Cl_2 (10ml) was added to each side. Inversion of the sealed reaction vessel resulted in the slow diffusion through the separating grade three sinter of a solution of PhCNSeSeN into the former limb to yield a deep red solution over unreacted [$Pd(PPh_3)_4$]. After 3-4 days all the $Pd(PPh_3)_4$ had reacted, yellow crystals of $(PPh_3)_2PdCl_2$ had started to form and the solution became yellow in colouration.

8.4. CONCLUSION.

The final chapter in this thesis has concentrated on the physical properties and preliminary complexation reactions of Phenyl 1,2,3,5-Diselenadiazolyl. The frozen glass e.s.r. spectrum of this species has enabled a comparison to be made between the nature of the singly occupied molecular orbital on [PhCNSeSeN]$^{\bullet}$ and previously reported radicals especially the sulfur analogue [PhCNSSN]$^{\bullet}$.

Similar chemistry to the research outlined in the previous chapters on [PhCNSSN]$^{\bullet}$ has also been undertaken on [PhCNSeSeN]$^{\bullet}$. As such a new simplified preparation of the dimeric species $(PhCNSeSeN)_2$ has been outlined and preliminary complexation reactions have been undertaken. In the reaction of [PhCNSeSeN]$^{\bullet}$ with $[Pt(PPh_3)_4]$ the first diselenadiazolyl complex, $[Pt(SeNC(Ph)NSe\text{-}Se,Se)(PPh_3)_2]$, has been observed in solution by e.s.r. spectroscopy. Also reaction between [PhCNSeSeN]$^{\bullet}$ and $[Pd(PPh_3)_4]$ has resulted in the isolation of $[Pd_3(\mu_{Se\text{-}Se}SeNC(Ph)NSe)_2(PPh_3)_4]$ as a stable solid. Clearly further complexation reactions (perhaps with zero-valent dppe complexes of Pt and Pd) could result in the formation of more complexes.

8.5. REFERENCES.

1. P.D. Belluz, A.W. Cordes, E.M. Krislof, S.W. Liblong and R.T. Oakley, *J.Am.Chem.Soc.*, 1989, **111**, 9276.

2. A.W. Cordes, S.H. Glarum, R.C. Haddon, R. Haliford, R.G. Hicks, D.K. Kennepohl, R.T. Oakley, T.T.M. Palstra and S.R. Scott, *J.Chem Comm.*, 1992, 1265.

3. R.T. Boeré, K.H. Moock and M. Parvez, *Z.Anorg.Allg.Chem.*, 1994, **620**, 1589.

4. C.D. Bryan, A.W. Cordes, R.C. Haddon, R.G. Hicks, R.T. Oakley, T.T.M. Palstra, A.S. Perel and S.R. Scott, *Chem.Mater.*, 1994, **6**, 508.

5. M.P. Andrews, A.W. Cordes, D.C. Douglas, R.M. Fleming, S.H. Glarum, R.C. Haddon, P. Marsh, R.T. Oakley, T.T.M. Palstra, L.F. Schneemeyer, G.W. Trucks, R. Tycko, J.V. Waszczak, K.M. Young and N.M. Zimmerman, *J.Am.Chem.Soc.*, 1991, **113**, 582.

6. A.W. Cordes, R.C. Haddon, R.T. Oakley, L.F. Schneemeyer, J.V. Waszczak, K.M. Young, M.N. Zimmerman, *J.Am.Chem.Soc.*, 1991, **113**, 582.

7. A.W. Cordes, R.C. Haddon, R.G. Hicks, R.T. Oakley, T.T.M. Palstra, L.F. Schneemeyer and J.V. Waszczak, *J.Am.Chem.Soc.*, 1992, **114**, 1729.

8. I. Lavender, PhD Thesis, University of Durham, 1992.

9. R.T. Boeré, private communication, 1994.

10. A.W. Cordes, C.D. Bryan, W.M. Davis, R.H. de Laat, S.H. Glarum, J.D. Goddard, R.C. Haddon, R.G. Hicks, D.K. Kennepohl, R.T. Oakley, S.R. Scott and N.B.C. Westwood, *J.Am.Chem.Soc.*, 1993, **115**, 7232.

11. S.A. Fairhurst, K.M. Johnson, L.H. Sutcliffe, K.F. Preston, A.J. Banister, Z.V. Hauptman and J. Passmore, *J.Chem.Soc., Dalton Trans.*, 1986, 1465.

12. E.G. Awere, J. Passmore, K.F. Preston and L.H. Sutcliffe, *Can.J.Chem.*, 1988, **66**, 1776.

13. F.L. Lee, K.F. Preston, A.J. Williams, L.H. Sutcliffe, A.J. Banister and S.T. Wait, *Magn.Reson.Chem.*, 1989, **27**, 1161.

14. J.R. Morton, J.R. Rowlands and D.H. Whiffen, National Physical Laboratory Report, BPR13, National Physical Laboratory, Teddington, 1962.

15. H.M. McConnell, *J.Chem.Phys.*, 1956, **25**, 709.

16. K.F. Preston, J.P. Charland and L.H. Sutcliffe, *Can.J.Chem.*, 1988, **66**, 1299.

17. J.R. Morton and K.F. Preston, *J.Magn.Reson.*, 1978, **30**, 577.

18. J.M. Rawson, A.J. Banister and I. Lavender, *Adv. Hetero. Chem.*, 1995, **62**, 137.

19. S.A. Fairhurst, L.H. Sutcliffe, K.F. Preston, A.J. Banister, A.S. Partington, J.M. Rawson, J. Passmore and M.J. Schriver, *J.Magn.Reson.*, 1993, **31**, 1027.

20. T. Chivers, M. Edwards, A. Meetsma, J.C. Van der Lee, *Inorg. Chem.*, 1992, **31**, 11.

APPENDIX 1
SUPPLEMENTARY X-RAY STRUCTURAL DATA

This appendix contains selected structural details for the X-ray structures discussed during the course of this thesis.

[Pt(SNC(Ph)NS-*S,S*)(PPh$_3$)$_2$].MeCN.

Empirical formula:	$C_{45}H_{38}N_3P_2S_2Pt$	
Crystal system:	triclinic	
Space group:	$P\bar{1}$	
Cell dimensions:	a = 13.240(6)Å,	α = 63.57(1)°
	b = 13.366(6)Å,	β = 76.38(2)°
	c = 14.090(8)Å,	γ = 60.71(2)°
Volume:	1946.9(7)Å^3	
Z:	2	
Density (calc):	1.607mg/m^3	
Final R indices:	0.0353 (R_w = 0.0946)	

[Pt(SNC(Ph)NS-*S,S*)(dppe)]

Empirical formula:	$C_{35}H_{29}N_2P_2S_2Pt$	
Crystal system:	orthorhombic	
Space group:	$P2_12_12_1$	
Cell dimensions:	a = 11.618(11)Å,	α = 90°
	b = 12.65(13)Å,	β = 90°
	c = 20.994(6)Å,	γ = 90°
Volume:	2.992(4)Å^3	
Z:	4	
Density (calc):	1.720mg/m^3	
Final R indices:	0.0633 (R_w = 0.1683)	

[Pd(SNC(Ph)NS-*S,S*)(dppe)]

Empirical formula:	$C_{33}\ H_{29}\ N_2\ P_2\ S_2\ Pd$
Crystal system:	orthorhombic
Space group:	$P2_12_12_1$
Cell dimensions:	a = 11.653(4)Å, $\alpha = 90°$
	b = 12.258(8)Å, $\beta = 90°$
	c = 20.826(11)Å, $\gamma = 90°$
Volume:	1974.8(9)Å^3
Z:	4
Density (calc):	1.532mg/m^3
Final R indices:	0.0444 (R_w = 0.1142)

[$Pt_3(\mu_{S\text{-}S}SNC(Ph)NS)_2(PPh_3)_4$].2MePh.

Empirical Formula:	$C_{100}\ H_{86}\ N_4\ P_4\ S_4\ Pt_3$
Crystal system:	monclinic
Space group:	$P2_1/c$
Cell dimensions:	a = 12.704(16)Å, $\alpha = 90°$
	b = 24.988(11)Å, $\beta = 101.94(3)°$
	c = 12.888(6)Å, $\gamma = 90°$
Volume:	4313(3)Å^3
Z:	2 (Pt on inversion centre)
Density (calc):	1.679mg/m^3
Final R indices:	0.0477 (R_w = 0.1271)

[$Pt_3(\mu_{S\text{-}S}SNC(3,4FC_6H_3)NS)_2(PPh_3)_4$].4CDCl$_3$.

Empirical formula:	$C_{90}\ H_{70}\ Cl_{12}\ F_4\ N_4\ P_4\ Pt_3\ S_4$
Crystal system:	monclinic
Space group:	$P2_1/c$
Cell dimensions:	a =13.5111(13) Å, a = 90°
	b = 20.902(2)Å, b = 111.330(5)°
	c = 17.588(2)Å, g = 90°
Volume:	4626.9(8)Å^3
Z:	2
Density (calc):	1.828mg/m^3
Final R indices:	0.0531 (R_w = 0.1223

$[Pd_3(\mu_{S,S}SNC(Ph)NS)_2(PPh_3)_4].2MePh.$

Empirical formula:	$C_{88}\ H_{78}\ C_{14}\ N_4\ P_4\ Pd_3\ S_4$
Crystal system:	triclinic
Space group:	P-1
Cell dimensions:	a = 14.2420(10)Å, α = 73.440(10)°
	b = 14.2610(10)Å, β = 89.190(10)°
	c = 24.512(2)Å, γ = 62.090(10)°
Volume:	4174.9(5)Å^3
Z:	2
Density (calc):	1.515mg/m^3
Final R indices:	0.0674 (R_w = 0.1347)

$[Pd_2(\mu_{S,S}SNC(Ph)N(H)S)_2(dppe)_2][BF_4]_2.3CDCl_3.$

Empirical formula:	$C_{62}\ H_{57}\ B_2\ Cl_9\ F_8N_2\ P_4\ Pd_2\ S_2$
Crystal system:	monoclinic
Space group:	P21/c
Cell dimensions:	a = 11.0729(7)Å, a = 90°
	b = 23.3848(14)Å, b = 94.7180(10)°
	c = 27.300(2)Å, g = 90°
Volume:	7045.1(8)Å^3
Z:	4
Density (calc):	1.625mg/m^3
Final R indices:	0.0684 (R_w = 0.1382)

APPENDIX 2
CONFERENCES AND LECTURES ATTENDED

A.2.1. Conferences Attended.

The following is a list of conferences and post-graduate meetings which were attended by the author and the poster and oral presentations give by the author at these meetings.

1. 27th International Conference on E.S.R. Spectroscopy (Cardiff March 94).
Poster: *"E.S.R. studies of some dithiadiazolyl Pt and Pd complexes with phosphine ligands"*

2. 7th Inorganic Ring Systems Conference (Banff, Canada, August 94)
Poster: *"Metal Insertion into the S-S Bond of Phenyl Dithiadiazolyl"*

3.The R.S.C. Autumn Meeting (Glasgow University, September 94)
Oral Presentation: *"Metal Insertion into the S-S Bond of Phenyl Dithiadiazolyl"*

4. I.C.I. Poster competition (Durham University, December 94)
Poster: "Applications of Dithiadiazolyls and their Complexes"

5. Graduate Talk (Durham University, June 95)
Oral Presentation: *"Preparation, properties and applications of the platinum-dithiadiazolyl complex* [Pt(SNC(Ph)NS-S,S)$(PPh_3)_2$]"

A.2.2. Lectures Attended.

The following is a list of colloquia, lectures and seminars from invited speakers to the Department of chemistry, University of Durham, during the period of this research. An asterix (*) indicates those lectures which were attended by the author of this Thesis.

1992

October 15	Dr M. Glazer & Dr. S. Tarling, Oxford University & Birkbeck College, London *It Pays to be British! - The Chemist's Role as an Expert Witness in Patent Litigation.*
October 20	Dr. H. E. Bryndza, Du Pont Central Research *Synthesis, Reactions and Thermochemistry of Metal (Alkyl) Cyanide Complexes and Their Impact on Olefin Hydrocyanation Catalysis.*
October 22	Prof. A. Davies, University College London *Ingold-Albert Lecture The Behaviour of Hydrogen as a Pseudometal.* *

October 28 Dr. J. K . Cockcroft, University of Durham
Recent Developments in Powder Diffraction.

October 29 Dr. J. Emsley, Imperial College, London
The Shocking History of Phosphorus. *

November 4 Dr. T. P. Kee, University of Leeds
Synthesis and Co-ordination Chemistry of Silylated Phosphites. *

November 5 Dr. C. J. Ludman, University of Durham
Explosions, A Demonstration Lecture. *

November 11 Prof. D. Robins†, Glasgow University
Pyrrolizidine Alkaloids : Biological Activity, Biosynthesis and Benefits.

November 12 Prof. M. R. Truter, University College, London
Luck and Logic in Host - Guest Chemistry.

November 18 Dr. R. Nix†, Queen Mary College, London
Characterisation of Heterogeneous Catalysts.

November 25 Prof. Y. Vallee. University of Caen
Reactive Thiocarbonyl Compounds.

November 25 Prof. L. D. Quin†, University of Massachusetts, Amherst
Fragmentation of Phosphorous Heterocycles as a Route to Phosphoryl Species with Uncommon Bonding. *

November 26 Dr. D. Humber, Glaxo, Greenford
AIDS - The Development of a Novel Series of Inhibitors of HIV.

December 2 Prof. A. F. Hegarty, University College, Dublin
Highly Reactive Enols Stabilised by Steric Protection.

December 2 Dr. R. A. Aitken†, University of St. Andrews
The Versatile Cycloaddition Chemistry of $Bu_3P.CS_2$. *

December 3 Prof. P. Edwards, Birmingham University
The SCI Lecture - What is Metal? *

December 9 Dr. A. N. Burgess†, ICI Runcorn
The Structure of Perfluorinated Ionomer Membranes.

1993

January 20 Dr. D. C. Clary†, University of Cambridge
Energy Flow in Chemical Reactions.

January 21 Prof. L. Hall, Cambridge
NMR - Window to the Human Body. *

January 27 Dr. W. Kerr, University of Strathclyde
Development of the Pauson-Khand Annulation Reaction : Organocobalt Mediated Synthesis of Natural and Unnatural Products.

January 28 Prof. J. Mann, University of Reading
Murder, Magic and Medicine. *

February 3 Prof. S. M. Roberts, University of Exeter
Enzymes in Organic Synthesis.

February 10 Dr. D. Gillies†, University of Surrey
NMR and Molecular Motion in Solution.

February 11 Prof. S. Knox, Bristol University
The Tilden Lecture: Organic Chemistry at Polynuclear Metal Centres.

February 17 Dr. R. W. Kemmitt†, University of Leicester
Oxatrimethylenemethane Metal Complexes.

February 18 Dr. I. Fraser, ICI Wilton
Reactive Processing of Composite Materials.

February 22 Prof. D. M. Grant, University of Utah
Single Crystals, Molecular Structure, and Chemical-Shift Anisotropy.

February 24 Prof. C. J. M. Stirling†, University of Sheffield
Chemistry on the Flat-Reactivity of Ordered Systems.

March 10 Dr. P. K. Baker, University College of North Wales, Bangor
'Chemistry of Highly Versatile 7-Coordinate Complexes'. *

March 11 Dr. R. A. Y. Jones, University of East Anglia
The Chemistry of Wine Making. *

March 17 Dr. R. J. K. Taylor†, University of East Anglia
Adventures in Natural Product Synthesis.

March 24 Prof. I. O. Sutherland†, University of Liverpool
Chromogenic Reagents for Cations.

May 13 Prof. J. A. Pople, Carnegie-Mellon University, Pittsburgh, USA
The Boys-Rahman Lecture: Applications of Molecular Orbital Theory

May 21 Prof. L. Weber, University of Bielefeld
Metallo-phospha Alkenes as Synthons in Organometallic Chemistry *

June 1 Prof. J. P. Konopelski, University of California, Santa Cruz
Synthetic Adventures with Enantiomerically Pure Acetals

June 2 Prof. F. Ciardelli, University of Pisa
Chiral Discrimination in the Stereospecific Polymerisation of Alpha Olefins

June 7 Prof. R. S. Stein, University of Massachusetts
Scattering Studies of Crystalline and Liquid Crystalline Polymers

June 16 Prof. A. K. Covington, University of Newcastle
Use of Ion Selective Electrodes as Detectors in Ion Chromatography.

June 17 Prof. O. F. Nielsen, H. C. Arsted Institute, University of Copenhagen
Low-Frequency IR - and Raman Studies of Hydrogen Bonded Liquids.

September 13 Prof. Dr. A. D. Schlüter, Freie Universität Berlin, Germany
Synthesis and Characterisation of Molecular Rods and Ribbons.

September 13 Prof. K. J. Wynne, Office of Naval Research, Washington, U.S.A.
Polymer Surface Design for Minimal Adhesion

September 14 Prof. J. M. DeSimone, University of North Carolina, U.S.A.

Homogeneous and Heterogeneous Polymerisations in Enviromentally Responsible Carbon Dioxide.

September 28 Prof. H. Ila., North Eastern University, India
Synthetic Strategies for Cyclopentanoids via OxoKetene Dithiacetals.

October 4 Prof. F. J. Feher†, University of California at Irvine
Bridging the Gap between Surfaces and Solution with Sessilquioxanes.

October 14 Dr. P. Hubberstey, University of Nottingham
Alkali Metals: Alchemist's Nightmare, Biochemist's Puzzle and Technologist's Dream.

October 20 Dr. P. Quayle†, Unversity of Manchester
Aspects of Aqueous Romp Chemistry.

October 23 Prof. R. Adams†, University of S. Carolina
The Chemistry of Metal Carbonyl Cluster Complexes Containing Platinum and Iron, Ruthenium or Osmium and the Development of a Cluster Based Alkyne Hydrogenating Catalyst. *

October 27 Dr. R. A. L. Jones†, Cavendish Laboratory
'Perambulating Polymers'.

November 10 Prof. M. N. R. Ashfold†, University of Bristol
High-Resolution Photofragment Translational Spectroscopy: A New Way to Watch Photodissociation.

November 17 Dr. A. Parker†, Laser Support Facility
Applications of Time Resolved Resonance Raman Spectroscopy to Chemical and Biochemical Problems.

November 24 Dr. P. G. Bruce†, University of St. Andrews
Synthesis and Applications of Inorganic Materials. *

November 25 Dr. R.P. Wayne, University of Oxford
The Origin and Evolution of the Atmosphere

December 1 Prof. M. A. McKelvey†, Queens University, Belfast
Functionlised Calixerenes.

December 8 Prof. O. Meth-Cohen, Sunderland University
Friedel's Folly Revisited.

December 16 Prof. R. F. Hudson, University of Kent
Close Encounters of the Second Kind.

1994

January 26 Prof. J. Evans†, University of Southhampton
Shining Light on Catalysts.

February 2 Dr. A. Masters†, University of Manchester
Modelling Water Without Using Pair Potentials.

February 9 Prof. D. Young†, University of Sussex
Chemical and Biological Studies on the Coenzyme Tetrahydrofolic Acid.

February 16 Prof. K. H. Theopold, University of Delaware, U.S.A
Paramagnetic Chromium Alkyls: Synthesis and Reactivity.

February 23 Prof. P. M. Maitlis†, University of Sheffield
Why Rhodium in Homogenous Catalysis. *

March 2 Dr. C. Hunter†, University of Sheffield
Non Covalent Interactions between Aromatic Molecules.

March 9 Prof. F. Wilkinson, Loughborough University of Technology
Nanosecond and Picosecond Laser Flash Photolysis.

March 10 Prof. S.V. Ley, University of Cambridge
New Methods for Organic Synthesis.

March 25 Dr. J. Dilworth, University of Essex
Technetium and Rhenium Compounds with Applications as Imaging Agents.

April 28 Prof. R. J. Gillespie, McMaster University, Canada
The Molecular Structure of some Metal Fluorides and Oxo Fluorides: Apparent Exceptions to the VSEPR Model. *

May 12 Prof. D. A. Humphreys, McMaster University, Canada
Bringing Knowledge to Life *

October 5 Prof. N. L. Owen, Brigham Young University, Utah, USA
Determining Molecular Structure - the INADEQUATE NMR way

October 19 Prof. N. Bartlett, University of California
Some Aspects of Ag(II) and Ag(III) Chemistry *

November 2 Dr P. G. Edwards, University of Wales, Cardiff
The Manipulation of Electronic and Structural Diversity in Metal Complexes - New Ligands *

November 3 Prof. B. F. G. Johnson, Edinburgh University
Arene - Metal Clusters - DUCS Lecture *

November 9 Dr J. P. S. Badyal, University of Durham
Chemistry at Surfaces, A Demonstration Lecture

November 9 Dr G. Hogarth, University College, London
New Vistas in Metal Imido Chemistry *

November 10 Dr M. Block, Zeneca Pharmaceuticals, Macclesfield
Large Scale Manufacture of the Thromboxane Antagonist Synthase Inhibitor ZD 1542

November 16 Prof. M. Page, University of Huddersfield
Four Membered Rings and b-Lactamase

November 23 Dr J. M. J. Williams, University of Loughborough
New Approaches to Asymmetric Catalysis

December 7 Prof. D. Briggs, ICI and University of Durham
Surface Mass Spectrometry

1995

January 11 Prof. P. Parsons, University of Reading
Applications of Tandem Reactions in Organic Synthesis

January 18	Dr G. Rumbles, Imperial College, London *Real or Imaginary 3rd Order non-Linear Optical Materials*
January 25	Dr D. A. Roberts, Zeneca Pharmaceuticals *The Design and Synthesis of Inhibitors of the Renin-Angiotensin System*
February 1	Dr T. Cosgrove, Bristol University *Polymers do it at Interfaces*
February 8	Dr D. O'Hare, Oxford University *Synthesis and Solid State Properties of Poly-, Oligo- and Multidecker Metallocenes* *
February 22	Prof. E. Schaumann, University of Clausthal *Silicon and Sulphur Mediated Ring-opening Reactions of Epoxide*
March 1	Dr M. Rosseinsky, Oxford University *Fullerene Intercalation Chemistry*
March 22	Dr M. Taylor, University of Auckland, New Zealand *Structural Methods in Main Group Chemistry* *
April 26	Dr M. Schroder, University of Edinburgh *Redox Active Macrocyclic Complexes : Rings, Stacks and Liquid Crystals*
May 3	Prof. E. W. Randall, Queen Mary and Westfield College *New Perspectives in NMR Imaging*
May 4	Prof. A. J. Kresge, University of Toronto *The Ingold Lecture - Reactive Intermediates : Carboxylic Acid Enols and Other Unstable Species*

† Invited specially for the graduate training programme.